

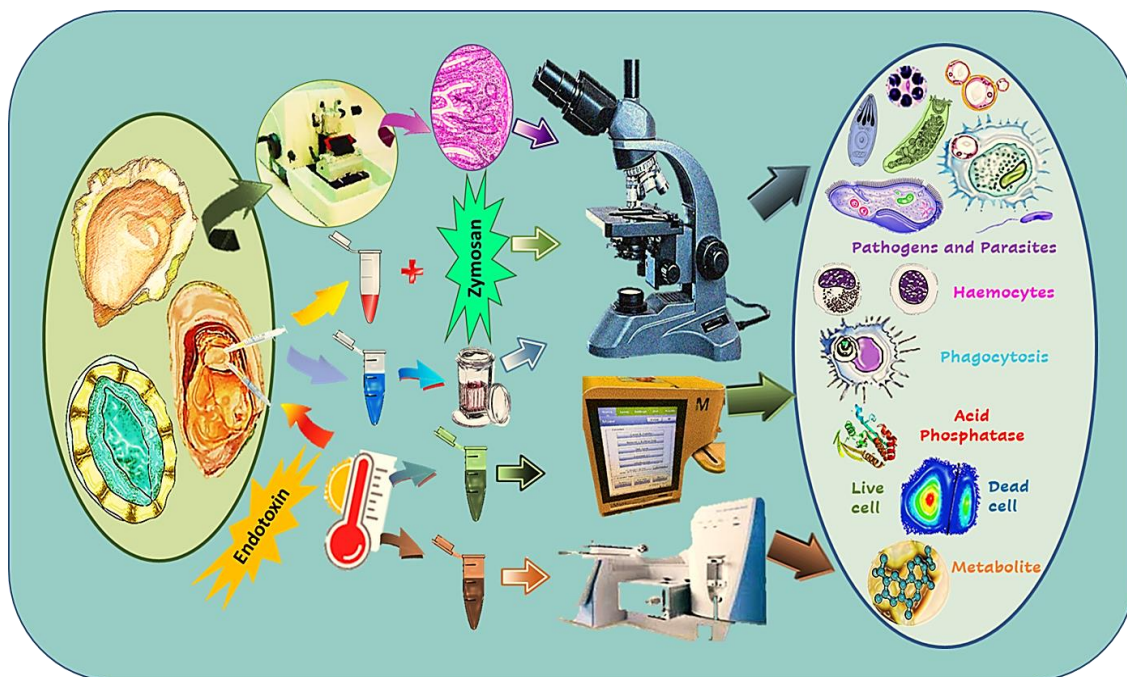
Investigation and Characterization of Pathogens and Parasites on New Zealand Aquaculture Shellfish

Farhana Muznebin

A thesis submitted to Auckland University of Technology in
fulfilment of the requirements for the degree of Doctor of Philosophy
(PhD)

Faculty of Health and Environmental Sciences
School of Science
2022

Abstract



Shellfish, including New Zealand Greenshell™ mussels (*Perna canaliculus*), New Zealand black-footed abalone (*Haliotis iris*) and flat oysters (*Ostrea chilensis*) are susceptible to a number of pathogens and diseases which threaten the aquaculture industry. In recent years, the high mortality of these species in both wild and farm settings has increased in frequency and magnitude. These mortality events often take place in summer (summer mortality), with shellfish succumbing to heat stress and pathogen loadings. However, there is a lack of information on the combined effects of acute heat stress and immune stimulation, as well as the specific mechanisms of the effects, susceptibility and resilience. Therefore, a better understanding is needed of the health status and capacity of shellfish to survive and overcome these events. Key to this understanding is the investigation of host-pathogen-environment interactions during mortality events and transmission pathways of infections.

Histology, one of the most useful and imperative diagnostic techniques, was applied for the detection and identification of protozoa (*Perkinsus olseni*, apicomplexan X [APX], *Bonamia exitiosa* and *B. ostreae*, gut protozoan), ciliates (*Scyphidia*-like, *Sphenophrya*-like and unidentified disintegrated), fungi (*Microsporidium rapuae*), cestodes (*Bucephalus longicornutus* and Gymnophallid-like metacercaria), microbes (intracellular microcolonies of bacteria, *Vibrio*-like bacteria) and copepods from different tissues of *H. iris*, *O. chilensis* and *P. canaliculus* collected from Moana Blue Abalone Ltd., Kaiarau mussel farms and oyster farms in the Marlborough Sounds, New Zealand. Subsequent *in situ*-hybridization confirmed the

identity of *P. olseni* in *H. iris* and *P. canaliculus*. This is the first detailed description of *P. olseni* in *H. iris*. There is a close relationship between the health status of abalone and the presence or absence of parasites, which may assist with identifying and characterising abalone health risks. Consequently, the findings of this thesis increase our in-depth understanding of pathogen infections in abalone, including host immune responses which may be used as early warning signs of health issues in wild and cultivated abalone in New Zealand. Furthermore, this is the first report on seasonal variations of *P. olseni* and APX in *P. canaliculus*. There was a significant association between seasons and the presence of *P. olseni* and APX in mussels.

The abundance of *B. ostreae*, *P. olseni* and APX for whole animals and different tissues was evaluated semi-quantitatively using modified grading scales. Inflammatory tissue responses and abnormal tissue structures were also assessed semi-quantitatively. The modified grading schemes were employed to assess the health state of oysters, as well as improve the understanding of the progression of *B. ostreae* disease in oyster tissues. In this investigation, *B. ostreae* microcells were detected inside haemocytes of *O. chilensis*. The haemocytes presence in a variety of tissues within oysters indicated *B. ostreae* was present at these sites. Moreover, diapedesis was noticed in tissues containing *B. ostreae* in haemocytes and suggesting a route of disease transmission.

A new classification scheme for *P. canaliculus* haemocytes was developed using Giemsa-stained smears, which is improved and more representative for the characterization of haemocytes (eight distinct types). The successful observation of phagocytic performance indicates that granulocytes only exhibit phagocytosis, and the phagocytic activity changed with season and temperature.

Multidisciplinary methods including enzyme staining reactions, flow cytometry, and metabolomic profiling were used to investigate the combined effects of acute thermal stress and immune stimulation on mussels exposed to different temperatures (26°C vs 15°C) and endotoxin injection (with vs without). Positive enzyme reactions of the marker enzymes (acid phosphatase [ACP] and phenoloxidase [PO]) only detected in granulocytes, and for the first time, ACP and PO were evaluated in *P. canaliculus*. At the higher water temperature, free fatty acid constituents increased in mussel haemolymph and free amino acids decreased which supports higher energy demand and metabolic rate due to thermal stress. Survival data confirmed a severe physiological impact of the high-temperature treatment through incidences of mortality. However, thermal stress combined with endotoxin exposure did not lead to a synergistic effect on mortality. These findings provide new insights into the relationship between thermal stress and immunity to better understand the immune defence system in mussels.

In summary, the information of this thesis helps to draw inferences about specific infection patterns relating to disease development and transmission mechanisms, assess host-pathogen interactions, to better understand the immune function and the overall health of shellfish for disease mitigation of these important aquaculture species. This information is crucial to develop disease management strategies and early warning systems for aquaculture species to ensure the sustainability of wild and farmed shellfish populations.

Table of Contents

Abstract.....	i
Table of Contents.....	iv
List of Tables.....	ix
List of Figures.....	xi
Attestation of Authorships.....	xvii
Co-author Contributions.....	xviii
Acknowledgements.....	xx

Chapter 1: Introduction and Literature Review

1.1 General Introduction and Literature Review.....	2
1.1.1 Worldwide aquaculture.....	2
1.1.2 New Zealand Aquaculture.....	2
1.1.3 Disease outbreaks in aquaculture species.....	5
1.1.4 Potential disease risk of New Zealand aquaculture species.....	7
1.1.4.1 Mussels.....	7
1.1.4.2 Oysters.....	8
1.1.4.3 Abalone.....	10
1.1.5 Summer mortality events and host-pathogen-environment interactions in aquaculture species.....	11
1.1.6 Immunity of aquaculture species.....	12
1.1.6.1 Bivalve molluscs immune studies.....	13
1.1.6.2 Gastropod molluscs immune studies.....	13
1.1.7 Overview of haemolymph and haemocytes of molluscs.....	14
1.1.7.1 Haemolymph components and their roles.....	14
1.1.7.2 Haemocyte classifications and their functions.....	14
1.1.8 Phagocytosis in defence function of molluscs.....	16
1.1.9 Enzyme activity in defence function of molluscs.....	16
1.1.10 Immunological tissue responses of molluscs.....	17
1.1.11 Techniques and approaches to study shellfish pathology.....	17
1.2 Thesis Aims.....	20
1.3 Thesis Structure.....	21

1.4 Research Outputs	23
1.4.1 Peer-reviewed papers	23
Published.....	23
Revised.....	23
In preparation	24
1.4.2 Presentations at Conferences and Symposiums	24
Poster presentations (first or main author).....	24
Oral presentation (presented by co-author).....	25
1.4.3 Scholarship/Award/Travel grants	25
<u>Chapter 2: Occurrence of <i>Perkinsus olseni</i> and other parasites in New Zealand black-footed abalone (<i>Haliotis iris</i>)</u>	
2.1 Introduction.....	28
2.2 Materials and Methods.....	30
2.2.1 Sample collection and preparation.....	30
2.2.2 Histology.....	30
2.2.3 <i>In-situ</i> hybridization (ISH).....	31
2.2.4 Microscopic observations	32
2.2.5 Epidemiological parameters and data analysis	32
2.2.6 Statistical analyses	35
2.3 Results.....	35
2.3.1 Prevalence and mean intensity of pathogens and parasites.....	35
2.3.2 Observations of pathogens and parasites	37
2.3.2.1 <i>Perkinsus olseni</i>	37
2.3.2.2 Specificity test of <i>Perkinsus olseni</i> by ISH.....	38
2.3.2.3 Ciliates	39
2.3.2.4 Apicomplexan-like.....	39
2.3.2.5 Intracellular microcolonies of bacteria (IMCs).....	39
2.3.2.6 Rod-shaped bacteria.....	39
2.3.3 Severity of immunological tissue responses	41
2.3.3.1 Haemocytes in muscle tissues.....	41
2.3.3.2 Ceroid infiltration in different organs	41
2.3.3.3 Pathological condition of gills of abalone.....	41
2.3.4 Gross appearance of the samples and the occurrence of parasites	42
2.4 Discussion.....	43
2.4.1 <i>Perkinsus olseni</i>	43
2.4.2 Other pathogens and parasites	44
2.4.3 Immunological tissue responses.....	45

2.5 Conclusions.....	46
<u>Chapter 3: <i>Bonamia ostreae</i> (Haplosporidia) and other parasites in New Zealand flat oysters (<i>Ostrea chilensis</i>): a histopathological study</u>	
3.1 Introduction.....	49
3.2 Materials and methods	51
3.2.1 Sample collection, histological preparation and microscopic examination	51
3.2.2 Quantification of parasites	52
3.2.3 Quantification of <i>Bonamia</i>	52
3.2.3.1 <i>Bonamia</i> relative abundance per tissue (0-3)	52
3.2.3.2 The mean of <i>Bonamia</i> microcells per haemocyte	52
3.2.4 <i>Bonamia</i> species diagnosis	56
3.2.5 Haemocytosis associated with <i>B. ostreae</i> infection	56
3.2.6 Presence of ceroid granules or lipofuscin with <i>B. ostreae</i> infection.....	56
3.2.7 Other pathogens and parasites	57
3.2.8 Overall condition	57
3.2.9 Statistical analysis.....	57
3.3 Results.....	57
3.3.1 Infection with <i>Bonamia</i>	57
3.3.2 <i>B. ostreae</i> epidemiological and health parameters.....	59
3.3.3 Infection with other parasites and pathogens	63
3.4 Discussion.....	67
3.5 Conclusions.....	72
<u>Chapter 4: <i>Perkinsus olseni</i> and other parasites and abnormal tissue structures in New Zealand Greenshell™ mussels (<i>Perna canaliculus</i>) across different seasons</u>	
4.1 Introduction.....	75
4.2 Materials and methods	78
4.2.1 Sample collection, Histology and <i>In-situ</i> hybridization (ISH).....	78
4.2.2 Quantitative and semi-quantitative evaluation of parasite infections, inflammatory tissue responses and abnormal tissue structures	78
4.2.3 Inflammatory responses	80
4.2.4 Tissue conditions	80
4.2.4.1 Digestive tubule structures.....	81
4.2.4.2. Gill structures.....	81
4.2.5 Statistical analyses	82
4.3 Results.....	82
4.3.1 Epidemiological parameters of <i>P. olseni</i> infection	82

4.3.2 Epidemiological parameters of APX infection	86
4.3.3. Co-infection of <i>P. olsenii</i> and APX	90
4.3.4 Epidemiological parameters of other parasite infections	91
4.3.5 Immunological tissue responses (Haemocytosis)	92
4.3.6 Immunological tissue responses (ceroid/brown material).....	94
4.3.7 Digestive tubule structures.....	96
4.3.8 Gill structures.....	97
4.3.9 Observation of pathogens and parasites.....	99
4.3.9.1 Infection with <i>P. olsenii</i>	99
4.3.9.2 Specificity test of <i>Perkinsus olsenii</i> by ISH.....	101
4.3.9.3 Infection with APX.....	101
4.3.9.4 Infection with other parasites.....	103
4.4 Discussion.....	105
4.4.1 Infection with <i>P. olsenii</i>	105
4.4.2 Infection with APX.....	106
4.4.3 Other parasites and pathogens.....	107
4.4.4 Gill pathology and digestive tubule pathology	108
4.5 Conclusions.....	109
<u>Chapter 5: Characterization of mussel (<i>Perna canaliculus</i>) haemocytes and their phagocytic activity across seasons</u>	
5.1 Introduction.....	113
5.2 Materials and Methods.....	115
5.2.1 Mussel samples	115
5.2.2 Sample size and experimental design	115
5.2.3 Haemolymph collection	115
5.2.4 Differential Haemocyte Counts (DHC)	116
5.2.5 Phagocytosis assay.....	116
5.2.6 Grading scale for bacterial association	117
5.2.7 Grading scale for granules of granulocytes.....	117
5.2.8 Statistical analyses	117
5.3 Results.....	118
5.3.1 Classification scheme.....	118
5.3.2 Differential Haemocyte Counts (DHC)	124
5.3.3 Bacteria (<i>Vibrio</i> -like) associated with haemocytes.....	126
5.3.4 Phagocytosis assay.....	128
5.4 Discussion.....	131
5.4.1 Haemocyte classification	131

5.4.2 Haemocyte types and functions	132
5.4.3 Bacterial association	134
5.4.4 Phagocytic activity	135
5.5 Conclusions.....	136

Chapter 6: Acute thermal stress and endotoxin exposure modulate metabolism and immunity in marine mussels (*Perna canaliculus*)

6.1 Introduction.....	139
6.2 Materials and Methods.....	140
6.2.1 Biological samples and experimental setup	140
6.2.2 Enzyme activity	142
6.2.3 Flow cytometry	143
6.2.4 Metabolite profiling	143
6.2.5 Statistical analyses	144
6.3 Results.....	144
6.3.1 Enzyme activity	144
6.3.2 Flow cytometry	146
6.3.3 Metabolomics.....	148
6.3.4 Mortality	150
6.4 Discussion.....	151
6.5 Conclusions.....	155

Chapter 7: General Discussion and Conclusions

7.1 General discussion	157
7.2 Limitations and future perspectives	162
7.3 Conclusions.....	166

Chapter 8: References

8. References.....	169
--------------------	-----

Chapter 9: Appendixes

9.1 Appendixes (Chapter 1)	203
9.2 Appendixes (Chapter 6)	204

List of Tables

Table 2.1 Semi-quantitative grading scale for the severity of haemocytes and ceroid material occurrence. See the figures below for visual grading	33
Table 2.2 Grading scale for gill pathology.	33

Table 2.3 Overall prevalence and mean intensity (\pm SE) index of parasites in abalone.....	36
Table 2.4 Prevalence and mean intensity (\pm SE) of parasites in different tissues and organs of abalone.....	37
Table 3.1 A semi-quantitative <i>B. ostreae</i> grading scale for whole oysters modified from Hine (1991a), compared with the original scheme of Hine (1991a).....	54
Table 3.2 The distribution of <i>B. ostreae</i> grading levels within the sample population (n = 94) an the concurrence of microcells infecting haemocytes in blood spaces or undergoing diapedesis within haemocytes. X = absence, \surd = presence.....	60
Table 3.3 Diffuse, focal and multi focal haemocytosis and ceroid abundance in different tissues of oysters [n = number of samples, % = occurrence rate].....	62
Table 3.4 Prevalence of all observed parasites or pathogens associated with flat oysters (n = 94) in this survey.....	65
Table 3.5 Statistical analysis: Chi-square test and Odds Ratio (OR) for the association between histological observation of <i>B. ostreae</i> and other pathogens (n = 94).....	65
Table 3.6 Statistical analysis: Chi-square test and Odds Ratio (OR) for the association between <i>B. ostreae</i> (as detected via PCR) and other pathogens as detected via histology and/or PCR (n = 94).....	66
Table 3.7 Statistical analysis: Chi-square test and Odds Ratio (OR) for the association between histological observation of <i>B. ostreae</i> and other pathogens in oysters (n = 60).	66
Table 3.8 Statistical analysis: Chi-square test for the association between histological observation of <i>B. ostreae</i> and oyster health condition (n = 94).	67
Table 3.9 Statistical analysis: Chi-square test for the association between <i>B. ostreae</i> presence as detected via PCR and oyster health conditions (n = 94).....	67
Table 4.1 Whole animal grading for <i>P. olseni</i> infection (for each mussel, 10 random fields for each tissue were examined at 100 \times magnification).	79
Table 4.2 Whole animal grading for APX infection (for each mussel, 10 random fields for each tissue were examined at 100 \times magnification).....	79
Table 4.3 Tissue grading for <i>P. olseni</i> (0-3) and APX (0-4) infection (for each mussel, 10 random fields for each tissue were examined at 100 \times magnification).....	80
Table 4. 4 Grading for digestive tubule structures (Fig. 4.14A-D).....	81
Table 4.5 Grading for gill structures (Fig. 4.15A-D).....	81

Table 4.6 Prevalence of <i>P. olsenii</i> associated with mussels in different months [n = number of mussels infected with parasites].....	83
Table 4.7 Prevalence of APX associated with mussels in different months [n = number of mussels infected with parasites].....	87
Table 4.8 Statistical analysis: Chi-square test for the association between <i>P. olsenii</i> and APX infection in mussels.....	90
Table 4.9 Prevalence of parasites associated with mussels in different months [n = number of mussels infected with parasites].....	92
Table 4.10 Statistical analysis: Chi-square test for the association between parasites and health condition of mussels.....	98
Table 5.1 <i>Perna canaliculus</i> haemocyte characterization showing the criteria of Chandurvelan et al. (2013) compared with the new classification in this study.	119
Table 5.2 Percentages of different types of haemocytes. Bold values indicate Mean percentages (\pm SE) of the haemocyte categories.	124
Table 5.3 Percentages of samples (n = 80) associated with bacteria (<i>Vibrio</i> -like).	127
Table 5.4 Tukey's HSD Post Hoc tests (n = 50) for the season-wise estimates of differences (Mean \pm SE) in the percentage of cells with phagocytic activity along with 95% confidence intervals	131
Table 2.A.1 Statistical analysis: Chi-square test for the association between <i>P. olsenii</i> and other pathogens and parasites.....	203
Table 2.A.2 Statistical analysis: Chi-square test for the association between <i>P. olsenii</i> and gills pathology.	203
Table 2.A.3 Statistical analysis: Chi-square test for the association between <i>P. olsenii</i> and gross appearance of abalone.	203
Table 2.A.4 Statistical analysis: Chi-square test for the association between <i>P. olsenii</i> and unhealthy gross appearance of abalone.....	204
Table 2.A.5 Statistical analysis: Chi-square test for the association between unidentified disintegrated ciliates and gross appearance of abalone.....	204
Table 6.A.1 Mean percentage \pm SE of PO positive granulocytes, ACP positive granulocytes, total granulocytes and total hyalinocytes were calculated from the slides incubated in ACP and PO enzyme-substrate solutions at 15°C and 26°C temperature after 24 hours and 48 hours	

incubation period from non-injected control, FSW injected and endotoxin injected mussels. [Total sample number (n) = 60 and 100 cell counts from each sample].....	204
Table 6.A.2 2-Way ANOVA summary table for Enzyme reactions.....	205
Table 6.A.3 2Way ANOVA summary table for Flow cytometry	207
Table 6.A.4 Metabolites significantly affected ($p < 0.05$) in green-lipped mussels due to the effect of temperature, immune stimulation or the interaction of both.	208
Table 6.A.5 Average metabolite abundance of metabolites found in green-lipped mussels significantly affected by temperature.....	209
Table 6.A.6 Average metabolite abundance of metabolites found in green-lipped mussels significantly affected by immune stimulation.....	210
Table 6.A.7 Average metabolite abundance of metabolites found in green-lipped mussels significantly affected by the interaction of temperature and immune stimulation.....	210

List of Figures

Figure 1.1 Major aquaculture areas in New Zealand (Adapted from New Zealand Aquaculture Fact, 2012 & NZMFA, 2010).....	4
Figure 1.2 Production of New Zealand aquaculture in 2017. Data was obtained from FAO FishStat (FAO, 2019).....	5
Figure 1. 3 Thesis structure.....	21
Figure 2.1 Gross appearance of <i>Haliotis iris</i> showing (A) brown creamy substance/fluid (pus), (B) abnormal tissue (spongy), (C) and (D) abnormal tissue with nodules on foot, (E)-(G) shell deformities (scars and damage), (H) infestation of spirorbid worms (commensals) on the shell.	30
Figure 2.2 Grading scale for the occurrence of haemocytes in muscle tissues according to Table 2.1 (A) grade 1-light haemocytosis (H1), (B) grade 2-moderate haemocytosis (H2), (C) grade 3-heavy with diffuse haemocytosis (H3) and (D) grade 4- heavy with focal haemocytosis (H4). Scale bars in (A-C) = 30 μm and in (D) = 25 μm	34
Figure 2.3 Grading scale for the occurrence of ceroid material (arrows) in muscle tissues according to Table 2.1 (A) grade 1-light ceroid material (C1), (B) grade 2-moderate ceroid material (C2) and (C) grade 3-heavy ceroid material (C3). Scale bars = 30 μm	34
Figure 2.4 Grading scale for gill pathology according to Table 2.2 (A) grade 1- normal without ceroid material and parasites (G1), (B) grade 2- gills with ceroid material (green arrow) and ciliate parasites (black arrows) (G2), (C) grade 3- disrupted (showing areas of destruction) gills (black arrows) with ceroid materials (green	

arrow) and ciliate parasites (blue arrow), and without haemocytosis (G3) and (D) grade 4- swollen gills with haemocytosis (blue arrows) and *Perkinsus olseni* (black arrow) (G4). Scale bars = 30 μm 35

Figure 2.5 *Perkinsus olseni* in histological sections from infected abalone (*H. iris*) gills and mantle tissue, (A) vacuolated signet-ring trophozoite of *P. olseni* with eccentric prominent nuclei (black arrows) inside swollen gill, (B) single vacuolated signet-ring trophozoite (black arrow) of *P. olseni* with prominent eccentric nucleus and a large vacuole containing vacuoplast (green arrow) inside swollen gill, (C) and (D) vacuolated (containing vacuoplast) (green arrows) sibling daughter trophozoites (blue arrows) of *P. olseni* and trophozoite stage with rosette-like arrangement (orange arrow) inside a wall in mantle tissue. Scale bars = 20 μm 38

Figure 2.6 (A) and (B) *In situ* hybridization detection (blue staining) (black arrows) of *P. olseni* vegetative cells in tissue sections of *H. iris*. Scale bars = 20 μm 39

Figure 2.7 Parasites and pathogens in different organs in abalone (*H. iris*), (A) elongated pear-shaped *Sphenophrya*-like ciliates (black arrows) in the gills, (B) ovoid or spherical shaped *Scyphidia*-like ciliates (black arrow) with a conspicuous brush-like adhesive disc or scopula (blue arrow) and a dark macronucleus (orange arrow), (C) and (D) unidentified disintegrated ciliate (black arrows) and *Sphenophrya*-like ciliates (blue arrows) in the gills, (E) intracellular microcolonies of bacteria (IMCs) (black arrow) in the muscle, (F) intracellular microcolonies of bacteria (IMCs) (black arrow) in the gill blood spaces, (G) unidentified apicomplexan-like structures appearing in vacuoles within the intestinal epithelium (black arrows) inside digestive epithelium, (H) Bacteria (rod-shaped) in foot muscle tissue. Scale bars = 40 μm 41

Figure 2.8 Immunological tissue responses (haemocytosis and ceroid material) and *Perkinsus olseni* in abalone tissues, (A) inflammatory lesion showing haemocytosis (orange arrows) surrounding *P. olseni* (black arrows) in muscle tissue, (B) inflammatory lesion showing ceroid material (green arrows) in mantle connective tissues near *P. olseni* (black arrows). Scale bars = 30 μm 42

Figure 3.1 *B. ostreae* microcells (black arrows) in different tissues of flat oysters, (A) gills, (B) muscle, (C) connective tissue around the digestive tubules (presence of ceroid indicated with a blue arrow), (D) haemocytes around the gut wall, (E) *Bonamia* microcells in haemocyte (black arrow) inside blood sinus, (F) *Bonamia* microcell infected haemocytes (black arrow) inside blood spaces of gills and diapedesis with *Bonamia* microcells (blue arrow) in the gills, (G) diapedesis (blue arrow) and haemocyte with *Bonamia* microcells (black arrow) in the gut, (H) diapedesis (blue arrow) and haemocyte with *Bonamia* microcells (black arrow) in the mantle. Scale bars = 20 μm 59

Figure 3.2 Prevalence of different *B. ostreae* histological whole-oyster infection grades. 60

Figure 3.3 Percentage of *B. ostreae* abundance grading (0-3) in different tissues of *O. chilensis*. 61

Figure 3.4 Box and whiskers plot showing the distributions of the number of *B. ostreae* microcells per infected haemocyte in gills, mantle, digestive tubules and gut tissues of oysters

(Minimum, Q1, Median, Q3, Maximum). [In each case, Mean is greater than the Median, distributions are slightly positively skewed, Minimum values of all the tissues are similar, Median and Maximum values are higher in digestive tubules than other tissues]..... 62

Figure 3.5 (A) Haemocytosis (blue arrow) around a sporocyst (black arrow) of *B. longicornutus* containing a cercaria (black arrow) and sections of the cercarial tail (green arrow) in connective tissue, (B) zooites of APX (black arrows) in the connective tissue around digestive tubules, (C) cyst containing spores of *M. rapuae* (black arrow) in the connective tissue under the gut wall, (D) intracellular microcolonies of bacteria (IMCs; black arrow) in the digestive tubule epithelium, (E) fragment of a copepod (black arrow) and copepod parts (blue arrow) in the mantle cavity, (F) gymnophallid-like metacercaria (black arrow) in the mantle cavity and (G-H) bacteria (black arrow) in oyster gill filament. Scale bar = 60 μ m (A and E), Scale bar = 20 μ m (B, D, G and H), and Scale bar = 30 μ m (C and F). 64

Figure 4.1 Cumulative percentage of *P. olseni* abundance grading (0-3) of mussels in different tissues, N = 256 (abundance here applied only to organs/tissues rather than the whole mussel). 83

Figure 4.2 Cumulative percentage of *P. olseni* abundance grading (whole animal grading = 0-4) of mussels in different months..... 84

Figure 4.3 Mean prevalence (\pm SE) of *P. olseni* in summer, winter, spring and autumn. [summer (n = 40), winter (n = 80), spring (n = 60), autumn (n = 76)]. 85

Figure 4.4 Cumulative percentage of *P. olseni* abundance grading (0-4) of mussels in different seasons (summer, winter, spring and autumn) [summer (n = 40), winter (n = 80), spring (n = 60, autumn (n = 76)]. 86

Figure 4.5 Cumulative percentage of APX abundance grading (0-4) of mussels in different tissues, N = 256 (abundance here applied only to organs/tissues rather than the whole mussels). 87

Figure 4.6 Mean prevalence (\pm SE) of APX in summer, winter, spring and autumn. [summer (n = 40), winter (n = 80), spring (n = 60), autumn (n = 76)]. 89

Figure 4.7 Cumulative percentage of APX abundance grading (whole animal grading = 0-5) of mussels in different months..... 89

Figure 4.8 Cumulative percentage of APX abundance grading (0-5) of mussels in different seasons (summer, winter, spring and autumn). [summer (n = 40), winter (n = 80), spring (n = 60, autumn (n = 76)]. 90

Figure 4.9 Mean prevalence (\pm SE) of parasites and microorganisms associated with mussels (per slide of the whole animal) (N = 256). 91

Figure 4.10 Haemocytosis (orange arrows) in the different tissues of *P. canaliculus*, (A) mantle,

(B) connective tissue surrounding digestive tract epithelium, (C) connective tissue surrounding digestive tubules and (D) connective tissue surrounding gonads. Scale bars = 10 μ m. 93

Figure 4.11 Cumulative percentage (occurrence rate) of hemocytosis grading (0-3) in different tissues of mussels, N = 256, % = occurrence rate [the term occurrence rate was used rather than prevalence to avoid confusion between organ/tissue values and prevalence]..... 94

Figure 4.12 Ceroid/brown material accumulation (orange arrows) in *P. canaliculus*, (A) connective tissue surrounding gonads, (B) connective tissue surrounding digestive tubules, (C) mantle, (D) gills (blood space). Scale bars = 10 μ m..... 95

Figure 4.13 Cumulative percentage of ceroid material accumulation levels (0-3) in different tissues, N = 256, % = occurrence rate..... 96

Figure 4.14 Digestive tubule structures (orange arrows) of *P. canaliculus* (A) normal or cruciform or Y shaped lumen (D1), (B) normal lumen but sloughed epithelial cells inside lumen (D2), (C) small or no lumen (D3) and (D) large lumen, with a thin epithelial wall (D4). Scale bars = 10 μ m. 97

Figure 4.15 Gill structures of *P. canaliculus*, (A) and (B) normal structure with ciliated lateral cilia (blue arrow) in the frontal zone of gill filament and with a medium number of haemocytes (orange arrows) in the gill blood space (G1), (C) normal structure with ciliary discs (green arrow) appear in the abfrontal zone of gill filament and with a medium number of haemocytes (orange arrow) in the gill haemolymph space (G1), (D) ciliary discs (black arrow) appear in the abfrontal zone of gill filament and destroyed/broken epithelium (blue arrow) of gill filament and few haemocytes in the gill haemolymph space (G2), (E) and (F) without ciliated lateral cilia in the frontal zone of gill filament, ciliary discs are atrophied/separated in the abfrontal zone of gill filament and very few haemocytes (orange arrow) in the gill hemolymph space (G3). Scale bars = 10 μ m..... 98

Figure 4.16 (A) and (B) Histology of Greenshell™ mussel (*P. canaliculus*) showing *P. olseni* cells phagocytosed by haemocytes in space between digestive tubules (orange arrows). Scale bar = 10 μ m. 99

Figure 4.17 Trophozoites (orange arrows) of *P. olseni* in (A) connective tissue surrounding digestive epithelium, (B) connective tissue surrounding digestive tubules, (C) gills (blood space), (D) gills (outside the gill epithelium), (E) mantle, (F) adductor muscle, (G) connective tissue surrounding female gonads and (H) connective tissue surrounding male gonads. Scale bars = 10 μ m. 101

Figure 4.18 (A) and (B) ISH of New Zealand Greenshell™ mussels showing blue labelled *P. olseni* trophozoites near digestive tubules (green arrows). Scale bar = 10 μ m..... 101

Figure 4.19 APX (orange arrows) in different tissues of *P. canaliculus*, (A) connective tissue surrounding digestive epithelium, (B) gills (blood space), (C) connective tissue surrounding digestive tubules, (D) phagocytosis by haemocytes near digestive tubules, (E) mantle, (F) adductor muscle, (G) connective tissue surrounding female gonads and (H) connective tissue surrounding male gonads. Scale bars = 10 μ m. 102

Figure 4.20 Parasites (orange arrows) and microorganisms (orange arrows and black arrow) in tissues of *P. canaliculus*, (A) *M. rapuae* sporocyst in connective tissue near digestive epithelium, (B) part of copepod (*P. spinosus* or *L. uncus*) exoskeleton inside the gut, (C) and (D) IMCs in muscle and near the mantle respectively, (E) bacteria (bacilli = orange arrow and cocci = black arrow) in the connective tissues near male gonads and (F) rod-shaped bacteria (bacilli) in the connective tissues surrounding digestive tubules. Scale bars = 10 μ m. 104

Figure 5. 1 A) Eosinophilic granulocytes and B) basophilic granulocytes. Scale bar = 10 μ m. 122

Figure 5.2 A) Dense-granulocytes (blue arrow), semi-granulocytes (black arrow) and small semi-granulocytes (orange arrow), B) dense-granulocyte (blue arrow), C) semi- granulocyte (black arrow) and D) small semi-granulocytes (orange arrows). Scale bar = 10 μ m. 122

Figure 5.3 A) Eosinophilic basophils (orange arrows) and B) mixed granulocytes (black arrows). Scale bar = 10 μ m. 123

Figure 5.4 (A) Large hyalinocytes (blue arrow), Filopodia (orange arrow), (B) and (C) small hyalinocytes (black arrows). Scale bar = 10 μ m. 123

Figure 5.5 Distributions of overall (n = 80) percentages of haemocytes (eosinophilic granulocytes = a, basophilic granulocytes = b and hyalinocytes = c), and those for different types of eosinophilic granulocytes (d, e and f) and hyalinocytes (g and h). The different letters denote significant differences among haemocyte categories. 125

Figure 5.6 Mean percentages of eosinophilic granulocytes, basophilic granulocytes and hyalinocytes based on monthly observation. 125

Figure 5.7 A) and B) Rod-shaped *Vibrio*-like bacteria (orange arrow) near haemocytes. Scale bar = 10 μ m. 127

Figure 5.8 Distributions of overall (n = 80) percentages of haemocytes (eosinophilic granulocytes = a, basophilic granulocytes = b and hyalinocytes = c), and those for different types of eosinophilic granulocytes (d, e and f) and hyalinocytes (g and h) using the samples where bacteria were present. The different letters denote significant differences among haemocyte categories. 128

Figure 5.9 Monolayer of haemocytes challenged with zymosan particles (orange arrows), (A) non-phagocytosing haemocytes (basophilic granulocytes) (blue arrow), (B) phagocytosing haemocytes (basophilic granulocytes) (blue arrow) with ingested zymosan particles, (C) eosinophilic semi-granulocytes (green arrow) with adhered zymosan particles (orange arrows) and (D) phagocytosing haemocytes with ingested zymosan particles (orange arrows) and numerous rod-shaped bacteria (green arrows) surrounding haemocytes (black arrows). Scale bar = 10 μ m. 129

Figure 5.10 Mean \pm SE percentage of phagocytosis based on microscopic observation. Exposure

time- a = 30 min, b = 60 min and c = 120 min. Each letter (a, b and c) indicates a significant difference. 130

Figure 6.1 Experimental design. Haemolymph was collected after 6h, 24h, and 48h for a combination of flow cytometry, enzyme activity and metabolomic-based analyses. Vehicle controls consisted of 0.22 μ m filtered seawater (FSW) injections. 142

Figure 6.2 Differential haemocyte cell-types and detection of their acid phosphatase (ACP) and phenoloxidase (PO) in *Perna canaliculus*: A) mean percentage (\pm SE) of total granulocytes and hyalinocytes at 15°C and 26°C after 24h and 48h incubation periods which were calculated from the slides incubated in ACP enzyme-substrate solutions, along with B) positively-stained granulocytes for ACP activity (inset bar plot; scale = relative %), C) light micrograph of a granulocyte showing PO enzyme reaction at the peripheral margin (orange arrows), D) light micrograph of a granulocyte showing numerous granules (green arrows) positive for ACP enzyme activity (orange arrows) and nucleus (black arrow), E) mean percentages (\pm SE) of granulocytes and hyalinocytes at 15°C and 26°C after 24h and 48h incubation periods which were calculated from the slides incubated in PO enzyme-substrate solutions, F) along with positively stained granulocytes for PO activity (inset bar plot; scale = relative %). 145

Figure 6.3 Average enzyme activity data (\pm SE) showing mean percentages of acid phosphatase and phenoloxidase, over 2 sampling times (24h and 48h) in all experimental groups (non-injected control, FSW injection and endotoxin injection) housed at 15°C and 26°C. 146

Figure 6.4 Average flow cytometry data (\pm SE) depicting total haemocyte counts, cell viability and reactive oxygen species production over 3 sampling times (6h, 24h and 48h) in all experimental groups (non-injected control, FSW injection and endotoxin injection) housed at 15 and 26°C. 147

Figure 6.5 Effect of thermal stress and immune stimulation via endotoxin exposure on mussel (*P. canaliculus*) haemolymph metabolites. Venn diagram (A) showing total numbers of compounds (annotated and unidentified) influenced by temperature (26°C vs 15°C), immune stimulation, and their interaction (2-Way ANOVA; $p < 0.05$). Main effects of temperature (B) and immune stimulation (C) on central metabolic pathways; annotated metabolites ($p < 0.05$) are highlighted with their relative changes in abundances (up/down arrows) compared to control conditions. 149

Figure 6.6 Cumulative mussel (*P. canaliculus*) mortality over 120 hours (Incubation period: 0 = 0h, 1 = 6h, 2 = 24h, 3 = 48h, 4 = 120h) in response to a thermal challenge (26°C vs 15°C) and endotoxin exposure. 151

Attestation of Authorship

I hereby declare that this submission is my own work and that, to the best of my knowledge and belief, it contains no material previously published or written by another person (except where explicitly defined in the acknowledgements), nor material which to a substantial extent has been submitted for the award of any other degree or diploma of a university or other institution of higher learning.

Farhana Muznebin

July 2022

Co-authored works

Chapter	Authors	Contribution	Total	Signature
2– Case study 1	Farhana Muznebin	- Experimental design - Sampling - Sample analysis - Data processing and Analysis - Writing	90%	
	Andrea C. Alfaro	- Review/edit	4%	
	Stephen C. Webb	- Review/edit - Experimental design	6%	
3 – Case study 2	Farhana Muznebin	- Experimental design - Sample analysis - Data processing and Analysis - Writing	80%	
	Andrea C. Alfaro	- Experimental design - Review/edit	2%	
	Stephen C. Webb	- Experimental design - Review/edit	8%	
	Anne Rolton Vignier	- Experimental design - Review/edit	2%	
	Zoë Hilton	- Experimental design - Review/edit	8%	
4 – Case study 3	Farhana Muznebin	- Experimental design - Sample analysis - Data processing and analysis - Writing	88%	
	Andrea C. Alfaro	- Experimental design - Review/edit	6%	
	Stephen C. Webb	- Experimental design - Review/edit	6%	

Chapter	Authors	Contribution	Total	Signature
5– Case study 4	Farhana Muznebin	- Experimental design - Sampling - Sample analysis - Data processing and analysis - Writing	91%	
	Andrea C. Alfaro	- Review/edit	2%	
	Stephen C. Webb	- Experimental design - Review/edit	6%	
	Fabrice Merien	- Experimental design	1%	
6 – Case study 5	Farhana Muznebin	- Experimental design- - Sampling - Sample analysis - Data processing and analysis - Writing	80%	
	Andrea C. Alfaro	- Experimental design - Review/edit	1%	
	Leonie Venter	- Experimental design - Sampling - Data processing and analysis - Writing & Review/edit	9.5%	
	Tim Young	- Experimental design - Sampling - Data processing and analysis - Writing & Review/edit	9.5%	

Acknowledgements

I would like to thank Almighty Allah for all blessings and for making everything possible. Thank you Allah!

This PhD thesis would not have been conceivable without the monetary help from various associations, including the New Zealand Government for a New Zealand Commonwealth Scholarship, a research budget from the Auckland University of Technology (AUT), the New Zealand Society of Parasitology for Travel Fellowships, and the New Zealand Department of Economics, Innovation and Employment (MBIE) contract the Aquatic Health Program CAWX1707.

My special thanks to my primary supervisor, Professor Andrea C. Alfaro. “Thank you so much, Andrea, for your incredible help over the years, being so understanding, patient while editing this thesis and a wonderful supervisor”. Your steady consolation, inspiration, motivation, helpful suggestions, enthusiastic guidance, diligent academic support, professional academic writing skills and vision have certainly elevated me above my capabilities. You are not only my supervisor but also a guardian who has accompanied me from academic and non-academic perspectives. A big thanks to you for providing me with mental support during my troublesome time and for assisting me with enhancing my insight and experience. In addition to my primary supervisor, I would like to thank my excellent co-supervisor Professor Fabrice Merien for his guidance and encouragement.

I would also like to especially acknowledge Dr. Steve Webb’s contribution to this thesis. Thank you so much Steve for training me on histopathology, providing expert knowledge on aquaculture pathology, valuable guidance and advice. I am grateful to you for having such an open mind and leaving me space to thrive. Your broad view and intellectual questions boosted my practical skill and histopathological knowledge. Without your extraordinary assistance in histopathology and haemocyte studies and revising manuscripts, I was unable to complete four manuscripts.

I am deeply indebted to my co-authors for helping undertake the research and edit the manuscripts within this thesis. I thank my co-authors: Professor Andrea C. Alfaro, Professor Fabrice Merien, Dr. Steve Webb, Dr. Zoe Hilton, Dr. Tim Young, Dr. Leonie Venter and Dr. Anne Rolton for their contribution. Andrea thank you for the in-depth reviews, anecdotes and significant input of all the manuscripts and Thesis Chapters, the skills and knowledge from which I will take throughout my career. I would like to express my gratitude to Steve, who had the tolerance and time to help me in fostering my exploration technique on histopathology and had an incredible commitment during the manuscripts production. Thank you, Zoe, for your

constructive criticism and careful review of the manuscript. A big thanks for editing the draft and assisting with methodology development, especially in Chapter 3. I also thank Fabrice for his assistance and supervision in developing enzyme experiment and phagocytic activity protocols. I would like to thank Tim and Leonie for their support in setting up the experiment, methodology development and big contribution during the manuscript production, especially in Chapter 6. A special thanks to both of you for helping me with metabolomics and flow cytometry analyses and draft writing. Thank you, Anne, for your participation in reviewing and editing the manuscripts, particularly Chapter 3. All my co-authors' significant reviews, advice, valuable comments and suggestions on the manuscripts carried my writing to the journal level.

Thanks to Ryan Lanauze, Operations Manager at Moana Blue Abalone Ltd. for providing abalone samples and Kaiaua mussel farms for supplying the mussels for this study. I would also like to thank the following people for their technical help: Dr. Henry Lane, Dr. Cara Brosnahan, Dr. Brian Jones and the staff at MPI Animal Health Laboratory, Biosecurity New Zealand for their help with histological sampling and assistance in the laboratory for *In-situ* hybridization (ISH). I am grateful to Dr. P. M. Hine for his advice and help with creating the modified grading scale. Taranaki Medlab, New Plymouth and Gribbles Veterinary Pathology Ltd., Christchurch are acknowledged for their assistance with histological sectioning, staining and slide preparation. AquaGene NZ is acknowledged for screening samples (PCR). Thanks go to the team from the Mass Spectrometry Centre at the University of Auckland for metabolomics assistance.

I would like to thank –the AUT School of Science, Technicians, staff and officials for various sorts of support during my study. I am profoundly thankful to Jinan, Meie, Saeedeh, Mena, Iana and Eileen for being supportive and assisting me with reagents preparation. I also like to thank Sharita Meharry, Senior Lecturer for helping me with the histological techniques. I would like to thank members of the Aquaculture Biotechnology Research Group, especially Dr. Tim Young, Dr. Leonie Venter, Dr. Thao Nguyen, Dr. Carine Burgois, Dr. Sara Masoomi Dezfooli, Shaneel Sharma, Si Ming Li, Awanis Azizan and Natalia Bullon Zegarra for their assistance with sampling. I am thankful to Awanis for assisting me with reagent preparation for the Enzyme experiment. I want to express gratitude toward Dr. David Parker for his proofreading of a manuscript. Thanks to Margaret Leniston, Sacha Pointon, Petrina Hibben, Sandelyn Agnes Su Kuan Lua, Prerna Taneja and George Kimani for their great work and kind supports at the scholarship office.

I am grateful to my friends Shanta Budha-Magar, Dr. Nishat Sultana, Dr. Sridevi Ravi, Anna Ishihara and Jamie Pamu who helped me to relieve mental stress and made me smile. Thank you so much for the endless conversations, fun, lunches, dinners, travel and so forth and above

all for being such a wonderful person. Shanta, thank you for being by my side even when we were away. At the point when I felt completely helpless, you stayed there to help me. “Thank you” can never make up for what you did for me. Unfortunately, Dr. Sridevi has passed away just a couple of months ago who was a gentle soul with a pure heart. I am grateful to late Sridevi for spending her precious time helping me with writing and sharing academic information, providing me with companionship and mental strength. I might likewise want to say thanks to Dr. Ronald Lulijwa (Ronnie) for assisting me with sharing research ideas and academic information. Much appreciated, Ronnie, for consistently with me, particularly during my hard times. Above all, I must thank you all most for helping me spark my inner strength by stimulating me in difficult situations.

For my time being in New Zealand, I thank my compassionate hosts: Nizam Uddin & Tania, Professor Andrea C. Alfaro & Professor Kathleen Campbell, Dr. Steve Webb & Kathy, Dr. Rosemary Barraclough and Dr. Leonie Venter who welcomed me furnished with delicious food. Magnificent couple Nizam & Tania were always beside me, especially in my difficult time to help me with warm accommodation, delicious food and incredible help. Their hospitality was such a blessing to me. Andrea & Kathleen were the remarkably amazing host. I can't thank you enough for the amazing hospitality you offered me. Without the super warm reception on the first day of Nelson, extraordinary help, care and gracious hospitality from Steve & Kathy, I certainly would have confronted a huge load of challenges in setting myself in Nelson during the histology training sessions. Those are great memories that I will treasure forever. Rosemary, I will never forget our catch up and coffee times. Leonie, I appreciate your kind hospitality. I am so glad for the generosity all of you showered.

I would like to say a heartfelt Thank you to my loving husband Dr. Abu Zar Md. Shafiullah who sacrifices a lot to help me live my dream and achieve my goal and offers me the motivation to keep going in life. He even aided me with the statistical analysis of some of my results. Without his continuous support, encouragement, great sacrifice and cooperation I am not able to pursue and continue my higher study here in New Zealand.

I express my sincere and deepest gratitude to my wonderful family in my home country of Bangladesh. I would like to thank my beloved parents, parents-in-law and the whole family who were always there to support me in every possible way.

Lastly, it was sudden that my beloved Father and Mother-in-law passed away during the final stage of my PhD journey and which funeral I was unable to join. I believe that my late father and mother-in-law would be amazingly glad for what I achieved. I could not be thankful enough for my family members who supported and prayed for me through this period.

**Dedicated to my beloved parents, parents-in-law
and husband**

Chapter 1

Introduction and Literature Review



New Zealand aquaculture species (New Zealand Greenshell™ mussels, New Zealand black-footed abalone and flat oysters)

1.1 General Introduction and Literature Review

1.1.1 Worldwide aquaculture

Aquaculture production is anticipated to rise by 109 million tonnes in 2030, a rise of 32% (26 million tonnes) over 2018 (FAO, 2020). From 2001 to 2018, the global aquaculture production of farmed aquatic animals increased by an average of 5.3% per year. Asia is expected to continue to boost the aquaculture sector with 89% of the global production by 2030. Overall, aquaculture production takes place in all corners of the globe, particularly in Africa (up to 48%) and Latin America (up to 33%). Since 1991, the amount of farmed aquatic food produced in China exceeded that of the rest of the world combined (FAO, 2020). Among major aquaculture producing countries, Egypt, Chile, India, Indonesia, Vietnam, Bangladesh and Norway have enhanced their share in regional or global production to a varying degree over the past two decades (FAO, 2020). The second-largest species production in the world is molluscs, with an output of 17.7 million tonnes and US\$34.6 billion; bivalves, including mussels, clams, scallops and oysters, with a production of 9.4 million tons and US\$69.3 billion in 2017 (FAO, 2020). Today, aquaculture is by far the dominant source of bivalve resources for human consumption. However, throughout the world, the growth and sustainability of the aquaculture industry are adversely affected by summer mortality events and high pathogen loads. Thus, good biosecurity practices are vital for successful marine and land-based farming and the future of the aquaculture industry.

1.1.2 New Zealand Aquaculture

New Zealand aquaculture products are well accepted by the international market and the industry continues to evolve to meet demands. The New Zealand flagship species are Greenshell™ mussels (*Perna canaliculus*), followed by King salmon (*Oncorhynchus tshawytscha*) and Pacific oysters (*Crassostrea gigas*) with some new species currently being investigated for their commercial value. There are well-established aquaculture regions at the top of the South Island and the top of the North Island. The aquaculture industry is spread mainly across five regions; mussels in Marlborough, Coromandel and Southland; oysters in Northland, Auckland and Coromandel; abalone in Marlborough and Canterbury (New Zealand Aquaculture Fact, 2012) (Fig. 1.1). Northland dominates Pacific oyster production (51%), with the remaining production being split between the Coromandel (26%), Auckland (21%) and Marlborough (3%) (New Zealand Aquaculture Fact, 2012).

New Zealand's aquaculture industry employs more than 3,000 people, and its revenue in 2019 is approximately US\$600 million (<https://www.aquaculture.org.nz/>). In 2018, the total aquaculture production in New Zealand was 104,500 tonnes (FAO, 2020). New Zealand aquaculture products are considered the world's best seafood and are exported to 79 countries

throughout the world (Aquaculture New Zealand, 2016). Over the past 50 years, New Zealand's aquaculture has grown from a small scale to a major key industry with sustainably producing the world's best seafood— Greenshell™ mussels, King salmon and Pacific oysters. (<https://www.aquaculture.org.nz/>). The Greenshell™ mussel (*P. canaliculus*) is New Zealand's most iconic premium seafood. In 2017, the production of oysters, salmon and mussels represented 1.5%, 12.8% and 85.6% respectively (FAO, 2019) (Fig. 1.2). In this country, total bivalve production in 2018 was 88,200 tonnes (FAO, 2020). The production of two bivalves (*P. canaliculus* and *C. gigas*) has made great contributions to the national economy. Other cultured species with smaller productions include New Zealand black-footed abalone/ pāua (*Haliotis iris*) and flat oysters (*Ostrea chilensis*). *H. iris* has been grown on a broader commercial scale, and its flesh and decorative shells have been recognized by the great commercial markets of the world. Statistics from the Food and Agriculture Organization of the United Nations (FAO) show that the world's production of farmed abalone has reached 22,000 tonnes. Abalone exports increased from \$34 million in 1991 to a top of \$80 million in 2001, before falling to \$51 million in 2003 (<https://www.paua.org.nz/>). New Zealand's abalone/pāua industry predominantly contributes to an international market (Cook & Gordon, 2010; Hooker & Creese, 1995) where the exported product of fresh, frozen and processed New Zealand abalone has increased the commercial tariffs. In 2016, New Zealand exported \$37.5 million capital of abalone with a bulk of 763.5 tonnes from processed products, 37 tonnes from frozen products and 29.1 tonnes from fresh products (Seafood New Zealand, 2016). Another aquaculture species under development, the New Zealand geoduck (*Panopea zelandica*) has also expanded as is one of the most profitable products in the seafood market (Le et al., 2017). New Zealand aims to develop other potential aquaculture species, such as yellowtail kingfish (*Seriola lalandi lalandi*), gropers (*Polyprion oxygeneios*) and eels (*Anguilla australis*, *A. dieffenbachia*) (<https://www.niwa.co.nz/>).

In New Zealand, the aquaculture industry has been perceived by the government as a top potential income source through the New Zealand aquaculture strategy and action plan (Ministry for Primary Industries, 2020). Therefore, the government has announced a strategy that will help "streamline" the aquaculture industry toward turning into a \$3 billion industry by 2035. However, marine shellfish diseases and summer mortality pose significant threats to the industry. Addressing these health threats requires a thorough understanding of the immune systems of these commercially important New Zealand aquaculture species and their ability to cope with the increased burden of pathogens.



Figure 1.1 Major aquaculture areas in New Zealand (Adapted from New Zealand Aquaculture Fact, 2012 & NZMFA, 2010).

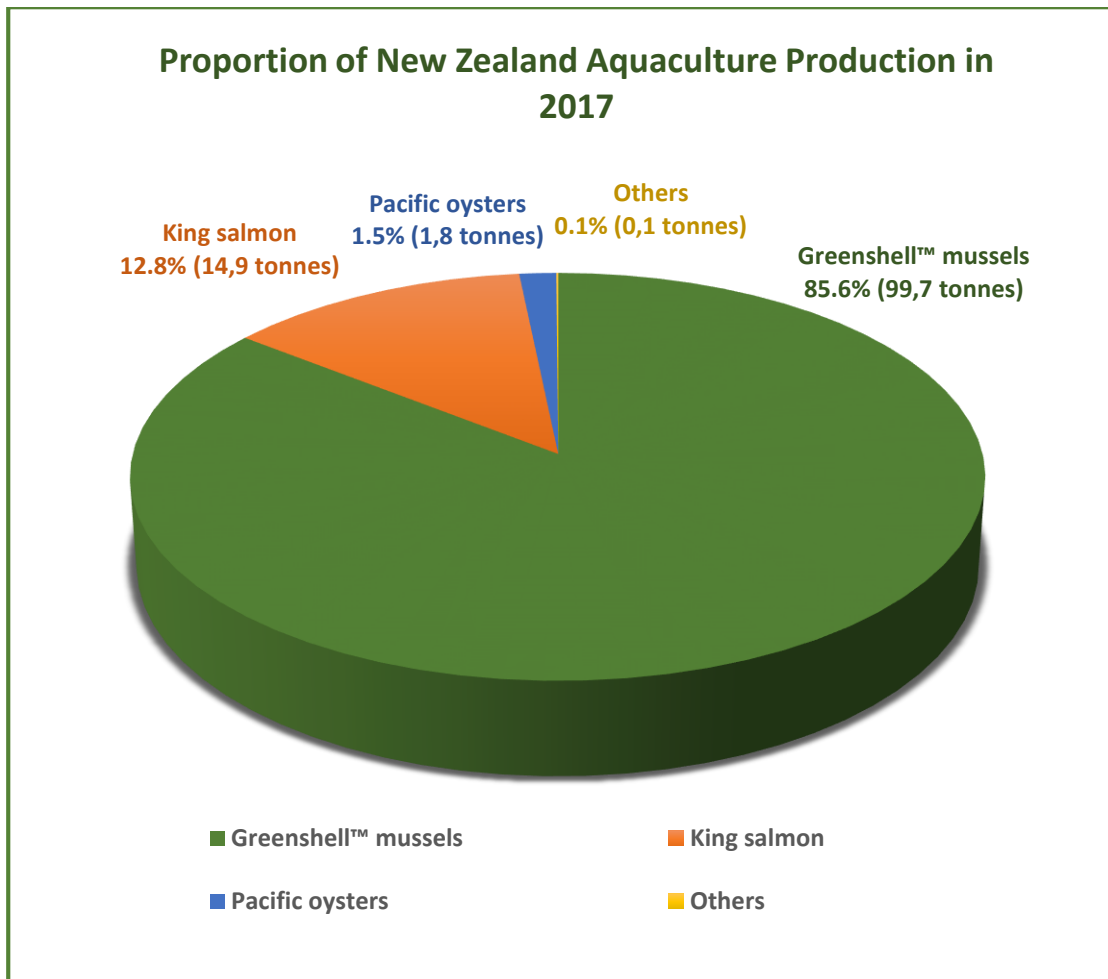


Figure 1.2 Production of New Zealand aquaculture in 2017. Data was obtained from FAO FishStat (FAO, 2019).

1.1.3 Disease outbreaks in aquaculture species

Disease can be simply defined as a lack of health. However, diseases are often associated with host-pathogen interactions. Infectious diseases have always been one of the top issues for the growth and sustainability of the seafood industry. They have negative impacts on the production of both farm and wild harvest, as well as the development of seafood quality. In recent decades, aquaculture diseases have attracted attention because they can seriously compromise production and profitability. The ongoing development of aquaculture together with the international trade of seafood, transfers and introduction of shellfish seed and stocks have escalated the threat of disease spread throughout the world. Disease outbreaks may be due to the spread of wild populations, accidental transfer of sick animals between farms, use of pathogen-infected feed, poor water quality, lack of sanitary barriers, lack of identification and isolation of unhealthy organisms, and impaired animal welfare as a result of overstocking and malnutrition, among others (Alfaro & Young, 2016). Disease outbreaks in aquaculture are often associated with viruses, bacteria and parasites. It is estimated that up to 1/5 of potential

aquaculture production in China, which is responsible for over two-thirds of the world's production, is lost due to the emergence of diseases (Li et al., 2011). In some cases, large-scale deaths caused by epidemics of serious diseases caused a large number of deaths in certain sectors, leading to the total collapse of the industry and a large socio-economic impact (for example, the herpes virus in oysters, white spot syndrome virus in shrimp) (Peeler et al., 2012; Sánchez-Martínez et al., 2007). Thus, disease outbreaks are considered to be a major constraint on aquaculture production and trade, affecting the economic development and socio-economic income of this sector in many countries around the world.

Several pathogens that have a major impact on the aquaculture industry have been identified worldwide. For example, a digenetic trematode, *Cercaria tenuans*, was the probable causative agent of extensive mortality of cultured mussels (*Mytilus edulis* = *Mytilus galloprovincialis*) in the southern part of the Laguna Veneta, Italy (Munford et al., 1981). In addition, disseminated neoplasia, also called leukemia or hemic neoplasia, has been discovered in blue mussels (*M. galloprovincialis*) from the coast of the Romanian Black Sea (Ciocan et al., 2005). The disease is characterized by the presence of single anaplastic cells with enlarged nuclei and sometimes frequent mitosis in hemolymph vessels and sinuses. The neoplastic cells gradually replace normal haemocytes leading to increased animal mortality.

Viral infections, such as the Oyster Herpes Virus (OsHV-1) have severely impacted oyster populations in Europe, Australia and New Zealand. It has long been believed that the oyster herpes virus occasionally causes the death of larvae and juveniles of bivalve species, most notably the Pacific oyster, *C. gigas*, and the flat oyster, *Ostrea edulis* (Hine, 2002a; Renault & Novoa, 2004). However, in 2008, a new variant (OsHV type 1 microvar) was described in association with mass mortalities of Pacific oyster spat in the United Kingdom, France, Ireland and Asia (Hwang et al., 2013; Peeler et al., 2012; Segarra et al., 2010). This virus without associated mortality was also detected in *C. gigas* in Spain and Italy (Dundon et al., 2011; Roque et al., 2012). In 2010, New Zealand and Australia recorded the first mortality outbreaks associated with OsHV-1 microvar (Bingham et al., 2013; Jenkins et al., 2013). These outbreaks have received considerable attention from shellfish farmers and scientists, but there is currently little information about these infections and their impacts. In late 2005, an acute disease, abalone viral ganglioneuritis (AVG), occurred in a land farm in Victoria, Australia, which was associated with very high mortality (up to 100%) in farmed abalone (Hooper et al., 2007). In May 2006, the disease was discovered in wild abalone, first near the affected farms, and subsequently spread along the Victorian coastline. After abalone was transferred from the wild to the farm, all three farms exploded almost simultaneously. The history of the abalone movement linking farms, the spread of outbreaks on farms, within and between farms, as well

as clinical observations of moribund and dead abalone, were all significantly indicative of a virulent infectious agent.

Bacterial infections are a constant risk to stocks in aquaculture facilities, such as hatcheries, nurseries and grow-out tanks (Webb, 2012). Bacterial pathogens, especially *Vibrio* spp. seriously affect aquaculture species and cause mortality outbreaks of marine bivalves in hatcheries, commercial farms and natural habitats (Travers et al., 2015). Some common *Vibrio* species include *V. splendidus*, *V. harveyi*, *V. tubiashii/coralliilyticus*, *V. aestuarianus*, and *V. crassostreae*; and other members of the genus *Nocardia* and *Roseovarius* are also considered important pathogenic bacterial species affecting bivalve aquaculture (Travers et al., 2015). *Xenohalictis californiensis* is a proposed new genus and new species of Rickettsiaceae that causes the disease known as “withering syndrome”, occurring in the epithelium of the intestinal tract of abalone and responsible for mortality (Friedman et al., 2000). *Xenohalictis californiensis* is listed by the OIE Manual of Diagnostic Tests for Aquatic Animals (OIE, 2019a).

Protozoan parasites belonging to the genera *Perkinsus*, *Haplosporidium*, *Marteilia*, and *Bonamia* severely affect a variety of mollusc species, such as abalone, clams, mussels, oysters, and scallops; which are commercially harvested or farmed around the world (Robledo et al., 2014). In particular, *Perkinsus marinus*, *Perkinsus olseni*, *Marteilia refringens*, *Mikrocytos mackini*, *Bonamia ostreae*, and *Bonamia exitiosa* can infect abalone, clams, mussels, oysters, and scallops, and are therefore currently under surveillance by the World Organization for Animal Health (OIE, 2019a). Infectious diseases are still a major concern for aquaculture and causing massive losses, and sometimes even shutting down certain operations completely. Therefore, the management of infectious diseases is a priority for aquaculture sustainability.

1.1.4 Potential disease risk of New Zealand aquaculture species

There is credible evidence that various pathogens and diseases have adverse effects on New Zealand aquaculture species. Potential disease risks to New Zealand aquaculture species are discussed below:

1.1.4.1 Mussels

New Zealand Greenshell™ mussels (*P. canaliculus*) support the largest shellfish industry in this country. However, due to their filter-feeding nature, mussels act as reservoirs for bacteria, including *Vibrio* spp., and can release them into seawater (Prado et al., 2014). Currently, there has been little information published in regards to diseases of *P. canaliculus* in New Zealand.

Pathogens observed in *P. canaliculus* are the unenveloped RNA virus in the epithelial cells of the digestive tract (Jones et al., 1996); phenotypic identification of two non-reactive gram-negative bacteria- *V. splendidus*, *V. coralliilyticus/neptunius*-like isolate in larval tissue (Kesarcodi-Watson et al., 2009a); protozoan parasite apicomplexan X (APX) in the gonad (Diggles et al., 2002a); flatworm- *Enterogonia orbicularis* inside body and mud worms- *Boccardia* spp. and *Polydora* spp. within the shell (Diggles et al., 2002a). Pathogens and parasites associated with *P. canaliculus* that have been recorded in New Zealand include APX, *B. exitiosa*, digestive epithelial virosis (DEV), invasive ciliates, shell-boring worms (mud worms) and *Vibrio* spp. bacteria (Castinel et al., 2014, 2019). The significant pathogen, APX was also identified in different mussels- *P. canaliculus*, *M. galloprovincialis* and *Modiolus areolatus* in New Zealand (Suong et al., 2019). *Perkinsus olseni* which is associated with inflammatory responses and mass mortalities was noted in *P. canaliculus* from the top of the South Island in New Zealand (OIE, 2016). *P. olseni* was first reported in farmed *P. canaliculus* at the top of the South Island in 2014 (OIE, 2014, 2016) and then in 2018 (Webb & Duncan, 2019). Relatively few studies have focused on *Perkinsus* and APX infection and their relation with seasonal temperature variations in New Zealand Greenshell™ mussels. Therefore, seasonal changes in *P. olseni* and APX infections in New Zealand Greenshell™ mussels (*P. canaliculus*) are first reported in Chapter 4. Since *Perkinsus* infection is usually related to key environmental factors, such as water temperature, salinity, animal density, and substrate type, it is important to continuously monitor *Perkinsus* infection during all seasons.

The greatest potential threat to New Zealand Greenshell™ mussels aquaculture appears to be posed by parasites introduced by invading species of blue mussels (e.g., *Mytilus edulis*). These common ship-borne fouling organisms are a likely source of overseas pathogens. The hybridisation of invasive and indigenous blue mussels (*M. galloprovincialis*) presents additional potential pathological risks due to the production of more susceptible reservoir hosts suitable for these pathogens. Evidence for such a risk is reported by Beaumont et al. (2004) who found the slower performance of *M. edulis* × *M. galloprovincialis* hybrids compared with pure species. Furthermore, Fuentes et al. (2002) reported lower viability of hybrids challenged by heat shock or infection with *Marteilia refringens*. If *Mytilus* spp. were to become infected with *Marteilia* and if appropriate intermediate hosts (or local substitutes) were available, there is the possibility of transmission to Greenshell™ mussels (Webb et al., 2007).

1.1.4.2 Oysters

Flat oysters (*Ostrea chilensis*) and Pacific oysters (*C. gigas*) are filter-feeding animals and are important aquaculture species in New Zealand. However, several diseases and parasites

associated with oysters have been reported, most of which are also globally ubiquitous and pose some commercial threats to oysters production. The haplosporidian parasites *Bonamia* spp. have had significant impacts on both farmed and wild populations of flat oysters around the world (Carnegie et al., 2016; Doonan et al., 1994; Engelsma et al., 2014). Due to its ongoing impact on the flat oyster fishery in New Zealand, there has been both experimental and observational work carried out examining the epidemiology and pathology of *B. exitiosa* affecting *O. chilensis* in New Zealand (Cranfield et al., 2005; Diggles & Hine, 2002; Hine et al., 2002; Hine, 1991a). *B. ostreae* is a parasite that can fatally infect flat oysters and poses a substantial threat to this species of oyster. *B. ostreae* was first discovered in the upper South Island in 2015, then in Big Glory Bay oyster farms in 2017. *B. ostreae* and *B. exitiosa* alone have caused serious internationally notifiable disease outbreaks (OIE, 2018a; OIE, 2018b; OIE, 2012). They were responsible for heavy stock losses (80 to 90%) in oyster populations (Elston et al., 1987; Farley et al., 1988; Hine, 1996). Hine (2002a) reported severe apicomplexan and *B. exitiosa* infection in the oyster, *O. chilensis*. In addition, *Bonamia* spp. have been found within the haemocytes of flat oysters, and *Bonamia* co-infections have been observed in *O. chilensis* in New Zealand (Lane et al., 2016). The mortality outbreaks of *O. chilensis* were caused by *Bonamia* spp. (Castinel et al., 2013) which led to the removal of all the farmed oysters in New Zealand in 2017. Therefore, clarifying the disease progression pattern of *B. ostreae* infections within *O. chilensis* is paramount in helping to determine appropriate disease management strategies. Chapter 3 introduces *B. ostreae*, *B. exitiosa*, and other parasites in flat oysters in New Zealand, as well as the specific pattern of *B. ostreae* disease progression in oysters' tissues, to elucidate host-parasite interactions and transmission of infection.

Several other pathogen and parasites such as *Bucephalus longicornutus*, APX, *Microsporidium rapuae* and ciliates in digestive tubule lumen; copepod in digestive gland connective tissue and *Rickettsia* in digestive tubule epithelium also have been reported in flat oysters (Lane et al., 2016). Diggles et al. (2002a) noticed viruses-iridovirus, herpes-like virus in gill, mantle and adductor muscle; bacteria-*Nocardia crassostreae* (gram-positive bacteria) in the mantle, gill, adductor muscle and heart; *Cytophaga* spp. in hinge ligament; rickettsia like organisms (RLOs) (now referred to as intracellular microcolonies of bacteria [IMCs] by Cano et al., 2020) in mantle and gill; protozoa- *Marteilioides chungmuensis* in ovarian follicle; *Mikrocytos mackini* in the body wall, labial pulp and mantle; *Haplosporidium nelsoni*; and *Perkinsus marinus* in the mantle of Pacific oysters.

Other diseases and parasites associated with New Zealand oysters have also been reported. These include flatworms *Enterogonia orbicularis* inside the body, mud worms- *Boccardia* spp. and *Polydora* spp. within the shell (Diggles et al., 2002a); spionid mud-worms (Handley &

Bergquist, 1997; Handley, 1995) and ostreid herpes virus OsHV-1 (Dinamani, 1971; Hine et al., 1992; Jenkins & Meredyth-Young, 1979), which also infects oyster larvae and spat. Potential problems could arise from RLOs/IMCs, granuloma-like lesions and inflammatory lesions suggestive of haemocytic neoplasia, and severe cases of mud worm can cause significant shell embrittlement (Webb, 2012). The least affected organisms (Dinamani, 1986) include turbellarians, chironomids, nematodes, mud worms and pea crabs. Hine and Jones (1994) mentioned the copepod *Pseudomyicola spinosus* but asserted that it appears to have little effect on its hosts. In 2010, New Zealand recorded the first outbreak of mortality involving OsHV1 microvariants (Bingham et al., 2013; Jenkins et al., 2013). These outbreaks have received considerable attention from shellfish farmers and scientists, but at present, there is currently little information on these infections and their impacts.

1.1.4.3 Abalone

New Zealand black-footed abalone or pāua (*H. iris*) are currently farmed in New Zealand. However, abalone cultured at high densities (up to 45% of the cultured *H. iris*) usually show erosion and exfoliation damage of the foot and epipodium, which are usually associated with infections of various bacteria (Diggles & Oliver, 2005). In addition, pathogenic transmissions from one species to another are common in intensive aquaculture settings. Diggles and Oliver (2005), observed Flexibacter/Cytophaga-like rods bacteria in the epithelium of the foot and epipodium of pāua. Diggles et al. (2002a) reported pustule disease caused by *Vibrio* spp. bacteria. *Vibrio* species are commonly associated with moribund abalone. Infection with *V. harveyi* is marked by tissue inflammation generally leading to the formation of pustules that are analogous to vertebrate abscesses. In organized lesions (such as foot muscle abscess), a large number of live and necrotic haemocytes are often seen to accumulate, and many bacteria are surrounded by a well-developed haemocyte response. *V. harveyi* and *V. splendidus* have been observed to pose a significant risk to other cultured mollusc species in New Zealand (Webb, 2013). Diggles et al. (2002a) also reported *Flavobacterium*-like gliding bacteria in shell, epipodium, mantle and foot of juvenile abalone. Abalone also exhibit a fungal shell mycosis (Diggles et al., 2002a; Grindley et al., 1998) as well as the shell boring spionid mud worms *Polydora* spp. and *Boccardia* spp. (Bower, 2006b; Diggles et al., 2002a) that can be a problem in the culture of abalone. Severe cases of mud worm can cause significant shell embrittlement (Webb, pers. obs.). In addition to damaging the shell, it can also cause a deterioration of health: *H. iris* infected with *Polydora hoplura* can be underweight and produce abnormal deposits of conchiolin (Diggles & Oliver, 2005). Diggles and Oliver (2005) reported haplosporidia, epithelial erosion, rickettsial inclusions in the gut, coccidian-like protozoa in foot epithelium, bacterial infection (Bower, 2006a), non-specific necrosis, granuloma-like lesions, haemocytic neoplasia like inflammation and gregarines (apicomplexans) in *H. iris*. In New Zealand,

Diggles et al. (2002a) mentioned that except for one type of abalone disease known to affect brown lesions within the abalone shell and cause death in severe cases, there is not much research on abalone diseases. The disease can also have detrimental effects on economic value as it can cause damage to the shells (Grindley et al., 1998), rendering them unsuitable for decorative purposes.

Perkinsus olseni (protozoan parasite) has been a notifiable species to the World Organisation for Animal Health (OIE, 2019a). From the top of the South Island, *P. olseni* has been reported in *H. iris* (OIE, 2017). Although *P. olseni* has now been confirmed in *H. iris*, there is no detailed information about *P. olseni* in this species. To fill up this knowledge gap, infection with *P. olseni* and other parasites in *H. iris* is described in Chapter 2 which is the first detailed description of *P. olseni* along with other pathogens and parasites in New Zealand black-footed abalone. While the New Zealand abalone aquaculture industry is relatively free of dangerous parasites and pathogens compared to other countries, *Perkinsus* spp. has potential disease risks that need to be monitored and managed.

1.1.5 Summer mortality events and host-pathogen-environment interactions in aquaculture species

In some seasons, pathogen and parasite loads can be extremely high, especially in summer with high temperatures, which can cause massive mortalities. Summer mortality events are often associated with various types of pathogens, such as viruses (e.g., *Ostreid herpesvirus 1*) (Alfaro et al., 2018; Nguyen et al., 2018a), bacteria (e.g., *Vibrio* spp.) (Allam & Raftos, 2015), and parasites (e.g., protozoans) (Lane et al., 2016). Effects due to rising water temperatures have been reported in New Zealand Greenshell™ mussels (*P. canaliculus*), where mortalities on mussel farms (Nguyen & Alfaro, 2020) and alterations in energy and immune-related metabolic pathways were highlighted in unhealthy mussels (Li et al., 2020).

Summer mortality events are a consequence of complex interactions between pathogens and environmental factors and often are associated with temperature increases (Berthelin et al., 2000) and reproductive cycles (Cheyney et al., 1998). The rise of water temperature in the summer season may be responsible for bacterial proliferation in the water, and bacterial accumulation in the tissues, leading to stress (Mitta et al., 2000), disease and mortality (Gagnaire et al., 2007). Multiple factors, including infections of microbes and parasites, environmental stressors and imbalanced immune systems are responsible for creating diseases in aquaculture. Disease dynamics are greatly influenced by environmental factors such as elevated temperature, salinity, water quality and hydrodynamic forces; and cultivation practices such as rearing history, rearing systems and farming sites (Alfaro et al., 2018). Since high mortalities of molluscs in both wild harvest and farms have become a frequent phenomenon in

recent years; this knowledge gap remains a big challenge for better understanding the complex host-pathogen-environment interactions during mortality events and transmission of infection to develop the disease management strategies for aquaculture species.

Continuing trends in the environment variables controlled by the global climate change motivates researchers to measure environmental and physiological effects with changes in the host organism and pathogens (Maynard et al., 2016). Changes in the environment can consequence in outcomes that indulge either host or pathogen, increasing or decreasing indigenous infection rates (Danovaro et al., 2011; Burge et al., 2014). High temperature increases pathogenicity of numerous marine pathogens (Burge et al., 2014) through increasing pathogen metabolism and fitness, it's finally leading to higher transmission rates (Karvonen et al., 2010). Temperature is an important factor that affects physiology, behavior and ecology of marine organisms. Initially, as the temperature rises, metabolism and energy consumption usually increase but can eventually kill marine life (Brauko et al., 2020). Therefore, the effects of acute thermal stress on the physiology of mussels have been included in Chapter 6 for better understanding their defence system during summer mortality and evaluating the host-pathogen-environment interactions.

1.1.6 Immunity of aquaculture species

The health of marine organisms is uniquely related to their immediate environments. When conditions become conducive to reproduction, microorganisms are capable of infecting marine life (Ellis, 2001). Due to their filter-feeding behaviour, aquaculture species are constantly being exposed to pathogens and parasites from the surrounding water. Therefore, molluscs can accumulate many pathogens from the surrounding water. For organisms grown in aquaculture environments, they are more likely to come into contact with pathogens, because these "controlled environments" generally promote the growth of pathogens (such as bacteria, viruses, and fungi). However, under normal conditions and good aquaculture practices, marine invertebrates maintain a healthy status by defending themselves against these potential invaders using a repertoire of innate defences (Bachère et al., 2004; Schmitt et al., 2012). To cope with the challenge of the pathogen-rich marine environment, molluscs have evolved both external and internal defence systems. The external defence is made up of several layers of physical or mechanical barriers, including the shell and the mucosal layer. The internal defence mainly depends on the innate immune system which relies primarily on several significant defence processes, including extracellular and intracellular neutralization, melanization, encapsulation, apoptosis, phagocytosis, chemotaxis and recognition (Allam & Raftos, 2015). Immune priming (memory), which affects molluscs, is the ability to store or re-use the information from a

pathogen or parasite encounter to induce an intensified resistance or tolerance to subsequent infections (Lafont et al., 2017). This enhanced immune response may increase with re-exposure and may result in extreme levels of specificity between hosts and pathogens, and thus host protection occurs (Portela et al., 2013). Detailed research is necessary to expand our understanding of the mollusc immune system.

1.1.6.1 Bivalve molluscs immune studies

Bivalves mainly rely on the innate immune system, including cellular and humoral components (Song et al., 2010). Several studies have been conducted to understand the mechanisms involved in the innate immune system of marine bivalves, including mussels (Costa et al., 2009; Coles & Pipe, 1994; Wootton et al., 2003) and oysters (da Silva et al., 2008; Hégaret et al., 2003; Lin et al., 2014), clams (Cima et al., 2000; Matozzo & Bailo, 2015; Munari et al., 2011; Prado- Alvarez et al., 2012). *Perna canaliculus*, which is the most important cultivated aquaculture species in New Zealand. However, there are few studies on *P. canaliculus* immunity and its cellular and molecular pathways in responses to pathogens (Kesarcodi-Watson et al., 2009a; Kesarcodi-Watson et al., 2009b). Since high mortalities of *P. canaliculus* in both hatcheries and commercial farms have become a frequent phenomenon in recent years, there is an urgent need to perform immunological studies of mussels to understand the disease process and consequently the development of management strategies. To fill this knowledge gap, haemocyte immune function and the relationship between thermal stress and immunity of mussels are presented in Chapters 5 and 6 for better understanding their defence system during summer mortality and evaluating the host-pathogen interactions.

1.1.6.2 Gastropod molluscs immune studies

The immune system of gastropods such as abalone consists of the cellular immune system and the humoral response (Hooper et al., 2006). Numerous studies have been performed to understand the mechanisms involved in the innate immune system of abalone. These studies have focused on cell-mediated responses (Cheng, 1981; Martello & Tjeerdema, 2001; Sahaphong et al., 2001; Travers et al., 2008), humoral responses (Cheng, 1981; Vakalia & Benkendorff, 2005), and stress responses (Baldwin et al., 1992; Malham et al., 2003; Ryder et al., 1994). To defend against infections caused by pathogens, most abalone rely on innate immunity (Elvitigala et al., 2013). Observation of the invertebrate immune system offers the possibility of some degree of specificity and memory in the immune strategies of abalone (Rowley & Powell, 2007). Therefore, more in-depth investigations are needed to clarify how the immune system can defend the animal in a pathogen-rich environment.

1.1.7 Overview of haemolymph and haemocytes of molluscs

Haemolymph and the circulating haemocytes are the major components of the immune system and have been the focus of most immunological studies in molluscs. Examples of these studies include many aquaculture species, such as *Mya arenaria* (Beckmann et al., 1992), *Tapes philippinarum* (Cima et al., 2000), *Ruditapes decussatus* (López et al., 1997a), *Saccostrea glomerata* (Aladaileh et al., 2007), *Meretrix lusoria* and *Crassostrea gigas* (Chang et al., 2005).

1.1.7.1 Haemolymph components and their roles

Hemolymph is composed of haemocytes and various humoral defence factors secreted by haemocytes that float in the colourless plasma (Allam & Raftos, 2015; Gosling, 2015). Respiratory pigment usually absences in the haemolymph because its oxygen concentration is equal to or slightly larger than that of seawater (Bayne et al., 1979). The haemolymph is a circulatory fluid that plays various significant roles in bivalve physiology, such as internal defence, gas exchange, osmoregulation, nutrient distribution, waste elimination and hydrostatic pressure, and is used for the structural support of organs including, labial palps, foot and mantle edges (Gosling, 2015).

1.1.7.2 Haemocyte classifications and their functions

Haemocytes are cells circulating in the bloodstream and are primarily responsible for defence against pathogens responses within invertebrate organisms (Karp & Coffaro, 1980). Haemocytes play significant roles in haemocytosis, phagocytosis, nacrezation and encapsulation, but they are also involved in other biological functions, such as wound healing, food digestion and transport of nutrients, gonad resorption, shell formation, and secretion of humoral factors (Allam & Raftos, 2015; Bachere et al., 2015; Grandiosa et al., 2018).

Haemocytes are the principal immuno-effector cells that play a key role in the innate immune system of molluscs. Changes in total haemocyte counts (THC) in haemolymph are an important immunological parameter to evaluate the health state of the host. Alterations in circulating haemocytes have shown a common response of molluscs to infections or diseases (Allam et al., 2000; Jones et al., 1996; Mateo et al., 2009; Nguyen et al., 2018) and environmental stresses (Couch, 1985; Hauton et al., 2000; Wedderburn et al., 2000). Flow cytometry (FCM) analyses in molluscs have focused on the characterization of haemocyte types, response of haemocytes to stress, diseases or toxic agents and diagnosis of diseases (Nguyen & Alfaro, 2019). Assessing health parameters of bivalve haemocytes has become a popular tool in aquaculture-based studies to assess haemocyte cell viability, cell number and the production of reactive oxygen species (ROS) (Nguyen & Alfaro, 2019).

Molluscan haemocytes vary greatly from species to species, and there is currently no unified nomenclature that applies to haemocytes of all aquaculture species. Generally, bivalve haemocytes are divided into two broad categories based on the presence of cytoplasmic granules, including granulocytes and agranulocytes (Cheng & Foley, 1975; Cheng, 1981; Wootton & Pipe, 2003). These cell types have been observed in many bivalve species including the mussels *Dreissena polymorpha*, *Mytilus edulis*, *Anodonta cygnea*, *Perna canaliculus* (Chandurvelan et al., 2013; Giamberini et al., 1996; Pipe et al., 1997; Rolton et al., 2020; Soares-da-Silva et al., 2002), the oyster *Crassostrea gigas* (Allam et al., 2002; Chang et al., 2005), the clams *Ruditapes philippinarum*, *Mercenaria mercenaria*, *Meretrix lusoria* (Allam et al., 2002; Chang et al., 2005) and the peppery furrow shell mollusc *Scrobicularia plana* (Wootton & Pipe, 2003). However, not all haemocyte types are observed in all bivalve species (Hine, 1999). Depending on the granular affinity to specific dyes (acidophilic/eosinophilic, basophilic and neutrophilic granulocytes), granulocytes are further sub-classified into different categories (Bayne et al., 1979; Hine, 1999). Indeed, granulocytes have many cytoplasmic granules and are the most abundant cell type. Conversely, hyalinocytes have few or no granules and have a hyaline (translucent) cytoplasm (Hine, 1999). Hyalinocytes have been divided into two types: small hyalinocytes and large hyalinocytes (Cheng, 1981). Interestingly, granulocytes have been rarely observed in the haemolymph of marine gastropods such as abalone (Hooper et al., 2007; Nakatsugawa et al., 1999; Travers et al., 2008; Zhengli & Handlinger, 2004). The presence of granulocytes in the haemolymph has only been reported in *Haliotis asinina* (Sahaphong et al., 2001). In *Haliotis iris*, two types of haemocytes were identified, including type I (monocyte-like) and type II (lymphocyte-like) cells (Grandiosa et al., 2015). It has been suggested that for the haemocytes of marine gastropods, the usual hyalinocytes and granulocytes classification might not be appropriate (Martello & Tjeerdema, 2001). Haemocytes play an important role and are actively involved in immune defence in innate immune responses within invertebrate organisms. Although as part of the internal innate immune system, haemocytes act as mediators of cellular defences, various active particles in haemolymph secreted by haemocytes are key components of humoral defences (Allam & Raftos, 2015; Song et al., 2010). Therefore, haemocytes are the foundation of the bivalve innate immune system, and haemocyte-mediated immunity is recognized to be the main internal defence mechanism of bivalves (Zannella et al., 2017). In order to gain a deeper understanding of this topic, most studies have used the observation of haemocytes as a technique to investigate molluscan immunity. Haemocyte morphological distinctions are necessary for a better understanding of haemocyte functions and the development of a health assessment system that can be used to evaluate immune parameters of aquaculture species. In this contribution, light microscopical studies were carried out to characterize the haemocytes of *Perna canaliculus*, in

order to establish a novel and complete classification scheme for the haemocytes of this species to better understand the immune functions of aquaculture species (Chapter 5).

1.1.8 Phagocytosis in defence function of molluscs

Haemocytes play a key role in phagocytosis, perhaps the most important mechanism of molluscs to eliminate pathogens, which is the engulfment of foreign particles (e.g., bacteria, algae, cellular debris, protozoan parasites) by haemocytes (Gosling, 2015). Due to the open circulatory system of mollusc, haemocytes are freely circulated, and abundant haemocytes have been found in peripheral compartments; and these peripheral haemocytes can phagocytise foreign particles (Allam & Raftos, 2015). Granulocytes are phagocytic cells, which eliminate foreign microorganisms that invade the haemolymph and tissue (Tame et al., 2015). In granulocytes, high levels of intracellular enzymes associated with immunological activity allow them to kill pathogens after phagocytosis (Gosling, 2015). Phagocytosis is a temperature-dependent process of bivalve molluscs (Oliver & Fisher, 1999) and phagocytosis can be affected by water acidification, increased temperature and changes in salinity (Ellis et al., 2011; Matozzo et al., 2012). The growth and sustainability of the aquaculture industry can be adversely affected by thermal stress and/or high pathogen loads. To address these health threats, it is important to investigate phagocytosis like haemocyte immune function in aquaculture species. Phagocytic activity of mussels (*P. canaliculus*) haemocytes in different seasons is included in Chapter 5 to better understand the haemocyte immune function of the mollusc.

1.1.9 Enzyme activity in defence function of molluscs

Lysosomal enzymes within the haemocytes of molluscs participate in the killing and degradation of phagocytosed materials (Cheng, 1975, 1981). Sometimes, to degrade foreign materials, lysosomal enzymes are released from haemocytes into the plasma or extracellular compartments of other tissues (Mohandas et al., 1985). Acid phosphatase (ACP) is a lysosomal marker enzyme that is detected inside cytoplasmic granules of granulocytes and can be taken as a reliable tool for the biological assessment of heavy metal pollution (Aladaileh et al., 2007; Rajalakshmi & Mohandas, 2005). Phenoloxidase (PO) is a key enzyme involved in melanisation, and also serves as an innate defence mechanism in several bivalves (Gerdol et al., 2018; Vaillant, 2001). The strong activity of PO and its zymogen form, prophenoloxidase (ProPO), has been observed in the haemolymph of different bivalve species (Gerdol et al., 2018). Enzymatic elimination of antigens in marine molluscs occurs through ACP activity and reactive oxygen species (ROS), such as hydrogen peroxide produced by the haemocyte (Tiscar & Mosca, 2004). Temperature and salinity changes can affect bivalve defence mechanisms involving haemocytes that contain hydrolytic enzymes and produce ROS related to the

degradation of pathogens (Donaghy et al., 2012; Gagnaire et al., 2006). Therefore, it is vital to investigate the enzyme activity of haemocytes for understanding the immune responses of the mollusc to pathogens. Research into enzyme activity in defence function of mollusc rarely examines in New Zealand aquaculture species and researchers have not treated this topic in much detail. To fill up the knowledge gap, a detailed study of ACP and PO enzyme activity exposure to endotoxin and acute temperature in defence functions of haemocytes of *Perna canaliculus* was added in Chapter 6 to a better understanding of the mussel immune defence system during acute increases in water temperature.

1.1.10 Immunological tissue responses of molluscs

The inflammatory response after pathogenic infection and/or cell injury is a local defence reaction in host tissues (Cone, 2001). An inflammatory tissue response, such as haemocytosis (abnormally high number of haemocytes), is an attempt to destroy, dilute or isolate the destructive agent and the affected host cells (Sparks, 1972). Accumulation of lipofuscin pigment (ceroid material) or brown material-like immunological tissue responses is caused by nutritional deficiencies, toxicity, or disease in molluscs which are associated with disturbances in the lipid metabolism in several pathological conditions (Zarogian & Yevich, 1993; Webb & Duncan, 2019). However, very few studies have been conducted in New Zealand to evaluate immunological tissue responses associated with pathogens in aquaculture species. To fill this gap, the detailed studies of immunological tissue responses (haemocytosis and brown material/ceroid accumulation) associated with pathogens in abalone, oysters and mussels were included in Chapters 2, 3 and 4.

1.1.11 Techniques and approaches to study shellfish pathology

There are several immunological techniques (e.g., histopathology, haematology, *in situ* hybridization, polymerase chain reaction) and novel approaches (e.g., metabolomics, flow cytometry) that can be applied to diagnose pathogens, investigate host-pathogen interactions and better understand the immune defence system of shellfish. The combination of these techniques is likely to provide more valuable information for elucidating the complex mechanisms of disease progression, and how the immune response deals with pathogens and remediation in aquatic organisms.

Histological techniques (microscopic examination of fixed and stained tissue sections) involve evaluating tissues for determining the prevalence of parasites and the occurrence of pathologies. Moderate to heavy infections with pathogens and parasites are relatively easy to detect by histological techniques. The diagnosis of molluscan diseases has primarily been achieved using

histological methods and transmission electron microscopy (Anderson et al., 1994; Azevedo et al., 1990; Hervio et al., 1996; Howard et al., 2004; Longshaw et al., 2001). Histology provides a large amount of information not only on the general health of a shellfish but also the detection of a wide range of pathogens, lesions associated with the interaction of the pathogen with the immune system of molluscs (Aranguren et al., 2016). However, some parasites are difficult to detect in moderate to light infections and measurement of their prevalence or occurrence does not give a true indication of the health of an organism (Hervio et al., 1996). To solve this problem, histopathological observations can be analysed both quantitatively and semi-quantitatively which are important approaches for the health assessment of individuals and populations of aquatic animals. Pathogens, parasites or tissue inflammation are recorded for intensity or abundance or severity using either quantitative or semi-quantitative scales. Most parasites are counted quantitatively (Chapters 2, 3 & 4). The abundance of *Bonamia ostreae*, *Perkinsus olseni* and apicomplexan parasite X (APX) in flat oysters (*O. chilensis*) and New Zealand Greenshell™ mussels (*P. canaliculus*) was evaluated with semi-quantitative grading scales (Chapters 3 & 4). Tissue inflammation (haemocytosis and ceroid accumulation) and abnormal tissue structures (digestive tubule atrophy and gills pathology) were evaluated using semi-quantitative scales (light, moderate and high). Quantitative histopathological analysis of aquaculture species is a valuable approach for assessing the health of individuals and populations and is often applied to investigate the impacts of disease and parasite infestation in mussels (Robledo et al., 1994; Svärth, 1999), providing direct and reliable evidence of cellular injury and inflammatory responses. To evaluate the intensity of diseases and parasites, and the extent of tissue pathologies, rather than simply prevalence measures, intensity or extent of tissue alteration may more reliably correspond to measures of exposure (Ellis et al., 1998). Tissue appearance (Quick & Mackin, 1971), histological grading (Bowmer et al., 1991), or summation of total parasite load (Wilson-Ormond et al., 2000) are usually considered to better assess the health of sampled populations.

While a considerable amount of information regarding the innate immune system of marine invertebrates has been gathered over the years, there are huge gaps in our knowledge, especially about the detailed mechanisms of action when invertebrates are exposed to pathogens and the development of infections within various tissues. Therefore, it is essential to identify specific infection patterns relating to this disease progression. To fill up the knowledge gap, a modified grading scale for determining *B. ostreae* infection levels of oysters, as well as for providing a method for investigating *B. ostreae* disease progression are introduced in Chapter 3 to clarify host-parasite interactions, disease development and transmission mechanisms.

Molecular-based methods or molecular techniques of polymerase chain reaction (PCR) are more sensitive than light microscopy-based methods (Diggles et al., 2003; da Silva & Villalba,

2004; Flannery et al., 2014). Since, *B. exitiosa* and *B. ostreae* are morphologically similar (Lane et al., 2016), it is difficult to distinguish the two types of *Bonamia* spp. through histology technique. Moreover, Deoxyribonucleic Acid (DNA) sequencing is a reliable method for distinguishing between *Bonamia* species (Cochennec et al., 2000). Therefore, the *Bonamia* species were confirmed as either *B. ostreae* or *B. exitiosa* in New Zealand flat oysters by PCR (Chapter 3).

In situ hybridization (ISH) is an incredible adjunct to traditional histopathology and PCR-based diagnosis techniques and it combines advantages of both (Carnegie et al., 2003). Like traditional histopathology, ISH reveals the location of the infected tissue and the host response and similar to PCR, ISH is specific and highly sensitive. Therefore, successful hybridization of ISH offers a distinct phylogenetic confirmation that a specific pathogen is associated with specific host tissue (Carnegie et al., 2003). Since degraded or non-viable pathogen DNA may create false-positive PCR results and false-negative results, as with histopathology, may occur due to sampling errors (Burreson, 2000), the efficacy of ISH exceeds conventional diagnosis (Carnegie et al., 2003). *Perkinsus* infections in histological sections can be confirmed by ISH analysis of tissues from histological sections (Moss et al., 2006, 2008; Navas, 2008; Ramilo et al., 2015). Moss et al. (2006) confirmed *P. olseni* infection in *Crassostrea ariakensis* using the ISH assay and both ISH and histology analyses helped to diagnose lesions in gills of Chinese oysters for *Perkinsus beihaiensis* infection (Moss et al., 2008). As ISH is a useful species-specific assay that can confirm *P. olseni* detected in the tissues of aquaculture species by histology, we used (included in Chapters 2 and 4) ISH assay for the confirmation of *P. olseni* infections in *H. iris* and *P. canaliculus*, which is the first ISH-confirmed occurrence of *P. olseni* in New Zealand black-footed abalone (Chapter 2).

Various criteria or approaches have been used to categorize haemocytes according to their morphology, cytochemistry, and function (Wang et al., 2012). Multiple studies have used light microscopy (Nakayama, 1997; Wootton et al., 2003) and flow cytometry (Hégaret et al., 2003; Xue et al., 2001) to examine the type, structure and function of bivalve haemocytes (Hine, 1999). A new optimised haemocyte classification scheme for *P. canaliculus* (Chapter 5) was developed using Giemsa-stained hemolymph smears, and *in vitro*, phagocytosis activity assays were applied to measure phagocytosis-like haemocyte immune function.

The occurrence of several enzymes in shellfish haemocytes was demonstrated by different techniques. The staining reactions method is a cytochemical technique carried out for light microscopy to identify the number of enzyme reactive haemocytes. Staining reaction techniques were used to determine a range of enzymes in aquaculture species by Wootton and Pipe (2003), Lopez et al. (1997a), Carballal et al. (1997a). Enzyme staining reaction tests were

applied (Chapter 6) for determining the percentages and localization of two marker enzymes (acid phosphatase and phenoloxidase) in haemocytes of *P. canaliculus*.

Flow cytometry (FCM) is a standard laboratory instrument used for both fundamental and applied research in immunological researches, especially for clinical analyses (Cordier, 1986; Cossarizza et al., 2017; Fleisher & Oliveira, 2019). The application of FCM has been developed to various parameters of molluscan immunology, including cell count and viability, cell types, phagocytosis, oxidative stress, apoptosis, DNA and protein content (Nguyen & Alfaro, 2019). Haemocyte immune functions, involving total haemocyte count (THC), haemocyte viability and reactive oxygen species (ROS) production were investigated by flow cytometry (Chapter 6).

Metabolomics (a biotechnological approach) is the comprehensive analysis of metabolites in biological samples, and it is a rapidly growing field with significant pertinence in aquaculture research, such as larval production, nutrition and diet, disease and immunology and post-harvest quality control (Alfaro & Young, 2018). Metabolomics offers a novel application for understanding endogenous metabolic alterations of organisms in all biological activities organized by disease or environmental agitation (Klassen et al., 2017). Metabolomics is utilized to differentiate endogenous metabolic changes in biological samples under various environmental conditions and biomarkers involved in these processes (Nguyen & Alfaro, 2019). The metabolomics approach has been developed and applied over the past few years in aquaculture species in New Zealand and has become a powerful tool to monitor molluscan health (Alfaro & Young, 2016; Nguyen & Alfaro, 2019; Young et al., 2016). To this end, metabolomics (gas chromatography-mass spectrometry-based) of *P. canaliculus* exposed to endotoxin and acute thermal stressors were applied (Chapter 6) to investigate the changes of metabolites in mussel haemocytes.

1.2 Thesis Aims

This study was conducted to gain information and fill knowledge gaps about the histopathology of New Zealand shellfish and their immune defence system. This thesis aims to assess the health condition of New Zealand aquaculture species and to investigate their defence functions and disease susceptibility/resistance. The thesis objectives are to identify different pathogens and parasites in New Zealand Greenshell™ mussels, New Zealand black-footed abalone/pāua and flat oysters and to evaluate immunological tissue responses associated with pathogens, to understand the patterns of disease progression that may help elucidate host-parasite interactions and transmission of infections, and to investigate the individual and combined effects of acute thermal stress and endotoxin exposure on immunological responses to better understand the

immune defence system. This research will contribute to disease management strategies for the wild and farmed shellfish aquaculture industries in New Zealand and overseas.

1.3 Thesis Structure

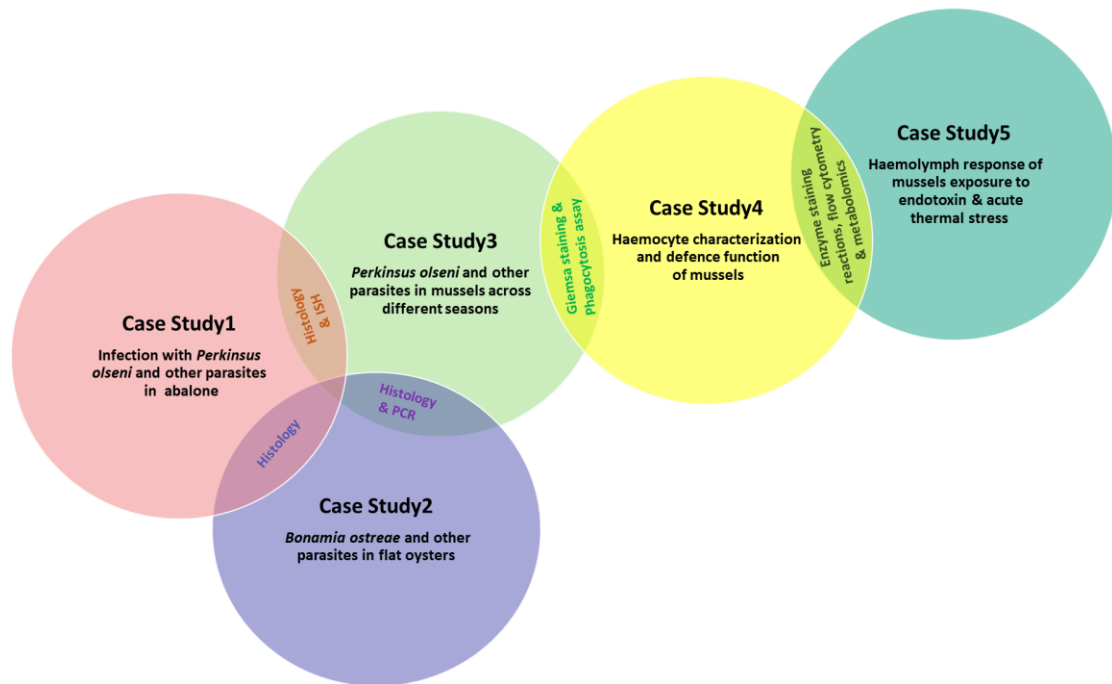


Figure 1. 3 Thesis structure.

To achieve the aims of this thesis, seven chapters are included. Chapters 1 and 7 are the general introduction, and final discussion and conclusions, respectively. Description from Chapter 2 through 6 are as follows:

Chapter 2 (Case study 1): Occurrence of *Perkinsus olsenii* and other parasites in New Zealand black-footed abalone (*Haliotis iris*)

Objectives i) To identify, confirm and characterise the main parasites including *Perkinsus olsenii* of farmed New Zealand black-footed abalone (*Haliotis iris*).

ii) To describe pathological conditions and severity of inflammatory responses such as the proliferation of haemocytes and ceroid material in different tissues of *H. iris*.

iii) To investigate the relationship between the health status (gross appearance of healthy and unhealthy abalone) and the presence or absence of parasites.

Chapter 3 (Case study 2): *Bonamia ostreae* (Haplosporidia) and other parasites in New Zealand flat oysters (*Ostrea chilensis*): a histopathological study

Objectives

i) To determine the presence of *Bonamia ostreae* (and other parasites) in different tissues of New Zealand flat oysters (*Ostrea chilensis*).

ii) To clarify the patterns of disease progression (from a mild infection to a systemic infection) through the individual tissue grading for *B. ostreae* infections within oysters.

Chapter 4 (Case study 3): *Perkinsus olseni* and other parasites and abnormal tissue structures in New Zealand Greenshell™ mussels (*Perna canaliculus*) across different seasons

Objectives

i) To identify the pathogens and parasites and their seasonal variations in New Zealand Greenshell™ mussels through histopathological technique.

ii) To determine the prevalence and abundance of parasites (e.g., *Perkinsus olseni*, APX) in different tissues of mussels across different seasons.

iii) To study inflammatory tissue responses (haemocytosis, ceroid material) and abnormal tissue structures (gill pathology and digestive tubule pathology) of mussels.

Chapter 5 (Case study 4): Characterization of mussel (*Perna canaliculus*) haemocytes and their phagocytic activity across seasons

Objectives

i) To develop a new optimised classification scheme for *Perna canaliculus* haemocytes to assess mussel health.

ii) To quantify different types of haemocytes of mussels and to compare their haemocyte profiles within different levels of *Vibrio*-like bacterial association.

iii) To better understand the immune function of haemocytes in *P. canaliculus* through in vitro phagocytosis activity assays over the seasons.

Chapter 6 (Case study 5): Acute thermal stress and endotoxin exposure modulate metabolism and immunity in marine mussels (*Perna canaliculus*)

Objectives

- i) To identify and determine the percentages of marker enzymes (acid phosphatase and phenoloxidase) in haemocytes of *Perna canaliculus* exposed to two stressors: 1) endotoxin exposure (lipopolysaccharide) and 2) thermal stress (26°C vs 15°C) by enzyme staining reaction tests.
- ii) To study the cell viability, total haemocyte count (THC), reactive oxygen species (ROS) production of *P. canaliculus* exposed to 1) endotoxin exposure (lipopolysaccharide) and 2) thermal stress (26°C vs 15°C) using flow cytometry.
- iii) To inspect the changes of metabolites in haemocytes of *P. canaliculus* exposed to 1) endotoxin exposure (lipopolysaccharide) and 2) thermal stress (26°C vs 15°C) utilizing gas chromatography-mass spectrometry-based metabolomics.
- iv) To investigate the individual and combined effects of acute thermal stress and endotoxin exposure on the survival of *P. canaliculus*.

1.4 Research Outputs

1.4.1 Peer-reviewed papers

Published

1. Muznebin, F., Alfaro, A. C., & Webb, S. C. (2021). Occurrence of *Perkinsus olseni* and other parasites in New Zealand black-footed abalone (*Haliotis iris*). *New Zealand Journal of Marine and Freshwater Research*, 1-21. <https://doi.org/10.1080/00288330.2021.1984950>
2. Muznebin, F., Alfaro, A. C., Webb, S. C., & Merien, F. (2022). Characterization of mussel (*Perna canaliculus*) haemocytes and their phagocytic activity across seasons. *Aquaculture Research*. <https://doi.org/10.1111/are.15926>

Revised

1. Farhana Muznebin, Andrea C. Alfaro, Leonie Venter & Tim Young. Acute thermal stress and endotoxin exposure modulate metabolism and immunity in marine mussels (*Perna canaliculus*). *Journal of Thermal Biology*.

2. Farhana Muznebin, Andrea C. Alfaro & Stephen C. Webb. *Perkinsus olseni* and other parasites in New Zealand Greenshell™ mussels (*Perna canaliculus*) across different seasons. Journal of Aquaculture International.

In preparation

1. Farhana Muznebin, Andrea C. Alfaro, Stephen C. Webb, Anne Rolton & Zoë Hilton. *Bonamia ostreae* (Haplosporidia) and other parasites in New Zealand flat oysters (*Ostrea chilensis*): a histopathological study.

1.4.2 Presentations at Conferences and Symposiums

Poster presentations (first or main author)

1. Muznebin, F., Alfaro, A. C. & Webb, S. C. (2021, September). Occurrence of *Perkinsus olseni* and other parasites in New Zealand black-footed abalone (*Haliotis iris*). Poster session presented at the Physiomar & Australia New Zealand Marine Biotechnology Society Joint Conference, Nelson, New Zealand.

2. Muznebin, F., Alfaro, A. C. & Webb, S. C. (2021, July). Occurrence of *Perkinsus olseni* and other parasites in New Zealand black-footed abalone (*Haliotis iris*). Poster session presented at the New Zealand Marine Sciences Society Conference, Tauranga, New Zealand.

3. Muznebin, F., Alfaro, A. C., Webb, S. C., Rolton, A. & Hilton, Z. (2019, October). Infection intensity and disease progression of *Bonamia* parasites in New Zealand flat oysters (*Ostrea chilensis*). Poster session presented at the New Zealand Society for Parasitology (NZSP) Conference, Dunedin, New Zealand.

4. Muznebin, F. (2019, August). Infection of *Bonamia* parasites in New Zealand flat oysters (*Ostrea chilensis*). Poster session presented at the Auckland University of Technology Postgraduate Research Symposium, Auckland, New Zealand.

5. Muznebin, F., Alfaro, A. C. & Webb, S. C. (2018, October). Parasites and pathogens of cultured pāua (*Haliotis iris*) in New Zealand. Poster session presented at the New Zealand Society for Parasitology Conference, (NZSP) Palmerston North, New Zealand.

Oral presentation (first or main author)

1. Muznebin, F. (2018, August). A histopathological study of New Zealand black-footed abalone (*Haliotis iris*). Paper presented at the Auckland University of Technology Postgraduate Research Symposium, Auckland, New Zealand.

Oral presentation (presented by co-author)

1. Hilton, Z., Rolton, A., **Muznebin, F.**, Webb, S. C., Fidler, A. & Alfaro, A. C (2021, September). The impact of the exotic pathogen *Bonamia ostreae* on the NZ native flat oyster (*Ostrea chilensis*), and potential for selective breeding for resilience. Paper presented at the Physiomar & Australia New Zealand Marine Biotechnology Society Joint Conference, Nelson, New Zealand.

1.4.3 Scholarship/Award/Travel grants

1) April 2017: New Zealand Commonwealth Doctoral Scholarship by New Zealand Ministry of Foreign Affairs and Trade.

2) The best poster presentation award at the New Zealand Society for Parasitology (NZSP) Conference, Dunedin, 2019.

3) Conference grant (500 NZ\$) to attend the New Zealand Society for Parasitology Conference (NZSP), Dunedin, 2019.

4) Conference grant (500 NZ\$) to attend the New Zealand Society for Parasitology Conference, (NZSP) Palmerston North, 2018.

Chapter 2

Occurrence of *Perkinsus olseni* and other parasites in New Zealand black-footed abalone (*Haliotis iris*)



New Zealand black-footed abalone (*Haliotis iris*)

Muznebin, F., Alfaro, A. C., & Webb, S. C. (2021). Occurrence of *Perkinsus olseni* and other parasites in New Zealand black-footed abalone (*Haliotis iris*). *New Zealand Journal of Marine and Freshwater Research*, 1-21.

<https://doi.org/10.1080/00288330.2021.1984950>

Abstract: The culture of endemic New Zealand black-footed abalone (*Haliotis iris*) represents a growing aquaculture industry, which is potentially threatened by pathogens and parasites. To identify and characterise health risks, a targeted sampling event was conducted of healthy- and unhealthy-looking abalone (shell deformities, tissue damage and brown creamy substance/fluid in tissues) at a land-based farm. Histological analysis showed signs of ill health, including disrupted and swollen gills with haemocytosis, ceroid material and parasites, and muscle tissues with focal haemocytosis with parasites. For the first time in *H. iris*, detailed histological observations, followed by confirmatory *in situ* hybridization (ISH) resulted in the identification of *Perkinsus olseni* (5% prevalence). *Scyphidia*-like ciliates (56%), *Sphenophrya*-like ciliates (55%), unidentified disintegrated ciliates (26%), intracellular bacterial microcolonies (IMCs) (9%), apicomplexan-like cells (1%) and bacteria (2%) were also identified across organs. There was a significant association between presence of *P. olseni* and IMCs. Immunological tissue responses (haemocytosis and ceroid material) and gill pathology were evaluated semi-quantitatively, and were significantly associated with *P. olseni*. Gross abalone appearance was also significantly associated with *P. olseni* and unidentified disintegrated ciliates. These findings indicate the types of pathogens and parasites found in cultured *H. iris* for future health assessment studies of this important aquaculture species.

2.1 Introduction

Abalone are haliotid gastropods of increasing importance in the global aquaculture sector. While they are found throughout the world, the New Zealand black-footed abalone (*Haliotis iris*) is endemic to this country. This species supports a growing aquaculture industry (production of 60 mt in 2016/17) as well as commercial and recreational fisheries (Cook, 2019; Diggles et al., 2002a; Reece & Stokes, 2003). Like most wild and cultivated molluscs, abalone are susceptible to pathogens and parasites, but there are few published studies that focus on their characterisation and health effects (Diggles & Oliver, 2005). Of specific concern is a renewed interest in the study of the alveolate protozoan parasite *Perkinsus olseni* and other protozoan parasites that affect wild and cultured abalones (Handler et al., 2006; Liggins & Upston, 2010; Mouton & Gummow, 2011).

Members of the *Perkinsus* genus are well-known causes of disease and production loss in aquaculture across their wide global distribution and host range (Choi & Park, 2010; OIE, 2019b). Seven species of *Perkinsus* are now documented: *P. beihaiensis* (Moss et al., 2008), *P. chesapeakei* (McLaughlin et al., 2000), *P. honshuensis* (Dungan & Reece, 2006), *P. marinus* (Mackin et al., 1950), *P. mediterraneus* (Casas et al., 2008), *P. olseni* (Lester & Davis, 1981) and *P. qugwadii* (Blackbourn et al., 1998). Two species (*P. marinus* and *P. olseni*) are notifiable to the World Organisation for Animal Health (OIE, 2019a). With regard to other abalone species, *P. olseni* has been associated with massive mortalities and significant economic losses in *H. rubra* in NSW, Australia in the 1980s (Liggins & Upston, 2010). *Perkinsus* infections have also been detected in *H. rubra*, *H. laevigata* and *H. cyclobates* in South Australia (Goggin & Lester, 1995). However, information on *P. olseni* in New Zealand is limited, especially with regards to its effects on *H. iris* within wild and cultured populations, which are economically important. To date, *P. olseni* has been reported in bivalves, including the clams *Austrovenus stutchburyi*, *Macomona liliana*, *Barbatia novaezelandia* and *Paphies australis* in northern New Zealand (Diggles et al., 2002a). From the top of the South Island of New Zealand, *P. olseni* has been reported in abalone (*H. iris*), scallops (*Pecten novaezelandiae*) and mussels (*Perna canaliculus*) and confirmed by histopathology and Ray's fluid thioglycollate medium (RFTM) assays (OIE, 2017). Although *P. olseni* has now been reported in *H. iris*, detailed observations and characterisation are lacking, as well as detection and confirmation using species-specific *in situ* hybridisation (ISH) assays.

Previous studies on New Zealand abalone have resulted in the identification of a range of disorders and pathologies. Diggles & Oliver (2005) documented haplosporidia, epithelial erosion, and rickettsia-like organisms (RLOs) (now referred to as intracellular microcolonies of bacteria [IMCs] by Cano et al., 2020) in the gut and protozoa in the foot epithelium of *H. iris*. Diggles and Oliver (2005) also observed mud worms (*Polydora hoplura*), bacterial

infections, non-specific necrosis, abnormal deposits of conchiolin along with shell damage, granuloma-like lesions and haemocytic neoplasia-like cell proliferation and gregarines in *H. iris*. In addition, Diggles et al. (2002a) noted a pustule disease (light coloured, sometimes yellowish pustules or abscesses) caused by *Vibrio* bacteria on the base of the foot of *H. iris*. Shell-related pathologies, include shell-boring spionid mud worms (*Polydora websteri* and *P. hoplura*) and *Boccardia* spp. (*B. acus*, *B. knoxi*, and *B. chilensis*) which are involved in shell blistering (mud blisters), burrows within the shell structure and brittle shell (Diggles et al., 2002a), endobiont sponges and polychaetes (Dunphy & Wells, 2001) and shell mycosis (disease associated with an opportunistic fungal infection) have been observed in *H. iris*, and in some cases result in shell loss (Grindley et al., 1998).

Pathogens and parasites, as well as other foreign agents (e.g., inorganic particles, contaminants), may trigger inflammation processes, which result from the accumulation of large numbers of haemocytes (immune-effector cells) around the damaged or affected areas to destroy or mitigate the intrusion (Darriba Couñago, 2017). Such inflammations have been noticed in tissues of *H. iris* after infection with haplosporidian parasites (Diggles et al., 2002b), and shell lesions (Nollens et al., 2004). Other studies have investigated the inflammation process by characterising the immune response or haemocytosis (high number of haemocytes in tissues) in *H. iris* (Grandiosa et al., 2016; Nollens et al., 2004), but information on this process remains limited. Another inflammatory tissue response is ceroid material accumulation in tissues, which is observed as brownish-yellow pigment caused by nutritional deficiencies, toxicity, or disease stemming from several pathological conditions (Webb & Duncan, 2019; Zaroogian & Yevich, 1993). Although the presence of yellow pigment or ceroid was reported in the oyster *Crassostrea virginica* (Mackin, 1951) and Mediterranean clam *Ruditapes semidecussatus* (Sagrìstà et al., 1995) and Greenshell™ mussel *Perna canaliculus* (Webb & Duncan, 2019), such tissue-specific immune responses are not well-characterised in New Zealand black-footed abalone (*Haliotis iris*). Therefore, characterisation of the immunological tissue responses, which can be useful warning signs for the diagnosis of ill health may require further investigation.

To fill the knowledge gap, a sampling snapshot of healthy- and unhealthy-looking abalone was conducted at one land-based farm to identify, characterise and quantify the main pathogens and parasites and their infections in different tissues of farmed abalone (*H. iris*), using histopathological techniques and ISH assays for confirmation of *P. olseni*. Moreover, the severity of immune host responses, such as haemocytosis and ceroid material accumulation was assessed with regards to pathogen presence. The relationship between the health status (gross appearance of healthy and unhealthy abalone) and the presence or absence of parasites was also investigated.

2.2 Materials and Methods

2.2.1 Sample collection and preparation

A total of 86 adult abalone (shell size ranging from 51 to 97 mm, mean \pm SE of 66.5 \pm 7.0 mm) were collected from Moana Blue Abalone Ltd. (Ruakaka, New Zealand) in August (austral winter season) 2017. The culture water was maintained at a temperature of \pm 15°C, salinity of 35 ppt, pH 8.0, and a dissolved oxygen content above 7.0 mg L⁻¹. Gross appearance (criteria by which live abalone were determined as healthy or unhealthy) of samples showed unhealthy animals (n = 27) with a brown creamy substance or fluid or pustules (Fig. 2.1A), damaged and abnormal tissues or spongy (Fig. 2.1B), nodules (Fig. 2.1C & D), shell deformities (Fig. 2.1E-H), and healthy animals (n = 59) with normal-appearing tissue and shell structures.

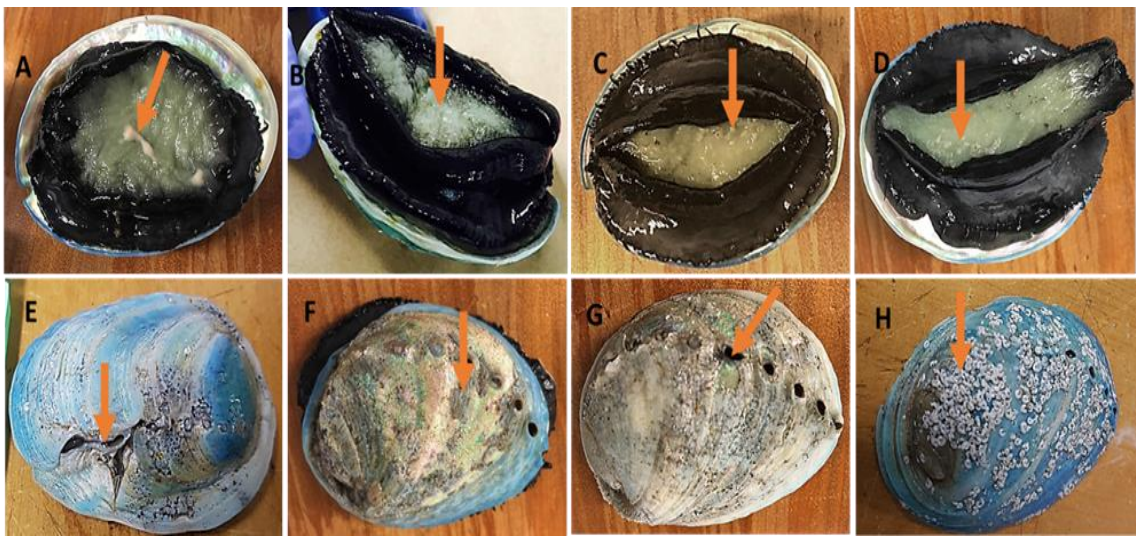


Figure 2.1 Gross appearance of *Haliotis iris* showing (A) brown creamy substance/fluid (pus), (B) abnormal tissue (spongy), (C) and (D) abnormal tissue with nodules on foot, (E)-(G) shell deformities (scars and damage), (H) infestation of spirorbid worms (commensals) on the shell.

All samples were transported to the Auckland University of Technology (AUT) in a container that was kept cool with ice packs that were not in direct contact with the animals.

2.2.2 Histology

On arrival at the AUT laboratory, specimens (86 abalone) were dissected on the same day, and 2–5 mm thick slices containing different tissues and organs (e.g., gills, foot, mantle, gonad, digestive gland, esophageal pouch) were placed in histological cassettes (two cassettes per animal) before fixation (Howard et al., 2004), followed by standard histological processing (OIE, 2016). Samples were fixed in Davidson's solution (48 h), then stored in 70% ethanol and processed for paraffin histology (Luna, 1968). Sections of 5 μ m were obtained using a

microtome. Deparaffinised, 5 µm sections were stained with hematoxylin and eosin (H&E) stains. DPX mountant was used to seal glass coverslips over the sections.

2.2.3 In-situ hybridization (ISH)

ISH was used to corroborate *Perkinsus* infections for the 4 abalone in which *Perkinsus* was encountered during histological assessment. ISH analyses were conducted at the Animal Health Laboratory, Wallaceville, Upper Hutt, New Zealand. Sections of wax-embedded blocks corresponding to histological slides showing *Perkinsus* infections were used for ISH. Tissue sections of 5 µm in thickness, each on silane-prep™ slides (Sigma-Aldrich, France), were dewaxed in two changes of xylene for 5 min and 2 min and rehydrated in a descending alcohol series. Subsequently, the sections were rinsed in distilled water for 1 min and then in phosphate-buffered saline (PBS) for 1 min. The sections were treated with 100 µl proteinase K (concentration of 100 µg/ml) for 15 min at 37°C, washed in 1% glycine in PBS for 5 min and briefly air-dried at room temperature before pre-hybridization. Sections were then incubated at 42°C for 30 min with 100 µl of pre-hybridization buffer containing 10 µl of digoxigenin (DIG)-labelled probes (Eurogentec). A DIG-labelled ISH probe (10µl) was prepared using the DIG PCR probe synthesis kit (Roche). A DIG-labelled probe was generated using the PCR primers Pals140F (5' GAC CGC CTT AAC GGG CCG TGT T 3') and PalsITS-600R (5' GGR CTT GCG AGC ATC CAA AG 3') (Moss et al., 2006). The DIG-labelled probe was used at a concentration of 5 ng/µl. A no-probe control (25 µl of hybridization buffer only) was included with each experiment. Target DNA and DIG-labelled probes were denatured at 95°C for 5 min and the hybridization was carried out overnight at 42°C. The next day sections were washed in 2×SSC at RT (2×5 min), in 0.75×SSC at 42 °C (10 min) and in solution 1 (100 ml maleic acid buffer, 205g NaCl, pH 7.5) for 5 min at RT. Tissues were then blocked for 30 min at RT with 100 µl blocking solution 1. Specifically, bound probe was detected using 100 µl anti DIG conjugate in blocking solution (2 h, RT). Washed with Solution 1, 2×1 min and equilibrated with detection buffer (solution 2) for 2 min at RT. Slides were incubated for 1 h at RT in NBT/BCIP, a chromogenic substrate for alkaline phosphatase, diluted in Solution 2 (100 µl) in the dark by covering humid chamber with foil. The reaction was stopped by rinsed briefly in distilled water (10–15 dips) and briefly in 1×PBS two times. Slides were counterstained for 1 min with Bismarck brown (0.5%), dehydrated with ethanol (96% ethanol 2×1 min and Absolute ethanol 3×15s) and cleared with xylene 3×15s, mounted with a drop of Eukitt resin and cover slipped.

Controls for each *Perkinsus olseni* species-specific probe were tested in the same manner except that they received hybridization buffer lacking probe during the hybridization step. Positive controls were tissue sections from susceptible host (*H. iris*) infected with *P. olseni* and negative controls were no-probe assays.

2.2.4 Microscopic observations

Prepared histological slides were examined under the microscope using 4× and 10× objectives. If any tissue needed to be examined more closely, 40× and 100× objectives were used to identify suspected pathogens and parasites. Images were taken from histological slides using a Leica DM2000 microscope.

2.2.5 Epidemiological parameters and data analysis

Prevalence and mean intensity of pathogens and parasites were calculated according to Bush et al., (1997).

$$\text{Prevalence} = \frac{\text{Number of hosts infected with a particular species}}{\text{Total number of samples examined}} \times 100$$

$$\text{Mean intensity} = \frac{\text{Total number of parasites of a particular species}}{\text{Number of hosts infected with that parasite}}$$

Prevalence was calculated quantitatively as the percentage of the sample population showing a given condition. Mean intensity was calculated quantitatively as the total number of parasites of a particular species in each individual or specified organ or thin section of the entire animal divided by the number of hosts/samples infected with that parasite. Pathogens and parasites, including *Perkinsus olseni*, ciliates (*Scyphidia*-like, *Sphenophrya*-like and unidentified disintegrated) and intracellular microcolonies of bacteria (IMCs) were counted from different tissues (gills, muscle, digestive gland and esophageal pouch) to calculate their prevalence and mean intensity. One histological section per animal was used for histopathological evaluation. Pathogens and parasites were counted across the entire slide after a thorough examination.

Host responses were evaluated semi-quantitatively with a grading scale (light, moderate and heavy) modified from Hine (2002a) representing the severity of inflammation features (haemocytosis and ceroid material) in an animal, organ, tissue or histological section (Table 2.1).

Several tissue conditions were also assessed semi-quantitatively. A grading scale (1-4) was applied for evaluating gill pathology (normal gills without ceroid material and parasites, gills with ceroid material and parasites, disrupted gills with ceroid material and ciliate parasites, and without haemocytosis, and swollen gills with haemocytosis and *Perkinsus*) (Table 2.2).

Table 2.1 Semi-quantitative grading scale for the severity of haemocytes and ceroid material occurrence. See the figures below for visual grading.

Inflammatory lesions	Score	Description
Haemocytosis	1	Light haemocytosis: (H1), few (< 30) haemocytes per field at 40× magnification (Fig. 2.2A)
	2	Moderate haemocytosis: (H2), medium number (31-200) of haemocytes per field at 40× magnification (Fig. 2.2B)
	3	Heavy with diffuse haemocytosis: (H3), haemocytes (> 200-500 per field at 40× magnification) are distributed broadly over a large section of tissue without a clear centre or focal point of highest haemocyte concentration (Fig. 2.2C)
	4	Heavy with focal haemocytosis: (H4), a more intense type of haemocytosis with marked centres or focal points of haemocyte (>500 per field at 40× magnification) concentration (Fig. 2.2D)
Ceroid material	1	Light ceroid material: (C1), low concentration of ceroid material (Fig. 2.3A)
	2	Moderate ceroid material: (C2), medium concentration of ceroid material (Fig. 2.3B)
	3	Heavy occurrence of ceroid material: (C3), (Fig. 2.3C)

Table 2. 2 Grading scale for gill pathology.

Score	Description
1	Normal gills without ceroid material and parasites (G1) (Fig. 2.4A)
2	Gills with ceroid material and ciliate parasites (G2) (Fig. 2.4B)
3	Disrupted (showing areas of destruction) gills with ceroid material and ciliate parasites, and without haemocytosis (G3) (Fig. 2.4C)
4	Swollen gills with haemocytosis and <i>Perkinsus olseni</i> (G4) (Fig. 2.4D)

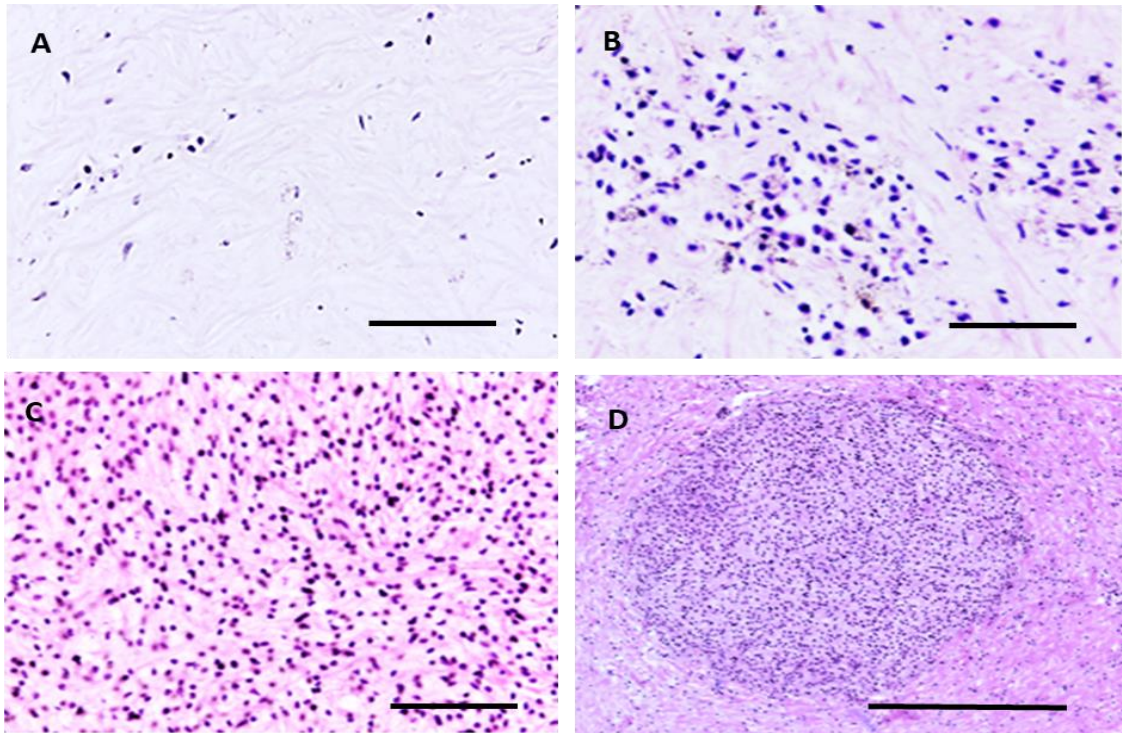


Figure 2.2 Grading scale for the occurrence of haemocytes in muscle tissues according to Table 2.1 (A) grade 1-light haemocytosis (H1), (B) grade 2-moderate haemocytosis (H2), (C) grade 3-heavy with diffuse haemocytosis (H3) and (D) grade 4- heavy with focal haemocytosis (H4). Scale bars in (A-C) = 30 μ m and in (D) = 25 μ m.

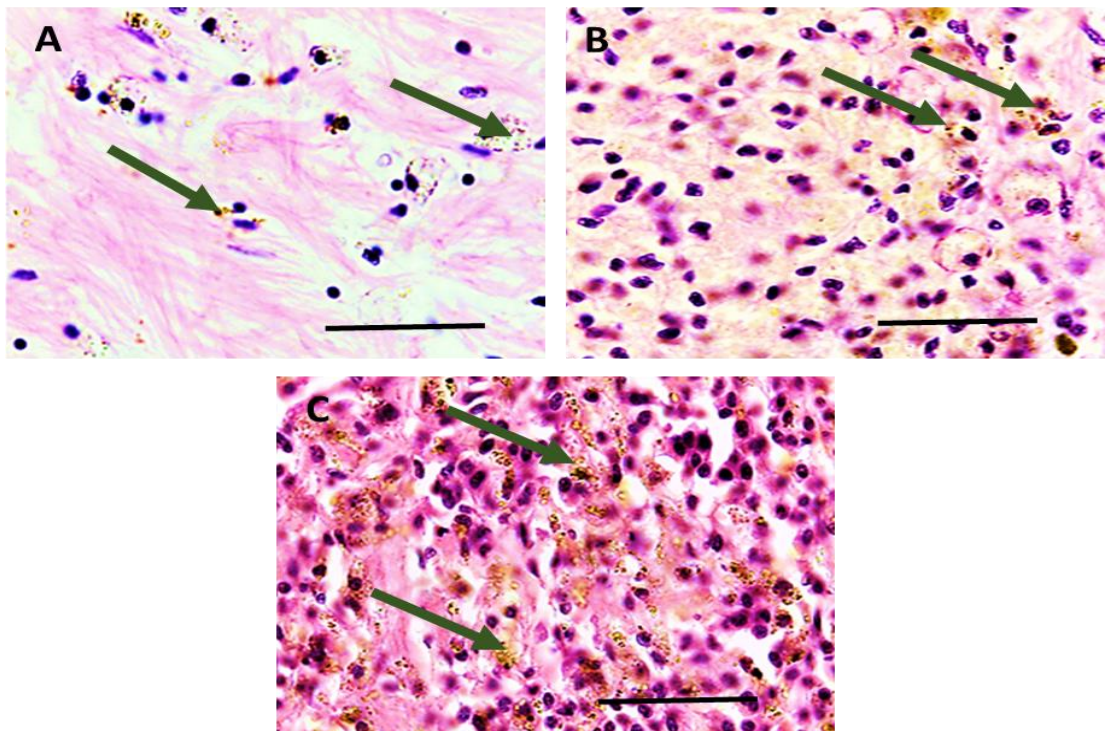


Figure 2.3 Grading scale for the occurrence of ceroid material (arrows) in muscle tissues according to Table 2.1 (A) grade 1-light ceroid material (C1), (B) grade 2-moderate ceroid material (C2) and (C) grade 3-heavy ceroid material (C3). Scale bars = 30 μ m.

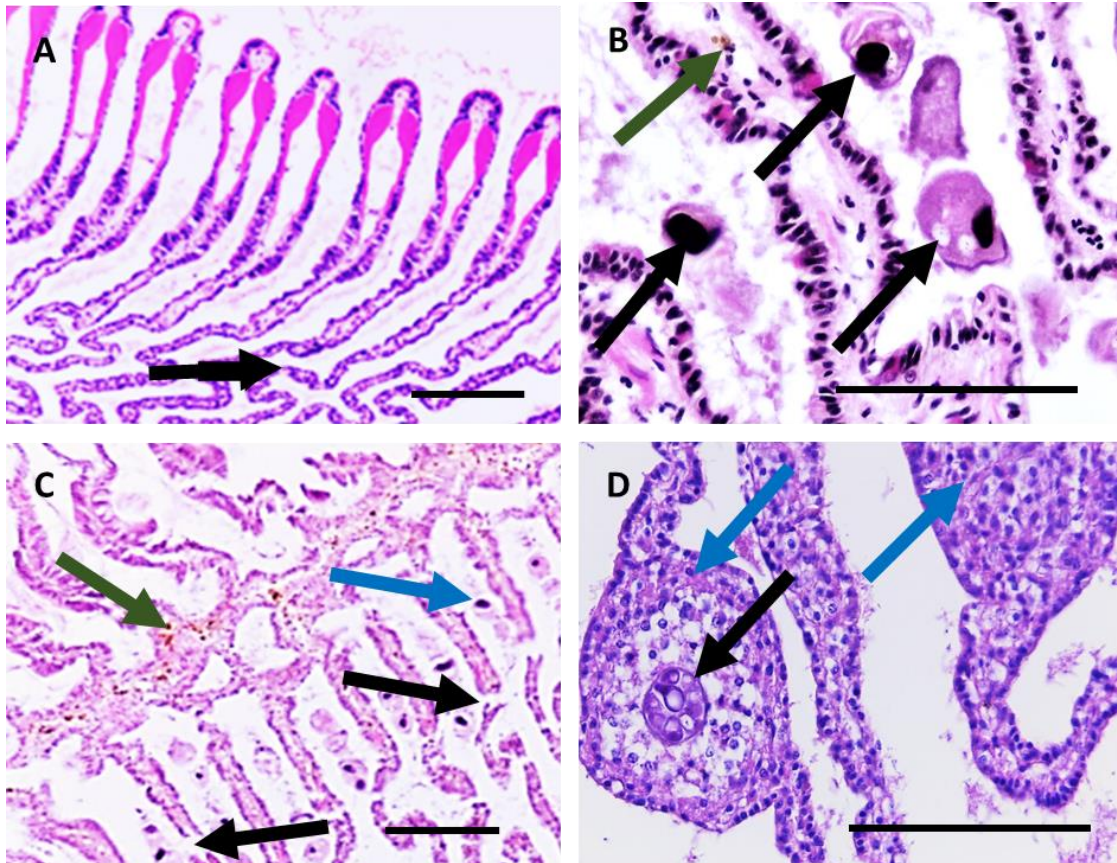


Figure 2.4 Grading scale for gill pathology according to Table 2.2 (A) grade 1- normal without ceroid material and parasites (G1), (B) grade 2- gills with ceroid material (green arrow) and ciliate parasites (black arrows) (G2), (C) grade 3- disrupted (showing areas of destruction) gills (black arrows) with ceroid materials (green arrow) and ciliate parasites (blue arrow), and without haemocytosis (G3) and (D) grade 4- swollen gills with haemocytosis (blue arrows) and *Perkinsus olseni* (black arrow) (G4). Scale bars = 30 µm.

2.2.6 Statistical analyses

Chi-square tests were used to identify associations between the health status (gross appearance of healthy and unhealthy abalone) and presence or absence of parasites, and the association between pathogens/parasites and presence or absence of *P. olseni*. These tests were performed using IBM's SPSS Statistics software (version 23).

2.3 Results

2.3.1 Prevalence and mean intensity of pathogens and parasites

A number of pathogens and parasites, including *Perkinsus olseni*, *Scyphidia*-like ciliates, *Sphenophrya*-like ciliates, unidentified disintegrating (dead/dying) ciliates, intracellular microcolonies of bacteria (IMCs), apicomplexan-like cells and bacteria were observed in different tissues and organs (Table 2.3) of 86 abalone. Prevalence and mean intensity of

parasites varied greatly from one host organ to another (Table 2.4). Since this mean intensity is only from a part of the surveyed individual, organ or tissue, it is, therefore, indicative and comparative rather than an absolute value. *Sphenophrya*-like ciliates and *Scyphidia*-like ciliates had the highest overall prevalence (55 and 56%, respectively) and mean intensity (39 ± 3.8 and 30 ± 2.8 , respectively), and infected host number ($n = 47$ and 48 , respectively) and were observed in gills (infected host number = 42 and 44 , respectively), oesophageal pouch (infected host number = 5 and 7 , respectively), and muscle tissues (infected host number = 4 and 5 , respectively). The prevalence, mean intensity of abalone infected with *P. olseni* was 5% ($n = 4$) and 18.5 ± 0.6 , respectively, and these protozoa were distributed in a variety of organs, but mainly in gills (infected host number = 2) and foot muscle (infected host number = 3).

Dead/dying ciliates had a prevalence and mean intensity of 26% ($n = 22$) and 3.5 ± 0.2 , respectively, and were noted in gills (infected host number = 19), oesophageal pouch (infected host number = 3), and muscle tissues (infected host number = 1). Their poor condition rendered them unidentifiable. Unidentified structures appearing in vacuoles within the intestinal epithelium that could correspond to apicomplexan-like were also found with a prevalence of only 1%. Intracellular microcolonies of bacteria (IMCs) (prevalence of 9%, $n = 8$ and mean intensity of 21.3 ± 1.0) were observed in a variety of organs, such as gills (infected host number = 1), muscle (infected host number = 1), digestive gland (infected host number = 5) and the oesophageal pouch (infected host number = 3) of abalone.

A Chi-square test indicated a significant association ($p = 0.042$) between abalone infected with *P. olseni* and IMCs (Table 2.A.1 in the Appendix). Rod-shaped bacteria (2%) commonly occurred on epithelial surfaces of gills, mantle cavity, and organ surfaces within the body cavity.

Table 2.3 Overall prevalence and mean intensity (\pm SE) index of parasites in abalone.

Parasite type	Prevalence %	Mean intensity \pm SE
<i>Perkinsus olseni</i>	5%	18.5 ± 0.6
<i>Scyphidia</i> ciliates	56%	30 ± 2.8
<i>Sphenophrya</i> ciliates	55%	39 ± 3.8
Unidentified disintegrated ciliates	26%	3.5 ± 0.2
Intracellular microcolonies of bacteria (IMCs)	9%	21.3 ± 1.0

Table 2.4 Prevalence and mean intensity (\pm SE) of parasites in different tissues and organs of abalone.

Parasite type	Organ names							
	Gills		Muscle		Digestive gland		Esophageal pouch	
	Prevalence %	Mean intensity \pm SE	Prevalence %	Mean intensity \pm SE	Prevalence %	Mean intensity \pm SE	Prevalence %	Mean intensity \pm SE
<i>Perkinsus olseni</i>	2.33 %	8 \pm 0.2	3.5 %	19.3 \pm 0.5	0 %	0 \pm 0	0 %	0 \pm 0
<i>Scyphidia</i> ciliates	51.2 %	28.3 \pm 2.6	5.8 %	3.4 \pm 0.1	0 %	0 \pm 0	8.1 %	26 \pm 1.1
<i>Sphenophrya</i> ciliates	50 %	40 \pm 3.4	4.7 %	3 \pm 0.1	0 %	0 \pm 0	5.8 %	22 \pm 0.6
Unidentified disintegrated ciliates	22.1 %	4 \pm 0.2	1.2 %	1 \pm 0.01	0 %	0 \pm 0	3.5 %	3 \pm 0.1
Intracellular microcolonies of bacteria	1.2 %	45 \pm 0.5	1.2 %	3 \pm 0.04	5.8 %	14.4 \pm 0.4	2.3 %	25 \pm 0.4

2.3.2 Observations of pathogens and parasites

2.3.2.1 *Perkinsus olseni*

Perkinsus olseni (Fig. 2.5A-D) is a dinoflagellate-like protozoan parasite. *Perkinsus* trophozoites commonly occur in gills, digestive glands, mantle and gonadal connective tissues. Single or multiple trophozoites (Fig. 2.5A-D) of *P. olseni* were observed in the swollen (swelling consists mostly of haemocytes) blood space of gills and the connective tissues of mantle tissues of *H. iris*. Spherical trophozoites (8–13 μ m diameter) exhibited the characteristic signet ring shape with an eccentric nucleus and a large vacuole occupying most cytoplasm and containing vacuoplast (Fig. 2.5A-D). Trophozoites were also observed as a cluster of cells of up to 10-20 sibling daughter cells that stay together in a rosette-like arrangement inside a wall (Fig. 2.5C & D).

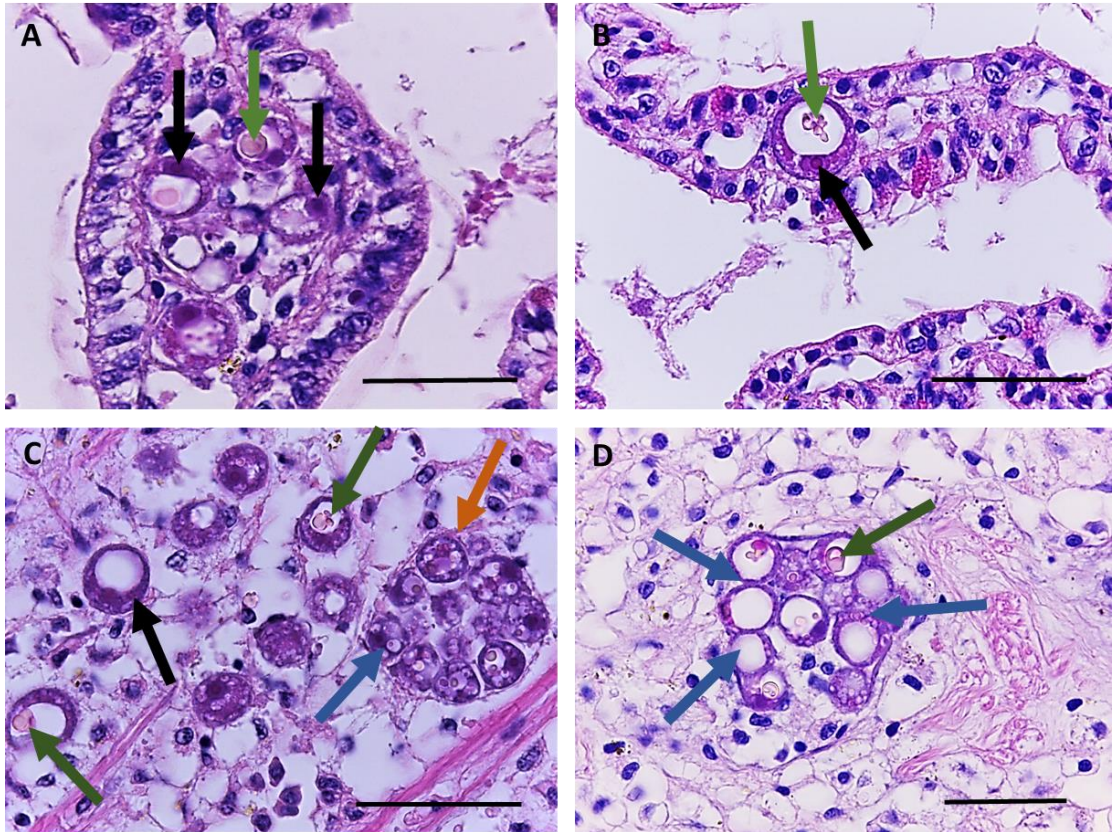


Figure 2.5 *Perkinsus olseni* in histological sections from infected abalone (*H. iris*) gills and mantle tissue, (A) vacuolated signet-ring trophozoite of *P. olseni* with eccentric prominent nuclei (black arrows) inside swollen gill, (B) single vacuolated signet-ring trophozoite (black arrow) of *P. olseni* with prominent eccentric nucleus and a large vacuole containing vacuoplast (green arrow) inside swollen gill, (C) and (D) vacuolated (containing vacuoplast) (green arrows) sibling daughter trophozoites (blue arrows) of *P. olseni* and trophozoite stage with rosette-like arrangement (orange arrow) inside a wall in mantle tissue. Scale bars = 20 μm .

2.3.2.2 Specificity test of *Perkinsus olseni* by ISH

The digoxigenin-labelled probes (species-specific ISH assay) demonstrated hybridization to *P. olseni* cells in all the tissue sections (gills, mantle and foot) as blue staining (Fig. 2.6A & B) and all controls performed as expected. No hybridization of parasite cells of other species was observed. No probe labelling was detected within slides that had been incubated either in the absence of the probe nor from the negative control tissue sections (Fig. not shown).

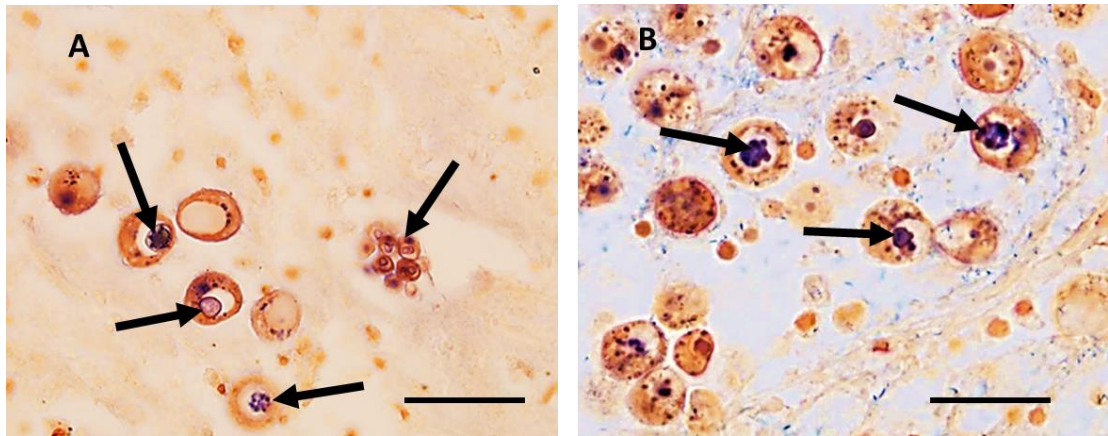


Figure 2.6 (A) and (B) *In situ* hybridization detection (blue staining) (black arrows) of *P. olseni* vegetative cells in tissue sections of *H. iris*. Scale bars = 20 μ m.

2.3.2.3 Ciliates

Sphenophrya-like and *Scyphidia*-like free-living ectocommensal ciliates (Fig. 2.7A & B) were found in gills, oesophageal pouch, and muscle tissues of abalone. Large numbers of ciliates appear without any adverse effect on the host, and there are no reports of mortalities associated with this type of infection. Dead/dying ciliates, were noted (Fig. 2.7C & D) in gills, oesophageal pouch, and muscle tissues, whose poor condition (including disintegration of nuclei) rendered them unidentifiable. Such ciliate mortalities have not previously been seen in other abalone health surveys where many ciliate infections have been encountered. The cause for this is unclear. A host response seems unlikely as the ciliates occur externally to the gill epithelium and there is no evidence of elevated haemocyte numbers in the gill cavity or clustering around the ciliates.

2.3.2.4 Apicomplexan-like

Unidentified apicomplexan-like structures were observed in vacuoles within the intestinal epithelium that (Fig. 2.7G) seem to have an insignificant pathological effect.

2.3.2.5 Intracellular microcolonies of bacteria (IMCs)

Intracellular microcolonies of bacteria (IMCs) (Fig. 2.7E & F) are usually observed as colonies or cysts. Intracellular microcolonies of bacteria (IMCs) were found in a variety of organs, such as gills, muscles, and the oesophageal pouch of abalones.

2.3.2.6 Rod-shaped bacteria

Bacteria other than (IMCs) (Fig. 2.7H) are Gram-negative curved rod-shaped bacteria. Rod-shaped bacteria commonly occur on epithelial surfaces of gills, mantle cavity, and organ

surfaces within the body cavity. In this study, the presence of bacteria appears of insignificant pathological importance on individual unhealthy (decaying) abalones.

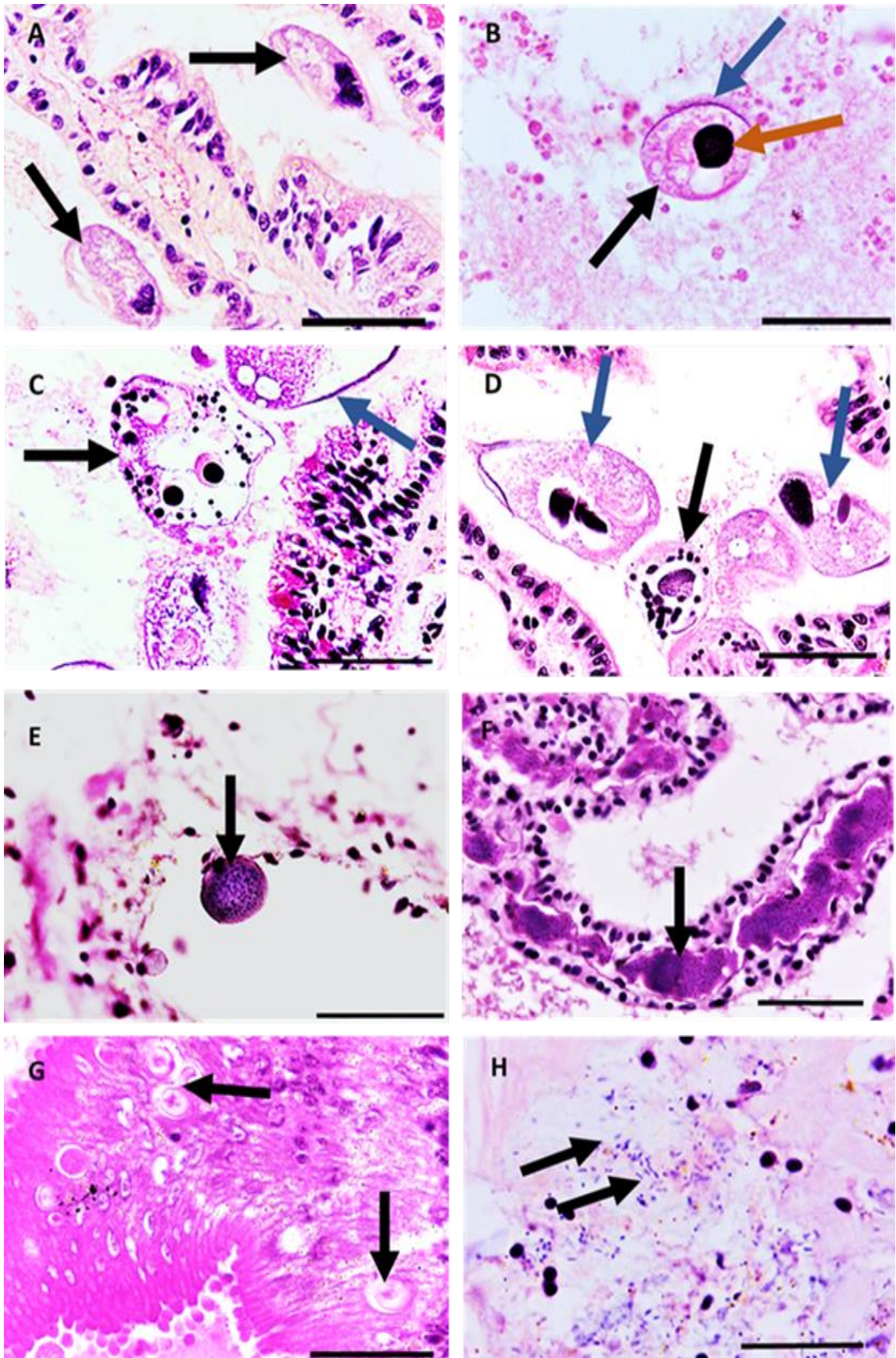


Figure 2.7 Parasites and pathogens in different organs in abalone (*H. iris*), (A) elongated pear-shaped *Sphenophrya*-like ciliates (black arrows) in the gills, (B) ovoid or spherical shaped *Scyphidia*-like ciliates (black arrow) with a conspicuous brush-like adhesive disc or scopula (blue arrow) and a dark macronucleus (orange arrow), (C) and (D) unidentified disintegrated ciliate (black arrows) and *Sphenophrya*-like ciliates (blue arrows) in the gills, (E) intracellular microcolonies of bacteria (IMCs) (black arrow) in the muscle, (F) intracellular microcolonies of bacteria (IMCs) (black arrow) in the gill blood spaces, (G) unidentified apicomplexan-like structures appearing in vacuoles within the intestinal epithelium (black arrows) inside digestive epithelium, (H) Bacteria (rod-shaped) in foot muscle tissue. Scale bars = 40 μ m.

2.3.3 Severity of immunological tissue responses

2.3.3.1 Haemocytes in muscle tissues

Most abalone showed severity 3 (Heavy and diffuse) haemocyte infiltration (n = 55, occurrence rate of 64%), and the smallest number of abalone samples showed severity 1 (Light) haemocyte infiltration (n = 11, occurrence rate of 13%). On the other hand, 36 samples showed severity 2 (Moderate) and 26 samples showed severity 4 (Heavy with focal haemocytosis) haemocyte infiltration and the occurrence rates were 42% (n = 36) and 30% (n = 26), respectively. In heavy infections, abalone tissues were congested with *Perkinsus olseni* and haemocytosis showing focal inflammation where large numbers of haemocytes surrounded the trophozoites (Fig. 2.8A).

2.3.3.2 Ceroid infiltration in different organs

Ceroid infiltrations across tissues/organs were often associated with *P. olseni*, and ceroid material accumulation was evident as brown material in pathogen-associated tissues (Fig. 2.8B). Therefore, ceroid could be a warning for the presence of *P. olseni* or other pathogens and parasites. In the foot muscle, most abalone (33%) had severity 2 (Moderate) ceroid concentration, followed by severity 1 (Light) at 24% and severity 3 (Heavy) at a 12% occurrence rate. In gills, 42% of abalone showed severity 1 (Light) ceroid concentration, whereas 7% and 1.2% had ceroid concentrations at severity 2 (Moderate) and 3 (Heavy), respectively.

2.3.3.3 Pathological condition of gills of abalone

Parasites were often associated with tissue haemocytosis and elevated levels of ceroid material. Indeed, 4 abalone (5%) showed swollen gills with ceroid material, haemocytosis and *Perkinsus* (grade 4) and 31 abalone (36%) had gills with ceroid material and ciliate parasites (grade 2). Another 8 abalone (9%) had disrupted gills (showing areas of destruction) with ceroid material and without haemocytosis (grade 3). A significant association between *P. olseni* and swollen gills with

ceroid material and haemocytosis (grade 4) was observed ($p = 0.032$) (Table 2.A.2 in the Appendix).

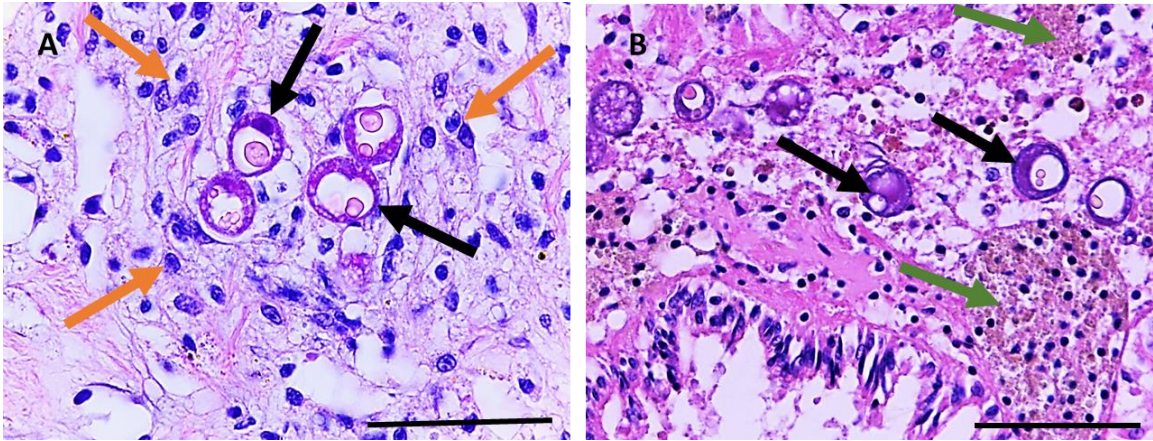


Figure 2.8 Immunological tissue responses (haemocytosis and ceroid material) and *Perkinsus olseni* in abalone tissues, (A) inflammatory lesion showing haemocytosis (orange arrows) surrounding *P. olseni* (black arrows) in muscle tissue, (B) inflammatory lesion showing ceroid material (green arrows) in mantle connective tissues near *P. olseni* (black arrows). Scale bars = 30 μm .

2.3.4 Gross appearance of the samples and the occurrence of parasites

A total of 34 abalone (40%) had no parasites, and 27 of these were from the healthy and 7 from the unhealthy samples as identified by gross examination. Of the remaining 52 abalone (60%), which had at least one individual parasite type, 32 were from the healthy samples and 20 were from the unhealthy samples. *P. olseni* was identified in 5% ($n = 4$) of the unhealthy samples. No trace of *P. olseni* was observed in the healthy-appearing samples. A Chi-square test indicated a significant association (p -value = 0.008) between the gross appearance (healthy and unhealthy) of abalone and the presence or absence of *P. olseni* (Table 2.A.3 in the Appendix). A significant association ($p = 0.024$) was found between the unhealthy gross appearance (pustules) of abalone and the presence or absence of *P. olseni* (Chi-square test) (Table 2.A.4 in the Appendix). A Chi-square test also indicated a significant association ($p = 0.001$) between the unhealthy gross appearance (nodules) of abalone and the presence or absence of *P. olseni* (Table 2.A.4 in the Appendix). The gross appearance was also significantly associated with the presence or absence of unidentified disintegrated ciliates ($p = 0.036$) (Table 2.A.5 in the Appendix).

2.4 Discussion

2.4.1 *Perkinsus olseni*

This is the first ISH-confirmed occurrence of *P. olseni* in New Zealand black-footed abalone (*H. iris*), with a detailed histological description of this parasite. In this study, only a few (5%) *H. iris* samples were infected by *P. olseni*. However, a higher prevalence of *P. olseni* in *H. rubra* examined by Lester and Hayward (2005) at Taylor Island, South Australia, ranged from 19 to 68% in three different samples. Lester et al. (2001) noted that infections of *P. olseni* in wild *H. rubra* were positively correlated with increasing water temperature. The lower prevalence of *P. olseni* in the present study may be related to the fact that sampling was conducted in the austral winter season. Therefore, it is important to monitor *P. olseni* infection continuously throughout all seasons, especially in summer, to better understand the susceptibility of *H. iris* to this parasite.

Spherical *P. olseni* trophozoites with an eccentric nucleus and a large vacuole were found in the blood spaces of gills and the connective tissues of the foot muscle of four *H. iris*. Lester and Davis (1981) also observed similar trophozoites of *P. olseni* in *H. rubra*. In this study, there was a significant association between *P. olseni* and swollen gills with ceroid material and haemocytosis. This result is in agreement with the findings of Choi and Park (1997, 2010), Park et al. (1999), Park and Choi (2001), who described similar inflammatory responses due to *Perkinsus* infections. According to Dungan et al. (2007), *P. olseni* induced a strong host response with infiltration of numerous haemocytes in the surrounding tissue and the trophozoite stage occurring in the tissues of the New Zealand clam *Austrovenus stutchburyi*. Although the potential *P. olseni* infection was accompanied by inflammatory tissue responses (large numbers of haemocytes surrounding the trophozoites), mortalities due to this parasite were not assessed in this study. Lesions were relatively scarce among histological sections from our sampled abalone. However, Dungan et al. (2007) reported a wide range of histological lesions, including both light infections and intense systemic infections of *P. olseni* in clams (*A. stutchburyi*). Moreover, heavy infection with *P. olseni* in Manila clams often results in tissue inflammation, reduced growth and impaired reproduction (Pretto et al., 2014). Liggins and Upston (2010), reported that in the abalone *Haliotis rubra* with heavy infection of *P. olseni*, there was evidence of substantial tissue and organ impairment, including tissue necrosis, damage of normal tissue structure, necrosis of gills due to the inadequate blood supply, and significant accumulation and infiltration of haemocytes into tissues. According to Goggin and Lester (1995), 30-40% mortality occurred in abalone infected by *P. olseni* in Australia, which highlights a potential risk for *H. iris* in New Zealand.

In this study, *Perkinsus*-infected abalone showed a brown fluid (pus) and nodules in their foot and mantle. Bower (2010), also reported a similar characteristic on the foot and mantle of abalone infected with *P. olseni*. *P. olseni* was only detected in abalone deemed unhealthy (presence of pustules and nodules) by gross appearance, with a significant association between abalone health status and the presence or absence of *P. olseni*. A significant association was also found between the abalone gross appearance (healthy and unhealthy) and the presence or absence of unidentified disintegrated ciliates, which were also present around the visible ulcers/pustules that were attributed to *P. olseni* infection. These findings suggest that there is a close relationship between the health status of abalone and the presence or absence of parasites which may assist with identifying and characterising abalone health risks.

2.4.2 Other pathogens and parasites

The most common parasites in *H. iris* were ciliates (*Scyphidia*-like and *Sphenophrya*-like). According to Diggles and Oliver (2005), *Sphenophrya*-like ectocommensal ciliates are particularly common in larger and older farmed abalone. In this study, ciliates (*Scyphidia*-like and *Sphenophrya*-like) were observed in gills, oesophageal pouch, and muscle tissues of abalone and the highest prevalence of ciliates were recorded in the gills. This finding supports the results of Diggles and Oliver (2005), who noted that *Sphenophrya*-like ciliates are usually found living free between gill lamellae. According to Bower et al. (1994), ciliates lie on or in-between the gill lamellae, mantle cavity or esophageal pouch epithelium and appear in large numbers without any adverse effect on the host. Interestingly, we also observed unidentified disintegrated (dead/dying) ciliates in different organs of abalone whose poor condition rendered them unidentifiable. This has not previously been reported in ciliates associated with *H. iris*. This finding suggests that something might be killing the ciliates. Therefore, further investigation might help to reveal insights into control for ciliates.

Intracellular microcolonies of bacteria (IMCs) were observed in a variety of organs, such as gills, muscle, digestive gland, and the oesophageal pouch of abalone with a significant association between the presence of *P. olseni* and IMCs. Mouton and Gummow (2011) also found IMCs in digestive glands and suggested that IMCs were the most common parasite of abalone. Intracellular bacteria are associated with intracellular microcolonies of bacteria causing infection in marine molluscs (Cano et al., 2020). Infection with IMCs in abalone is usually light and not associated with a disease (Diggles & Oliver, 2005). In contrast, IMCs infections directly or indirectly linked with mortality have been noted in the abalone *Haliotis rufescens* (Moore et al., 2000). Moreover,

the IMCs-*Candidatus Xenohalotis californiensis*, the causative agent of the withering syndrome in black abalone (*Haliotis cracherodii*) is associated with mortalities up to 100% (Friedman et al., 1997; Moore et al., 2000). According to Cruz-Flores and Cáceres-Martínez (2020), temperature, host-susceptibility and pathogen-specificity can affect the proliferation of the IMCs and contribute to mortality in abalone *Haliotis corrugata*. Therefore, IMCs could become a disease threat if abalone are subjected to environmental challenges, high prevalence, and overcrowded culturing conditions.

Apicomplexan-like cells were detected in the intestinal epithelium of one abalone individual in this study. Apicomplexan-like structures were also reported in *H. iris* previously in the epithelium of the esophageal pouch (Diggles & Oliver, 2005).

Rod-shaped bacteria in the tissues of abalones were seen in this study. Handler et al. (2005) indicated that abalone mortalities were associated with bacterial infections, and higher mortalities were noted at higher temperatures. However, very few abalone samples were seen infected with this type of bacteria in the current study. The reason behind this observed low infection may be due to the limitations of H&E histology for bacterial detection, quantification and identification.

2.4.3 Immunological tissue responses

Haemocytosis was characterised as diffuse and focal inflammation in *H. iris* tissues. In this study, the accumulation of haemocytosis with focal inflammation was observed when large numbers of haemocytes surrounded *P. olseni* and sometimes also in foci with no *Perkinsus* cells. Similar haemocytosis was reported by other researchers in bivalves and indicated that diffuse haemocytosis is distinguished from focal haemocytosis when haemocytes are distributed broadly over a large section of tissue without a clear centre or focal point of highest haemocyte concentration (Kim et al., 2006; Kim & Powell, 2004, 2007; Villalba et al., 1997). Findings by Elston et al. (1992), McGladdery et al. (1993) and Smith and Conroy (1992) also support the results in the present study with their observations of intense haemocytic inflammatory lesions in at least 15 species of molluscs, including abalone following exposure to undetermined disease agents. Diggles and Oliver (2005) also noticed haemocytic inflammatory lesions due to pathological conditions in abalone, which suggests that haemocytosis may be an immunological response to local and systemic effects of parasites.

In this study, elevated amounts of ceroid material were observed in the gills and muscle tissues of *H. iris* where *P. olseni* and ciliates were detected. Darriba Couñago (2017) also reported similar material in the gills of clams, which were interpreted as evidence of chemical irritation from

pollutants and pathogens. Neves et al. (2015) recorded ceroid material in the digestive gland of snails (*Littorina littorea*) exposed to dinoflagellates. Apeti et al. (2014) stated that ceroids are common in oysters where their presence may indicate cell stress. Moreover, Carella et al. (2015a) noted that in molluscs, ceroid material accumulation has been associated with age and pollutant exposure. In this study, the occurrence of ceroid material was also observed in abalone tissues without parasitic association and this phenomenon might be due to the presence of other challenges such as pollutants, cell stress and age. Thus, ceroid material accumulation in *H. iris* tissues might be involved in the immunological response against pathogenic infections and other challenges which may be indicative of culturing conditions.

2.5 Conclusions

This manuscript presents the first report of *P. olseni* using ISH in the New Zealand black-footed abalone. This is the first detailed description of *P. olseni* along with other pathogens and parasites from histological sections in *H. iris* and their associations with health markers. In the case of co-infection of some parasites, hosts become weaker after infection with one parasite inevitably permitting entry by another. There was a significant association between infection of *P. olseni* and intracellular microcolonies of bacteria (IMCs). Abalone gross unhealthy appearances were corroborated by histological observations of poor health, signs such as disrupted and swollen gills with haemocytosis, ceroid material and parasites, and muscle tissue with focal haemocytosis with parasites. A significant association between abalone gross appearances and the presence or absence of *P. olseni* and unidentified disintegrated ciliates was recorded. Associations between *P. olseni* and swollen gills with ceroid material and haemocytosis were noted. Histology helped to visually recognise the immunological tissue responses (ceroid material and haemocytosis), but did not provide a definitive indication of the underlying causes for these conditions, which requires further investigation. However, the findings of this study increase our knowledge of the interactions between pathogens and abalone, including host immune responses which, with further work, may be used as early warning signs of health issues in wild and cultivated abalone in New Zealand.

Chapter 3

Bonamia ostreae (Haplosporidia) and other parasites in New Zealand flat oysters (*Ostrea chilensis*): a histopathological study



New Zealand flat oysters (*Ostrea chilensis*)

Abstract: *Bonamia exitiosa* and *B.ostreae* are protistan parasites responsible for Bonamiosis (microcell disease or haemocyte disease) in flat oysters. Whilst *B. exitiosa* is believed to be endemic to New Zealand (NZ) and has long been associated with periodic serious mortality in wild beds of the NZ native oyster *Ostrea chilensis*, *B. ostreae* has only recently been detected in NZ in 2015, and this was the first time the species was detected in the Southern Hemisphere. Since its first detection in farmed oysters, *B. ostreae* is believed to have caused significant mortalities, and this has severely impacted the NZ flat oyster aquaculture industry. A detailed histopathological examination was undertaken on *O. chilensis* collected from the aquaculture farming area of the Marlborough Sounds, NZ, in 2017, two years after the first detection of *B. ostreae* there. In this study, out of 94 flat oysters, *B. ostreae* and *B. exitiosa* were detected via histology in 34% and 1% of individuals respectively, and in 70% and 1% respectively via polymerase chain reaction (PCR). The only instance of detection of *B. exitiosa* was as a co-infection with *B. ostreae*. The connective tissue around digestive tubules, gonads, gills, gut wall and mantle cavity of *O. chilensis* were examined and several other parasites were also observed, including *Bucephalus longicornutus*, Apicomplexan X (APX), *Microsporidium rapuae*, Gymnophallid-like metacercaria, as well as intracellular microcolonies of bacteria (IMCs), copepods and other bacteria. Most other parasites were observed very rarely, but in contrast, there was an association between infection of *B. ostreae* and heavy infection of *B. longicornutus*. The abundance of *B. ostreae* microcells in different tissues, including gills, mantle, the connective tissue around digestive tubules, and haemocytes surrounding the gut were estimated semi-quantitatively by a grading scale that included the relative abundance of *B. ostreae* in various tissues and the average number of *B. ostreae* microcells per infected haemocyte per tissue. *B. ostreae* microcells infecting haemocytes were detected in blood spaces of gills and sinuses of oysters. Diapedesis was noticed in tissues where haemocytes contained *B. ostreae* microcells, and an association was noted between the number of intracellular microcells and diapedesis. A general 'health' rating was derived from examination of the gill structure, digestive tubule structure and the presence of bacteria and scored oysters as 'healthy', 'unhealthy', or 'moribund'. The highest prevalence of *B. ostreae* infection was observed in live but unhealthy oysters, whereas the lowest prevalence was recorded in moribund individuals. These findings provide new insights into the infection, disease progression, host-parasite interaction, and transmission mechanisms of *B. ostreae* in *O. chilensis* and may assist with disease management strategies.

3.1 Introduction

Haplosporidian parasites of the genus *Bonamia*, including *Bonamia ostreae* and *Bonamia exitiosa*, are intracellular parasites commonly of 1–3 µm in diameter, which infect haemocytes of flat oysters causing a disease known as bonamiosis (Hine & Jones, 1994; OIE, 2012). Both the native New Zealand flat oyster *Ostrea chilensis* and the European native flat oyster *Ostrea edulis* have been reported to be infected with *B. ostreae* (Elston et al., 1986; Lane et al., 2016; Pichot et al., 1979) and *B. exitiosa* (Arzul et al., 2011; Berthe & Hine, 2003; Hine et al., 2001) and both *Bonamia* species have caused serious disease outbreaks (OIE, 2012; OIE, 2018a; OIE, 2018b).

Mass mortalities of *O. edulis* due to *B. ostreae* infections have occurred throughout Europe and the United States for at least 25 years (da Silva et al., 2005). Severe effects were observed in farmed and wild populations when *B. ostreae* was accidentally introduced from the US and spread in Europe through the movement of infected oysters to France and Spain in the 1970s (Cigarría & Elston, 1997; Elston et al., 1986). The first occurrence of *B. ostreae* in the Southern Hemisphere was reported in New Zealand in 2015 and is believed to have been responsible for severe mortalities of naïve oysters on aquaculture farms at that time (Lane et al., 2016). Conversely, *B. exitiosa* is considered endemic to New Zealand flat oysters (*O. chilensis*), having been observed since at least the 1960s, although, this parasite has caused mass mortalities in wild populations, notably since the mid-1980s (Cranfield et al., 2005; Doonan et al., 1994; Michael et al., 2016). In order to support the future and sustainability of flat oyster populations, there is, therefore, an urgent need to understand the effect of *B. ostreae* on *Ostrea chilensis*.

B. ostreae is an intracellular protistan parasite that multiplies inside oyster haemocytes. In *O. edulis*, infection rarely results in clinical signs of disease, and many infected oysters appear normal (Bower et al., 1994); however, infected oysters may have yellow to black discolouration and extensive lesions, such as perforated ulcers on the gills and mantle (Arzul & Carnegie, 2015; Bower et al., 1994). During the early stages of infection, *B. ostreae* provokes a defence response in oysters, inducing lesions with heavy haemocytic infiltration in tissues (Bower et al., 1994; Dinamani et al., 1987; Elston et al., 1986; Hervio et al., 1995; Kroeck & Montes, 2005). Furthermore, *B. ostreae* causes diffused or generalized infections which seem to be linked with haemocyte destruction and diapedesis. Diapedesis (the passage of haemocytes through the epithelium) caused by the proliferation of the parasite (Bower et al., 1994). Although some flat oysters die with light infections, most perish with much heavier infections (Bower et al., 1994). Severely infected oysters tend to be in poorer condition (lesions, haemocyte destruction etc.) than lightly infected or uninfected oysters (Bower et al., 1994). However, despite the large amount known about the

progression of disease in *O. edulis*, there is almost nothing known about how *B. ostreae* may affect *O. chilensis*. Therefore, clarifying the patterns of disease progression for *B. ostreae* infections within *O. chilensis* is paramount in helping to determine appropriate disease management strategies.

The complete life cycles of *B. ostreae* and *B. exitiosa* are unknown, but both parasites are readily transmitted directly from oyster to oyster (Culloty & Mulcahy, 1996), and this may occur during respiration or filtration of seawater for food (Bucke, 1988; Montes et al., 1994). The parasites enter the host via the gill epithelia and enter into the haemocytes when they are detected as foreign particles and are phagocytised (Hine & Wesney, 1994; Montes et al., 1994), or through ingestion of the microcells and then entry into the haemolymph from the gut (Hine, 1991a; 1991b). If the haemocytes fail to destroy the parasites, microcells of *B. ostreae* may multiply rapidly via binary fission, and lyse or rupture the haemocytes, releasing more microcells that infect other haemocytes (Balouet et al., 1983; Culloty & Mulcahy, 2007), thus leading to haemocytic infiltration of surrounding tissues (Comps, 1983; da Silva et al., 2005). Haemocytosis (a high number of haemocytes) in the connective tissues of gills, mantle and gut indicates the initiation of infection by *B. ostreae* (Balouet et al., 1983; Poder et al., 1983) and also suggests that *Bonamia* microcells may migrate from the circulatory system to connective tissues (Cochennec-Laureau et al., 2003). In New Zealand flat oysters (*O. chilensis*), infection with *B. ostreae* has been shown to result in haemocytosis of the connective tissue around the digestive tubules, stomach, gills and mantle (Lane, 2018). In *O. edulis*, ten or more parasites have been observed within a single infected haemocyte (Poder et al., 1983). In *O. chilensis*, < 16 parasites were observed per infected haemocyte (Hine, 1991a). After lysing or rupture of haemocytes, or upon host death, the parasites are transmitted in the water to nearby oysters where the cycle begins again (Bucke, 1988; Carnegie et al., 2003; Montes et al., 1994).

In this study, a detailed histopathological examination was undertaken on New Zealand flat oysters (*O. chilensis*) collected from the Marlborough Sounds, New Zealand, two years after the first detection of *B. ostreae* in 2015. In addition to identifying the presence of *B. ostreae*, *B. exitiosa*, and other parasites in New Zealand flat oysters, we aim to clarify the pattern of disease progression following *B. ostreae* infection (from a mild infection to a systemic infection) by grading *B. ostreae* presence in different tissues within each individual. The abundance of *Bonamia* microcells in the whole oyster and different tissues, including gills, mantle, the connective tissue around digestive tubules and haemocytes surrounding the gut were assessed semi-quantitatively by a grading scheme modified from that of Hine (1991a). This information is used to draw inferences about specific

infection patterns of *B. ostreae* in *O. chilensis* relating to disease development, host-parasite interactions, and transmission mechanisms.

3.2 Materials and methods

3.2.1 Sample collection, histological preparation and microscopic examination

Flat oysters (shell size ranging from 50 to 85 mm, mean \pm SE of 68 \pm 0.9mm) were collected from oyster farms in the Marlborough Sounds, New Zealand on 27th November 2017. Samples were collected from 2 farming systems with different age groups by Ministry for Primary Industries (MPI) who were destroying all the oysters that were thought to have *Bonemia* so this was an opportunistic and unique sampling event. The oysters were kept alive on ice and freighted to the Ministry for Primary Industries' Animal Health Laboratory where they were held on ice in polystyrene bins in a humid environment for between 2 and 8 days before dissection. The animals were measured for size and weight, followed by shucking and sectioning for histological analyses.

Specimens were sectioned to give a 2–5 mm thick tissue slice (Howard et al., 2004), followed by standard histological processing (OIE, 2000). Samples were fixed in 4% formalin for 48 h and then stored in 70% ethanol. Specimens were dehydrated in a series of ascending ethanol concentrations, two changes of xylene, and then embedded in paraffin wax. Sections of 5 μ m were cut by microtome, mounted on slides, stained with haematoxylin-eosin and observed under a light microscope.

Prepared slides were examined under the microscope using 10 \times and 40 \times objectives. A 100 \times objective (oil) was used to identify suspected pathogens and parasites as required. Images were taken using a Leica DM2000 microscope with 40 \times and 100 \times objectives. The presence or absence of *Bonamia* microcells in four different tissues (gills, mantle, the connective tissue around digestive tubules and haemocytes surrounding the gut) was recorded, and the prevalence and abundance of microcells were assessed semi-quantitatively by grading scales as described below. All microscopic examination and grading were done blind to the size, health, or other identifying factors of the sampled individual.

3.2.2 Quantification of parasites

The prevalence of *B. ostreae* and other parasites was calculated according to Bush et al. (1997). A semi-quantitative scale was used for determining the abundance of parasites, as all the parasites were not counted in each host. Each tissue was examined to record the number of parasites, which was then used to calculate the prevalence and abundance of parasites per tissue and individual, by visual examination of a single histological section (the entire section) for each case at 40× and 100× magnification.

In this study, we use the term abundance instead of intensity, as according to Bush et al. (1997), intensity (a form of density) is the number of pathogens in each individual or specified tissue or thin section of the entire animal, and an abundance is also a form of density but differs from the intensity in that an intensity of “0” is not possible whereas an abundance of “0” is appropriate.

3.2.3 Quantification of *Bonamia*

The relative abundance of *Bonamia* microcells in haemocytes, individual tissues or the whole oyster was evaluated semi-quantitatively using grading scales of 0-3 or 0-5 modified from Hine 1991a (Table 3.1).

3.2.3.1 *Bonamia* relative abundance per tissue (0-3)

Although *B. exitiosa* infection was most significant in the gonad by Hine (1991a), in this study, there was little or no *Bonamia* infection in this tissue. Therefore, gonad was excluded from the tissues to choose for evaluating *Bonamia* abundance. The abundance of *B. ostreae* microcells in the different tissues, including gills, mantle, the connective tissue around digestive tubules and haemocytes surrounding the gut were evaluated semi-quantitatively on a scale of 0 to 3 where 0 = Absent, 1 = Low, 2 = Medium and 3 = Heavy. When combined across all four tissues, these combined as 3 = Heavy [3333, 3332 or 3322], 2 = Moderate [2222, 2223, 2221 or 2211], 1 = Light [0001, 0011, 0111 or 1111] and 0 = Nil/Absent [0000] (Table 3.1, Modified scheme column 2).

3.2.3.2 The mean of *Bonamia* microcells per haemocyte

When infected haemocytes were encountered, the number of *Bonamia* microcells in each infected haemocyte was counted (for up to 100 haemocytes) in each tissue. The mean number of *Bonamia* microcells per infected haemocyte was then calculated for each tissue (gills, mantle, the connective tissue around digestive tubules and haemocytes surrounding the gut). Then, the overall average number of *Bonamia* microcells per infected haemocyte was determined for the individual animal

by taking a mean of the tissue means. Based on the overall mean number of *Bonamia* microcells per infected haemocyte, ranges (0, 1, 1-2, 1-5, 4-9 and 7-12) of means of *Bonamia* microcells per haemocyte per tissue were fixed for evaluating the whole oyster grading, where Grade 0 = mean no. of microcells = 0; Grade 1 = mean no. of microcells = 1; Grade 2 = mean no. of microcells = 1-2; Grade 3 = mean no. of microcells = 1-5; Grade 4 = mean no. of microcells = 4-9; Grade 5 = mean no. of microcells 7-12 per infected haemocyte (Table 3.1, Modified scheme column 3).

The whole oyster grading system, which grades on a scale of 0-5 from absence to high-intensity systemic infection, was derived by combining the two other parameters above (relative abundance of *Bonamia* microcells per tissue (on a scale of 0-3), and the mean number of *Bonamia* microcells per infected haemocyte per tissue [mean of the 4 different tissue means]).

For example, an oyster with an overall grade of 5 showed all tissues at grade 3 [3333], the range of mean number of microcells per infected haemocyte = 7-12 per haemocyte across all tissues. An oyster at overall grade 4 = overall tissue grade = 3 [3332 or 3322], range of mean microcells per haemocyte = 4-9; oyster grade 3 = tissue grades = 2 [2222 or 2223], range of mean microcells per haemocyte = 1-5; oyster grade 2 = tissue grade = 2 [2221 or 2211], range of mean microcells per haemocyte = 1-2; and oyster grade 1 = tissue grade = 1 [0001, 0011, 0111 or 1111], range of mean microcells per haemocyte = 1; and oyster grade 0 = tissue grade = 0 [0000], range of mean microcells per haemocyte = 0 (Table 3.1). The differences between the new scheme and Hine's scheme for whole oyster *B. ostreae* infection level are presented in Table 3.1.

Table 3.1 A semi-quantitative *B. ostreae* grading scale for whole oysters modified from Hine (1991a), compared with the original scheme of Hine (1991a).

Grade	Scheme of Hine (1991a)		Modified scheme		
	Descriptions	No. of <i>Bonamia</i> microcells per haemocyte	Description of each grade	<i>Bonamia</i> relative abundance in all four tissues# (graded 0-3 in each tissue)	Mean <i>Bonamia</i> microcells per infected haemocyte
0	-	-	Grade 0 = No <i>Bonamia</i> microcells seen after extensive searching* of all tissues.	0000 (absent)	0
1	Very few (<10) <i>Bonamia</i> microcells observed after extensive searching of all tissues.	-	Grade 1 = Very few (<10) <i>Bonamia</i> microcells observed after extensive searching of all tissues.	0001, 0011, 0111 or 1111 (low)	1
2	<i>Bonamia</i> microcells observed only after searching, and then only one to two presents in each infected haemocyte.	1-2	Grade 2 = <i>Bonamia</i> only observed after extensive searching of all tissues, and then only one to two present in each infected haemocyte.	2221 or 2211 (low to medium)	1-2
3	<i>Bonamia</i> widespread, but only one to five microcells per infected haemocyte observed.	1-5	Grade 3 = <i>Bonamia</i> widespread in most or all tissues, but only one to five <i>Bonamia</i> microcells per infected haemocyte observed.	2222 or 2223 (medium)	1-5
4	<i>Bonamia</i> readily observed in all tissues, often associated with a haemocytosis.	-	Grade 4 = <i>Bonamia</i> readily observed in all tissues, but 4-9 <i>Bonamia</i> microcells per infected haemocyte observed and often associated with a heavy haemocytosis, and many extracellular microcells.	3332 or 3322 (medium to heavy)	4-9

5	<i>Bonamia</i> microcells common in all tissues, <16 per haemocyte, but often extracellular. Haemocytosis was always present; lesions sometimes observed.	<16	Grade 5 = <i>Bonamia</i> common in all tissues, with a mean of 7-12 per haemocyte, heavy haemocytosis was always present; high numbers of extracellular microcells, and sometimes lesions (due to rupture of haemocytes).	3333 (heavy)	7-12
---	--	-----	---	--------------	------

**Extensive searching was for 5 minutes per slide.*

#Gills, mantle, the connective tissue around digestive tubules and haemocytes surrounding the gut.

3.2.4 Bonamia species diagnosis

It was difficult to distinguish the two *Bonamia* spp. by histology. The *Bonamia* species were confirmed as either *B. ostreae* or *B. exitiosa* by polymerase chain reaction (PCR; Fidler unpublished results). *Bonamia* species-specific conventional PCR assays (Ramilo et al., 2013) were used to determine the total number of oysters infected with *B. ostreae* and/or *B. exitiosa*. For the *B. exitiosa* species-specific PCR, the forward primer BEXIT-F (5'-GCG CGT TCT TAG AAG CTT TG-3') was paired with the reverse primer B-EXIT-R (5'-AGA TTG ATG TCG GCA TGT CT-3') to produce an amplicon 246 bp in size. Thermal cycling conditions were 95°C for 2 min, followed by 35 cycles of 95°C for 10 s, 58°C for 10 s, and 72°C for 1 s. For the *B. ostreae* species-specific PCR, the forward primer BOSTRE-F (5'-TTA CGT CCC TGC CCT TTG TA-3') was paired with the reverse primer BOSTRE-R (5'-TCG CGG TTG AAT TTT ATC GT-3') to produce an expected amplicon of 208 bp. The thermal cycling conditions for *B. ostreae* were similar to *B. exitiosa*, but with an annealing temperature of 55°C. All amplicons were visualised under UV as described above, and the presence or absence of a band of the expected size was noted.

Only one oyster was confirmed as infected with *B. exitiosa*, and that individual was also infected with *B. ostreae*. All other samples were confirmed as *B. ostreae*. Thus, the discussion will only include observations of *B. ostreae*. The result for the specimen containing a co-infection with *B. exitiosa* was within the range of results observed for *B. ostreae*, and so has been included in the data analysis.

3.2.5 Haemocytosis associated with B. ostreae infection

A semi-quantitative scale of 0-3 (0 = Absent, 1 = Low, 2 = Medium and 3 = Heavy) was also applied to the amount of observed inflammatory response in the form of haemocytosis. Haemocytosis observed as an abnormally large number of haemocytes occurring in the tissues and can be either diffuse (where haemocytes are evenly distributed), focal (where there are distinct centres [foci] of haemocyte accumulation), or multi-focal.

3.2.6 Presence of ceroid granules or lipofuscin with B. ostreae infection

The presence or absence of brownish-yellow pigment that may indicate either ceroid or lipofuscin (inflammatory tissue response caused by nutritional deficiencies, toxicity, or disease) in the different tissues was recorded as a present (1) or absent (0).

3.2.7 Other pathogens and parasites

The presence and abundance of other parasites or pathogens in various tissues were also noted and quantified. Most were directly counted, but due to the high number of individuals of *Bucephalus longicornutus* encountered, a grading scheme was deemed necessary. Their abundance was recorded on a scale of 1 to 3 where 1 = Low (<50 individuals per slide), 2 = Medium (51-200 individuals per slide) and 3 = High (>200 individuals per slide). As a PCR method was available to detect the coccidian-like organism apicomplexan X (APX; Suong et al., 2018), a PCR assay was used to diagnose APX as well.

3.2.8 Overall condition

Flat oysters were categorised into 3 different general conditions: “live and healthy”, “live and unhealthy”, and “moribund” based on their gill structure, digestive tubule structure and the presence of bacteria. In live and apparently healthy oysters, the structure of the gills was good and typical, and the digestive tubules were thick with a cruciform lumen. In live but apparently unhealthy oysters, the structure of the gills was not typical (without cilia and with haemocytes in blood spaces), and bacteria (bacilli and/or cocci) were observed in the tissue. In moribund or near-dead oysters, the structure of the gills was destroyed, and deformed, and digestive tubules were thin and without a cruciform lumen. However, gill pathology (surface lesions of gills) with shedding *Bonamia* were observed in *O. chilensis* by Hine (1991a).

3.2.9 Statistical analysis

Tests for the association between *B. ostreae* and other pathogens (as detected via histology and PCR) were conducted by Odds ratios (OR) and Chi-square tests for whole samples (94 oysters). Pearson Chi-Square was applied for the association between the abundance of different grades across the different tissues. These tests were performed using SPSS Statistics software (IBM; version 23).

3.3 Results

3.3.1 Infection with Bonamia

A total of 32 (34%) of the 94 sampled oysters were observed to be infected with *Bonamia*, and all these observed infections were confirmed by PCR as *B. ostreae* except for one individual which had a co-infection of *B. ostreae* and *B. exitiosa*. The individual with a co-infection of both species was an apparently healthy individual. *Bonamia* was observed as a Grade 1 (low-level) infection in

the gills, mantle and haemocytes surrounding the gut, but was not observed in the connective tissue around digestive tubules. The animal did demonstrate a low level Grade 1 haemocytosis in the connective tissue around the digestive tubules, a medium level Grade 2 haemocytosis in gills and mantle, and a Grade 3 (high) level of haemocytosis in the haemocytes surrounding the gut. All haemocytosis were observed as diffuse.

Due to the very low sample size of observed *B. exitiosa* infections, the following results will describe only observations of *B. ostreae* infections.

Microcells of *B. ostreae* (1-2 μm) were observed within the haemocytes, as well as freely in the connective tissue around the digestive tubules, gut, gills and mantle (Fig. 3.1A-D) of *O. chilensis*. The parasites were often associated with an intense inflammatory reaction (local concentration of haemocytes (haemocytosis) and ceroid granules (Fig. 3.1C)). Microcells of *B. ostreae* were also detected within haemocytes in the blood spaces of sinuses (Fig. 3.1E) and the sinuses of gills (Fig. 3.1F). Diapedesis (the passage of haemocytes through the epithelium) was noticed in different tissues including the gills, gut and mantle (Fig. 3.1F-H), with haemocytes containing *B. ostreae* passing through the unruptured walls of tissues.

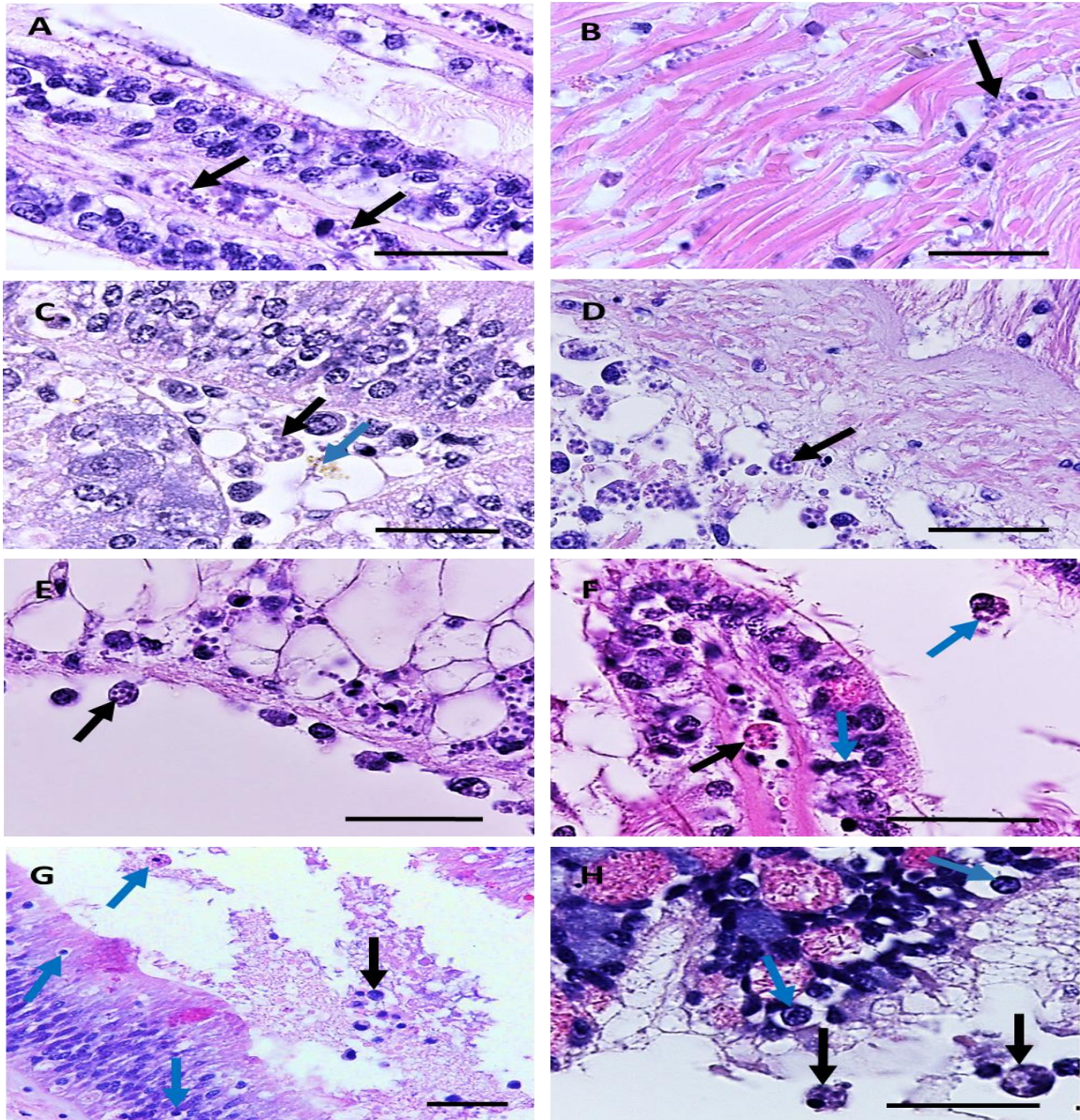


Figure 3.1 *B. ostreae* microcells (black arrows) in different tissues of flat oysters, (A) gills, (B) muscle, (C) connective tissue around the digestive tubules (presence of ceroid indicated with a blue arrow), (D) haemocytes around the gut wall, (E) *Bonamia* microcells in haemocyte (black arrow) inside blood sinus, (F) *Bonamia* microcell infected haemocytes (black arrow) inside blood spaces of gills and diapedesis with *Bonamia* microcells (blue arrow) in the gills, (G) diapedesis (blue arrow) and haemocyte with *Bonamia* microcells (black arrow) in the gut, (H) diapedesis (blue arrow) and haemocyte with *Bonamia* microcells (black arrow) in the mantle. Scale bars = 20 μ m.

3.3.2 *B. ostreae* epidemiological and health parameters

Of the 94 oysters sampled, 43% were live and apparently healthy (n = 40), 35% were live but unhealthy (n = 33) and a small number of oysters were moribund (n = 21, 22%). Out of the 40

healthy samples, 28% (n = 11) were *Bonamia* positive by histology and 73% (n = 29) were PCR positive, and of the 33 live unhealthy oyster samples, 42% (n = 14) were *Bonamia* positive by histology and 79% (n = 26) were PCR positive. Of the moribund oysters 33% (n = 7) were *Bonamia* positive by histology, and 48 % (n = 10) were *Bonamia* positive by PCR (n = 21).

Most oysters (65%, n = 62) had no observable *B. ostreae* infection (grade 0), with just 34% having an observable infection of grade 1 or higher. However, PCR results indicated that 70% of animals were indeed PCR positive for *B. ostreae*. Thus, only half of the animals that were PCR positive had an infection severe enough to be observable via histology. Just 2% (n = 2) were suffering from a severe grade 5 infection. Most infected animals (42% of those infected, 15% of total) had a grade 3 infection, with ‘medium’ tissue grades, and a range of 1 – 5 mean microcells per haemocyte. Only 9% of oysters were in grade 4, and just 4% and 5% of oysters were at grades 1 and 2, respectively (Fig. 3.2 & Table 3.2).

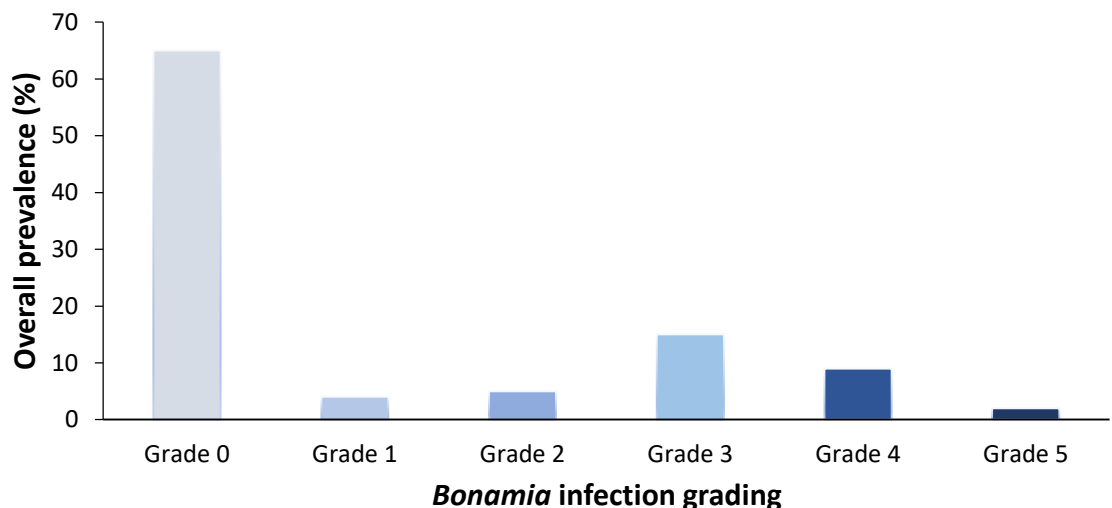


Figure 3.2 Prevalence of different *B. ostreae* histological whole-oyster infection grades.

Diapedesis with *B. ostreae* microcells was observed in various tissues of *O. chilensis* but only in tissues with a grade 4 or 5 level infection. Infected haemocytes were also only observed in blood spaces of gills and sinuses of oysters with grades 3, 4 or 5 level infection (Table 3.2).

Table 3.2 The distribution of *B. ostreae* grading levels within the sample population (n = 94) and the concurrence of microcells infecting haemocytes in blood spaces or undergoing diapedesis within haemocytes. X = absence, √ = presence.

Whole oyster <i>B. ostreae</i> abundance grade	Prevalence (%)	Frequency (n)	Diapedesis with <i>Bonamia</i> microcells	Blood spaces with <i>B. ostreae</i> infecting haemocytes
0	65	61	X	X
1	4	4	X	X
2	5	5	X	X
3	15	14	X	√
4	9	8	√	√
5	2	2	√	√

The percentages of *B. ostreae* abundance grading (0-3) in the different tissues (gills, mantle, the connective tissue around digestive tubules and haemocytes surrounding the gut) were observed. There is no significant difference ($p = 0.769$) between the abundance of different grades (0-3) of *B. ostreae* infection across different tissues (differences were considered significant when $P < 0.001$). The percentages of *B. ostreae* abundance grading across the different tissues is presented in Fig. 3.3.

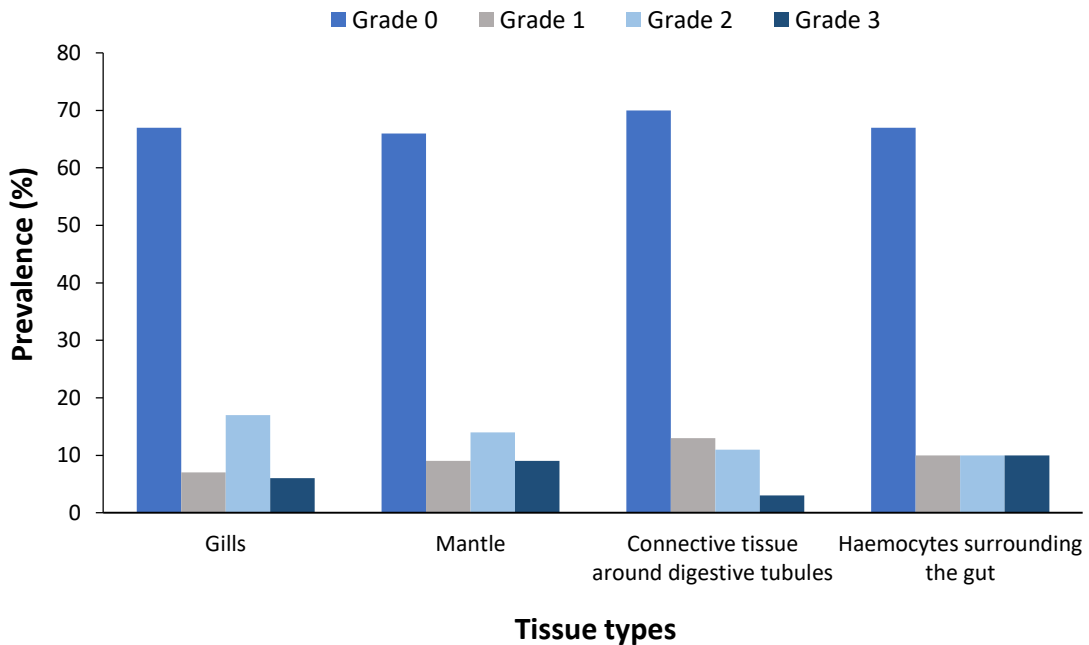


Figure 3.3 Percentage of *B. ostreae* abundance grading (0-3) in different tissues of *O. chilensis*.

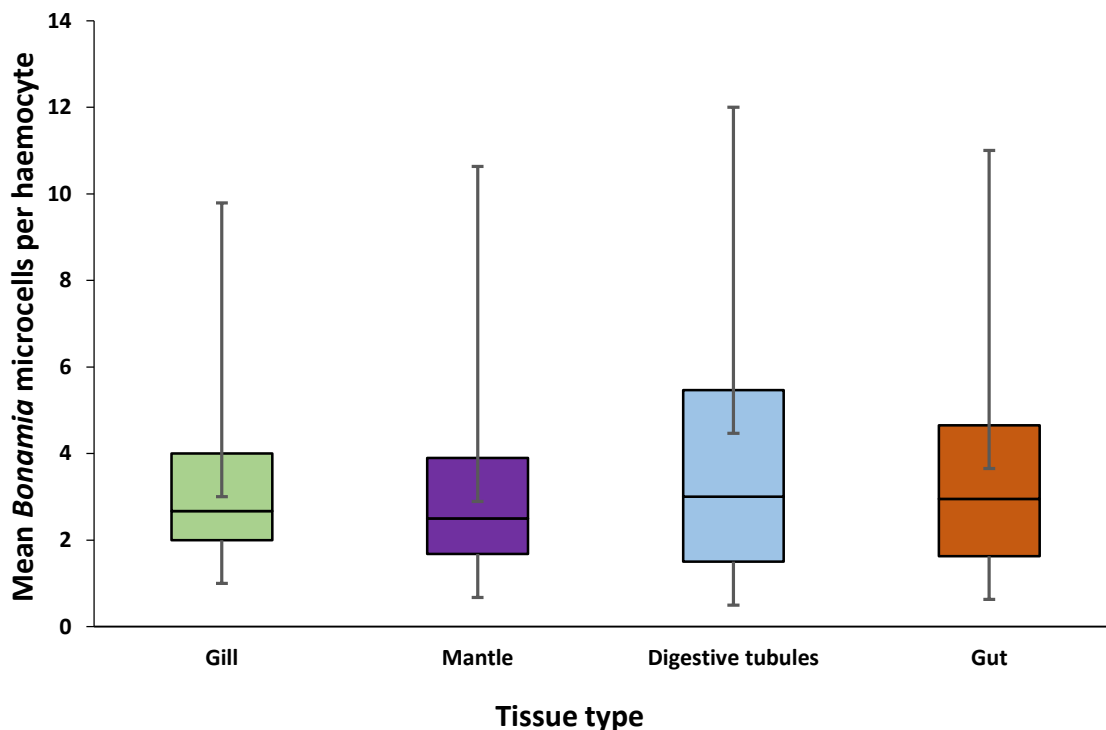


Figure 3.4 Box and whiskers plot showing the distributions of the number of *B. ostreae* microcells per infected haemocyte in gills, mantle, digestive tubules and gut tissues of oysters (Minimum, Q1, Median, Q3, Maximum). [In each case, Mean is greater than the Median, distributions are slightly positively skewed, Minimum values of all the tissues are similar, Median and Maximum values are higher in digestive tubules than other tissues].

All the tissues (gills, mantle, the connective tissue around digestive tubules and haemocytes surrounding the gut) showed a higher percentage (occurrence rate of above 80%) of diffuse haemocyte abundance than focal and multifocal haemocyte abundance. Moreover, 15% of samples indicated haemocyte abundance with multifocal haemocytosis in the mantle and only 6% of oysters showed haemocytes abundance with focal haemocytosis surrounding the gut (Table 3.3).

Out of 94 oysters, 70 (75%) had ceroid material in the cell bodies of digestive tubules and the surrounding connective tissues. Twenty nine percent of oysters showed ceroid material in gills (Table 3.3).

Table 3.3 Diffuse, focal and multi focal haemocytosis and ceroid abundance in different tissues of oysters [n = number of samples, % = occurrence rate).

Site	Different types of haemocytes abundance in different tissues			Brown/ceroid material in different tissues
	Diffuse	Focal	Multifocal	
Gills	n = 92 (98%)	n = 0 (0%)	n = 2 (2%)	n = 27 (29%)
Mantle	n = 77 (82%)	n = 5 (5%)	n = 12 (13%)	n = 14 (15%)
Connective tissue around digestive tubules	n = 91 (97%)	n = 3 (3%)	n = 0 (0%)	n = 70 (75%)
Haemocytes surrounding the gut	n = 79 (84%)	n = 6 (6%)	n = 9 (10%)	n = 19 (20%)

20-26% of oysters presented *B. ostreae* infected haemocytes at a low level (grade 1) in all the tissues (gills, mantle, the connective tissue around digestive tubules and haemocytes surrounding the gut). 5% of oysters demonstrated *B. ostreae* infected heavy hemocytosis (grade 3) in the mantle and the connective tissue around digestive tubules. A medium level (grade 2) of *B. ostreae* infected haemocytes was observed in the connective tissue around digestive tubules and surrounding the gut of 9% oysters.

3.3.3 Infection with other parasites and pathogens

Several other parasites and pathogens were noted in different tissues of oysters, but mostly at a very low frequency of occurrence. The one exception was *Bucephalus longicornutus* (Fig. 3.5A), a digenean trematode parasite. Sporocyst containing cercarial larval stages of this trematode was detected in the connective tissue around gonads, digestive tubules, mantle and gills, but mainly in gonads. Eighty-six percent of oysters with *B. ostreae* infection were also infected with a high-level (grade 3) of *B. longicornutus* (n = 12). Conversely, no oysters demonstrated *B. ostreae* co-infection with a low-level (grade 1) infection of *B. longicornutus*.

Other observed parasites included the coccidian-like organism, apicomplexan X (APX). This was noted in the connective tissue around digestive tubules and gonads of just 1 of the 94 flat oysters in histological analysis, but was found to be PCR positive in 31% (n = 29) (Fig. 3.5B & Table 3.4). Since histology and PCR analysis were not conducted from the same tissue layer of the samples, APX was not diagnosed by histology when it was in the samples and positive by PCR data. Cysts of *Microsporidium rapuae* (Fig. 3.5C) were recorded in connective tissue near the gut of a single individual. Intracellular microcolonies of bacteria (IMCs) were found in the digestive tubule epithelium of one individual (Fig. 3.5D) [Note: Rickettsia-like organisms (RLOs) are now referred

to as IMCs; Cano et al., 2020]. Also, copepods and parts of copepods were observed in the mantle cavity of two individuals (Fig. 3.5E). Gymnophallid-like metacercaria (a larval stage of cercaria) a digenean trematode occurred in the mantle cavity of one individual (Fig. 3.5F). Bacteria other than (IMCs) were recorded in gills, mantle cavity and organ surfaces within the body cavity of 17 of what appeared to be stressed and unhealthy individuals (Fig. 3.5G & H; Table 3.4).

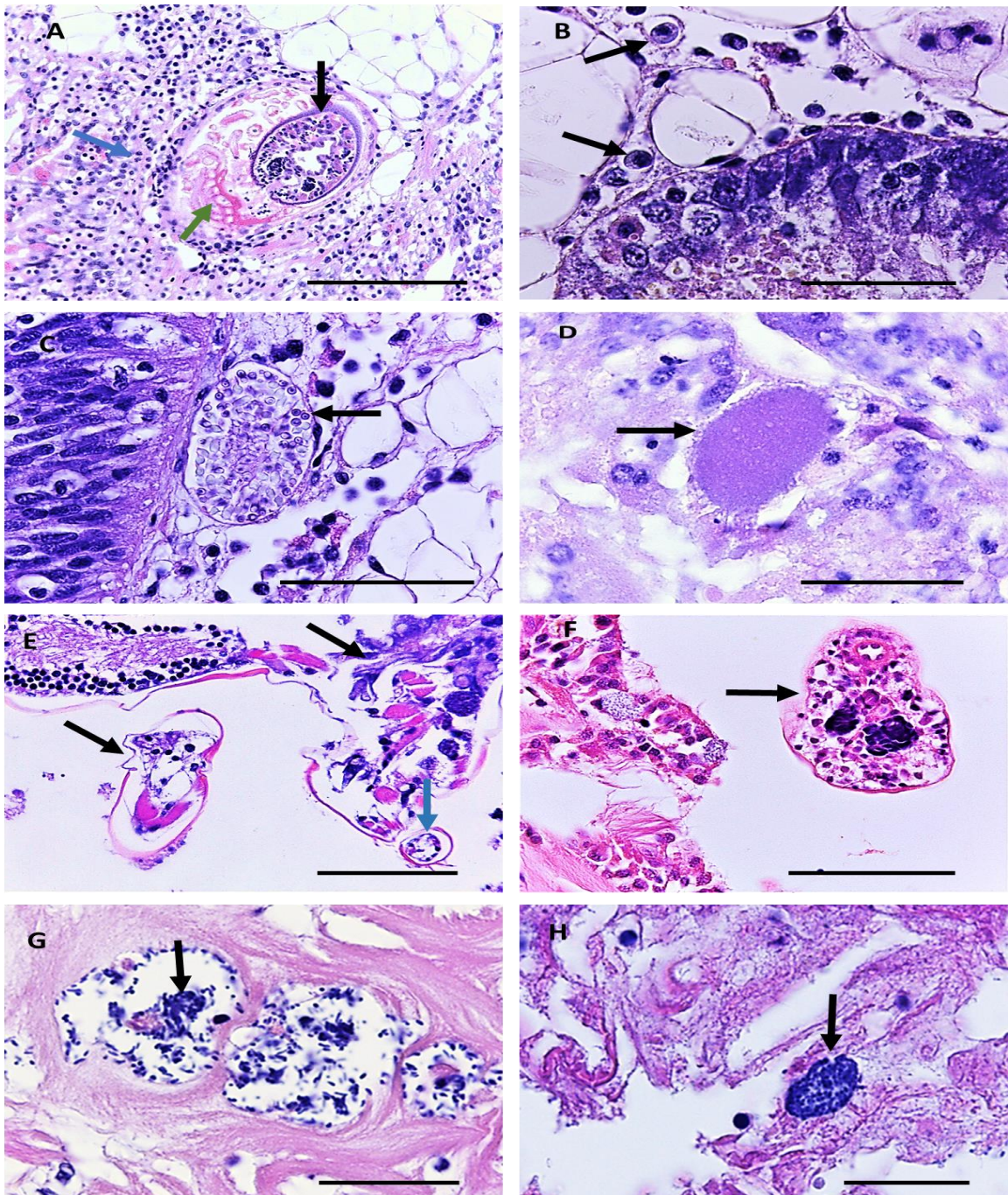


Figure 3.5 (A) Haemocytosis (blue arrow) around a sporocyst (black arrow) of *B. longicornutus* containing a cercaria (black arrow) and sections of the cercarial tail (green arrow) in

connective tissue, (B) zoites of APX (black arrows) in the connective tissue around digestive tubules, (C) cyst containing spores of *M. rapuae* (black arrow) in the connective tissue under the gut wall, (D) intracellular microcolonies of bacteria (IMCs; black arrow) in the digestive tubule epithelium, (E) fragment of a copepod (black arrow) and copepod parts (blue arrow) in the mantle cavity, (F) gymnophallid-like metacercaria (black arrow) in the mantle cavity and (G-H) bacteria (black arrow) in oyster gill filament. Scale bar = 60 μm (A and E), Scale bar = 20 μm (B, D, G and H), and Scale bar = 30 μm (C and F).

In this study, just 3 for *Bonamia* and 1 for APX were appeared positive via histology and negative via PCR (might be due to contamination), but these were excluded from the analysis. This was one of the reasons that PCR was used alongside the histological assessments (Table 3.4).

Table 3.4 Prevalence of all observed parasites or pathogens associated with flat oysters (n = 94) in this survey.

Organism	Histology		PCR	
	Overall Prevalence (%)	Overall Frequency (n)	Overall Prevalence (%)	Overall Frequency (n)
<i>Bonamia ostreae</i>	34	32	70	66
<i>Bonamia exitiosa</i>	1	1	1	1
<i>Bucephalus longicornutus</i>	15	14	-	-
Apicomplexan X	1	1	31	29
<i>Microsporidium rapuae</i>	1	1	-	-
Intracellular microcolonies of bacteria (IMCs)	1	1	-	-
Copepoda	2	2	-	-
Gymnophallid-like metacercaria	1	1	-	-
Bacteria other than (IMCs)	18	17	-	-

Table 3.5 Statistical analysis: Chi-square test and Odds Ratio (OR) for the association between histological observation of *B. ostreae* and other pathogens (n = 94).

Parasites/pathogens observed in oysters	<i>B. ostreae</i>		Chi-square test for association (<i>P</i> -value)	Odds Ratio (OR)
	Absent	Present		
<i>B. longicornutus</i>	Absent	60	0.000	18.00
	Present	2		
Apicomplexan X	Absent	61	1.000	-
	Present	1		
Bacteria	Absent	56	0.005	4.89
	Present	6		

Table 3.6 Statistical analysis: Chi-square test and Odds Ratio (OR) for the association between *B. ostreae* (as detected via PCR) and other pathogens as detected via histology and/or PCR (n = 94).

Parasites/pathogens detected in oysters	<i>B. ostreae</i>		Chi-square test for association (<i>P</i> -value)	Odds Ratio (OR)
	Absent	Present		
<i>B. longicornutus</i>	Absent	28	0.057	7.00
	Present	1		
Apicomplexan X	Absent	26	0.004	5.78
	Present	3		
Bacteria	Absent	28	0.018	9.14
	Present	1		

Table 3.7 Statistical analysis: Chi-square test and Odds Ratio (OR) for the association between histological observation of *B. ostreae* and other pathogens in oysters (n = 60).

Parasites/pathogens observed in oysters	<i>B.ostreae</i>		Chi-square test for association (<i>P</i> -value)	Odds Ratio (OR)
	Absent	Present		
<i>B. longicornutus</i>	Absent	26	0.006	7.80
	Present	2		
Apicomplexan X	Absent	27	0.467	-
	Present	1		

Bacteria	Absent	25	21	0.037	4.37
	Present	3	11		

Table 3.8 Statistical analysis: Chi-square test for the association between histological observation of *B. ostreae* and oyster health condition (n = 94).

Oyster health conditions		<i>B. ostreae</i>		Chi-square test for association (P-value)
		Absent	Present	
Live-healthy	No	33	21	0.278
	Yes	29	11	
Live –unhealthy	No	43	18	0.256
	Yes	19	14	
Moribund	No	48	25	1.000
	Yes	15	07	

Table 3.9 Statistical analysis: Chi-square test for the association between *B. ostreae* presence as detected via PCR and oyster health conditions (n = 94).

Oyster health conditions		<i>B. ostreae</i>		Chi-square test for association (P-value)
		Absent	Present	
Live-healthy	No	18	36	0.653
	Yes	11	29	
Live-unhealthy	No	22	39	0.165
	Yes	7	26	
Moribund	No	18	55	0.030
	Yes	11	10	

3.4 Discussion

Flat oyster (*Ostrea chilensis*) samples, collected from aquaculture farms located in the Marlborough Sounds in 2017 in this study using histological methods showed 34% infection with *Bonamia*

ostreae, and just 1% with *Bonamia exitiosa*, which was a coinfection with both species. Lane (2018) also observed a concurrent infection of *B. ostreae* and *B. exitiosa* from the same area (Marlborough Sounds) during the first detection of infection in New Zealand in 2015, with 40.3% of flat oysters showing infection with *B. ostreae*, 2.7% with *B. exitiosa* and 53.6% showing coinfection of the two species by PCR. In the study of Lane (2018), an overall *Bonamia* spp. infection rate of 96.6% was recorded via PCR yet, only 79.9% *Bonamia* spp. infection prevalence was recorded via histology. In the present study, the overall prevalence of *Bonamia* spp. (*B. ostreae* and *B. exitiosa*) in flat oysters detected by PCR was 70%, whereas the total prevalence of *Bonamia* spp. observed via histology was only 34%, highlighting the importance of PCR as an accurate detection tool, in particular for detecting light *Bonamia* spp. infections (Flannery et al., 2014).

In the present work, the abundance of *B. ostreae* for the whole oyster was evaluated semi-quantitatively by a grading scale modified from Hine (1991a). This modified grading scale was derived as a combination of individual tissue gradings, thus providing detailed information regarding the number of microcells per infected haemocyte across different tissues. The modified grading scale is an integration of the average number of *Bonamia* microcells per infected haemocyte per tissue and the abundance of *Bonamia* microcells per tissue. The purpose of the whole oyster grading of the modified scale is to measure the overall *B. ostreae* infection, whilst the individual tissue gradings help to clarify the progression of the disease.

In the current study, most *B. ostreae* infected oysters presented at grade 3 (*Bonamia* widespread in most or all tissues), a moderate number were considered grade 4 (microcells were readily observed in all tissues and often associated with a heavy haemocytosis) and just a few oysters were suffering from a severe, grade 5 infection, with microcells common in all tissues, with heavy haemocytosis and sometimes lesions. These findings indicate that by the time infection was detectable via histology, most of the oysters had a systemic infection and the *Bonamia* microcells were travelling throughout the body, infiltrating many tissues within the hosts, but only a small number showed tissue damage or lesions (due to rupture of haemocytes). Hine (2002a) also observed very few infections of *B. exitiosa* at grade 5 (heavy infection intensity and severe tissue damage) but most with grade 1, low infection intensity. Bower (1994) reported that in advanced infections, *B. ostreae* is distributed systemically; however, in early infections, microcells were often observed only within haemocytes and associated with heavy haemocyte infiltrations in the connective tissue of the gills and mantle, and the vascular sinuses around the stomach and intestine (Bower, 1994).

In the present study, *B. ostreae* microcells were recorded within haemocytes in the blood spaces of gills (the central part of the gill filament filled with haemolymph) and sinuses (a system of the circulatory system through which hemolymph largely flows). Blood spaces with *B. ostreae* infected haemocytes were also observed in oyster samples with heavy infection. These findings are consistent with Carnegie et al. (2006), who noted *B. perspora* in haemolymph sinuses of infected horse oysters (*Ostreola equestris*). Hine (2002a) also stated that *B. exitiosa* parasites spread from the haemolymph sinuses and move between Leydig cells in *O. chilensis*. Bower (1994) reported that *B. ostreae* are often detected within haemocytes and linked with heavy haemocytosis in the connective tissues and vascular sinuses.

Bower (1994) noted that *B. ostreae* were frequently seen within haemocytes and linked with heavy haemocyte infiltrations in the connective tissue of the gills and mantle of *O. edulis*. Similarly, Hine (2002a) observed that haemocytosis in *O. chilensis* was often related to *B. exitiosa* infection. The current study observed the same with infection of *B. ostreae* in *O. chilensis*: haemocytosis was often observed in *B. ostreae* infected oyster tissues such as gills, mantle, the connective tissue around digestive tubules and gut. According to Bower et al. (2005), bacterial clusters induced by microorganisms were surrounded by an intense accumulation of haemocytes in the tissues of oysters (*Crassostrea gigas*) and these massive haemocyte infiltration responses act as a flag to help to locate the pathogens. Therefore, *Bonamia* parasite associated haemocytosis in this study also indicates immunological tissue responses which help to detect *B. ostreae* in the oyster tissues.

Another immunological tissue response noted in the current study was brown pigmentation, which could be ceroid granules. These were noted in tissues including the digestive tubules, gills, mantle and gut of *O. chilensis* in this study. Ceroid granules were frequently noticed in many tissues, but mostly in the mantle, gonad and digestive gland interstitial tissues in various mollusc species by Webb and Duncan (2019) and digestive tubules of bivalves (*Mytilus galloprovincialis*) by Carella et al. (2015a). Moreover, Apeti et al. (2014) stated that ceroid is common in American oysters (*Crassostrea virginica*). According to Wood and Yasutake (1956), ceroid build up is caused by toxicity or disease.

Diapedesis was noticed in the mantle, gills and gut of *O. chilensis* with heavy infection of *B. ostreae* in the present study, and the infection seemed to be related to haemocyte destruction caused by the rapid increase of the parasite within haemocytes. Similar findings were observed by Bower et al. (1994) who reported that *B. ostreae* was associated with diffuse or generalised infections causing haemocyte destruction and diapedesis in European flat oysters (*Ostrea edulis*) due to the

proliferation of *B. ostreae*. Balouet et al. (1983) and Berthe (2004) also observed haemocyte destruction and diapedesis because of the rapid growth of *B. ostreae* in *O. edulis* in Brittany, western France. According to Hine (1991a), *B. exitiosa* infected haemocytes are initially observed in connective tissue, then, they can be found in all the tissues as the infection progresses and finally, they leave the oysters' tissues either by tissue leakage, haemocyte diapedesis, or host decomposition. Moreover, Hine (1991a, b) reported that *Bonamia* microcells infect the host during feeding where they pass through the oyster gut wall and infect their haemocytes. In the present study, diapedesis with *B. ostreae* microcells was noted in the gut epithelia, gills and mantle tissues, which hints that *Bonamia* microcells within haemocytes passed from one tissue to outside of the oyster through the process of diapedesis. Thus, diapedesis from gut epithelium to the lumen and from gill/mantle epithelium to the mantle cavity or external environment may be an important route for *B. ostreae* transmission in *O. chilensis*.

According to Elston et al. (1986), during feeding or respiration, *B. ostreae* passes from one infected flat oyster to nearby oysters. In addition, after infecting the oysters, the parasite proliferates in the haemocytes and they multiply to produce up to 20 parasites (Dunn et al., 2000; Elston et al., 1986). According to Lallias et al. (2008), a single highly infected flat oyster (*O. edulis*) contained 443×10^6 *B. ostreae*. Bower et al. (1994) noted that most flat oysters die from much heavier infections of *B. ostreae*. Hine (1991a, b) reported that after oyster deaths, *Bonamia* microcells freed and circulated into the water and finally, infect a new host. Although live oysters spread *Bonamia* microcells during feeding and respiration (Elston et al., 1986), dead ones spread even more because they shed the entire population when they die. Therefore, dead flat oysters are very important in disease transmission since they release large numbers of microcells into the water upon death. Although Brehélin et al. (1982) more often observed *B. ostreae* in moribund or dead oysters (*O. edulis*), in the present study, the heaviest infection (abundance) of *B. ostreae* was noted in live unhealthy oysters and the lowest infection (abundance) was found in moribund/dead oysters which indicate that the moribund oysters may have already lost or freed their microcells or were ill from another cause.

Other pathogenic parasites were recorded in the connective tissue around digestive tubules and gonads, gills and the gut of *O. chilensis* in the present study. These included *Bucephalus longicornutus* (with many sporocysts and cercaria) and apicomplexan parasite 'X' (APX). *B. longicornutus* and APX were also detected in *O. chilensis* by Hine and Jones (1994), Hine (2002a; 2002b; 1997; 1991a), Webb (2013), Lane et al. (2016), and Webb and Duncan (2019). In this study, the concurrent infections of *B. ostreae* with *B. longicornutus*, APX and bacteria were recorded in

different tissues of oysters. Co-infections of *B. ostreae* with APX and *B. longicornutus* were also observed by Lane et al. (2016). In the current study, an association between the infection of *B. ostreae* and the infection of *B. longicornutus* was demonstrated. According to Howell (1963) and Millar (1963), mass mortalities of flat oysters in Foveaux Strait, New Zealand occurred due to heavy infection of *B. longicornutus* (sporocysts and cercariae). Another parasite is APX which is endemic in New Zealand and the second most important pathogen in *O. chilensis*, following *Bonamia* spp. (Hine, 2002b; Webb, 2013). According to Hine (2002a), apicomplexan zoites may increase the susceptibility of oysters to *B. exitiosa* by occupying and destroying haemocytes and connective tissue cells and utilising the glycogen reserves of oysters. In this study, coinfection of *B. ostreae* with APX was observed in oysters and an association between the infection of *B. ostreae* and the infection of APX (PCR results) was found. Hine (2002a) noted that apicomplexan zoites with very light infection occurred in the connective tissue Leydig cells (CTC) around the haemolymph sinuses but haemocytosis occurred in heavy infections, causing congestion of CTC. Subsequent distribution of the zoites was related to CTC with early infections and forcing the zoites into the CTC of the gills (Hine, 2002a). Both *Bonamia* microcells and apicomplexan zoites appear in haemocytes (in which they undergo multiplication) and their pattern of distribution in oyster tissues might be similar (Hine, 1991a).

Several other parasites and pathogens such as *Microsporidium rapuae*, intracellular microcolonies of bacteria (IMCs), gymnophallid-like metacercaria, copepods and bacteria were observed in different tissues of oysters. *M. rapuae*, copepods and *Rickettsia*/intracellular microcolonies of bacteria (IMCs) were also observed in *O. chilensis* by Webb (2013), Lane et al. (2016), and Webb and Duncan (2019). *M. rapuae* observed in this study is not thought to be pathogenic and was only observed in a single specimen. Webb (2013) stated that cysts of *M. rapuae* are non-pathogenic and occur in connective tissue near the digestive tubules in *O. chilensis*. Intracellular microcolonies of bacteria (*Rickettsia*-like organisms) are common in the digestive epithelium of flat oysters without any significant pathological effects (Hine, 1997; Webb & Duncan, 2019). Copepods have been reported in several New Zealand bivalves with haemocytosis but their impact on the host may be not significant (Apeti et al., 2014; Caceres-Martinez & Vasquez-Yeomans, 1997; Webb & Duncan, 2019). Gymnophallid-like metacercaria is common in bivalves and most have no adverse effect on cultured bivalves (Webb, 1999). Travers et al. (2015) also identified *Vibrio* bacteria in marine bivalves. According to Webb and Duncan (2019), stressed, moribund and dead animals sometimes showed bacteria (rods and cocci) which related to autolytic and necrotic alterations in the epithelial surfaces of gills, mantle cavity and organ surfaces within the body cavity of bivalves (*P. canaliculus*, *C. gigas*, *O. chilensis* and *M. galloprovincialis*).

Therefore, *Bonamia* parasites along with other parasites and pathogens are common in oysters and other bivalves, and they are often associated with mild infection to mass mortalities (*Bonamia* being the most important component) in marine bivalves.

3.5 Conclusions

This study confirmed the presence of *Bonamia ostreae* and determined its prevalence and abundance in different tissues of flat oysters (*Ostrea chilensis*). A modified grading scale was used to determine *B. ostreae* infection levels of oysters, as well as to provide a means of investigating *B. ostreae* disease progression. This grading scale assessed the haemocyte presence in a variety of tissues within oysters and gives an indication of *B. ostreae* infections in those sites. Oysters presented systemic *Bonamia* infection with a small number showing tissue damage or lesions. Microcells of *Bonamia* spp. were recorded within haemocytes surrounding various tissues (gills, mantle, the connective tissue around digestive tubules and haemocytes surrounding the gut) as well as in the blood spaces of gills and mantle sinuses. Diapedesis was noticed in tissues including gut epithelia, gills and mantle where haemocytes contained *B. ostreae* microcells, and suggested a route of disease transmission. *B. ostreae* infection was detected mostly in live unhealthy oysters rather than the moribund/dead oysters indicating that moribund oysters may have shed their microcells or been ill due to other factors. Prevalence of *Bucephalus longicornutus*, APX, *Microsporidium rapuae*, Gymnophallid-like metacercaria, IMCs, copepods and other bacteria was also recorded. This study demonstrated an association or interaction between the infection of *B. ostreae* and the infection of *B. longicornutus* and APX in oysters. These findings provide new insights into *B. ostreae* disease development, host-parasite interactions, and transmission mechanisms in *O. chilensis* and may assist with disease management strategies for the wild harvest and future aquaculture industries.

Chapter 4

Perkinsus olseni and other parasites and abnormal tissue structures in New Zealand Greenshell™ mussels (*Perna canaliculus*) across different seasons



New Zealand Greenshell™ mussels (*Perna canaliculus*)

Abstract: The New Zealand Greenshell™ mussel (*Perna canaliculus*) supports the largest aquaculture industry in the country. However, summer mortality events and potential disease outbreaks may threaten the growth of this industry. As an approach to gauging potential threats through the seasons, a detailed histopathological examination was conducted on 256 adult cultured mussels, collected from a farm between April 2018 to September 2019, which covered the austral autumn, winter, spring and summer seasons. Histological sections followed by confirmatory *in situ* hybridization (ISH) resulted in the identification of *Perkinsus olseni* at an overall prevalence of 56%. Other parasites and pathogens were identified by histology: apicomplexan parasite X (APX) (78%), copepods (*Pseudomyicola spinosus* or *Lichomolgus uncus*) (1%), *Microsporidium rapuae* (1%), intracellular microcolonies of bacteria (IMCs) (2%) and, bacilli and cocci bacteria (4%) in gills, mantle, gonads, digestive epithelium and digestive tubules. There was a significant association between *P. olseni* and APX infection in mussels. This is the first report on seasonal variations of *P. olseni* and APX in New Zealand Greenshell™ mussels. There was a significant association between seasons and the presence of *P. olseni* and APX in mussels. A significant positive association between the brown material accumulation and parasites (*P. olseni* and APX) and between haemocytosis and *P. olseni* infections were recorded. A significant association between presence of parasites and health condition (healthy and unhealthy) of mussels was observed. Moreover, a significant association between digestive tubule deterioration (large lumen, with a thin epithelial wall) and *P. olseni* infection was noted. Therefore, this study provides information regarding the infections of potential parasites and pathogens for the first time in *P. canaliculus*, their seasonal variations and host-parasite interactions within a commercial farm.

4.1 Introduction

New Zealand Greenshell™ mussels (*Perna canaliculus*) are endemic to New Zealand and support the largest aquaculture industry in the country. Unlike other shellfish species, both cultured and wild Greenshell™ mussels have had relatively few disease issues (Castinel et al., 2019), but they are affected by several pathogens and parasites; including *Vibrio* spp. (Kesarcodi-Watson et al., 2009a, b), digestive epithelial virosis (Diggles et al., 2002a), *Microsporidium rapuae* and *Bucephalus* spp. (Castinel et al., 2019; Webb, 2008), *Tergestia agnostomi* (Jones, 1975), rickettsiae and apicomplexan parasite X (Hine, 2002a, b; Webb, 2013), and *Perkinsus olseni* (OIE, 2017; Webb & Duncan, 2019). Among them, the main pathogens and parasites of interest are *P. olseni* and APX, affecting these mussels (OIE, 2017; Suong, 2018).

P. olseni is a significant parasite associated with inflammatory responses and mass mortalities, in *Haliotis laevigata* (Goggin & Lester, 1995), where the presence of this parasite has just been reported for the first time in farmed *P. canaliculus* from the top of the South Island in New Zealand in 2014 (OIE, 2017), then in 2018 (Webb & Duncan, 2019). *Perkinsus* spp. (*P. olseni* and *P. marinus*) affect a variety of bivalve species around the world and are linked with severe mortalities (Ramilo et al., 2015; Villalba et al., 2011). Heavy *Perkinsus* spp. (*P. marinus*) infection results in the accumulation of massive haemocyte accumulation in epithelia, connective tissue, muscle fibres and blood spaces close to the parasite (Villalba et al., 2004). Moreover, the haemocytes phagocytose *P. marinus* cells and the phagocytosed parasites multiply inside the haemocytes causing them to rupture (Villalba et al., 2004). Therefore, *P. marinus* are involved with tissue damage and deformation of infected organs (La Peyre et al., 1995; Mackin, 1951; Perkins, 1996), and may eventually lead to organic abnormalities and death (Choi & Park, 2010). Mortalities associated with *P. olseni* infection are especially acute when environmental circumstances (e.g., elevated temperatures, increased salinity, host density) are favourable for the proliferation, activity (e.g., cell division, metabolism, reproduction) and transmission of the parasite (Park & Choi, 2001; Soudant et al., 2013; Villalba et al., 2004). Furthermore, studies reported the influence of temperature in the occurrence of annual patterns of perkinsosis (diseases caused by *P. olseni* and *P. marinus*) in the clam *Tapes decussatus* (Casas, 2002). Although some studies have focused on the annual and seasonal patterns of *P. olseni* infections in clams (*Ruditapes philippinarum* and *T. decussatus*) (Casas, 2002; Dang et al., 2010; Lassalle et al., 2007; Villalba et al., 2005), there is no information on infection by *P. olseni* and its seasonal variations in mussels (*P. canaliculus*).

Another potential parasite of New Zealand shellfish is apicomplexan X (APX), which is endemic to New Zealand and reported in different bivalves, such as *Ostrea chilensis* (Diggles et al., 2002a;

Hine, 2002a), *P. canaliculus* (Suong, 2018; Suong et al., 2019; Webb, 2013), *Mytilus galloprovincialis* and *Modiolus areolatus* (Suong, 2018; Suong et al., 2019). APX is often seen in the haemolymph sinuses and supra branchial sinuses of flat oysters, *Ostrea chilensis* (Hine, 2002a), but lesions are noticed in the digestive tract, gills and mantle with associated mortalities in acute APX infections (Hine, 2002a; Webb & Duncan, 2019). In addition, heavy infections of APX in flat oysters are related to the destruction of haemocytes and connective tissue (Hine, 2002a), and the depletion of host glycogen (Hine, 2002a; Suong, 2018). Furthermore, APX zoites frequently cause severe infection in oysters during the peak spawning period (summer or autumn) (Hine, 2002a). While seasonal changes of APX infection in New Zealand oyster *Ostrea chilensis* have been reported (Hine, 2002a), such studies on the mussel *P. canaliculus* are lacking.

Observations of inflammatory responses, tissues damages, or abnormal tissue morphologies in histology can be the signs of pathogenic and parasitic infection in shellfish. Inflammatory responses following pathogenic and parasitic infections, such as those caused by *Perkinsus* spp. are local defence reactions in host tissues (Cone, 2001; Choi & Park, 2010). The inflammatory response may be seen as abnormally elevated numbers of haemocytes in a tissue area (haemocytosis). This accumulation of haemocytes has been described as an attempt by the host to destroy, dilute or isolate the invading factors (Sparks, 1972). Another immunological tissue response is the presence of brownish-yellow pigmentation, (ceroid material or lipofuscin) frequently observed across tissues in many molluscan species (Webb & Duncan, 2019) and generally occurs in the vicinity of parasites, such as APX (Webb & Duncan, 2019). This brownish-yellow pigment is also associated with inflammation and contamination or necrotic lesions in *Crassostrea virginica* (Wood & Yasutake, 1956; Zaroogian & Yevich, 1993).

In addition to the occurrence of known pathogens and parasites, other conditions are also encountered in shellfish, including digestive gland and gill pathology caused by pathogens and parasites (*Perkinsus*) (Lee et al., 2001; Choi & Park, 2010). Digestive gland pathologies, such as abnormal tubule structures and lumen modifications, including thinning, sloughing and damage were seen in other bivalves *Cardium edule*, *Crassostrea virginica* and *Mytilus galloprovincialis* (Carella et al., 2015a; Morton, 1970; Winstead, 1995, 1998) have also been observed in *P. canaliculus* (Webb & Duncan, 2019). These digestive tubule abnormalities and morphological changes may occur during the digestive process or under stress conditions, such as changes in the food supply, starvation, or exposure to pollutants and biotoxins (Ellis et al., 1998; Rolton et al., 2019; Smolowitz & Shumway, 1997). The pathological changes in the digestive gland of the mussel (*Crenomytilus grayanus*) may be caused by chronic pollution and parasitic infestation (Usheva et

al., 2006), and affect the absorptive capacity of the digestive system. Another condition where causality is usually uncertain is the pathology of the gills, such as epithelial erosion, loss of cilia (Webb & Duncan, 2019) and alterations in the ciliary disks (the attachment connecting gill filaments laterally along their length) (Sunila & Lindstrom, 1985) which are common in aquaculture species. Depending on the level of the erosion and the extent of the obstructed area, the erosion of the gill epithelial cells could disrupt respiratory function (Webb & Duncan, 2019). In addition, the ciliary disks prevent gill filaments from separating in the mussels (de Oliveira David et al., 2008). Therefore, alterations in the ciliary disks of mussels will cause the gill filaments to separate and may lead to the disruption of the entire gill structure (de Oliveira David et al., 2008).

It is well known that seasonal temperature changes have a significant impact on the pathogen and parasite load in bivalves (Aagesen & Häse, 2014; Malham et al., 2009; Viergutz et al., 2012). Some parasites show positive responses to increases in temperature, including the increased transmission of parasites between hosts (Mouritsen & Jensen, 1997; Moore et al., 2000; Poulin, 2006) and can modify host-parasite interactions (Malek & Byers, 2018). Furthermore, a parasite such as *P. marinus* may expand its geographical range due to climate-induced rises in winter water temperatures (Ford & Chintala, 2006; Ford & Smolowitz, 2007). Although such increasing water temperatures have been reported to be associated with massive mortalities in *P. canaliculus* during summer (Dunphy et al., 2015), little is known about the relationship between seasonal temperature changes and parasitic and pathogenic infections in this species.

This study reports on presence of parasites and health conditions in *Perna canaliculus* collected from Kaiāua mussel farms. In this study, a detailed histopathological examination of a targeted survey/sampling of farmed mussels (*P. canaliculus*) was undertaken to identify potential pathogens and parasites and their seasonal variations, as well as to study the immunological tissue responses to pathogens and parasites to gauging potential threats (summer mortality events and potential disease outbreaks) at the farms. The prevalence and abundance of parasites (e.g., trophozoites of *Perkinsus olseni*, zoites of APX), inflammatory tissue responses (haemocytosis, ceroid material) and abnormal tissue structures (especially in the gills and digestive tubules caused by pathogens and parasites) which are indicative of host health condition (Howard et al., 2004), were assessed with quantitative and semi-quantitative approaches.

4.2 Materials and methods

4.2.1 Sample collection, Histology and In-situ hybridization (ISH)

A total of 256 adult (2 years old) mussels (shell size ranging from 69.2 to 121 mm, mean \pm SE of 94.2 \pm 0.9 mm), from the same batch of seed were obtained from Kaiaua mussel farms (Whakatiwai, New Zealand: 37°02' 51.2" S 175°18'56.1" E) between April 2018 to September 2019 (20 samples each month were collected randomly) and transported to the Auckland University of Technology (AUT) laboratory, Auckland, New Zealand. The monthly sampling covered the austral summer (average temperature 21°C; months: December, January, February), autumn (average temperature 17°C; months: March, April, May), winter (average temperature 12°C; months: June, July, August) and spring (average temperature 14°C; months: September, October, November).

On arrival, specimens were processed on the same day. After measuring the weight and shell length, specimens were shucked and the soft parts sectioned to give a 2–5 mm thick tissue slice (Howard et al., 2004) followed by standard histological processing (OIE, 2016). The tissue slices were placed in histological cassettes, fixed in 4% formalin (1-part concentrated formalin solution plus 9 parts filtered seawater) for 48 h, then stored in 70% ethanol and processed for paraffin histology (Luna, 1968). Specimens were dehydrated in a series of ascending ethanol concentrations with two changes of xylene and then embedded in paraffin wax. Sections of 5 μ m were obtained using a microtome. Slides with adhering tissue sections were dewaxed in xylene and then rehydrated through a descending series of ethanol concentrations followed by distilled water. Slides were stained with regressive Mayer's haematoxylin and eosin (H&E) stains, rinsed with deionized water and then taken through an ascending series of ethanol concentrations. After that, slides were rinsed in two changes of xylene. Then, DPX mountant was used to seal glass coverslips over the sections.

4.2.2 Quantitative and semi-quantitative evaluation of parasite infections, inflammatory tissue responses and abnormal tissue structures

The relative abundance of *P. olsenii* was evaluated by a semi-quantitative grading scale modified from Ray's scale (1954) and adapted by da Silva et al. (2013). Ray's scale (1954) estimated the intensity of infection in cultured tissues and the scale of da Silva et al. (2013) estimated the intensity of infection with *Perkinsus* spp. from the tissues stained with Lugol's solution (diagnosed *Perkinsus* spp. by Ray's fluid thioglycollate medium). Thus, a modified scale was used in this study to evaluate *P. olsenii* infection of histological sections (Table 4.1). Since the scale (0-4) modified from Ray's scale was not suitable for evaluating the abundance of APX, another grading scale (0-

5) modified by Hine (2002b) was used in this study to assess the relative abundance of APX [Hine's scale classified APX infected oysters into one to five grades of the intensity of infection]. Although Hine's scale evaluated APX infection from histological sections, observed parasites (zoites) numbers were not included in that grading scale (1-5). In this modified grading scheme (0-5) for APX infection, observed parasites (zoites) number for each scale were mentioned (Table 4.2). In the current study, the semi-quantitative grading scales were based on grading from 0 (indicating no infection) to 4 (indicating a high level of infection) for *P. olsenii* and from 0 (indicating no infection) to 5 (indicating a high level of infection) for APX.

Table 4.1 Whole animal grading for *P. olsenii* infection (for each mussel, 10 random fields for each tissue were examined at 100× magnification).

Score	Grading scale	Description
0	Null infection	No trophozoites observed after extensive searching of all tissues for 5 minutes per slide
1	Very light infection	Up to 10 trophozoites (in total) observed after extensive searching of all tissues (5 minutes)
2	Light infection	11-20 trophozoites observed per tissue
3	Moderate infection	>20-40 trophozoites readily observed in all tissues, scattered throughout the slide
4	Heavy infection	>40 trophozoites present in all tissues

Table 4.2 Whole animal grading for APX infection (for each mussel, 10 random fields for each tissue were examined at 100× magnification).

Score	Grading scale	Description
0	Null infection	No parasites (zoites) observed after extensive searching of all tissues for 5 minutes per slide
1	Light infection	A few (<5) parasites (zoites) present (in total), only observed after extensive searching of all tissues (5 minutes)
2	Light to moderate infection	>5-20 parasites (zoites) observed per tissue
3	Moderate infection	>20-40 parasites (zoites) readily observed in all tissues, scattered throughout the slide
4	Moderate to heavy	>40-100 parasites (zoites) present in all tissues
5	Heavy infection	>100 parasites (zoites) present, and tissues congested

The abundance of *P. olsenii* and APX for different tissues, including gills, mantle, the connective tissue around digestive tubules, gonads and digestive epithelium was evaluated with a grading scale from 0 to 4 (Table 4.3). Hine's (2002b) scheme recorded the distribution of APX zoites in different areas (tissues) of the oyster (*Ostrea chilensis*) at different levels of intensity (Grades 1-5) of

infection. Observed parasites (zoites) numbers were not included in Hine’s scale. However, in this modified grading scheme (0-4) for APX infection and (0-3) for *P. olseni* infection, observed parasites (trophozoites or zoites) number per tissue of mussels for each scale were mentioned (Table 4.3). Therefore, this modified scheme is more appropriate for evaluating tissue grading of *P. olseni* and APX infection in New Zealand Greenshell™ mussel (*Perna canaliculus*).

Table 4.3 Tissue grading for *P. olseni* (0-3) and APX (0-4) infection (for each mussel, 10 random fields for each tissue were examined at 100× magnification).

Score	Grading scale	Description
0	Null infection	Parasites (trophozoites/zoites) absent in tissue
1	Low infection	1-5 parasites (trophozoites/zoites) present per tissue
2	Medium infection	>5-20 parasites (trophozoites/zoites) present per tissue
3	High infection	>20-40 parasites (trophozoites/zoites) present per tissue
4	Extremely high infection	>40 parasites (zoites) present per tissue

4.2.3 Inflammatory responses

Inflammatory responses, such as haemocytosis and ceroid material in gills, mantle, and the connective tissue around digestive tubules, gonads and digestive epithelium were evaluated semi-quantitatively on a scale of 1-3, where Grade 1 = Light (few, <30 haemocytes per field at 40× magnification), Grade 2 = Moderate (medium number, 31-200 of haemocytes per field at 40× magnification), and Grade 3 = Heavy (high number, >200-500 of haemocytes per field at 40× magnification). All samples had some presence of haemocytes as this is the normal condition. Haemocyte proliferation (diffuse and focal hemocytosis) in blood spaces and tissues were observed. In *P. canaliculus*, hemocytosis can be a sign of infection by parasites (copepods or *Perkinsus*) (Webb & Duncan, 2019) and heavy haemocytosis might be indicative of health problems.

A semi-quantitative scale of 1-3 was also applied to the amount of observed inflammatory response in the form of ceroid material, where Grade 1 = Light (low concentration of ceroid material), Grade 2 = Moderate (medium concentration of ceroid material) and Grade 3 = Heavy (high concentration of ceroid material) (Muznebin et al., 2021). Ceroid material is often recognized as intra and extracellular granules associated with haemocytes (granulocytes and hyalinocytes) and may indicate an immune response (Webb & Duncan, 2019).

4.2.4 Tissue conditions

Digestive tubule structures and gill structures were also assessed semi-quantitatively (Table 4.4, 4.5).

4.2.4.1 Digestive tubule structures

A grading scale (1-4) was applied for evaluating digestive tubule structures, where Grade 1 = Very healthy, Grade 2 = Healthy to fair, Grade 3 = Poor and Grade 4 = Very poor (Table 4.4) [D1-D4 stand for the grading scale of digestive tubule pathology].

Table 4. 4 Grading for digestive tubule structures (Fig. 4.14A-D).

Score	Grading scale	Description
1	Very healthy	Normal, cruciform or Y shaped lumen (D1) (Fig. 4.14A)
2	Healthy to fair	Normal lumen but sloughed epithelial cells inside lumen (D2) (Fig. 4.14B)
3	Poor	Small or no lumen (D3) (Fig. 4.14C)
4	Very poor	Large lumen, with a thin epithelial wall (D4) (Fig. 4.14D)

4.2.4.2. Gill structures

A typical arrangement of mussel gills is composed of ascending and descending lamellae (Sunila & Lindström, 1985). Each gill lamellae consisted of filaments that have three different zones: frontal, intermediate and abfrontal (Gregory et al., 1996). The frontal zone differs from other zones by the presence of ciliated cells. Filaments are laterally joined along their length at regular intervals by discrete ciliary discs or ciliary junctions. Ciliary discs are formed by condensed tufts of simple cilia, which are fixed from a base extended from the latero-abfrontal surfaces of the lamellae (Akşit & Mutaf, 2014; Gregory et al., 1996). Interfilamentar junctions break up can occur either in a mechanical or chemical method (Sunila & Lindström, 1985). The ciliary discs of an interfilamentar junction can be changed and separated by the exposure of copper or cadmium (Sunila & Lindström, 1985). In this study, ciliary discs of *Perna canaliculus* can be atrophied or separated due to infection of parasites and might be indicative of health issues.

Gill structures were evaluated by a semi-quantitative grading scale (1-3), where Grade 1 = Healthy, Grade 2 = Fair and Grade 3 = Poor (Table 4.5).

[C1-C3 stand for the grading scale of gill pathology]

Table 4.5 Grading for gill structures (Fig. 4.15A-D).

Score	Grading scale	Description
1	Healthy	Normal structure with ciliated lateral cilia in the frontal zone, with ciliary discs in the abfrontal zone of gill filament and a medium number of haemocytes in the gill haemolymph space (G1) (Fig. 4.15A, B & C)

2	Fair	Ciliary discs appear in the abfrontal zone and destroyed/broken epithelium of gill filament and with few haemocytes in the gill haemolymph space (G2) (Fig. 4.15D)
3	Poor	Without ciliated lateral cilia, ciliary discs are atrophied/separated in the abfrontal zone of gill filament and very few haemocytes in the gill haemolymphspace (G3) (Fig. 4.15E & F)

4.2.5 Statistical analyses

Statistical analyses were performed using Pearson's chi-square test with IBM® SPSS® Statistics software (version 23). Pearson's chi-square test statistics and the associated p-values were applied for the comparisons between seasons and parasites, the association between *P. olseni* and APX infection, the association between haemocytosis and parasites infection and the association between tissue conditions and parasites infection and the association between health conditions and parasite infections. Prevalence of parasites and season* year were analyzed via two-way ANOVA. Associations were statistically significant at $p < 0.05$.

4.3 Results

4.3.1 Epidemiological parameters of *P. olseni* infection

Histological sections, followed by confirmatory *in situ* hybridization (ISH), resulted in the identification of *Perkinsus olseni* at an overall prevalence of 56%. Most *P. olseni* infected mussels were in whole animal grade 1 (prevalence 45%, $n = 112$), whereas, 0.4% ($n = 1$) were determined as grade 4.

Trophozoites of *P. olseni* were observed in the connective tissue surrounding the digestive tract epithelium, digestive tubules and gonads. They were also seen in the blood space of gills and outside the gill epithelium, in the space between digestive tubules, mantle, and adductor muscle (Fig. 4.17). Most organs/tissues showed a low prevalence (2-25%) of *P. olseni*. In gills, 20% of the mussels were infected with *P. olseni* at level 1. In the mantle, 10% of mussels showed *P. olseni* infection at grade 1 and 1% were suffering from a severe infection at grade 3. In the connective tissue around digestive tubules, 30% and 9% of the mussels were infected with *P. olseni* at grades 1 and 2, respectively. 13-15% of the mussels presented infection by *P. olseni* at grade 1 in the connective tissue surrounding digestive epithelium and gonads (Fig. 4.1).

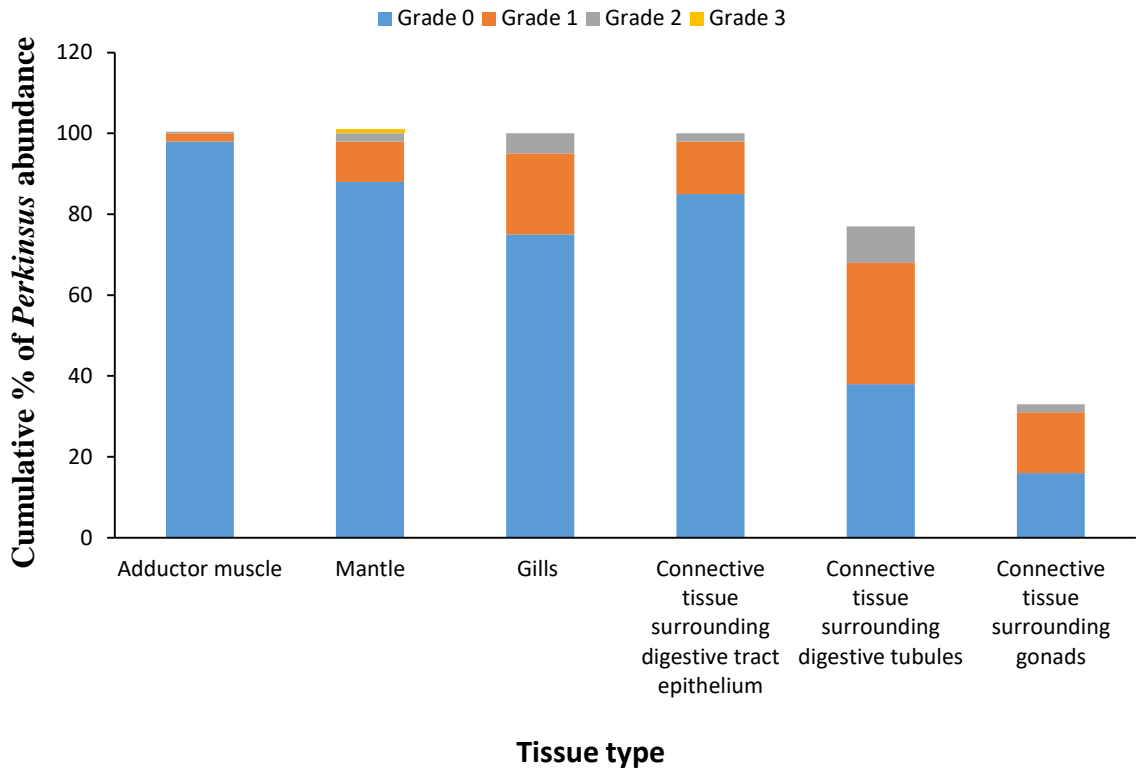


Figure 4.1 Cumulative percentage of *P. olseni* abundance grading (0-3) of mussels in different tissues, N = 256 (abundance here applied only to organs/tissues rather than the whole mussel).

The highest prevalence (80%-95%) of mussels with *P. olseni* infection was recorded in March 2019, May 2019 and July 2019, respectively (Table 4.6).

Table 4.6 Prevalence of *P. olseni* associated with mussels in different months [n = number of mussels infected with parasites]

Months & Years	Sample/mussels examined (N)	<i>Perkinsus olseni</i> prevalence (%)	<i>Perkinsus olseni</i> frequency (n)
Apr. 2018	18	50	9
May 2018	20	45	9
July 2018	20	15	3
Oct. 2018	20	65	13
Nov. 2018	20	60	12
Jan. 2019	20	35	7
Feb. 2019	20	70	14
Mar. 2019	20	95	19
May 2019	18	80	16
June 2019	20	75	15

July 2019	20	80	16
Aug. 2019	20	30	6
Sep. 2019	20	35	7

A high number (60-61%) of mussels showed *P. olsenii* infection at grade 1 in October 2018, March 2019, May 2019, June 2019 and July 2019 (Fig. 4.2).

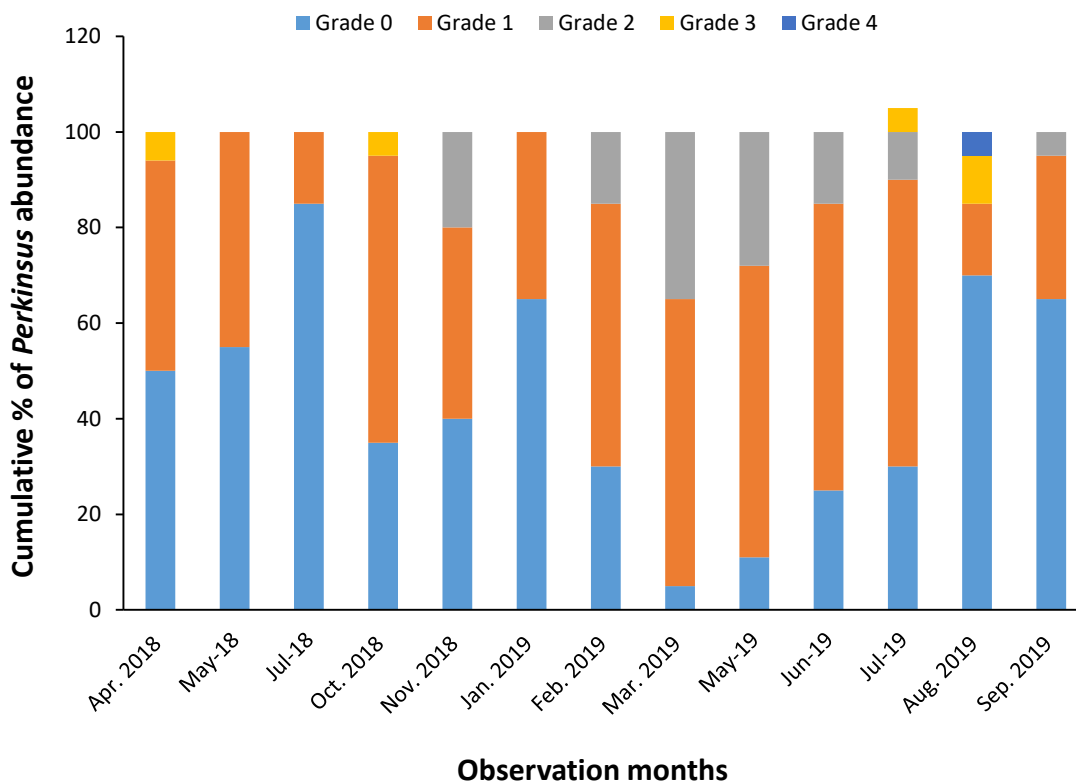


Figure 4.2 Cumulative percentage of *P. olsenii* abundance grading (whole animal grading = 0-4) of mussels in different months.

The highest prevalence (70%, n = 53) of mussels with *P. olsenii* infection was recorded in autumn. 53% of mussels presented with *P. olsenii* infection in both spring and summer (Fig. 4.3).

A Pearson's chi-square test resulted in a significant association between seasons (summer, winter, spring and autumn) and the presence of *P. olsenii* in mussels (p -value = 0.029). The prevalence of *P. olsenii* in summer, winter and spring are the same. However, the prevalence of *P. olsenii* in autumn was significantly higher than in the other three seasons. A significant (p -value = 0.004) number of

P. olseni was detected in mussels in both years (2018 and 2019) and seasons (summer, winter, spring and autumn) (2-way ANOVA's).

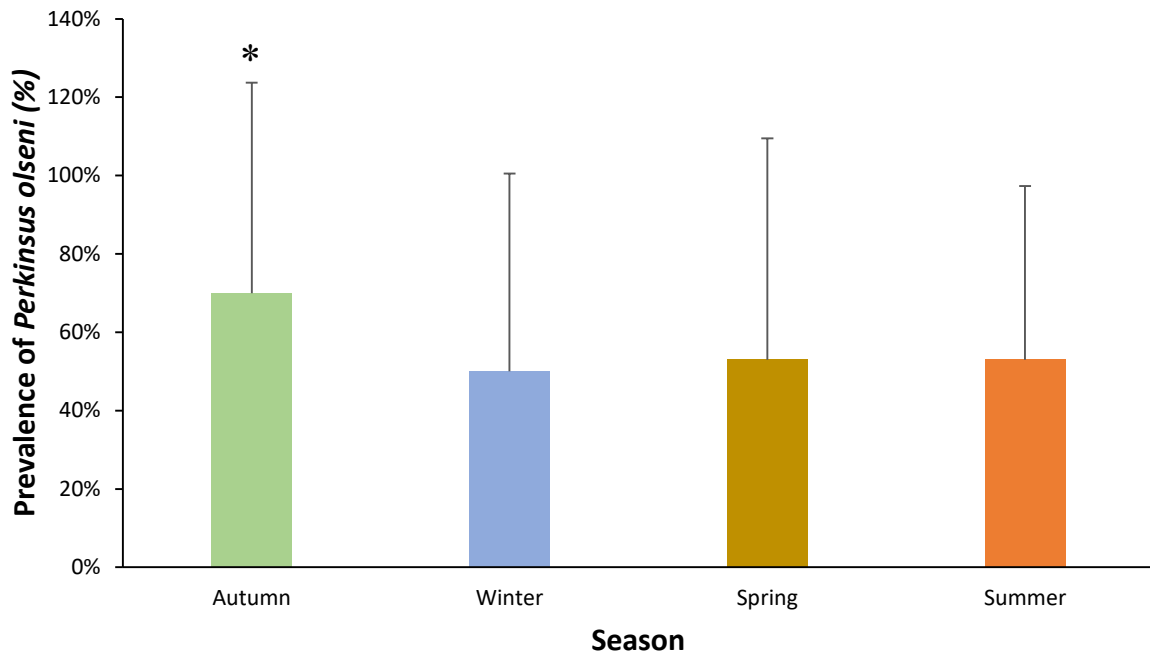


Figure 4.3 Mean prevalence (\pm SE) of *P. olseni* in summer, winter, spring and autumn. [summer (n = 40), winter (n = 80), spring (n = 60), autumn (n = 76)].

In autumn, mussel samples presented a high abundance (n = 40, 53%) of *P. olseni* with grade 1 (very light infection) and 16% of the mussels (n = 12) presented *P. olseni* abundance with grade 2. 8% (n = 6) of the mussels showed a mild infection (grade 2) by *P. olseni* in winter, spring and summer. In winter, 4% (n = 3) of mussels were infected with *P. olseni* at a medium level (grade 3). In contrast, grade 3 infection of *P. olseni* in mussel samples was not recorded during the summer. The severe infection of *P. olseni* (grade 4) in mussels was only noticed in winter (Fig. 4.4).

There was no significant association between seasons (summer, winter, spring and autumn) and *P. olseni* abundance gradings (0-4) in mussels (Pearson's chi-square test, p -value = 0.233).

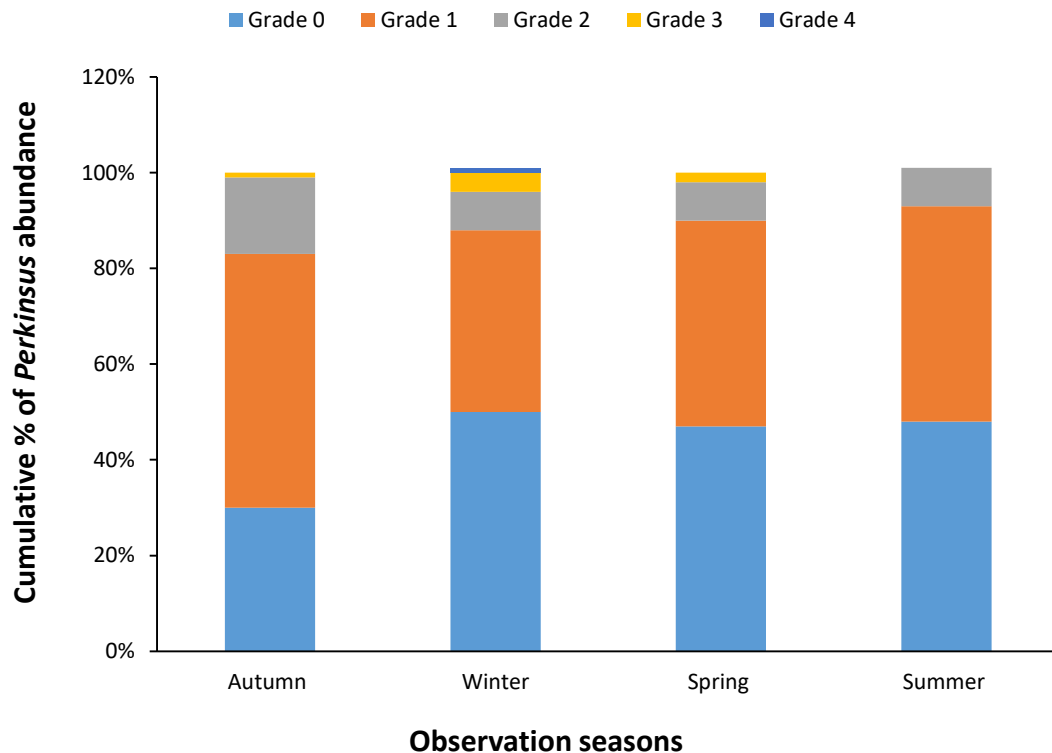


Figure 4.4 Cumulative percentage of *P. olseni* abundance grading (0-4) of mussels in different seasons (summer, winter, spring and autumn) [summer (n = 40), winter (n = 80), spring (n = 60, autumn (n = 76)].

4.3.2 Epidemiological parameters of APX infection

Out of total 256 mussel analyzed, 78% (n = 199) were APX positive. Most APX-infected mussels were in whole animal grade 2 (prevalence 27% [This is prevalence of the infection at this grade], n = 68) and only 2% (n = 4) had severe infection with abundance at grade 5. 26% of mussels (n = 67) were at APX abundance grade 1 and 22% (n = 57) had no observable APX infection (whole animal abundance grade 0).

Individual tissue grade 0 (null infection) with APX in the gills, mantle, adductor muscle, the connective tissue surrounding digestive tract epithelium, digestive tubules and gonads were observed from 45-79% mussels. For 31-37% of APX infected mussels with abundance grade 1, infections were observed in the mantle, and the connective tissue surrounding digestive tract epithelium and gonads. On the other hand, only 0.4% (n = 1)-1% (n = 3) of mussels presented a

tissue grade 4 (extremely high) infection of APX in the mantle and the connective tissue around digestive tubules and digestive epithelium. 3% of mussels was suffering from a high infection of APX with individual tissue grade 3 in the mantle and the connective tissue around digestive tubules (Fig. 4.5).

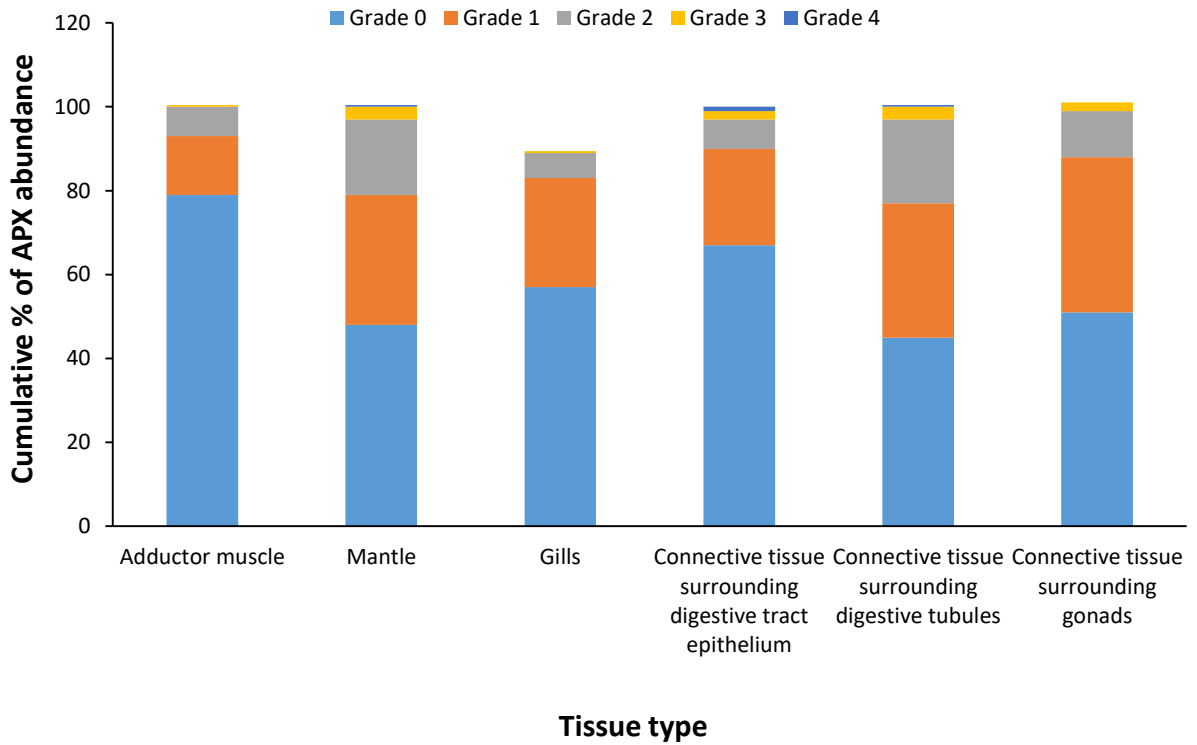


Figure 4.5 Cumulative percentage of APX abundance grading (0-4) of mussels in different tissues, N = 256 (abundance here applied only to organs/tissues rather than the whole mussels).

The highest prevalence (100%) of mussels with APX infection was observed in June 2019, August 2019 and September 2019 (Table 4.7).

Table 4.7 Prevalence of APX associated with mussels in different months [n = number of mussels infected with parasites].

Months & Years	Sample/mussels examined (N)	APX prevalence (%)	APX frequency (n)
Apr. 2018	18	72	13
May 2018	20	55	11
July 2018	20	60	12
Oct. 2018	20	85	17
Nov. 2018	20	70	14

Jan. 2019	20	65	13
Feb. 2019	20	45	9
Mar. 2019	20	75	15
May 2019	18	94	17
June 2019	20	100	20
July 2019	20	90	18
Aug. 2019	20	100	20
Sep. 2019	20	100	20

The highest prevalence (88%, $n = 70$) of mussels with APX infection was noted in winter. On the other hand, only 55% of mussels had APX infection in summer, a lower percentage than in other seasons (Fig. 4.6).

There was a highly significant association between seasons (summer, winter, spring and autumn) and the presence of APX in mussels (Pearson's chi-square test, p -value < 0.001). The prevalence of APX in winter and spring was almost the same. However, the prevalence of APX in autumn and summer was different from each other and also from the other two seasons. A significant ($p = 0.004$) number of APX was detected in mussels in both years (2018 and 2019) and seasons (summer, winter, spring and autumn) (2-way ANOVA).

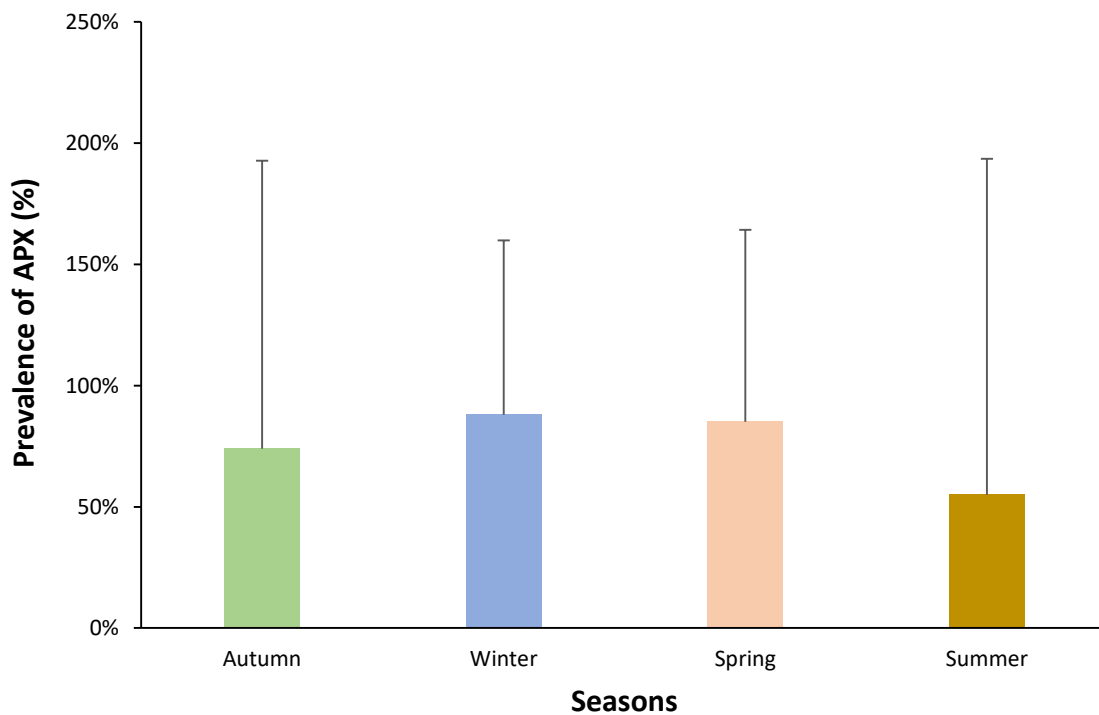


Figure 4.6 Mean prevalence (\pm SE) of APX in summer, winter, spring and autumn. [summer (n = 40), winter (n = 80), spring (n = 60), autumn (n = 76)].

A high number (45%) of mussels with heavy APX infection at whole animal grade 4 were recorded in June 2019. 50% mussels infected with APX abundance grade 3 in July 2019. The highest number of mussels (60%) with APX abundance whole animal grade 2 was found in September 2019. A higher number (55%) of mussels had no observable APX infection (grade 0) in February 2019. 55% of mussels presented with APX abundance grade 1 in March 2019. Mussels with medium to heavy (grade 3-grade 5) infection of APX was recorded in May 2019, June 2019, July 2019 and August 2019 (Fig. 4.7).

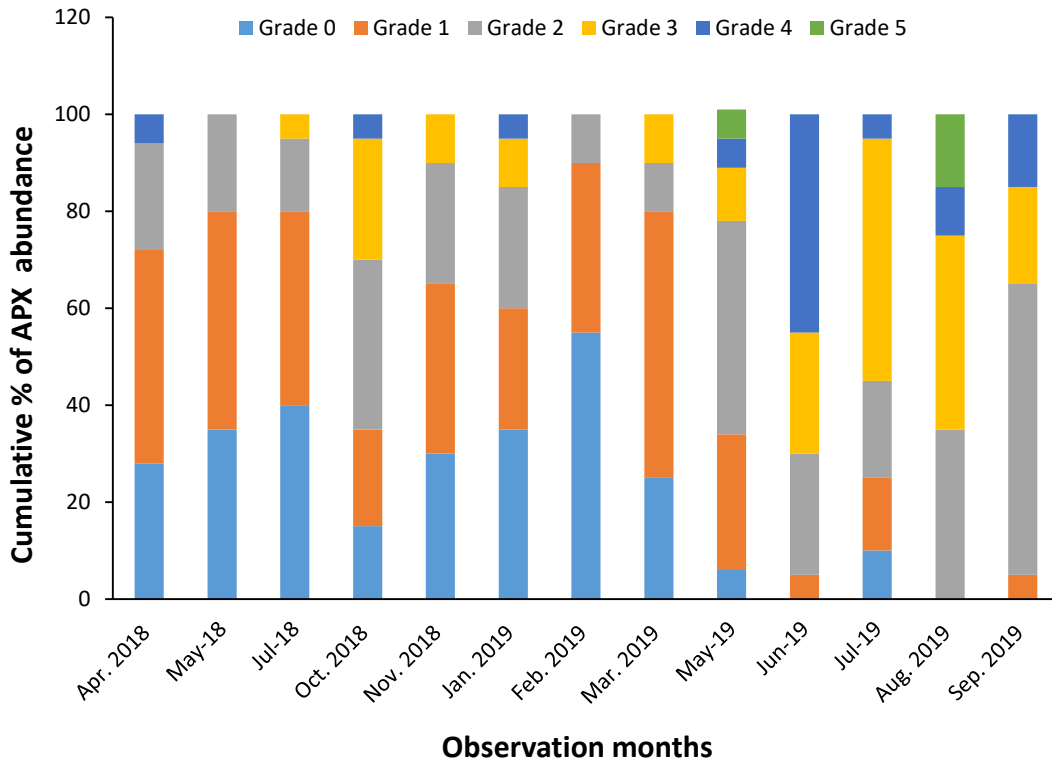


Figure 4.7 Cumulative percentage of APX abundance grading (whole animal grading = 0-5) of mussels in different months

In summer, 45% of the mussels (n = 18) had no observable APX infection (grade 0). On the other hand, 40-43% of mussels presented with an APX abundance at grade 1 in autumn and grade 2 in spring. 4% (n = 3) and 1% (n = 1) of the mussels were infected with a severe APX infection

(abundance grade 5) in winter and autumn respectively. In the winter season, 15% of the mussels (n = 12) showed a high level (grade 4) of APX infection (Fig. 4.8).

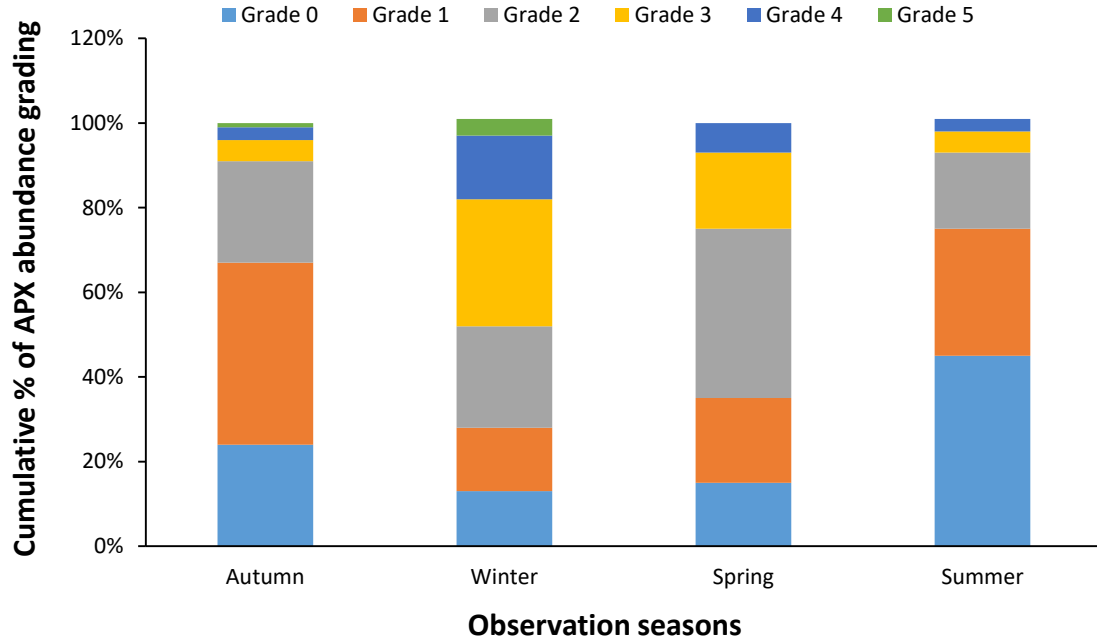


Figure 4.8 Cumulative percentage of APX abundance grading (0-5) of mussels in different seasons (summer, winter, spring and autumn). [summer (n = 40), winter (n = 80), spring (n = 60, autumn (n = 76)].

There was a highly significant association between seasons and APX abundance grading of mussels (Pearson's chi-square test, p -value < 0.001).

4.3.3. Co-infection of *P. olseni* and APX

There was a significant association between *P. olseni* and APX infection in mussels (Pearson's chi-square test, p -value < 0.017) (Table 4.8).

Table 4.8 Statistical analysis: Chi-square test for the association between *P. olseni* and APX infection in mussels.

Parasite	APX		Chi-square test for association (P -value)
	No	Yes	

<i>Perkinsus olseni</i>	Absent	32	78	0.017
	Present	25	121	

Heavily inflected *Perkinsus* mussels did not tend to carry heavy APX burdens.

4.3.4 Epidemiological parameters of other parasite infections

4% (n = 11) mussels were associated with bacteria (bacilli and cocci). On the other hand, few (1%-4%) mussels were infected with copepods (n = 2), *M. rapuae* (n = 3) and IMCs (n = 4) (Fig. 4.9).

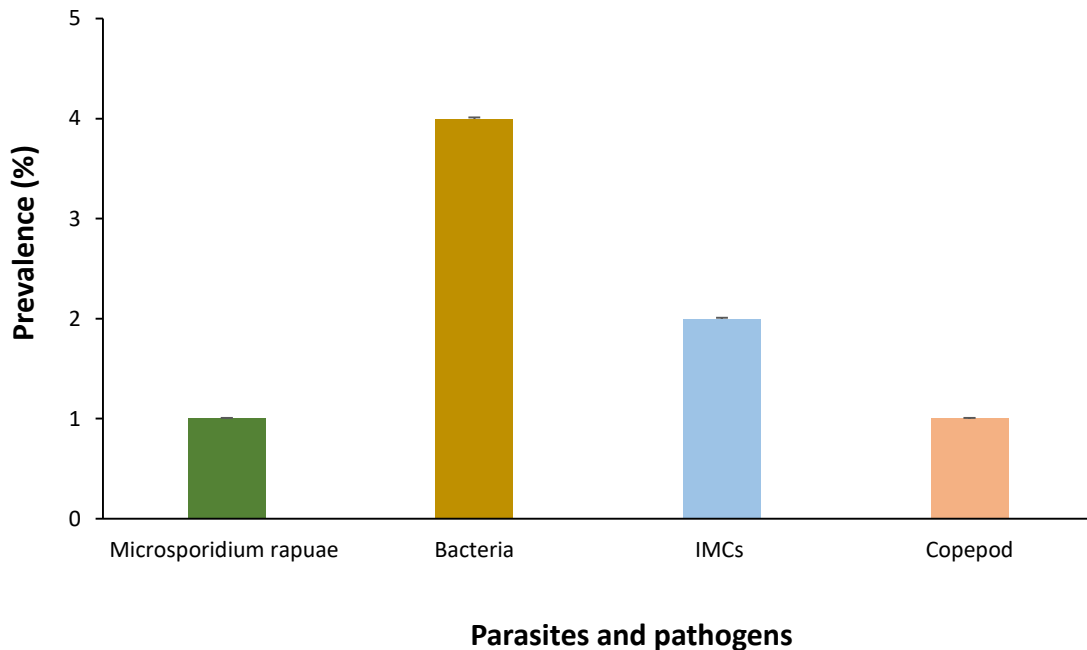


Figure 4.9 Mean prevalence (\pm SE) of parasites and microorganisms associated with mussels (per slide of the whole animal) (N = 256).

The highest prevalence of infection for most of the parasite species was recorded during September 2019, except for copepods, which were only present in June 2019. In April 2018, 28% of mussels with bacterial association were observed (Table 4.9).

All the parasites showed the same prevalence (3%, n = 2) in the winter season. However, the highest prevalence (10%) of mussels with the bacterial association was recorded in autumn. There was a significant association between seasons (summer, winter, spring and autumn) and the presence of bacteria in mussels (Pearson's chi-square test, p -value < 0.014). There was no association between seasons (summer, winter, spring and autumn) and the presence of copepods, *M. rapuae* and IMCs in mussels.

Table 4.9 Prevalence of parasites associated with mussels in different months [n = number of mussels infected with parasites].

Months & Years	Sample/mussels examined (N)	Bacteria		<i>M. rapuae</i>		IMCs		Copepod	
		n	%	n	%	n	%	n	%
Apr. 2018	18	5	28	0	0	0	0	0	0
May 2018	20	3	15	0	0	1	5	0	0
July 2018	20	0	0	1	5	0	0	0	0
Oct. 2018	20	0	0	0	0	0	0	0	0
Nov. 2018	20	0	0	0	0	0	0	0	0
Jan. 2019	20	0	0	0	0	0	0	0	0
Feb. 2019	20	0	0	0	0	0	0	0	0
Mar. 2019	20	0	0	0	0	0	0	0	0
May 2019	18	0	0	0	0	0	0	0	0
June 2019	20	0	0	1	5	2	10	2	10
July 2019	20	1	5	0	0	0	0	0	0
Aug. 2019	20	1	5	0	0	0	0	0	0
Sep. 2019	20	1	5	1	5	1	5	0	0

4.3.5 Immunological tissue responses (*Haemocytosis*)

Haemocytosis was observed in the mantle and connective tissue around digestive tubules, digestive epithelium and gonads (Fig. 4.10A-D). *P. olseni* parasites were observed associated with this response (Pearson Chi-square test, p -value = 0.03).

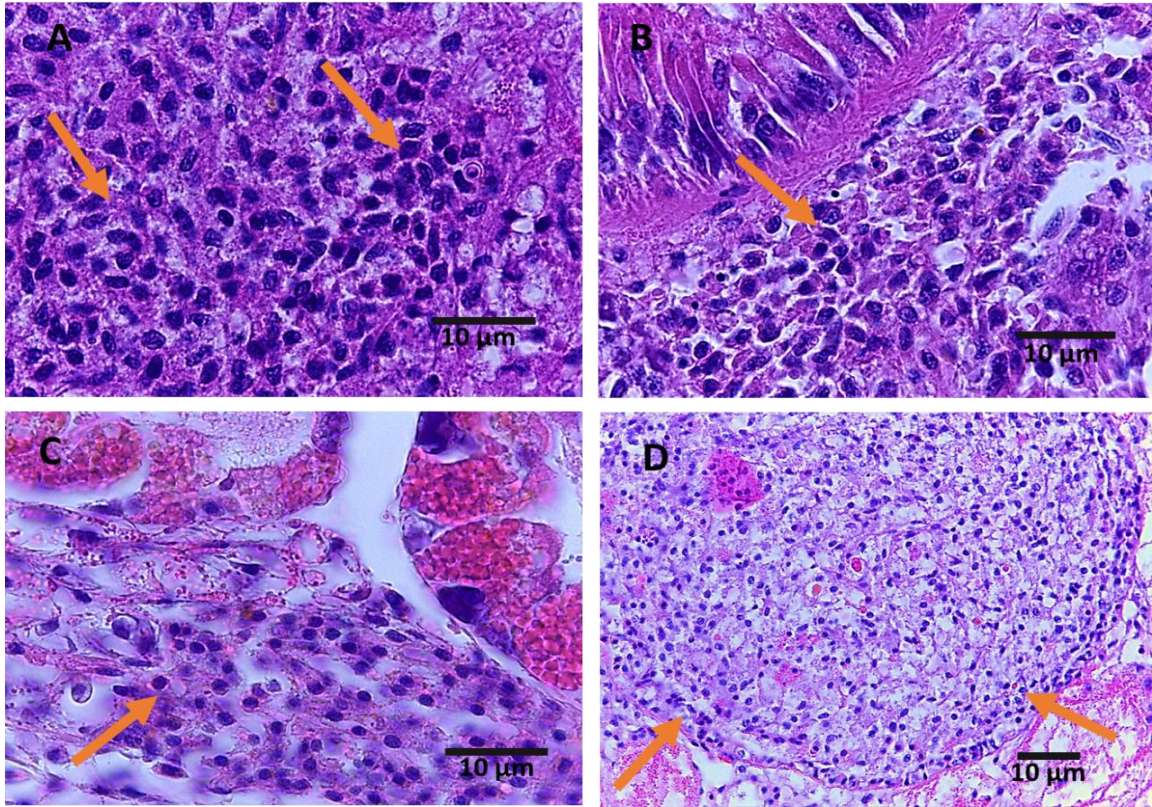


Figure 4.10 Haemocytes (orange arrows) in the different tissues of *P. canaliculus*, (A) mantle, (B) connective tissue surrounding digestive tract epithelium, (C) connective tissue surrounding digestive tubules and (D) connective tissue surrounding gonads. Scale bars = 10 µm.

Overall percentages (15-18%) of haemocytes were recorded in the mantle, and in the connective tissue around digestive tubules and gonads, whereas only 2% were observed in gills and the connective tissue surrounding the digestive epithelium of mussels.

A medium level (grade 2) of haemocytes was observed in the connective tissue surrounding digestive tubules of 68% of mussels, whereas 21% of mussels showed haemocytes at a high level (grade 3) in the connective tissue surrounding the digestive epithelium. 9-10% of mussels showed heavy haemocytes (grade 3) in the connective tissue surrounding digestive tubules, gills and mantle. 45% of mussels showed haemocytes at a low level (grade 1) in the connective tissue surrounding gonads (Fig 4.11).

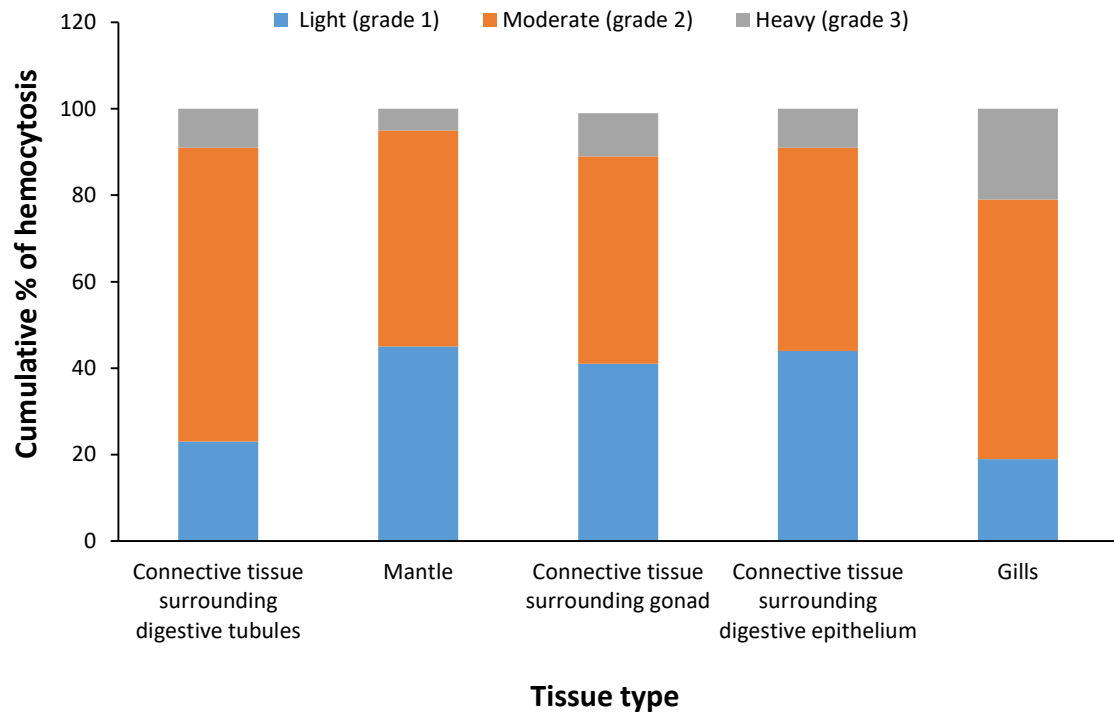


Figure 4.11 Cumulative percentage (occurrence rate) of hemocytosis grading (0-3) in different tissues of mussels, N = 256, % = occurrence rate [the term occurrence rate was used rather than prevalence to avoid confusion between organ/tissue values and prevalence].

4.3.6 Immunological tissue responses (ceroid/brown material)

Ceroid/brown material accumulation (light, moderate and heavy) was recorded in different tissues of *P. canaliculus* including the mantle, gills, and connective tissue surrounding gonads and digestive tubules (Fig. 4.12A-D). A chi-square test indicated a significant association (p -value = 0.016) between the brown material accumulation and *Perkinsus* infection. A significant association (p -value = 0.014) was also observed between the brown material accumulation and APX infection (Chi-square test). The presence of ceroid material was often noted in the tissues of mussels where APX was detected (Fig. 4.12A-D).

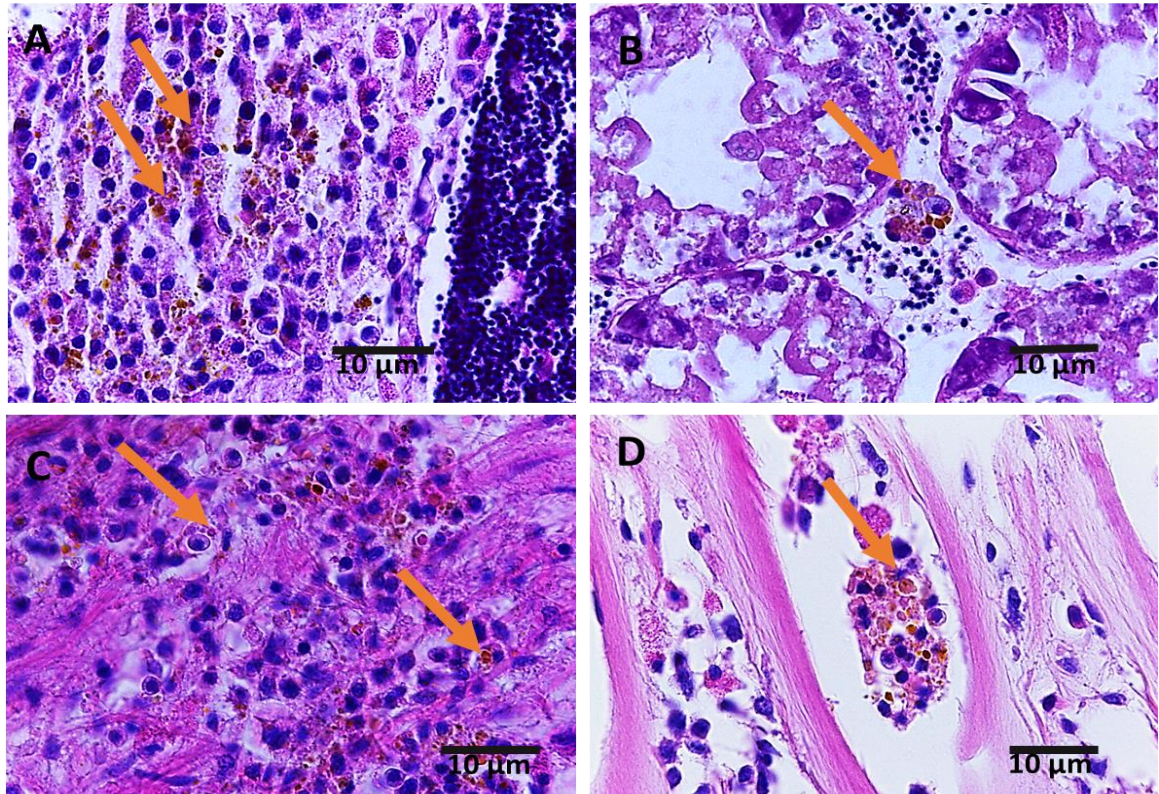


Figure 4.12 Ceroid/brown material accumulation (orange arrows) in *P. canaliculus*, (A) connective tissue surrounding gonads, (B) connective tissue surrounding digestive tubules, (C) mantle, (D) gills (blood space). Scale bars = 10 µm.

Most (70%) mussels showed ceroid material accumulation at low levels (grade 1) in gills and the connective tissue surrounding the digestive epithelium. In the connective tissue surrounding digestive tubules, 66% and 10% of mussels showed ceroid material accumulation at a medium level (grade 2) and high level (grade 3), respectively (Fig. 4.13). [Light/grade 1 = normal level].

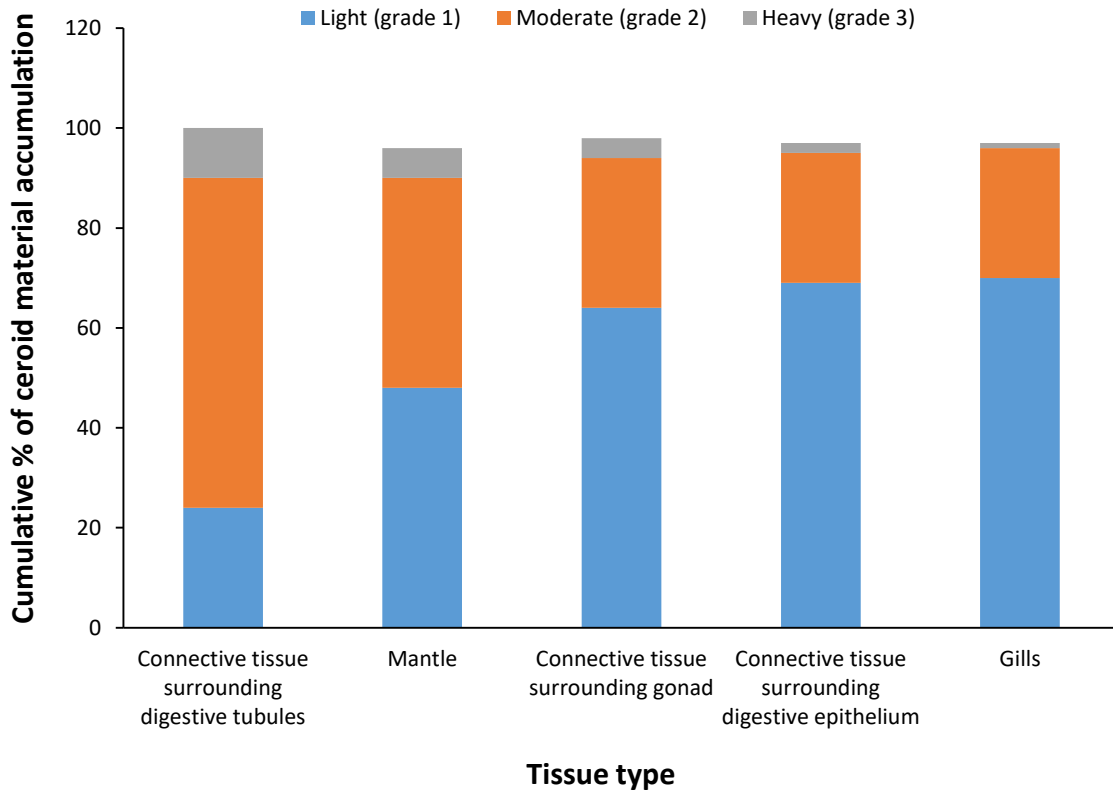


Figure 4.13 Cumulative percentage of ceroid material accumulation levels (0-3) in different tissues, N = 256, % = occurrence rate.

4.3.7 Digestive tubule structures

Most of the 256 mussel samples showed digestive tubule structures with the normal or cruciform or Y shaped lumen (D1) (n = 202, occurrence rate of 79%). However, 10% (occurrence rate) of mussels (n = 25) showed digestive tubule structure with normal lumen but sloughed epithelial cells inside lumen (D2) 18% (occurrence rate) of mussels (n = 45) showed digestive tubule structures with the large lumen, with a thin epithelial wall (D4) and small or no lumen (D3). A chi-square test indicated a highly significant association (p -value = 0.001) between digestive tubule structures and *Perkinsus* infection. However, there was an insignificant association (p -value = 0.484) between digestive tubule structures and APX infection.

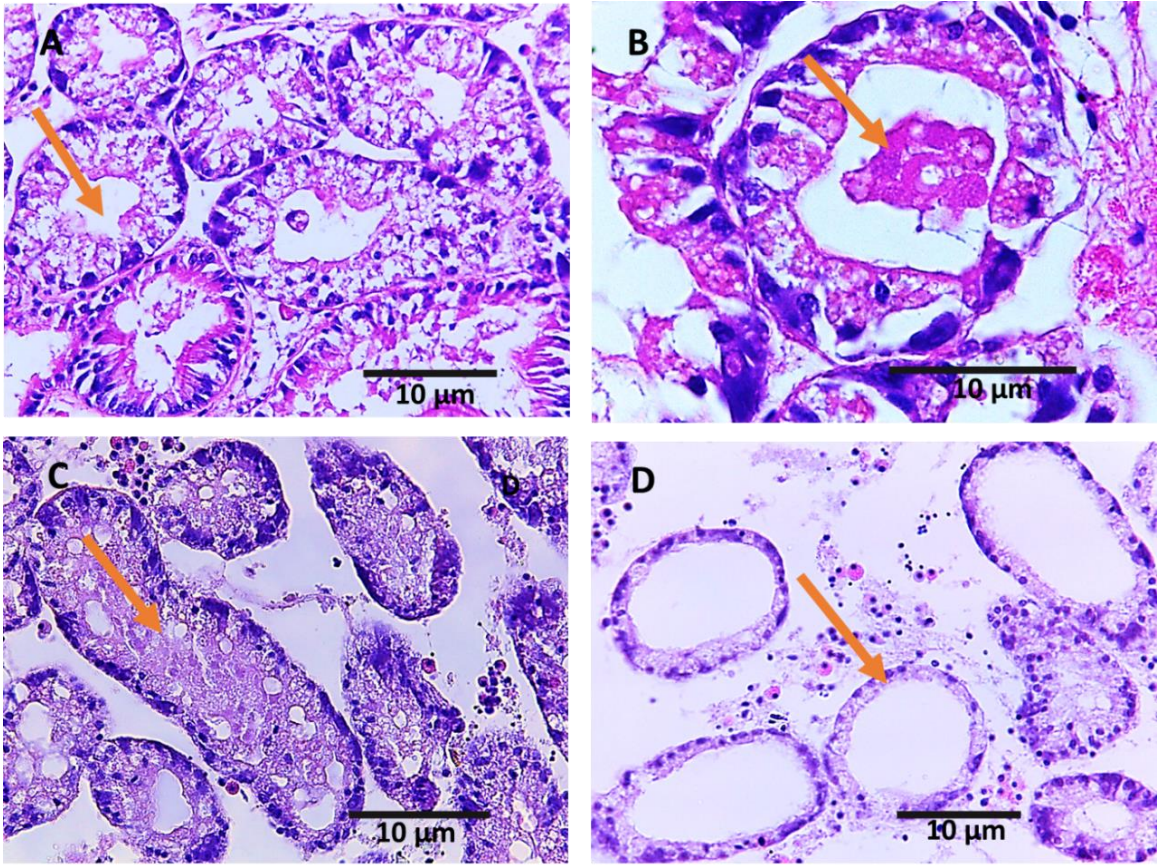


Figure 4.14 Digestive tubule structures (orange arrows) of *P. canaliculus* (A) normal or cruciform or Y shaped lumen (D1), (B) normal lumen but sloughed epithelial cells inside lumen (D2), (C) small or no lumen (D3) and (D) large lumen, with a thin epithelial wall (D4). Scale bars = 10 µm.

4.3.8 Gill structures

Out of 256 mussels, 190 samples (occurrence rate of 74%) showed gills with normal structure, with ciliated lateral cilia, ciliary discs and medium number of haemocytes in the gill haemolymph space (G1), whereas the 10% (occurrence rate) of samples (n = 26) showed gills with ciliary discs, destroyed/broken epithelium of gill filament and few haemocytes in the gill haemolymph space (G2). 24% (occurrence rate) of samples (n = 62) showed gills without ciliated lateral cilia, ciliary discs are atrophied/separated and with very few haemocytes in the gill haemolymph space (G3).

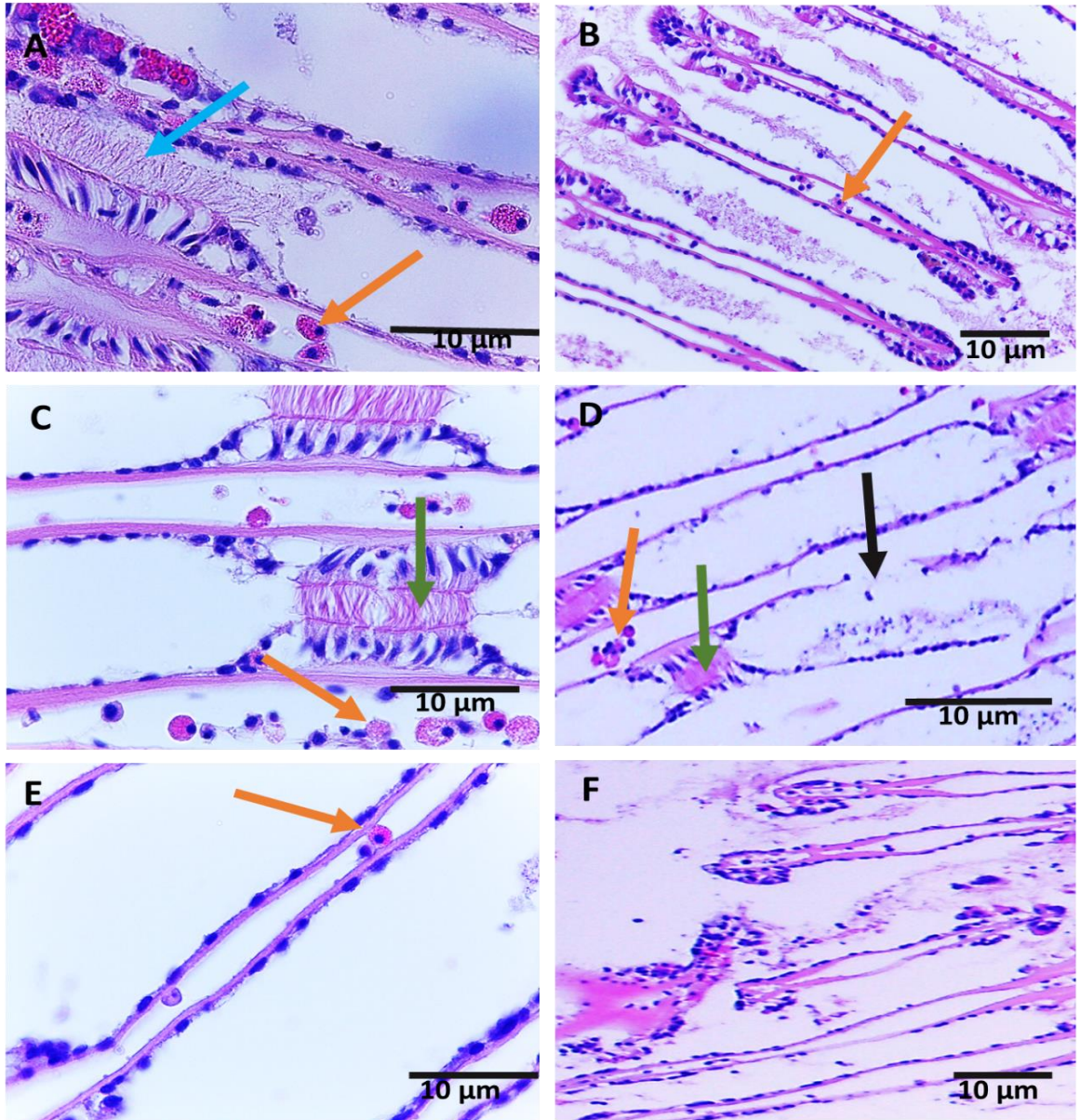


Figure 4.15 Gill structures of *P. canaliculus*, (A) and (B) normal structure with ciliated lateral cilia (blue arrow) in the frontal zone of gill filament and with a medium number of haemocytes (orange arrows) in the gill blood space (G1), (C) normal structure with ciliary discs (green arrow) appear in the abfrontal zone of gill filament and with a medium number of haemocytes (orange arrow) in the gill haemolymph space (G1), (D) ciliary discs (black arrow) appear in the abfrontal zone of gill filament and destroyed/broken epithelium (blue arrow) of gill filament and few haemocytes in the gill haemolymph space (G2), (E) and (F) without ciliated lateral cilia in the frontal zone of gill filament, ciliary discs are atrophied/separated in the abfrontal zone of gill filament and very few haemocytes (orange arrow) in the gill hemolymph space (G3). Scale bars = 10 µm.

A significant association between presence of parasites and health condition (healthy and unhealthy) of mussels was observed (Pearson Chi-square test, p -value = 0.030).

Table 4.10 Statistical analysis: Chi-square test for the association between parasites and health condition of mussels.

Health condition	Parasites		Chi-square test for association (P -value)
	No	Yes	
Healthy or Unhealthy	Healthy	124	0.030
	Unhealthy	21	

4.3.9 Observation of pathogens and parasites

4.3.9.1 Infection with *P. olseni*

Trophozoites of *P. olseni* are spherical cells, 3-5 μm in diameter, with a large, eccentric vacuole occupying most cytoplasm and a peripheral nucleus, giving them a “signet ring” appearance (Fig. 4.17A-H). Phagocytosis of *P. olseni* by mussel haemocytes was frequently observed (Fig. 4.16A & B).

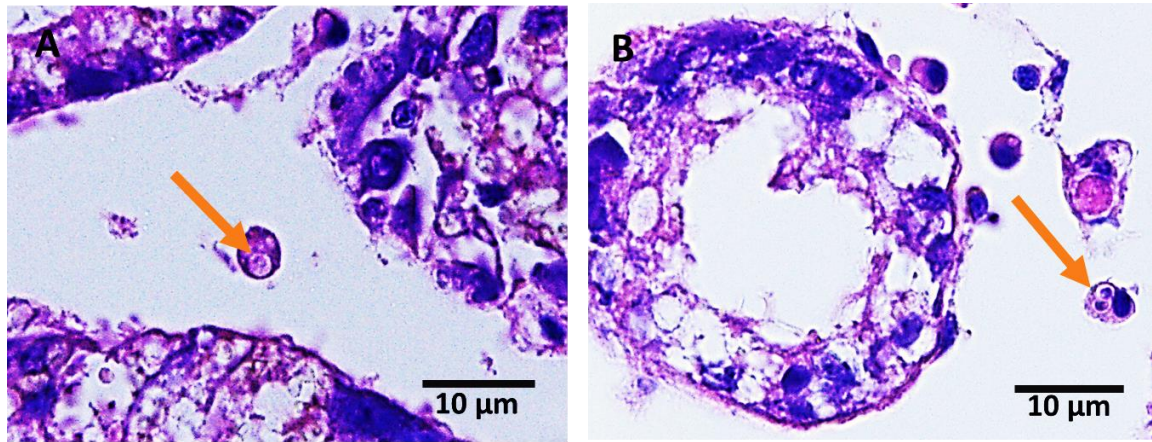


Figure 4.16 (A) and (B) Histology of Greenshell™ mussel (*P. canaliculus*) showing *P. olseni* cells phagocytosed by haemocytes in space between digestive tubules (orange arrows). Scale bar = 10 μm .

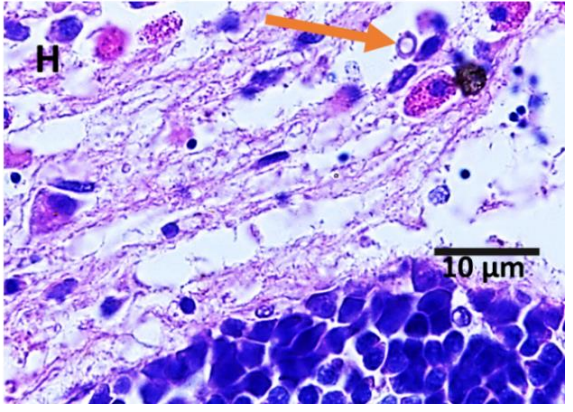
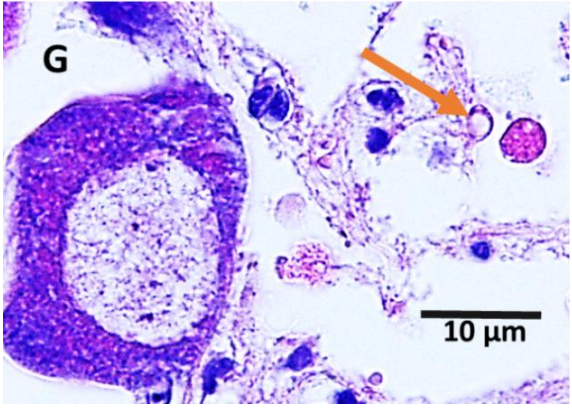
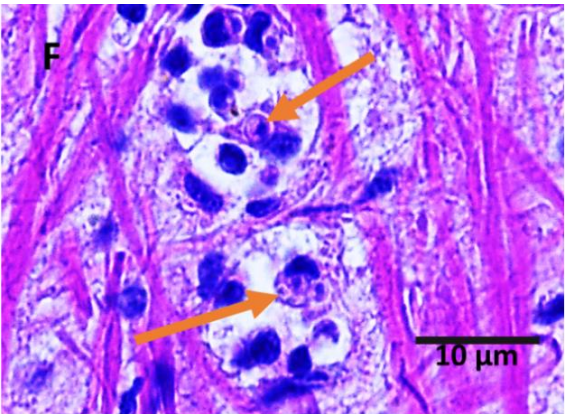
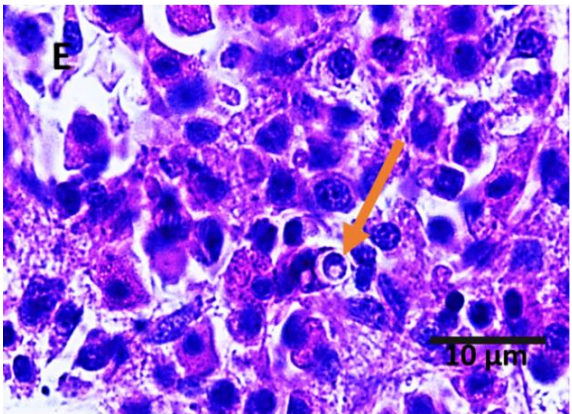
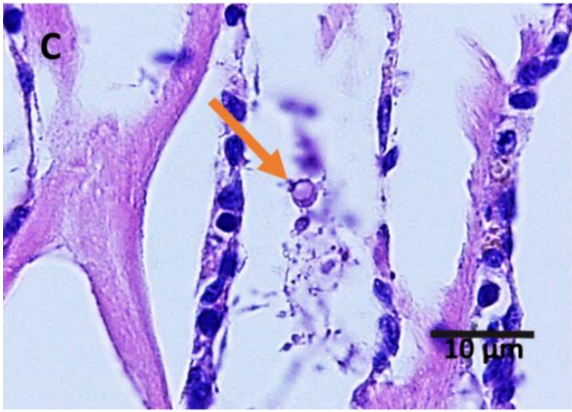
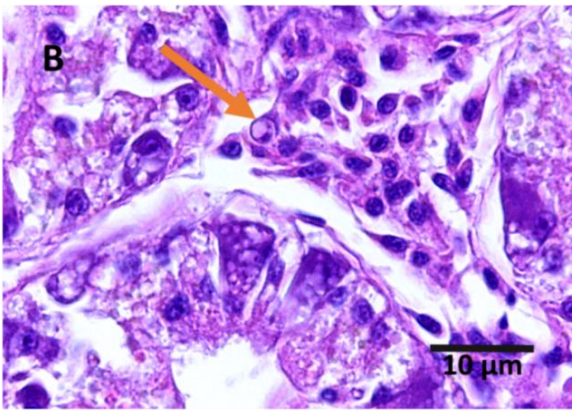
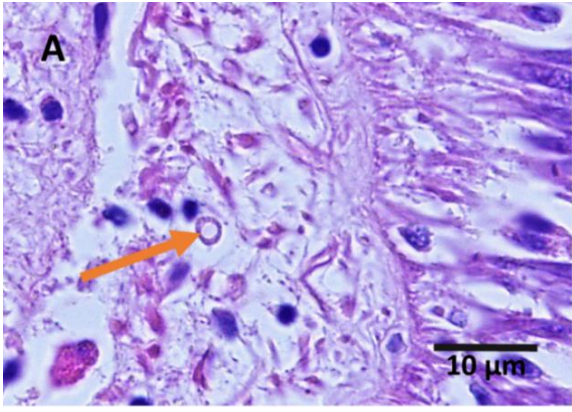


Figure 4.17 Trophozoites (orange arrows) of *P. olseni* in (A) connective tissue surrounding digestive epithelium, (B) connective tissue surrounding digestive tubules, (C) gills (blood space), (D) gills (outside the gill epithelium), (E) mantle, (F) adductor muscle, (G) connective tissue surrounding female gonads and (H) connective tissue surrounding male gonads. Scale bars = 10 μ m.

4.3.9.2 Specificity test of *Perkinsus olseni* by ISH

The digoxigenin-labelled probes (species-specific ISH assay) demonstrated hybridization to *P. olseni* cells in digestive epithelium, digestive tubules, gills, mantle, adductor muscle and gonads as blue staining (Fig. 4.18A & B). No hybridization of other parasite cells was observed.

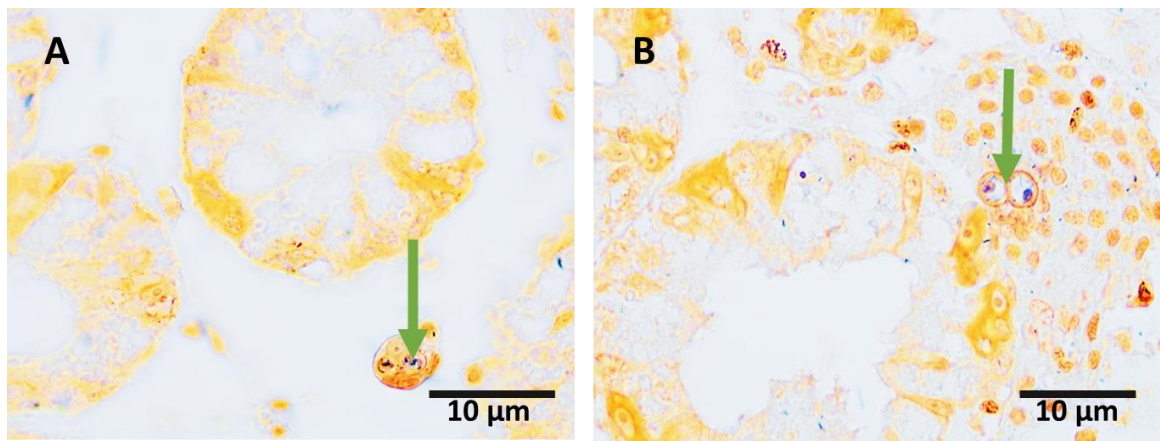


Figure 4.18 (A) and (B) ISH of New Zealand Greenshell™ mussels showing blue labelled *P. olseni* trophozoites near digestive tubules (green arrows). Scale bar = 10 μ m.

4.3.9.3 Infection with APX

APX zoites were observed in the connective tissue surrounding the digestive tract epithelium, digestive tubules and gonads. They were also seen in the blood space of gills, mantle and adductor muscle (Fig. 4.19). The zoites are oval/elongated and elliptical, 5-8 μ m long and 3-5 μ m wide with a round nucleus located to the middle of their length (Fig. 4.8). Phagocytosis of APX by mussel haemocytes was also observed (Fig. 4.19D).

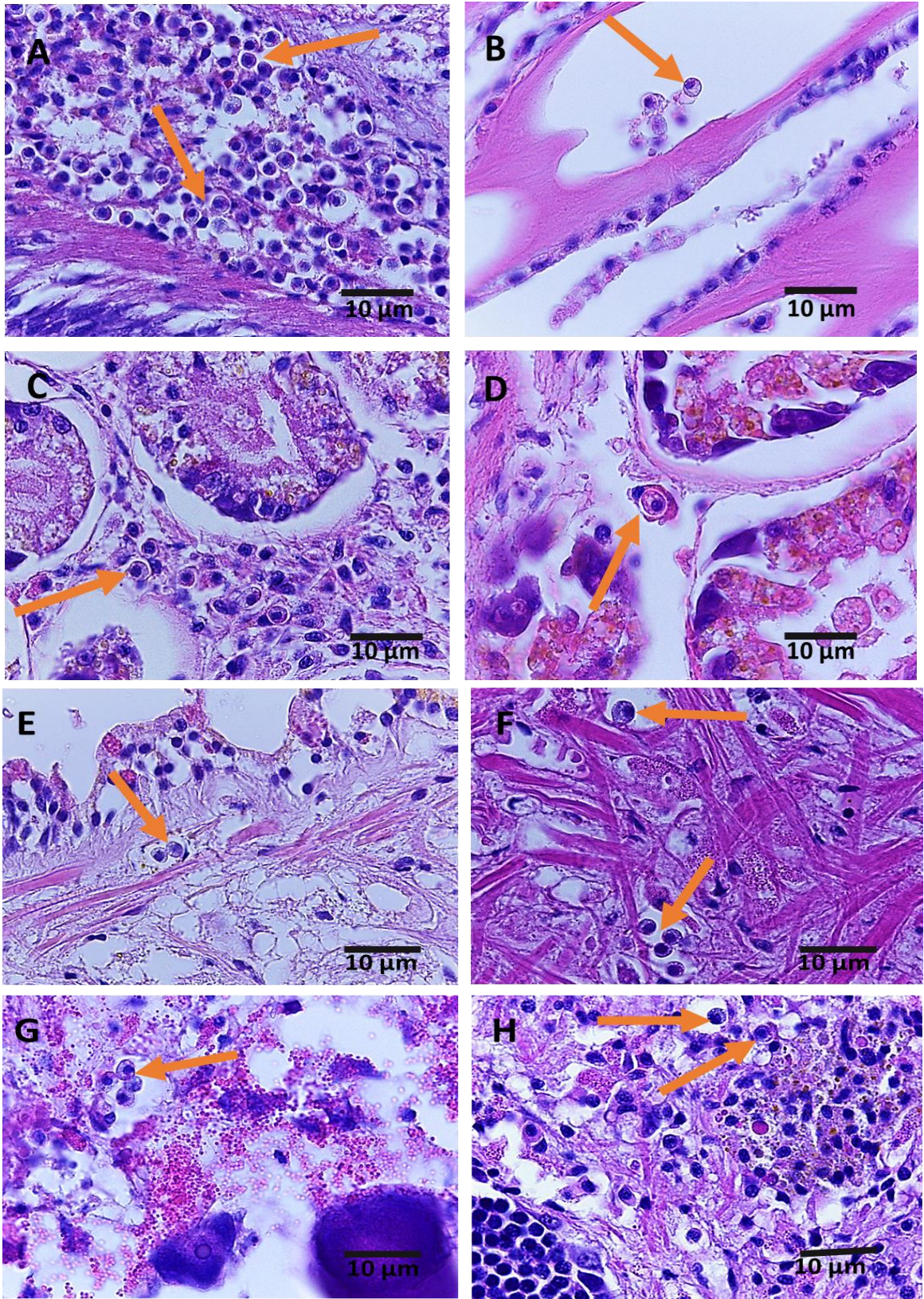


Figure 4.19 APX (orange arrows) in different tissues of *P. canaliculus*, (A) connective tissue surrounding digestive epithelium, (B) gills (haemolymph space), (C) connective tissue

surrounding digestive tubules, (D) phagocytosis by haemocytes near digestive tubules, (E) mantle, (F) adductor muscle, (G) connective tissue surrounding female gonads and (H) connective tissue surrounding male gonads. Scale bars = 10 μm .

4.3.9.4 Infection with other parasites

Other parasites and pathogens were noted (Fig. 20A-F). *Microsporidium rapuae* (sporocyst) was observed in connective tissue near the digestive epithelium. Copepods were found inside the gut lumen. Identification of the copepods is difficult in the histological section but that they might be *Pseudomyicola spinosus* or *Lichomolgus uncus* as they have been reported by Hine (2002a). Intracellular microcolonies of bacteria (IMCs) were observed as colonies or cysts in muscle tissue and in the mantle. Bacteria (bacilli and cocci) were found in the gills, mantle, connective tissues near gonads, digestive tubules and digestive epithelium of mussels.

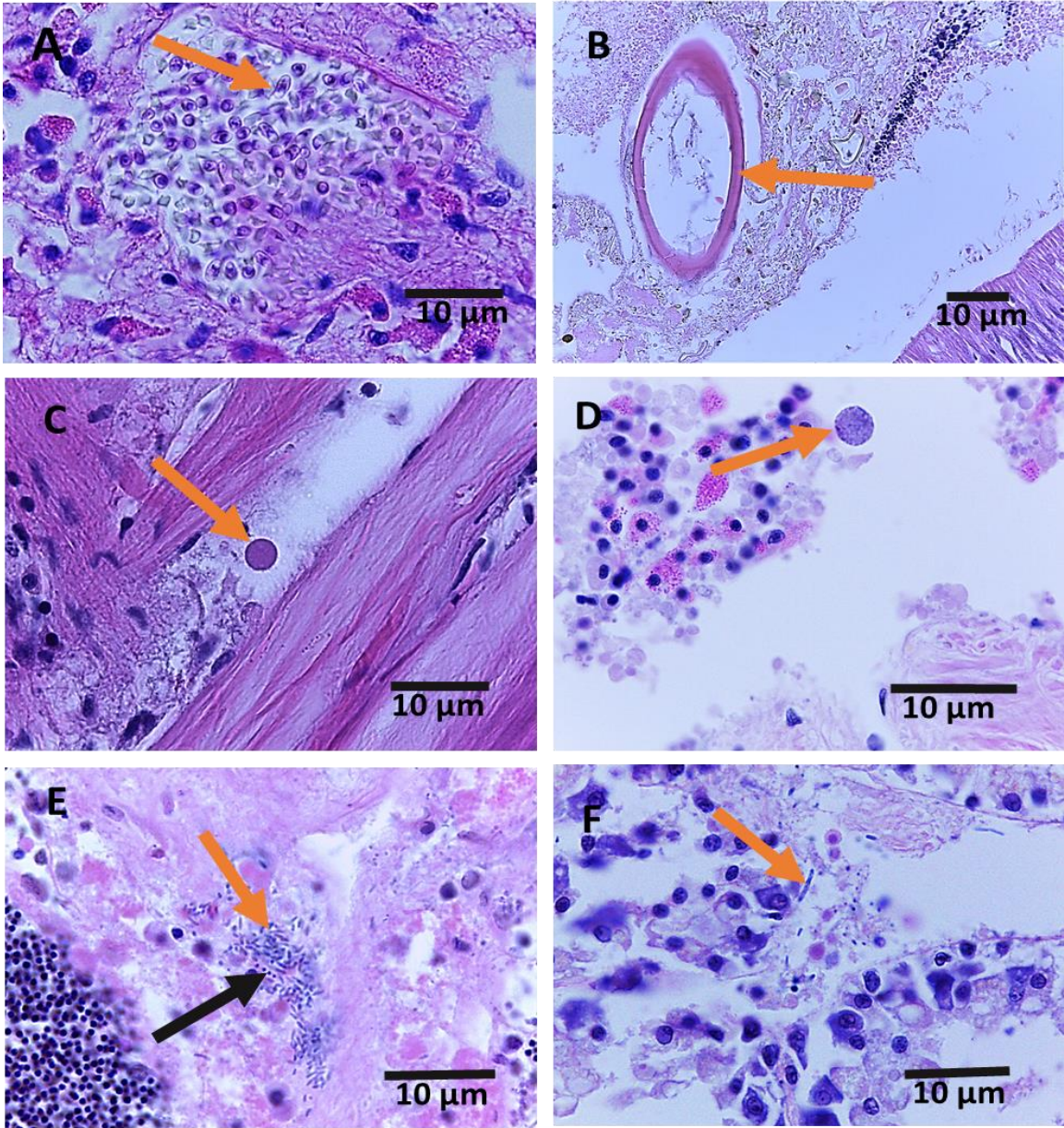


Figure 4.20 Parasites (orange arrows) and microorganisms (orange arrows and black arrow) in tissues of *P. canaliculus*, (A) *M. rapuae* sporocyst in connective tissue near digestive epithelium, (B) part of copepod (*P. spinosus* or *L. uncus*) exoskeleton inside the gut, (C) and (D) IMCs in muscle and near the mantle respectively, (E) bacteria (bacilli = orange arrow and cocci = black arrow) in the connective tissues near male gonads and (F) rod-shaped bacteria (bacilli) in the connective tissues surrounding digestive tubules. Scale bars = 10 µm.

4.4 Discussion

4.4.1 Infection with *P. olseni*

P. olseni was tentatively identified by histology and confirmed by ISH in mussels (*P. canaliculus*) (prevalence 56%) collected from Whakatiwai, North Island, New Zealand. *P. olseni* was also identified by histology and Ray's fluid thioglycollate medium (RFTM) from *P. canaliculus* in the South Island, New Zealand (OIE, 2017). In this study, more than 56% of mussel samples were infected with *P. olseni*. A similar finding was recorded in clams (*Ruditapes philippinarum*) in Isahaya Bay, Japan by Choi et al. (2002). A high prevalence (97%-100%) of *P. olseni* in clams (*R. philippinarum*) was observed in Ariake Bay, Kyushu, Japan and Komsae Bay, Korea by Park et al. (1999; 2008). Combined, these findings indicate that high infection rates of *P. olseni* are recorded in bivalves, including *P. canaliculus*.

In this study, trophozoites of *P. olseni* were recorded in connective tissues surrounding digestive tract epithelium, digestive tubules and gonads, and also in gills, mantle and adductor muscle. *Perkinsus* trophozoites were also observed in the same tissues of Manila clams (*Ruditapes philippinarum*) by Choi et al. (2002) and Park and Choi (2001). In the present study, trophozoites of *P. olseni* were mainly recorded in the connective tissue surrounding digestive tubules and gills, but fewer were noticed in the adductor muscle. Choi et al. (2002) also reported similar findings in Manila clams.

Seasonal variations of *P. olseni* infection in *P. canaliculus* were demonstrated in this study. The highest prevalence of mussels with *P. olseni* infection was registered in autumn, and heavy (high levels) infection of *P. olseni* was noticed in the winter season. However, Yang et al. (2012) observed no clear seasonality in *P. olseni* prevalence in adult Manila clam (*R. philippinarum*) in Gomsae Bay, Korea but reported the proliferation of *P. olseni* in clam tissues during winter. Park et al. (1999) noted extremely high levels of *P. olseni* in clams in late summer in Gomsae Bay, Korea. Uddin et al. (2010) also observed a seasonal difference in the prevalence (38–97%) annually, and the highest prevalence was in fall /autumn in Manila clams in Incheon Bay, Korea when most clams are in the post-spawning stage. In contrast, Villalba et al. (2005) found a high prevalence of *P. olseni* infection in the clam *Tapes decussatus* during spring and summer, when surface water temperatures increased. According to Yang et al. (2012), food accessibility is relatively low during late fall or autumn to winter, and during summer and early fall or autumn, spawning activities exhaust clams, which may impair their defense capacity. Therefore, the combined impacts of food shortage and poor physiological condition of clams will accelerate the spread of *P. olseni* in fall/autumn and winter (Yang et al., 2012). Further research may focus

attention to find out the link between *P. olseni* and seasonal variations, the food supply and physiological conditions of the mussels. *P. olseni* trophozoites were detected in the haemocytosis/haemocytic infiltration of mussel tissues and phagocytosis of *P. olseni* by the haemocytes was frequently seen (detection rate 47%). In addition, a significant association was recorded between the inflammatory tissue responses (haemocytosis and brown material accumulation) and *Perkinsus* infection in this study. According to Choi and Park (2010), heavy infection with *P. olseni* often involves tissue inflammation and results in mass mortalities in clam and oyster populations. Villalba et al. (2004) noted that severe infection with *Perkinsus* spp. in oysters (*Crassostrea virginica*) induces enormous haemocytic infiltration of tissues where the parasite is identified, and the haemocytes actively phagocytose *Perkinsus* cells. In addition, *Perkinsus* parasites multiply within the haemocytes and involve in their rupture (Villalba et al., 2004). Therefore, these findings indicate that *P. olseni* infections are linked with haemocytosis and brown material accumulation which may debilitate the mussels.

4.4.2 Infection with APX

APX zoites with a high prevalence rate (78%) correspond to the mean detection in whole mussels were recorded in different tissues of *P. canaliculus* collected from North Island (Whakatiwai), New Zealand. Suong (2018) also observed a high prevalence (60%) of APX in cultured *P. canaliculus* from North Island (Coromandel), New Zealand, in 2016. Other researchers have detected APX in *P. canaliculus* (Diggle et al., 2002a; Suong et al., 2019; Webb, 2013), Mediterranean mussels, *Mytilus galloprovincialis* (Suong et al., 2019) and hairy mussels, *Modiolus areolatus* (Suong et al., 2018). In the current study, light to moderate numbers of parasites were observed in most tissues, but a higher number of *P. canaliculus* showed infection with APX in the connective tissue surrounding digestive tubules and mantle. In contrast, Suong (2018) identified a few APX-like zoites in the connective tissues in other mussels including *P. canaliculus*. According to Suong (2018), all the mussel samples had only very light infections, and only a few APX-like zoites were scattered or gathered into small groups (3-5 zoites), mainly in the connective tissue of the digestive gland and mantle tissue. In this study, a higher prevalence with heavy infection of APX infection in mussels was found in the winter season. In addition, a highly significant association between seasons and the presence of APX in mussels was noted. A significant association was observed between the ceroid/brown material accumulation and APX infection, and the presence of ceroid/brown material was often noted close to APX. Consistent with this study, the presence of brown cells and the accumulation of haemocytes around APX-like cells have been recorded in the

tissues of several mussel species, including *P. canaliculus*, *M. galloprovincialis* and *M. areolatus* (Suong, 2018). Webb and Duncan (2019) also found areas of brown pigment in bivalve tissues, mostly in the mantle, gonad and digestive gland interstitial tissues, and brown pigmentation appears in the vicinity of parasites such as APX (Webb & Duncan, 2019). According to Suong (2018), APX may be related to the morbidity and mortality of mussels under certain stress conditions. Moreover, biotic factors (e.g., host density, common pathogens and host developmental stages) and abiotic factors (e.g., temperature, pH and salinity) can cause APX to propagate and result in harmful outbreaks in New Zealand aquaculture industry (Suong, 2018). These observations suggest that environmental factors affect the spreading of APX infection and, in severe cases, APX may be associated with disease outbreaks.

4.4.3 Other parasites and pathogens

Other parasites and pathogens were observed, including *Microsporidium rapuae* in the connective tissue near the digestive epithelium, copepods (*Pseudomyicola spinosus* or *Lichomolgus uncus*) inside the gut, IMCs in muscles and mantle, and bacteria (rods/bacilli and cocci) in the gills, mantle, connective tissues near gonads, and in the digestive tubules and digestive epithelium. A few mussels (low infection prevalence) were infected with these parasites and pathogens, and there were no noticeable pathological effects. *M. rapuae* was also identified in connective tissue near the digestive tract in *P. canaliculus* and *Ostrea chilensis* by Jones (1981) and Hine and Jones (1994). According to Webb (2013), *M. rapuae* appears to have no pathological impact on *P. canaliculus* and *O. chilensis*.

Webb (1999) and Webb and Duncan (2019) reported that copepods are frequently seen attached to gills or embedded in digestive tissues in bivalves such as South African *Perna perna*, *Aulacomya ater*, *Choromytilus meridionalis*, *M. galloprovincialis*, *P. canaliculus*, *Crassostrea gigas* and *O. chilensis*, and copepods are surrounded by heavy haemocytosis in the tissues of bivalves. According to Caceres-Martinez and Vasquez-Yeomans (1997), copepods are not host-specific and are found worldwide, and in light infestation, copepods are harmless to their host, but in heavy infestation, they may lead to gill erosion and haemocyte infiltration. Although the impact of copepods on the host may be negligible, the resultant haemocytosis can conceal other haemocytosis-activating infections, such as perkinsosis whose trophozoites are small and inconspicuous compared with the haemocyte profusion associated with them (Webb & Duncan, 2019).

IMCs/ RLOs were also reported in the cytoplasm of gills, digestive and mantle epithelial cells of mussels, oysters and other bivalves without significant pathological effects by Webb and Duncan (2019). Another pathogen such as bacteria (*Splendidus clade*, *Harveyi clade*, *Vibrio aestuarianus*, *V. tubiashii*, *V. coralliilyticus*, *V. tapetis*) was identified in marine bivalves as important aquaculture pathogens by. According to Travers et al. (2015), bivalves are adversely affected by many bacteria and are associated with mortality events of hatcheries and natural beds. In the present study, there was a significant association between seasons (summer, winter, spring and autumn) and the presence of bacteria in mussels. According to Nguyen and Alfaro (2020), in the summer season, aquaculture species may experience heat stress and pathogen loads which tends to overwhelm their immune systems and cause summer mortality events. Pathogens, parasites, and pests (PPP) are a long-lasting threat for the aquaculture sector, and the increase of production and amplified trade (Stentiford et al., 2012). Global cultivation of many bivalve species have has significantly threatened by the substantial mortality outbreaks (Nguyen & Alfaro, 2020). There is a critical need to investigate this health threat to safeguard the future of the industry. According to Assefa and Abunna (2018), implementation of best management practices (for example, for site and system selection, stocking densities, species rotations, broodstock, and feed quality, filtration and parasite monitoring and removal, and surveillance) has been the key ways of minimizing diseases (Assefa & Abunna, 2018). It is vital to conduct surveillance frequently in order to decrease the risk of the spread of pathogens (Oidtmann et al., 2011). Thus, strict quarantine measures, sanitation of equipment, disinfection of egg, traffic control, water treatments, use clean feed, removal of dead properly should be implemented during the introduction of new stock as well as implementing them for decreasing pathogens and to circumvent transferring pathogens from one stock to another (Assefa & Abunna, 2018). Therefore, it is important to monitor parasites and remove them throughout the year to minimize diseases and to reduce the risk of spread of pathogens and parasites.

4.4.4 Gill pathology and digestive tubule pathology

Gill pathology (e.g., loss of cilia, destroyed gill filament and no haemocytes in the gill blood space) were observed in *P. canaliculus*. Erosion of the gill epithelium and loss of cilia were observed in *C. gigas*, by Webb and Duncan (2019), who indicated that damage to the gill epithelial cells may lead to significant disturbance of respiratory functions in affected bivalves. Moreover, gill tissues may be affected by severe infection with *Perkinsus* which may result in deteriorating filtering activity and efficiency (Choi & Park, 2010).

The pathology of digestive tubules was noted in this study. Digestive tubule structural abnormalities, such as thinning and sloughing (Carella et al., 2015a; Morton, 1970; Winstead, 1995, 1998) have been recorded in *P. canaliculus*, *C. gigas* and *M. galloprovincialis* by Webb and Duncan (2019). Carella et al. (2015b) also assessed damage to the digestive epithelia in connection with lumen modifications in mussels exposed to the harmful dinoflagellate *Ostreopsis cf. ovata*. These digestive tubule structural anomalies have been related to stresses such as starvation, and xenotoxins (Rolton et al., 2019). In the present study, a significant association between digestive tubule structure (large lumen, with a thin epithelial wall) and *Perkinsus* infection was recorded. According to Lee et al. (2001), the infestation of the *Perkinsus* parasites in digestive tubules may cause digestive tubule atrophy and detrimental effects during food digestion. According to Morton (1970), the intracellular digestive procedure in the digestive diverticula is linked with the development, absorption, breakdown and reformative phases of the digestive tubules. Morton (1970) noted that the variations of the digestive tubules structure (due to different physiological factors) in the stage of the tidal cycle correlated with feeding and digestion. Thus, it is likely that the digestive tubule structural abnormalities observed in this study may have resulted from pathogen/parasite infections, natural cycle and/or biotic factors that lead to disruptions in digestive tubule functions, such as food digestion and nutrition absorption.

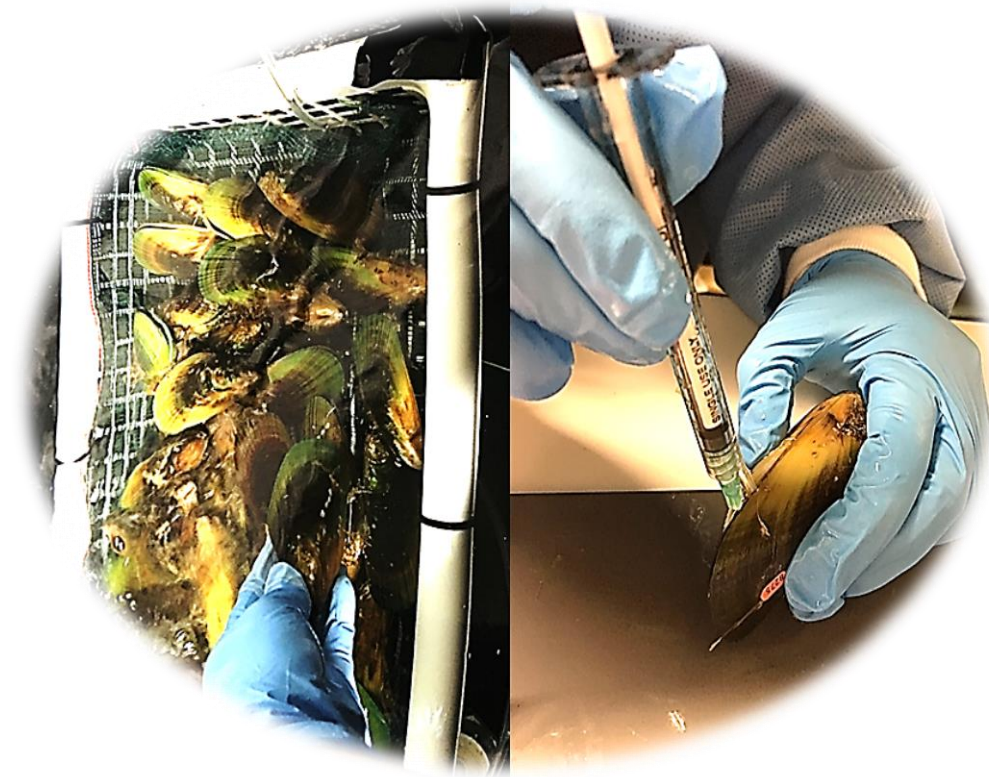
4.5 Conclusions

This is the first report on seasonal variations of *P. olseni* and APX in New Zealand Greenshell™ mussels (*P. canaliculus*). The presence of *P. olseni* and APX in mussels are significantly related to the seasons (summer, winter, spring and autumn). *P. olseni*, APX and other parasites were identified in different tissues of mussels. A high prevalence of *P. olseni* and APX was found in different tissues of mussels. There was a significant association between *P. olseni* and APX infection in mussels. However, a few moribund mussels were associated with bacteria (bacilli and cocci) and infected with copepods, *M. rapuae* and IMCs, and appears to have no pathological effect on *P. canaliculus* as indicated by histological condition. The abundance of *P. olseni* and APX in *P. canaliculus* was evaluated semi-quantitatively using two separate modified grading scales, which are suitable to assess *P. olseni* and APX infection of the histological section. In addition, tissue gradings for *P. olseni* and APX infection, inflammatory tissue responses (haemocytosis, ceroid material), abnormal tissue structures (gill pathology and digestive tubule pathology) were evaluated with semi-quantitative scales. An association between haemocytosis and *P. olseni* infection was noted. A significant association between the brown material accumulation and parasites (*P. olseni* and APX) infection was recorded. The pathologies of digestive tubules and gills were observed in

this study and *P. olseni* infection is related to digestive tubule deterioration (large lumen, with a thin epithelial wall). A significant association between presence of parasites and health condition (healthy and unhealthy) of mussels was observed. Therefore, the findings in this study provide information regarding the infections of potential parasites and pathogens and their abnormal tissue structures in *P. canaliculus* across different seasons.

Chapter 5

Characterization of mussel (*Perna canaliculus*) haemocytes and their phagocytic activity across seasons



Haemolymph collection from New Zealand Greenshell™ mussels (*Perna canaliculus*)

Muznebin, F., Alfaro, A. C., Webb, S. C., & Merien, F. (2022). Characterization of mussel (*Perna canaliculus*) haemocytes and their phagocytic activity across seasons. *Aquaculture Research*. <https://doi.org/10.1111/are.15926>

Abstract: *Perna canaliculus* is endemic to New Zealand and is the top shellfish export product. However, the growth of this industry is being adversely affected by summer mortality events. To assess these health threats, differential haemocyte counts (DHC) were performed on haemolymph smears stained with Giemsa, and *in vitro* phagocytosis activity assays were applied in *P. canaliculus* for several months covering three seasons (winter, spring and summer). A new optimised classification scheme was developed for *P. canaliculus* haemocytes where 55% eosinophilic and 27.2% basophilic granulocytes were identified. Eosinophilic granulocytes were classified as dense, semi and small semi and these new categories were reported herein for the first time in this species. A new haemocyte type (mixed granulocytes) which contains both acidophilic and basophilic granules is proposed for *P. canaliculus*. The phagocytosis percentages were significantly affected by incubation time, indicating an increase of zymosan particle uptake from $18.42 \pm 1.7\%$ after 30 min, $32.08 \pm 3.1\%$ after 60 min and $44.74 \pm 3.5\%$ (maximum) after 120 min of incubation. The lowest phagocytosis was observed in the winter season, and the highest phagocytosis in summer. This study findings provide a better understanding of the immune function of *P. canaliculus* haemocytes and serve as a reference for further investigations on the impacts of seasonal variations on haemocyte activity and phagocytosis.

5.1 Introduction

Increasing health threats, such as summer mortality, affect shellfish commercially important species worldwide (Berthelin et al., 2000; Newton & Webb, 2019). Summer mortality events are a consequence of complex interactions between pathogens and environmental factors and often are associated with temperature increases (Berthelin et al., 2000) and reproductive cycles (Cheyney et al., 1998). Seasonal temperature changes have a significant impact on growth, reproduction and mortality for bivalves (Aagesen & Häse, 2014; Malham et al., 2009; Viergutz et al., 2012). In addition, the rise in water temperature during summer often results in bacterial proliferation in the water, and bacterial accumulation in the tissues of shellfish, leading to stress (Mitta et al., 2000), disease and mortality (Gagnaire et al., 2007). Since high mortalities of molluscs in both wild harvests and farms have become a frequent phenomenon in recent years, it is important to better understand the complex host-pathogen-environment interactions during these mortality events.

Over the last decade, there has been growing awareness that temperature is related to disease incidence or mass mortality in marine bivalves as the temperature can significantly influence the immune responses of these animals (Matozzo & Marin, 2011; Monari, 2007; Perrigault et al., 2011). Summer mortality events are often associated with various types of pathogens, such as viruses (e.g., *Ostreid herpesvirus 1*, described by Alfaro et al., 2018; Nguyen et al., 2018a), bacteria (e.g., *Vibrio* spp., described by Allam & Raftos, 2015) and parasites (e.g., protozoans, described by Lane et al., 2016). High mortality events associated with pathogens have a significant impact on three important molluscan species in New Zealand, such as Greenshell™ mussels (*Perna canaliculus*), Pacific oysters (*Crassostrea gigas*) and flat oysters (*Ostrea chilensis*). In bivalves, the ability to counteract environmental stress and bacterial infections is mediated by plasma proteins, glycoproteins and the circulation of haemocytes (Mitta et al., 2000).

In bivalves, two types of haemocytes have been previously characterized, including granulocytes and hyalinocytes (Cheng, 1981; Wootton & Pipe, 2003). These cell types have been observed in many bivalve species, including the oyster *C. gigas* (Allam et al., 2002; Chang et al., 2005), the mussels *Mytilus edulis*, *Anodonta cygnea* and *P. canaliculus* (Chandurvelan et al., 2013; Pipe et al., 1997; Soares-da-Silva et al., 2002), the clams *Ruditapes philippinarum*, *Mercenaria mercenaria* and *Meretrix lusoria* (Allam et al., 2002; Chang et al., 2005) and the peppery furrow shell mollusc *Scrobicularia plana* (Wootton & Pipe, 2003). However, not all haemocyte types are found in all bivalve species (Hine, 1999). Different criteria, including a combination of morphology, function and cytochemistry, have been used to characterize bivalve haemocytes into two or more groups (Nakayama et al., 1997; Zhang et al., 2006). These include eosinophilic

granular, agranular, lymphoid, large granular, small granular and morula-like haemocytes. According to the staining affinities of their cytoplasmic granules, granulocytes may be further sub-classified into eosinophilic, basophilic and neutrophilic haemocytes, depending on the bivalve species (Hine, 1999; Lopez et al., 1997a; McCormickRay & Howard, 1991). Indeed, Hine (1999) described granulocytes as having many cytoplasmic granules and being the most abundant cell type. Conversely, hyalinocytes have few or no granules and have a hyaline (translucent) cytoplasm (Hine, 1999). Hyalinocytes have been divided into two types: small hyalinocytes with large nuclei and scanty cytoplasm and large hyalinocytes with lower nucleus/cytoplasmic ratios (Cheng, 1981). A wide range of bivalve haemocyte types circulate in the haemolymph and perform various crucial immune functions (e.g., destruction of potential pathogens, elimination of foreign material through phagocytosis, encapsulation and necrotization of invading pathogens and parasites) (Allam & Raftos, 2015; Cheng, 1981; Song et al., 2010). These haemocyte functional differences can be used to profile immune responses at a given time or under different health threats.

Phagocytosis is an effective cellular defence against pathogen invaders and foreign material. This process recognizes and eliminates non-self-components, such as invading microorganisms (Canesi et al., 2002; Ottaviani, 2006). In phagocytosis, the phagosome (the vacuole that contains the phagocytosed particles in the cytoplasm) fuses with the lysosome (cell organelle containing hydrolytic enzymes in the membrane) resulting in the intracellular digestion of the ingested microorganisms (Canesi et al., 2002). Some studies have shown that there are functional differences between bivalve haemocytes to recognize and eliminate pathogens. Granulocytes can phagocytise pathogens or foreign material, and they contain a mixture of hydrolytic enzymes that contribute to killing intracellular pathogens (López et al., 1997a; López et al., 1997b; Matozzo et al., 2007). Granulocytes are usually more active phagocytes than hyalinocytes (Cheng, 1981). In addition, hyalinocytes may be non-phagocytic (Carballal et al., 1997a). Generation of reactive nitrogen intermediates (RNIs) such as nitric oxide is an evolutionarily sustained strategy of phagocytosis, which are employed by bivalve haemocytes to combat pathogenic attacks (Araya et al., 2009; Chakraborty et al., 2009; Park et al., 2012). Most studies in the field of molluscan immunology have only focused on the phagocytic activity of bivalves, but relatively little information is available on phagocytic activity in different seasons and natural environmental changes, which are needed to understand seasonal impacts on the immune system of bivalves.

The New Zealand Greenshell™ mussel (*P. canaliculus*) is endemic to this country, and is the top shellfish export product, reaching \$NZ 272 million in 2018 (New Zealand Aquaculture, 2019). Despite the economic importance of *P. canaliculus* industry and the increasing threats of global

warming, there have been few studies on haemocyte characterization and phagocytic activity for this species (Chandurvelan et al., 2013). To address these health risks, a thorough understanding of the immune system and its capacity to cope with increased pathogen loads are needed for these commercially important species. Characterization of the functional differences between haemocytes and their immunological responses is the first step to investigate the effects of summer mortality and to assist farmers in mitigating these production risks. To fill this knowledge gap, a detailed characterisation of *P. canaliculus* haemocytes was conducted, leading to a novel and complete classification scheme for this species. The different types of haemocytes were quantified and the haemocyte profiles of mussels within different levels of *Vibrio*-like bacterial (gram-negative, rod-shaped) association were compared. In addition, *in vitro* phagocytic activity assays were carried out at different incubation periods over the seasons for a better understanding of the immune function of haemocytes in *P. canaliculus*.

5.2 Materials and Methods

5.2.1 Mussel samples

Adult *P. canaliculus* mussels (shell length: 8.06 ± 0.45 cm, weight: 55 ± 2.5 g) were obtained monthly from Kaiua Mussel Farms (Whakatiwai, New Zealand). Mussels were transported to the aquaculture lab at the Auckland University of Technology (Auckland, New Zealand) and acclimatized for 3-4 days in a re-circulation system (5 μ m filtered seawater [FSW]; temperature = 16 ± 0.5 °C; salinity = 35 ppt; pH = 8.0). The monthly sampling covered winter (June-August, 7-15°C), spring (September-November, 11-20°C) and summer (December, 15-22°C) seasons.

5.2.2 Sample size and experimental design

Mussel samples were collected to extract haemolymph for haemocyte characterization and phagocytic activity tests. A total of 80 adult mussels (5-15 mussels per month – July'18, September'18, October'18, June'19, July'19, August'19, October'19 and November'19) were used for haemocyte characterization and differential haemocyte counts, and a total of 50 mussels (5-15 mussels per month- June'19, July'19, August'19, October'19, November'19 and December'19) were used for phagocytosis analyses.

5.2.3 Haemolymph collection

Haemolymph was collected from each animal by gently inserting a needle (23 gauge \times 1.5 inches) attached to a 3 mL sterile syringe (Terumo, Japan) into the posterior adductor muscle. For each mussel, 1–2 mL of haemolymph was collected. Immediately after withdrawal, haemolymph

samples were transferred into 10 mL Eppendorf tubes and kept on ice. Hemolymph was analyzed for each individual (not a pool of hemolymph samples).

5.2.4 Differential Haemocyte Counts (DHC)

The DHC was performed by counting the different haemocyte types on haemolymph smears stained with Giemsa (Sigma-Aldrich, USA) from 80 animals (5-15 mussels per month were obtained for this experiment). Cold artificial seawater (ASW) was mixed with mussel haemolymph at the ratio 1:1 as the anti-coagulant (Gagnaire et al., 2006; Nguyen et al., 2018c; Zhou et al., 2017). Haemolymph cell monolayers (HCMs) method was adapted from Maedel and Doig (2012). HCMs were fixed by immersion with methanol at room temperature for 1 minute followed by air drying. HCMs were placed in Coplin jars of Giemsa stain for 4 minutes. Then, slides were removed with tweezers and placed in Coplin jars of diluted stain (1 Giemsa: 3 phosphate-buffered saline (PBS) (137 mM NaCl, 2.7 mM KCl, 2 mM KH₂PO₄, 10 mM Na₂HPO₄, pH 6.8) for 10 minutes. Glass slides were gently washed in deionized water for 1 minute and left to dry. Slides were then mounted and sealed with DPX mounting medium (Sigma-Aldrich, USA). A minimum of 100 cells per haemolymph sample was counted and classified into the different cell types based on size and morphology, and the relative percentages were calculated. Digital pictures were taken with proprietary Leica software, and measurements were processed using “ImageJ 1.48v” software (Rasband, 1997-2014) (Wayne Rasband, National Institute of Health).

5.2.5 Phagocytosis assay

In vitro, phagocytic activity assays were conducted using a modified method from Aladaileh et al. (2007). Briefly, zymosan suspensions were added to haemolymph samples in Eppendorf vials. Zymosan (cell walls of *Saccharomyces cerevisiae*, Sigma-Aldrich, Germany) was used as target cells for phagocytosis. Zymosan suspensions were prepared as described by Bachère et al. (1991). One milligram of zymosan was suspended in 10 mL of sterile-filtered seawater (FSW). To measure phagocytic activity, haemolymph samples were diluted 1:1 with modified Alsever’s solution (MAS). This anticoagulant solution was composed of glucose (20 g/L), Na citrate (8 g/L), EDTA (3.36 g/L) and Tween 80 (100 g/L) (Bachère et al., 1988).

A 50 µL dilution of haemolymph was placed on a glass coverslip and the cells were allowed to adhere for 30 minutes at room temperature in a moist chamber. The coverslips were rinsed five times with FSW, overlaid with 50 µL of zymosan solution (1×10^6 particles /mL) and incubated in a moist chamber for 30 minutes at room temperature. Non-ingested zymosan particles were

removed by dipping each coverslip in FSW 5 times. Haemocytes were stained by the Diff-Quick method. Coverslips were immersed into methanol and in eosin stain for 30 seconds and followed by methylene blue for 30 seconds. Then, coverslips were gently washed in deionized water and left to dry. The coverslips were carefully placed on glass slides and observed under a Leica DM 2000 microscope. Then, phagocytosis was observed at different times over a 2 hours incubation period (30, 60 and 120 minutes) and the accumulated phagocytosis was measured at each time interval. Phagocytic activity was determined as the percentage of haemocytes that had ingested at least one yeast cell after counting a minimum of 100 haemocytes on each coverslip.

5.2.6 Grading scale for bacterial association

Bacterial association analyses were performed by using the same HCMs slides prepared for DHC from 80 animals (5-15 mussels per month). HCMs slides preparation method was adapted from Maedel and Doig (2012) but this method was not vigorous enough for bacterial association as some bacteria might be detached from the slides during the fixation, washing steps, as they do not adhere to slides in the same way as haemocytes.

The number of *Vibrio*-like bacteria (Nguyen & Alfaro, 2020) for each haemolymph sample was assessed by a semi-quantitative (0-3) scale. Grading scale: 0 = Nil (bacteria absent), 1 = Low (<100 bacteria present per observed haemolymph sample), 2 = Medium (>100-500 bacteria present per observed haemolymph sample) and 3 = High (>500 bacteria present per observed haemolymph sample) were used to calculate the percentages of bacterial association.

5.2.7 Grading scale for granules of granulocytes

The number of granules for granulocytes were evaluated by a semi-quantitative (0-3) scale. Grading scale: 1 = Small (<50 number of granules present), 2 = Medium/average (>50-100 number of granules present) and 3 = Large (>100 number of granules present) were used to assess the number of granules for granulocytes.

5.2.8 Statistical analyses

Statistical analyses for phagocytosis assays were performed using one-way ANOVAs followed by Tukey's post-hoc test run with IBM® SPSS® Statistics software (version 23). Tukey's HSD was performed for pairwise comparisons of the season-wise percentages of phagocytosed zymosan. Moreover, Tukey's tests for pair-wise tests were used to compare different types of haemocytes. Data were presented as mean±SE. Differences were considered significant when $P<0.001$.

5.3 Results

5.3.1 Classification scheme

A total of six distinct haemocyte types (basophils, eosinophils, hyalinocytes, basophilic eosinophil, eosinophilic basophils and orange-brown cells) were identified in *P. canaliculus* by Chandurvelan et al. (2013) (see column 1, Table 5.1). At the beginning of this study, the scheme of Chandurvelan et al. (2013) was used to characterise the haemocytes of the *P. canaliculus* samples. However, when the scheme was found to be insufficiently representative for this mussel species, a new more inclusive scheme was developed (see column 3, Table 5.1). The differences between the new classification scheme proposed in this study and a previous classification by Chandurvelan et al. (2013) are shown in Table 5.1.

In this study, haemocytes of *P. canaliculus* were classified into 8 categories based on cell size, morphology, the nuclear/cytoplasmic (N/C) ratio of the cells, staining affinities of their cytoplasm and cytoplasmic granules. In hemacolor smears, two haemocyte categories, granulocytes (Fig. 5.1-5.3) and hyalinocytes (Fig. 5.4), were distinguished by light microscopy observation (LMO) according to the presence or the absence of cytoplasmic granules. Granulocytes could be further divided into two types- eosinophilic granulocytes and basophilic granulocytes (Fig. 5.1A & B) based on cytoplasm staining. Eosinophilic granulocytes were divided into three types -dense-granulocytes, semi-granulocytes and small semi-granulocytes according to cell size and granule density (Fig. 5.2A-D). Based on granule staining, granulocytes were classified as eosinophilic basophils granulocytes and mixed granulocytes (intermediate cells with both eosinophilic and basophilic granules) (Fig. 5.3A & B). Hyalinocytes could be further divided into two types-large hyalinocytes and small hyalinocytes according to cell size (Fig. 5.4A-C).

Table 5.1 *Perna canaliculus* haemocyte characterization showing the criteria of Chandurvelan et al. (2013) compared with the new classification in this study.

Chandurvelan et al. (2013)		This study				
Haemocyte name	Description	Haemocyte name	Haemocyte categories	Haemocyte sub categories	Description	
Absent	–	Granulocytes			Granulocytes were spherical or ovoid cells (6–14 µm) whose cytoplasm contains characteristic granules and the nucleus (spherical shaped) commonly eccentric with high nucleus/cytoplasm ratios (the cytoplasm volume is much more than the nuclear volume). Granulocytes could be further divided into two types- eosinophilic granulocytes and basophilic granulocytes based on cytoplasm staining. Based on granule staining, granulocytes were classified as eosinophilic basophils granulocytes and mixed granulocytes. (Note the shapes were reported after staining).	
Eosinophils	Eosinophils were identified as large, granular, pink-stained cells.				Eosinophilic granulocytes	A great number of cells exhibited small red granules (eosinophilic) within the cytoplasm. These cells were identified as eosinophilic granulocytes (Fig. 5.1A). Eosinophilic granulocytes were round or ovoid with the largest nucleus to cytoplasm ratio among granulocytes. The nucleus was spherical. Eosinophilic granulocytes were divided into three types (i.e., dense-granulocytes, semi-granulocytes and small semi-granulocytes) according to cell size and granule density.
Absent	–				Dense-granulocytes (eosinophilic)	Many large, dense (closely compacted) granules were observed in the cytoplasm of these cells (Fig. 5.2A & B). Granules were eosinophilic. Dense granulocytes were round or ovoid with pink colour cytoplasm. This type of cell was full of granules with less space inside and displayed a plump surface in contrast with semi-granulocytes (eosinophilic) and small semi-granulocytes (eosinophilic) (Fig. 5.2B, C & D).

Chandurvelan et al. (2013)		This study			
Haemocyte name	Description	Haemocyte name	Haemocyte categories	Haemocyte sub categories	Description
Absent	–			Semi-granulocytes (eosinophilic)	Medium/average number of granules were present, and they were small and red coloured. Semi-granulocytes were round or ovoid (10-14 µm) with pink coloured cytoplasm (Fig. 5.2A & C).
Absent	–			Small semi-granulocytes (eosinophilic)	Small semi-granulocytes only differed from semi-granulocytes in size (6-8 µm) (Fig. 5.2A & D). Medium/average numbers of granules were present. Granules were small and red coloured. Small semi-granulocytes were round or ovoid with pink cytoplasm.
Basophils	Basophils were identified as large, granular, blue-stained cells.		Basophilic granulocytes		Basophilic granulocytes (Fig. 5.1B) were characterized by a small amount of purple/blue-stained cytoplasm containing large dark violet to black dense granules. Basophilic granulocytes were round or ovoid cells. The nucleus to cytoplasm ratio was low (nuclear/cytoplasmic volumes are more similar). The nucleus was spherical.
Eosinophilic basophils	Eosinophilic basophils were identified as pink-stained cytoplasm and blue-stained granules.		Eosinophilic basophils (granulocytes)		A notable characteristic of the eosinic basophil granulocytes was the presence of many, blue granules in the eosinophilic pink cytoplasm (Fig. 5.3A). These cells were round or ovoid (10-14 µm) in shape.
Basophilic eosinophil	A basophilic eosinophil was characterised as a haemocyte with blue-stained cytoplasm and pink-stained granules.	Absent			–

Chandurvelan et al. (2013)		This study			
Haemocyte name	Description	Haemocyte name	Haemocyte categories	Haemocyte sub categories	Description
Abstent	-		Mixed granulocytes		Mixed granulocytes were characterised as intermediate cells, which contain both red eosinophilic) and blue (basophilic) granules (Fig. 5.3B). Round or ovoid cells (10-14 µm) with small nuclei (3-4 µm).
Orange-brown cells	The cell type identified was an orange-brown cell, which displayed a characteristic orange to brown-coloured cytoplasm and a blue nucleus.	Absent			—
Hyalinocytes	Hyalinocytes stained blue, but had very few, or no, granules in the cytoplasm.	Hyalinocytes			Hyalinocytes were characterized by larger (in comparison with the cytoplasm), ovoid or irregular eccentric nuclei. Hyalinocytes have basophilic (light blue-stained) cytoplasm with Giemsa staining with a minor (blue coloured) or absent granulation. Hyalinocytes could be further divided into two types (i.e., large hyalinocytes and small hyalinocytes) according to size.
Absent	—		Large hyalinocytes		Large cells that were 15–20 µm in diameter with large nuclei (10-15 µm). Large hyalinocytes had a low nucleus/cytoplasm ratio (nuclear/cytoplasmic volumes are more similar) (Fig. 5.4A). The larger hyalinocytes had a more abundant cytoplasm with thin filopodia (slender cytoplasmic projections).
Absent	—		Small hyalinocytes		Small hyalinocytes were small spherical cells that were 5–7 µm in diameter with nuclei that were 3-4 µm in diameter (Fig. 5.4B & C). Small hyalinocytes had a high nucleus/cytoplasmic ratio.

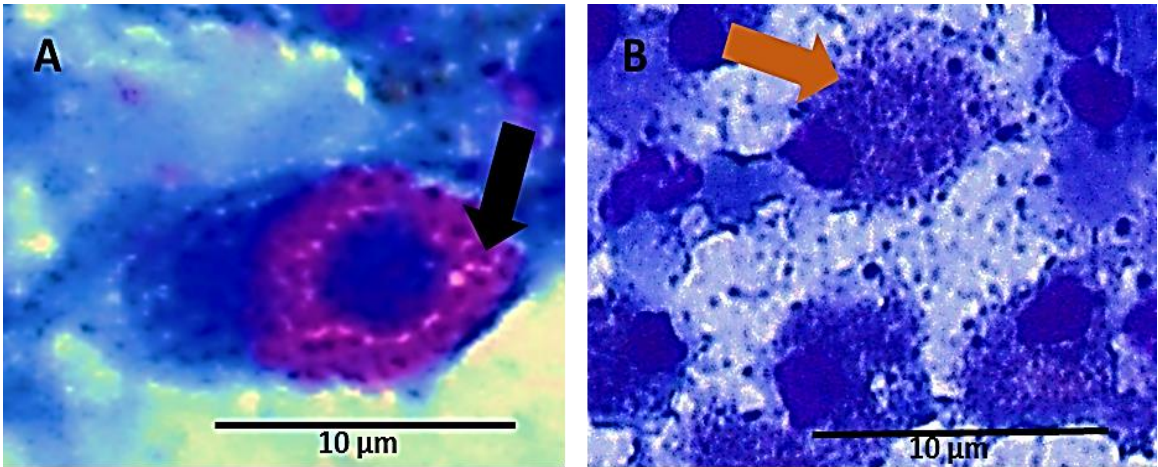


Figure 5.1 A) Eosinophilic granulocytes and B) basophilic granulocytes. Scale bar = 10 µm.

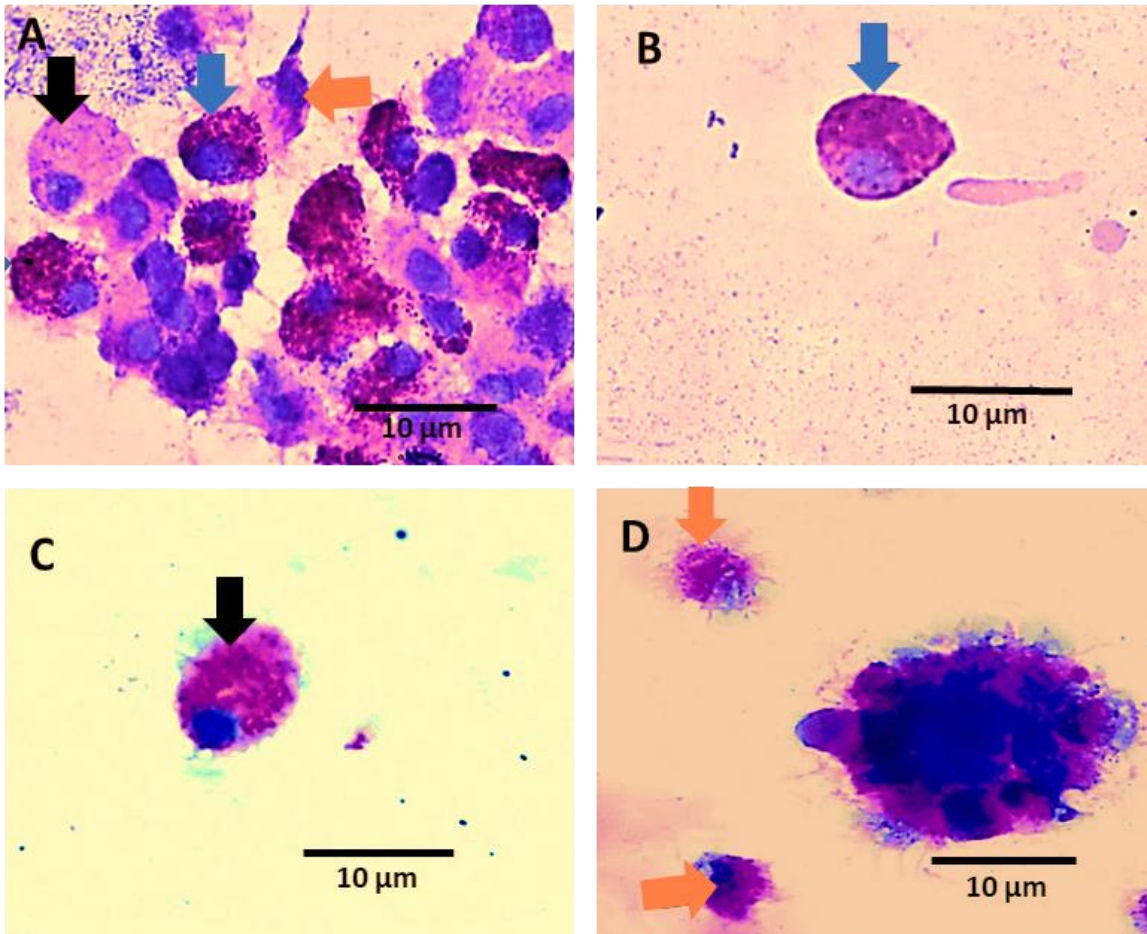


Figure 5.2 A) Dense-granulocytes (blue arrow), semi-granulocytes (black arrow) and small semi-granulocytes (orange arrow), B) dense-granulocyte (blue arrow), C) semi-granulocyte (black arrow) and D) small semi-granulocytes (orange arrows). Scale bar = 10 µm.

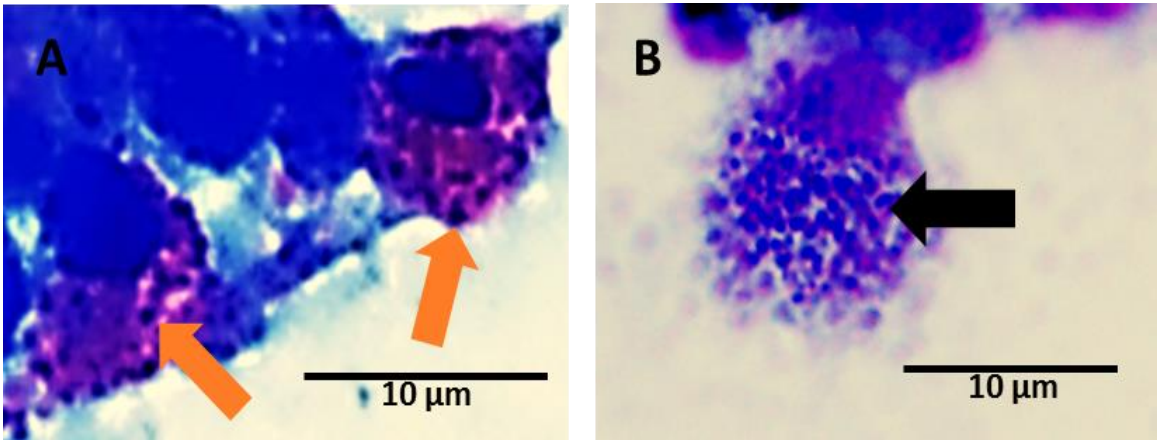


Figure 5.3 A) Eosinophilic basophils (orange arrows) and B) mixed granulocytes (black arrows). Scale bar = 10 μm.

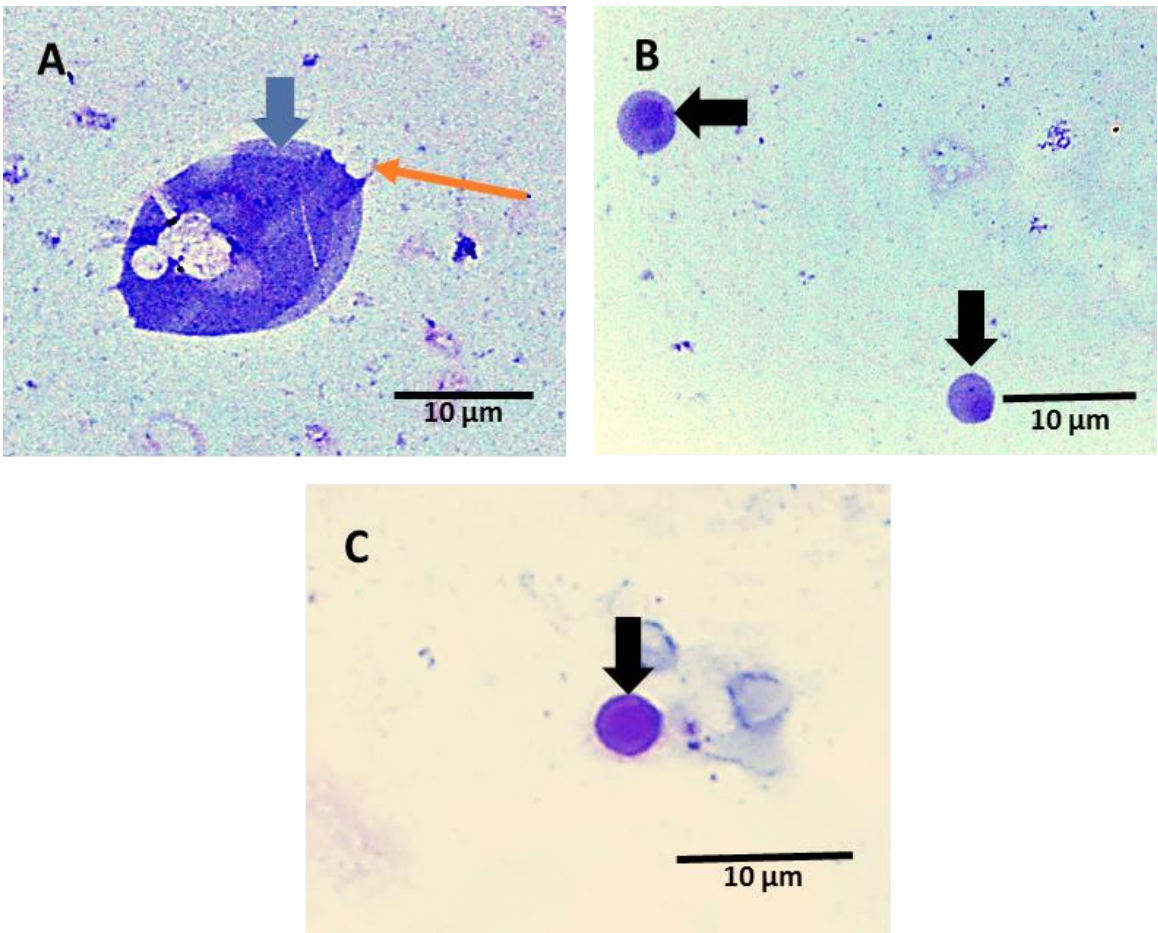


Figure 5.4 (A) Large hyalinocytes (blue arrow), Filopodia (orange arrow), (B) and (C) small hyalinocytes (black arrows). Scale bar = 10 μm.

[Note: The reason behind poorly staining of hyalinocytes might be that the reagents were not exchanged with new reagents at regular intervals].

5.3.2 Differential Haemocyte Counts (DHC)

Table 5.2 lists eight haemocyte types and the proportion of each type as a percentage of the total haemocyte count. The distributions of the overall percentages of haemocyte types (percent of eosinophilic granulocytes, basophilic granulocytes and hyalinocytes) and those for different types of eosinophilic granulocytes and hyalinocytes are shown in figure 5.5. Mean percentages of eosinophilic granulocytes, basophilic granulocytes and hyalinocytes were varied from one month to another (Fig. 5.6).

Table 5.2 Percentages of different types of haemocytes. Bold values indicate Mean percentages (\pm SE) of the haemocyte categories.

Differential Haemocyte Counts (DHC)		
Haemocyte types	Percentages (%)	Total sample
Dense-eosinophilic granulocytes	13.7 \pm 1.7	80
Semi-eosinophilic granulocytes	24.7 \pm 1.6	80
Small semi-eosinophilic granulocytes	16.4 \pm 1.4	80
Total eosinophilic granulocytes	55\pm3.2	80
Total basophilic granulocytes	27.2\pm2.9	80
Total eosinophilic basophil granulocytes	0.2\pm0.2	80
Total mixed granulocytes	0.1\pm0.0	80
Large hyalinocytes	6.6 \pm 1.4	80
Small hyalinocytes	13.3 \pm 2.2	80
Total hyalinocytes	19.7\pm3.4	80

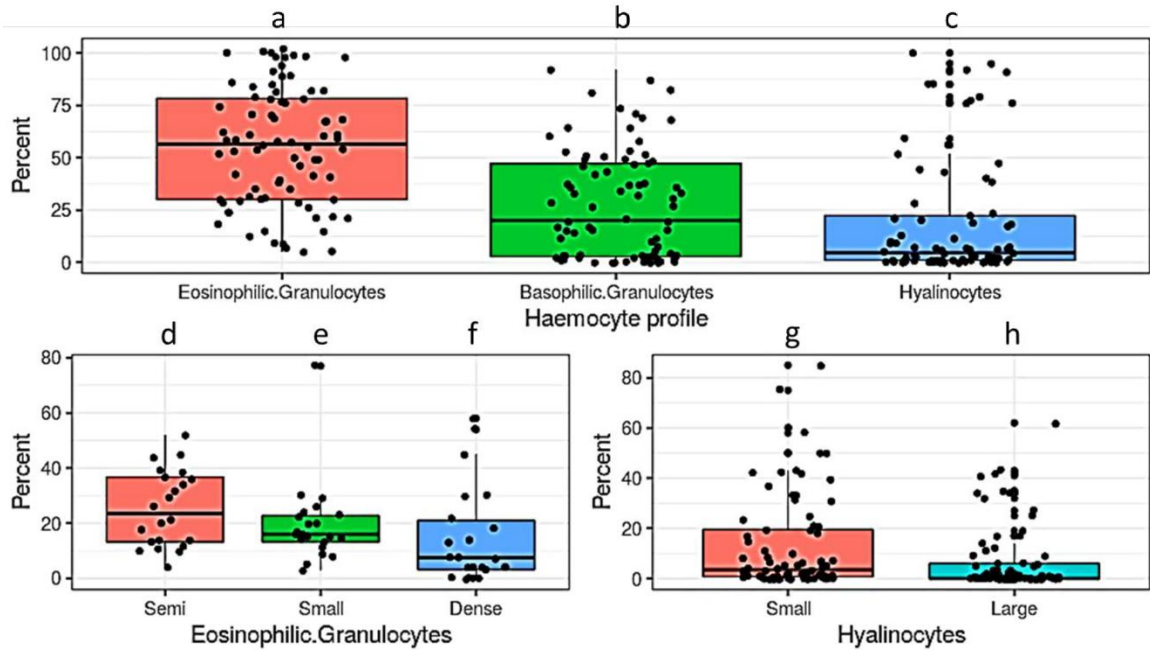


Figure 5.5 Distributions of overall (n = 80) percentages of haemocytes (eosinophilic granulocytes = a, basophilic granulocytes = b and hyalinocytes = c), and those for different types of eosinophilic granulocytes (d, e and f) and hyalinocytes (g and h). The different letters denote significant differences among haemocyte categories.

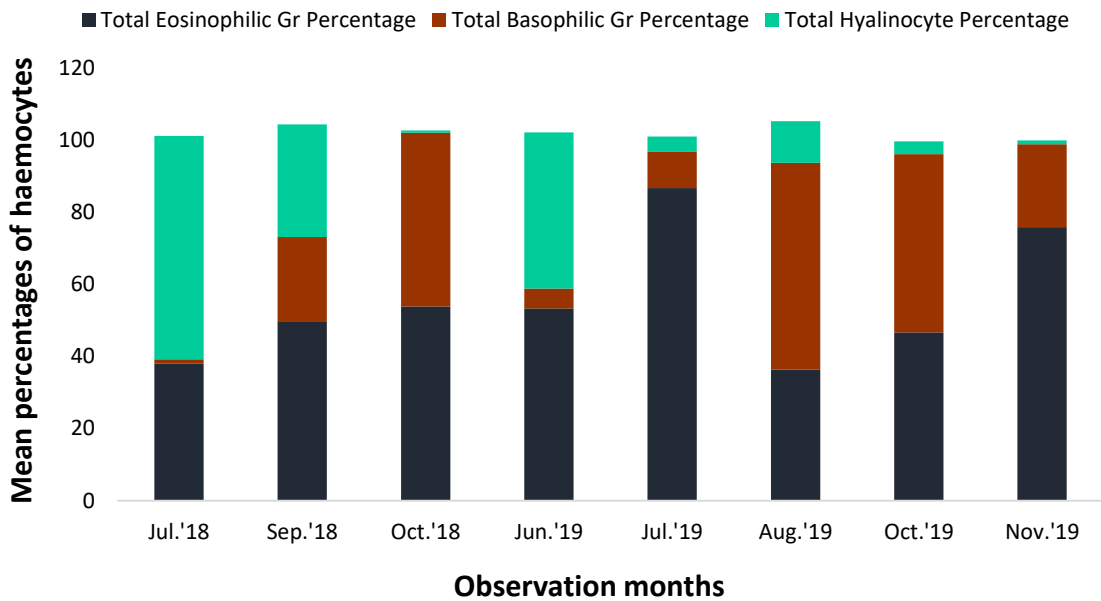


Figure 5.6 Mean percentages of eosinophilic granulocytes, basophilic granulocytes and hyalinocytes based on monthly observation.

Tukey's tests for pair-wise comparisons for equality of overall haemocytes (eosinophilic granulocytes, basophilic granulocytes and hyalinocytes), the types of eosinophilic granulocytes (small, semi and dense) and the types of hyalinocytes (small and large) were applied in this study. There was no significant difference (p -value = 0.164) in the percentage of hyalinocytes and basophilic granulocytes (Tukey's tests for pair-wise comparisons for equality) among mussel samples (between the replicates/each individual mussels). There were significant differences among eosinophilic granulocytes-basophilic granulocytes (p -value = 0.001) and eosinophilic granulocytes-hyalinocytes (p -value = 0.001) (Tukey's tests for pair-wise comparisons for equality). The percentage of eosinophilic granulocytes was higher than the expected percentage of basophilic granulocytes, which in turn was higher than hyalinocytes in the mussel samples. In the present study, it was observed that among the eosinophilic granulocytes, there was no significant difference (p -value = 0.431) in the percentage of small-dense mussel samples (Tukey's tests for pair-wise comparisons for equality). There were significant differences among small-semi (p -value = 0.001) and semi-dense (p -value = 0.001). The semi-granulocytes were slightly higher than small semi-granulocytes and dense-granulocytes among mussel samples. Moreover, the percentage of small hyalinocytes was significantly (p -value = 0.013) higher than large hyalinocytes (Tukey's tests for pair-wise comparisons for equality). The percentage of small hyalinocytes was higher than that of large hyalinocytes among the samples where hyalinocytes were identified.

5.3.3 Bacteria (Vibrio-like) associated with haemocytes

Some particles that looked like rod-shaped bacteria (*Vibrio*-like) were also found in the haemolymph (Fig. 5.7A-B). Since mussels have a semi-open circulatory system, to get bacteria in haemolymph is normal. The bacterial load can be of 10^4 CFU/ml haemolymph but can fluctuate with the seasons. However, in the present study, mussels haemocytes associated with bacteria were recorded in winter and spring seasons [5-15 mussels were collected per month – July'18, September'18, October'18, June'19, July'19, August'19, October'19 and November'19 which covered only two seasons-winter and spring] and there was no seasonal variation of bacterial association. In this study, 27.5% of the mussel haemocyte samples were positive/associated with bacteria. However, 1.3 % were observed in haemocyte samples with a low (1) number of bacteria. On the other hand, 21.3% of haemocyte samples showed a high (3) number of bacteria and 5% of haemocyte samples presented a medium (2) number of bacteria (Table 5.3).

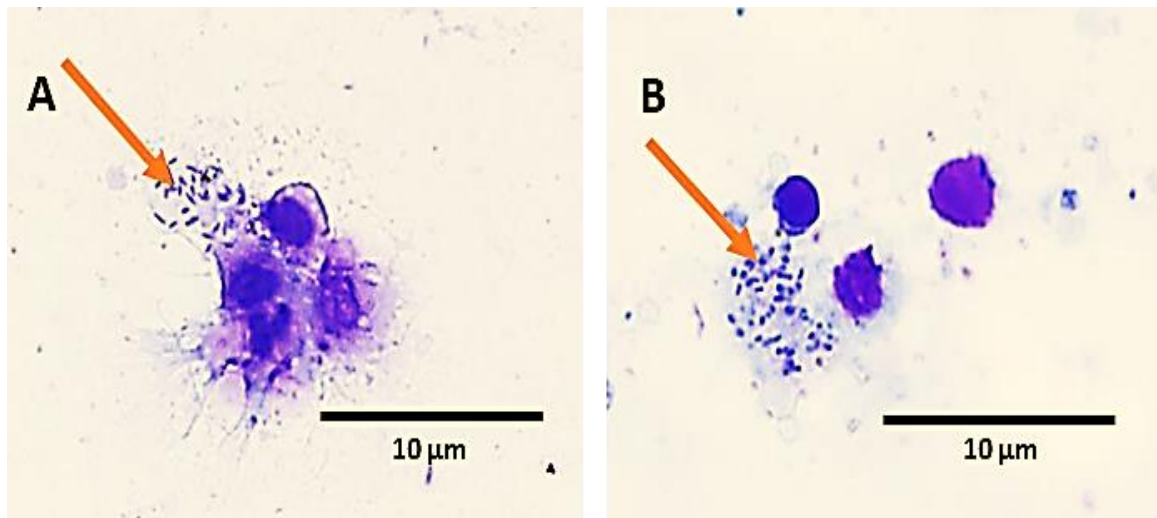


Figure 5.7 A) and B) Rod-shaped *Vibrio*-like bacteria (orange arrow) near haemocytes. Scale bar = 10 µm.

Table 5.3 Percentages of samples (n = 80) associated with bacteria (*Vibrio*-like).

Samples associated with bacteria			
Grading (0-3)	Percentages (%)	Frequency (n)	Total sample
No bacteria (0) = Nil (bacteria absent)	72.5	58	80
Bacteria number low (1) = <100 bacteria present per observed haemolymph sample	1.3	1	80
Bacteria number medium (2) = >100-500 bacteria present per observed haemolymph sample	5	4	80
Bacteria number high (3) = >500 bacteria present per observed haemolymph sample	21.3	17	80

In this study, there was no significant difference (p -value = 0.26) in the percentage of hyalinocytes and basophilic granulocytes among the bacteria-associated mussel samples. There were significant differences in the percentage of eosinophilic granulocytes and basophilic granulocytes (p -value = 0.0002) among the bacteria-associated mussel samples (Tukey's tests for pair-wise comparisons for equality). Moreover, there were significant difference in the percentage of hyalinocytes and eosinophilic granulocytes (p -value = 0.001) among the bacteria-associated mussel samples (Tukey's tests for pair-wise comparisons for equality). The percentage of eosinophilic granulocytes was higher than the percentage of basophilic granulocytes, which in turn was higher than hyalinocytes in samples with the presence of bacteria (Fig. 5.8). It was also observed that among the eosinophilic granulocytes-bacteria associated samples, the percentage of type "semi" was

significantly higher than the percentage of “dense” (p -value = 0.069) at a 10% significant level (Tukey’s tests for pair-wise comparisons for equality). Similarly, the percentage of small hyalinocytes was significantly higher than large hyalinocytes (p -value = 0.078) at a 10% significant level (Tukey’s tests for pair-wise comparisons for equality).

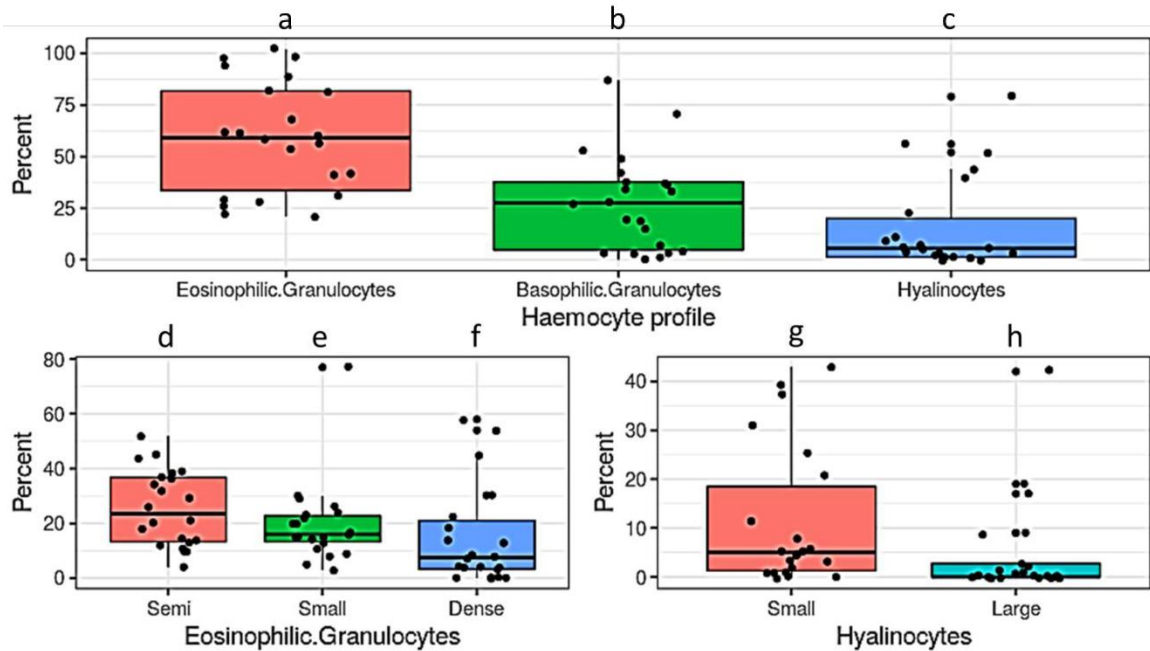


Figure 5.8 Distributions of overall ($n = 80$) percentages of haemocytes (eosinophilic granulocytes = a, basophilic granulocytes = b and hyalinocytes = c), and those for different types of eosinophilic granulocytes (d, e and f) and hyalinocytes (g and h) using the samples where bacteria were present. The different letters denote significant differences among haemocyte categories.

5.3.4 Phagocytosis assay

The observed differences between the phagocytic uptakes of the haemocyte types may indicate distinct roles in the host immune system. The phagocytosis index in this study was determined as the percentage of cells that had engulfed at least one zymosan particle. While the hyalinocytes exhibited no phagocytic activity, both types of granulocytes (basophilic and eosinophilic) were phagocytic (Fig. 5.9A-D). The basophilic granulocytes showed lower phagocytic activity than the eosinophilic granulocytes. Of the three eosinophilic granulocyte types, the semi-granulocytes exhibited the highest level of phagocytic activity.

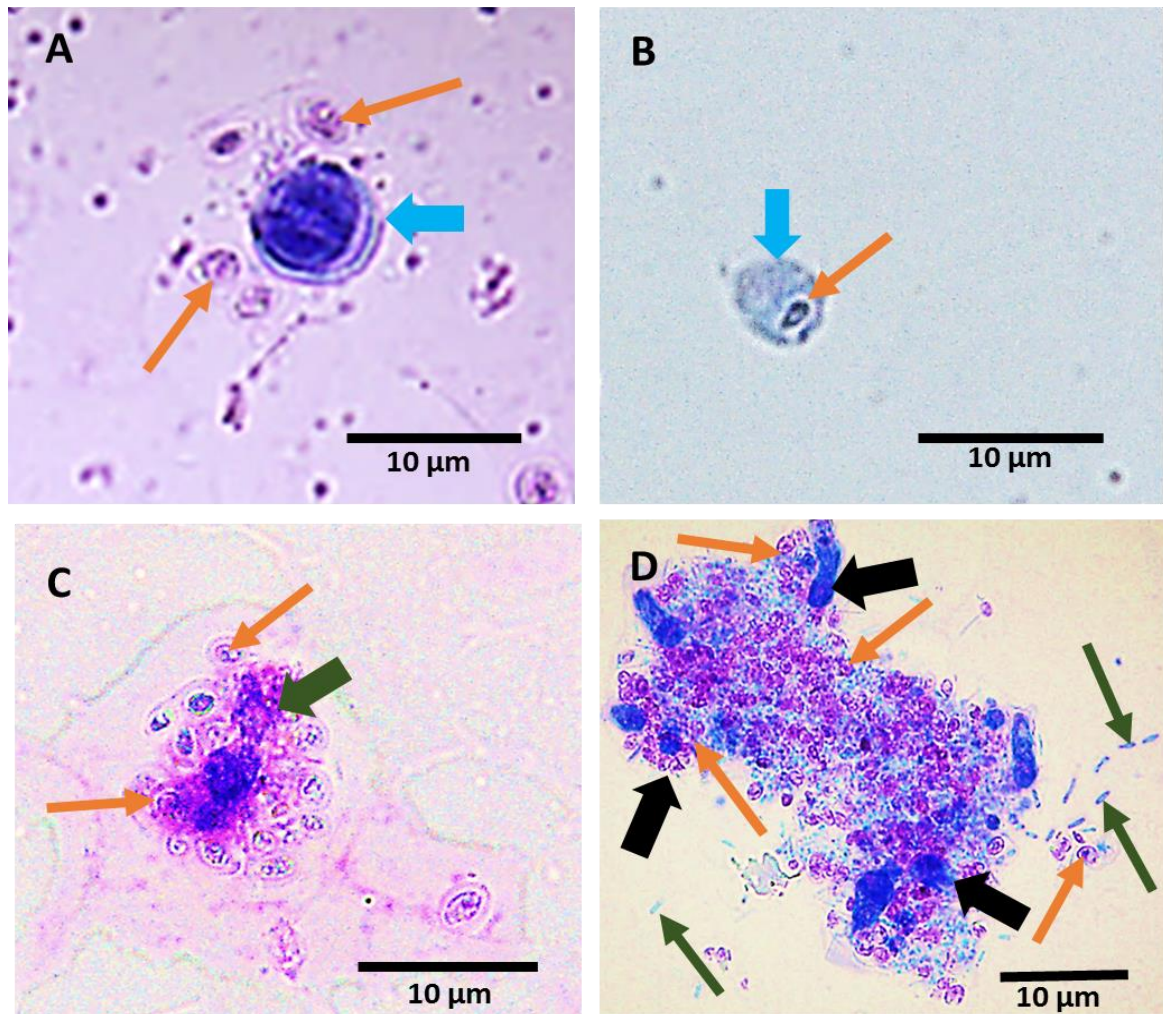


Figure 5.9 Monolayer of haemocytes challenged with zymosan particles (orange arrows), (A) non-phagocytosing haemocytes (basophilic granulocytes) (blue arrow), (B) phagocytosing haemocytes (basophilic granulocytes) (blue arrow) with ingested zymosan particles, (C) eosinophilic semi-granulocytes (green arrow) with adhered zymosan particles (orange arrows) and (D) phagocytosing haemocytes with ingested zymosan particles (orange arrows) and numerous rod-shaped bacteria (green arrows) surrounding haemocytes (black arrows). Scale bar = 10 μ m.

The percentage of all types of haemocytes with phagocytosed particles (zymosan) were affected by the incubation time (30, 60 and 120 minutes). The phagocytosis percentage increased over time, indicating an increase of zymosan particle uptake as follows 18.42 \pm 1.7% after 30 minutes, 32.08 \pm 3.1% after 60 minutes and 44.74 \pm 3.5% (maximum) phagocytic cells after 120 minutes of incubation. After this point, the phagocytosis index did not change over time (plateau phase). An ANOVA test demonstrated that phagocytosis percentages were significantly different from each other (n = 50) for incubation time 30 minutes (p -value = 0.001), 60 minutes (p -value = 0.001) and 120 minutes (p -value = 0.001) (Fig. 5.10).

The mean percentage of phagocytic cells for the incubation time (30, 60 and 120 minutes) decreased from June to July and from July to August. The lowest phagocytosis mean percentage was observed in August (winter season, 7-15°C). After that, the mean percentages of cells with phagocytosed zymosan for the incubation time (30, 60 and 120 minutes) increased from August to October (winter to spring) and October to November (spring season, 11-20°C). Then, the mean percentage of phagocytic cells for all the incubation time increased from November to December (spring to summer season) (Fig. 5.10). The highest phagocytic uptake was observed in the summer season (15-22°C).

A one-way ANOVA test was conducted separately for each incubation period. The tests revealed that on average, the percentages of cells with phagocytosed zymosan were significantly different (p -value <0.001) in winter, spring and summer of the study period. Thus, a follow-up test to ANOVA, i.e., Tukey's HSD was performed for pairwise comparisons of the season-wise percentages of phagocytosed zymosan (Table 5.4). The phagocytic uptake increased significantly from winter to spring and from spring to summer seasons (p -value<0.001). However, given a pair of seasons, on average, the percentage of cells with phagocytic uptake increased with the increase of incubation period. In this study, the highest percentage (81.8±4.8%) of phagocytic uptake was observed for 120 minutes incubation period in December, and the lowest percentage (8.2±0.6%) was observed for 30 minutes incubation period in June (Fig. 5.10).

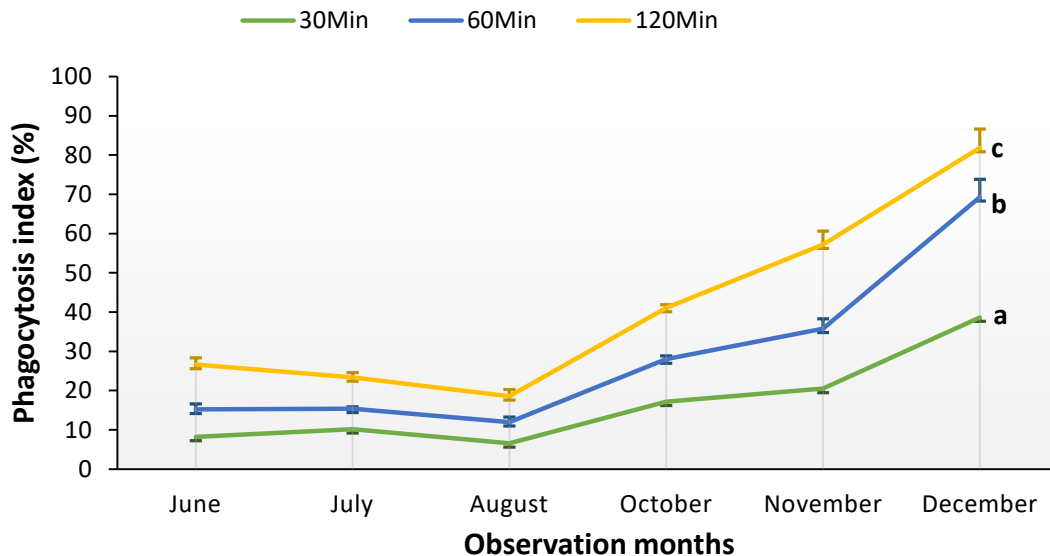


Figure 5.10 Mean±SE percentage of phagocytosis based on microscopic observation. Exposure time- a = 30 min, b = 60 min and c = 120 min. Each letter (a, b and c) indicates a significant difference.

Table 5.4 Tukey's HSD Post Hoc tests (n = 50) for the season-wise estimates of differences (Mean±SE) in the percentage of cells with phagocytic activity along with 95% confidence intervals.

Incubation period	Winter-Spring		Spring-Summer		Summer-Winter	
	Mean±SE	95% confidence intervals	Mean±SE	95% confidence intervals	Mean±SE	95% confidence intervals
30 minutes	-10.95*±1.30	-15.95, -5.95	-19.75*±1.60	-25.88, -13.62	30.70*±1.60	24.57, 36.83
60 minutes	-18.25*±2.53	-28.02, -8.48	-37.40*±3.10	-49.37, -25.43	55.65*±3.10	43.68, 67.62
120 minutes	-27.35*±3.29	-40.05, -14.65	-32.65*±4.03	-48.20, -17.10	60.00*±4.03	44.45, 75.55

*. The difference is significant at the 0.001 level.

[Table 5.4 showed the results of a post-hoc test, i.e., the pairwise tests for the significance of differences (diff) of percentages. In general, the negative value of a difference A-B implies that A is lower than B (or B is higher than A). Since, the post-hoc tests considered the differences between two proportions, not just the proportions, differences were negative or positive depending on the magnitude of former and later values in the differences].

Table 5.4 further presents the differences in the percentage of phagocytosis for each pair of seasons and incubation period. The 95% confidence interval further reveals that for different incubation periods (30 minutes, 60 minutes and 120 minutes), the phagocytic activity in summer was higher than that in winter. Conversely, the phagocytic activity in spring was lower than in summer, and the phagocytic activity in winter was lower than in spring (Table 5.4).

5.4 Discussion

5.4.1 Haemocyte classification

A new classification scheme that is more reflective of the actual state of haemocyte populations was developed for *Perna canaliculus*. In this study, differential haemocyte counts (DHC) were performed on haemolymph slides stained with Giemsa stain. Conversely, DHC were performed on haemolymph slides stained with 5% Wright stain by Chandurvelan et al. (2013). In the current study, haemocytes of *P. canaliculus* were classified based on cell size, morphology, the nuclear/cytoplasmic (N/C) ratio of the cells, staining affinities of their cytoplasm and cytoplasmic granules. However, the classification of *P. canaliculus* haemocytes presented by Chandurvelan et al. (2013) was based on the morphology and differential staining characteristics. The results of this

study revealed that *P. canaliculus* has 8 distinct haemocytes. In contrast, Chandurvelan et al. (2013) identified 6 distinct haemocyte types for *P. canaliculus*. Only a few haemocyte types (eosinophilic granulocyte, basophilic granulocytes, hyalinocyte and eosinophilic basophils granulocytes) are similar in both classification schemes, but dense-granulocytes (eosinophilic), semi-granulocytes (eosinophilic), small semi-granulocytes (eosinophilic), large hyalinocytes, small hyalinocytes and mix granulocytes were not identified by Chandurvelan et al. (2013). On the other hand, basophilic eosinophil and orange-brown cell that was observed by Chandurvelan et al. (2013), were not recognised in this study. Although Chandurvelan et al. (2013) identified six cell types, all were not considered for differential haemocyte counts (DHC). Three haemocyte types (basophilic eosinophil, eosinophilic basophils and orange-brown cell) were not considered as part of the DHC, as they occurred only rarely in scored slides (Chandurvelan et al., 2013). In this new classification, the eight types of haemocytes were described in detail and all the types were taken into account as part of differential cell count assessment. Therefore, the new scheme is more complete and more accurately describes the distribution and types of haemocytes.

5.4.2 Haemocyte types and functions

The results of this study indicate the presence of two general haemocyte categories: hyalinocytes and granulocytes, as described in other bivalves by several authors (Chang et al., 2005; Cheng, 1981; Hine, 1999; Wootton et al., 2003). In these studies, hyalinocytes are characterized as cells with no granules in their cytoplasm and a higher nucleus to cytoplasm ratio when compared with the granulocytes that have abundant granules. Therefore, the differentiation between hyalinocytes and granulocytes could be easily attained using light microscopy.

In the present study, hyalinocytes were identified into two categories (i.e., large hyalinocytes and small hyalinocytes) according to their size. Similar data were obtained by Dang et al. (2012) who also observed small hyalinocytes in the Sydney rock oyster *Saccostrea glomerata* and the pearl oyster *Pinctada fucata*.

It was possible to distinguish eosinophilic and basophilic granulocytes based on the staining affinities of their cytoplasmic granules. The characteristics of the eosinophilic granulocytes and basophilic granulocytes of *P. canaliculus* were similar to those of the eosinophilic granulocytes and basophilic granulocytes in *Bathymodiolus azoricus* (Bettencourt et al., 2009), *Mytilus edulis* (Pipe et al., 1997; Wootton et al., 2003), and *Mytilus galloprovincialis* (Carballal et al., 1997a; Carballal et al., 1997b).

Mixed granulocytes were found to be an intermediate cell type, which contains both red (eosinophilic) and blue (basophilic) granules. Carballal et al. (1997b) also reported this type of granulocyte in another mussel (*M. galloprovincialis*) and Chang et al. (2005) also observed mixed granulocytes in oysters (*Crassostrea gigas*).

Eosinophilic small semi-granulocytes, semi-granulocytes and dense-granulocytes, are here reported for the first time in *P. canaliculus*. Similar findings were also found in another mussel (*Perna viridis*) by Wang et al. (2012).

Granulocytes made up more than 80% of the haemocyte population with hyalinocytes making up less than 20% in *P. canaliculus*. Similar higher percentages of granulocytes were also observed in Mediterranean mussel *M. galloprovincialis* (60%) (Cajaraville et al., 1996) and hard clam *Mercenaria mercenaria* (75%) (Tripp, 1992). Conversely, higher percentages of hyalinocytes were observed in the clam *Chamelea gallina* (79%) (Pampanin et al., 2002), the mussel *Perna perna* (60%) (Barracco et al., 1999) and the scallop *Argopecten irradians* (55%) (Zhang et al., 2006). According to Wang et al. (2012), percentages of different haemocytes varied significantly among bivalve species. Variations in both the percentages of different haemocytes and the total number of circulating haemocytes in bivalves influenced by various exogenous (e.g. temperature, salinity or oxygen levels, Gagnaire et al., 2006; Hégaret et al., 2003; Wang et al., 2012) and endogenous factors (e.g. sex, Matozzo & Marin, 2010; age and reproductive state, Lachambre et al., 2017). In this study, monthly variations of mean percentages of eosinophilic granulocytes, basophilic granulocytes and hyalinocytes were recorded. Soudant et al. (2004) and Flye-Sainte-Marie et al. (2009) demonstrated the seasonal effects on the total number of circulating haemocytes and haemocyte size. According to Soudant et al. (2004) and Flye-Sainte-Marie et al. (2009), the size of haemocytes can be smaller than the size of mature cells when cell division occurred. Thus, more mature haemocytes can be bigger than less mature haemocytes and they are the same cell type but taken at different lifetimes and the total number of haemocytes fluctuate during the seasons. Since granulocytes are sticky and strongly attached to the smear slides but hyalinocytes are not sticky, in this study, many hyalinocytes cell types were lost during preparing the smear slides. Zhang et al. (2005) reported that small hyalinocytes easily lost from Giemsa-stained smear slides. Therefore, it is possible to vary the percentages of different haemocytes among bivalve species due to the mussels' age, physical status, biotic and abiotic factors, and the methods used.

Haemocytes were involved in phagocytosis-like immune function in *P. canaliculus* and they engulfed foreign particles. This finding supports the work of Tame et al. (2015) who also reported that haemocytes are phagocytic cells, which eliminate foreign microorganisms that invade the

haemolymph and tissue. According to Canesi et al. (2002) and Pruzzo et al. (2005), bivalves can eliminate pathogens from their tissues through haemocytes which can bind, phagocytize, and kill the bacteria, microbes and other pathogens. Thus, the findings confirm that haemocytes are associated with phagocytic activity and play a distinct role in the mussel immune system.

Among the haemocyte populations, phagocytic activity was only observed in granulocytes (eosinophilic and basophilic). Tame et al. (2015) described that both types of granulocytes (eosinophilic and basophilic) were phagocytic in deep-sea symbiotic mussels *Bathymodiolus japonicus*, *B. platifrons*, and *B. septemdiarium*. Granulocytes have been documented as having one of the most active phagocytic activities and containing abundant hydrolytic enzymes among bivalve species (Aladaileh et al., 2007; Chang et al., 2005; Goedken & de Guise, 2004; Zhang et al., 2006). Thus, these findings indicate that the two types (eosinophilic and basophilic) of granulocytes might be phagocytic cells and may play distinct roles in the defense system to engulf microorganisms and foreign particles to protect the body. Further experiments should be devised to explore this. The hyalinocytes in the present study were non-phagocytic. Hyalinocytes had limited phagocytic ability and lower levels of hydrolytic enzymes. Similar results were reported in other bivalves (Hine & Wesney, 1994; Mourton et al., 1992; Russell-Pinto et al., 1994). This study demonstrates that there are functional differences between mussel haemocyte types and these differences may indicate that granulocytes are involved in the host immune system and may target different types of microorganisms during the phagocytosis process.

5.4.3 Bacterial association

This study showed *Vibrio-like* bacteria associated with the mussel haemocytes. Haemolymph-associated microbiota was also recorded in marine bivalves- (*C. gigas*, *M. edulis*, *Pecten maximus* and *Tapes rhomboides*) by Desriac et al. (2014). Lau et al. (2018), also observed components of the opportunistic bacterial pathogen *Vibrio alginolyticus* (bacterial cells and extracellular products) in haemocytes of oysters (*Crassostrea virginica*). In this study, no seasonal variation was recorded for bacterial association with the mussel haemocytes. According to Wendling et al. (2014), *Vibrio* in the hemolymph of Pacific oysters *C. gigas* showed strong seasonal variation in diversity, prevalence and virulence. Opportunistic bacteria can infect pallial haemocytes through pallial organs (mantle, gills and body wall) (Lau et al., 2018) and can be transmitted directly through the water column from infected to uninfected oysters (Chu, 1996). Similarly, the *P. canaliculus* samples in this study were likely associated with microorganisms present in surrounding water through their pallial organs.

5.4.4 Phagocytic activity

The results of the present study show that the total phagocytic uptake in *P. canaliculus* haemocytes increased significantly over time up to 120 minutes and after that period, the phagocytosis index did not continue to change. Percentages of haemocytes with zymosan particles during different incubation times were significantly different from each other. Similar results were also reported in other bivalves, for example, the scallop *Pecten maximus* (LeGall et al., 1991; Mortensen & Glette, 1996), the percentage of phagocytic uptake by haemocytes of *P. maximus* increased over the incubation period. Since the highest percentage of phagocytic uptake was observed for 120 minutes incubation period and after this point it was a plateau phase, 2 hours might be the best time to incubate the haemocytes of *P. canaliculus* to measure the phagocytosis.

In this study, phagocytic performance was successfully observed in *P. canaliculus* (semi-granulocytes exhibited the highest level of phagocytic activity) in different seasons and temperatures. The percentage of phagocytic cells was significantly lowest in the winter (7-15°C) and highest in the summer (15-22°C). Similar observations were stated previously by Rahman et al. (2019), who noted that the phagocytic activity of haemocytes was significantly varied among different temperatures and increased from 15°C to 20–25°C in Pacific oysters (*C. gigas*), Mediterranean mussels (*M. galloprovincialis*) and mud cockles (*Katelysia rhytiphora*). Monari et al. (2007) also noticed high level of phagocytic activity at 20°C in the clam *Chamelea gallina*. Carballal et al. (1997c) found that the percentage of phagocytic haemocytes from *M. galloprovincialis* was lower at 10°C than at 20°C and 30°C. Mackenzie et al. (2014), also noted significantly increased phagocytosis in blue mussel (*M. edulis*) under increased temperatures (16°C temperature conditions). Inhibition of phagocytosis by low temperature (below 8°C) was seen in *C. virginica* and *Mercenaria mercenaria* haemocytes (Alvarez et al., 1989; Chu & La Peyre, 1993; Tripp, 1992). Phagocytosis is a temperature-dependent process in bivalve molluscs (Oliver & Fisher, 1999), which can influence haemocyte activity and important immune functions, (Chen et al., 2007; Hegaret et al., 2003; Perrigault et al., 2011; Yu et al., 2009). Fisher and Tamplin (1988) considered that the increase of phagocytic activity at high temperatures was the result of the increase of haemocyte locomotion which increased the number of haemocyte encounter with foreign particles. In this study, a greater number of circulating haemocytes were found to have increased haemocyte locomotion in the summer (higher temperature), which may be the result of an increased need to engulf pathogens, likely to be more abundant at this time of the year. Consequently, the higher summer temperatures may affect the haemocyte phagocytic function of *P. canaliculus* in a manner that increases their ability to respond to pathogens and foreign particles.

5.5 Conclusions

A new classification scheme for *Perna canaliculus* haemocytes was developed which is improved and more representative for haemocyte characterization. Under this new scheme, eight distinct types of haemocytes were identified. In this study, the phagocytic performance was successfully observed which demonstrated that granulocytes only showed phagocytosis while the hyalinocytes exhibited no phagocytic activity. Moreover, it was noticed that phagocytic activity changed with season and temperature. The lowest percentage of phagocytosis was seen in the winter season (lower temperature), and the highest phagocytosis was noted in the summer season (higher temperature). Furthermore, it was observed that among bacteria associated samples, the percentages of the different types of haemocytes varied significantly from one another, which suggests that these differences of haemocytes proportion due to the presence of bacteria will provide new diagnostic approaches to assessing mussel health. Therefore, such knowledge and approach would contribute to the development of disease management strategies of mussels, *P. canaliculus* and other aquaculture species.

Chapter 6

Acute thermal stress and endotoxin exposure modulate metabolism and immunity in marine mussels (*Perna canaliculus*)



New Zealand Greenshell™ mussels (*Perna canaliculus*)
exposure to endotoxin and thermal stressors

Abstract: Mass mortalities of New Zealand Green-lipped mussels (*Perna canaliculus*) are thought to be associated with increased water temperatures and immune challenges from opportunistic pathogens. However, the combined effects of acute thermal stress and immune stimulation on mussels are poorly understood. To investigate these responses, adult mussels were exposed to different temperatures (26°C [thermal stress] vs 15°C [ambient]) and a bacterial-derived endotoxin injection (with vs without) to mimic a pathogen infection. Various immunological and metabolic parameters were measured over two days via enzyme staining reactions, flow cytometry, and metabolomic profiling. None of the treatments impacted total and differential haemocyte counts, haemocyte viability or production of reactive oxygen species. Acid phosphatase and phenoloxidase activities were detected only within granulocytes (not in hyalinocytes), although their relative expressions also were not affected. Conversely, metabolite profiling exposed impacts of thermal stress and endotoxin exposure at a metabolic level, indicative of physiological changes in energy expenditure and partitioning. At the higher water temperature, free fatty acid and amino acid constituents increased and decreased, respectively, which supports an elevated energy demand and higher metabolic rate due to thermal stress. Ultimately, energy production is being sustained via multiple routes including the glycolysis pathway, TCA cycle, and β -oxidation. Additionally, branched-chain amino acids, the urea cycle and the glutathione pathway were affected by the higher temperature. The metabolic response of mussels exposed to endotoxin exposure resulted in increased metabolite response largely linked to protein and lipid degradation. After 5 days of exposure, survival data confirmed a severe physiological impact of the higher temperature through incidences of mortality. However, the thermal challenge in combination with the specific endotoxin treatment applied did not lead to a synergistic effect on mortality. These findings provide new insights into the relationship between thermal stress and immunity to better understand the immune defence system in mussels.

6.1 Introduction

Chronic and acute variations in ocean temperature are increasingly impacting on marine ecosystems. During the austral summers of 2017/2018 and 2018/2019, regions of New Zealand experienced intense and unprecedented ocean-atmosphere heatwaves, with higher sea surface temperatures (SSTs) than the monthly average at times (as warm as 5°C higher) (Chiswell & Sutton, 2020; Salinger et al., 2019;). Consequences of these changes in thermal gradients included abnormal and large-scale movements of fish, changes in ecosystem structure through localised extinction of kelp forests, and incidences of mass mortalities in fish and shellfish stocks (Genin et al., 2020; Lupo et al., 2021; Stillman, 2019).

The endemic green-lipped mussel (*Perna canaliculus*) industry is the largest aquaculture industry in New Zealand, based on tonnage and export value (Symonds et al., 2019). Marine heatwave events have been associated with on-farm mussel mortalities, with probable future occurrences being a concern for the industry. During the recent spikes in SSTs, mussels in the Firth of Thames (North Island, New Zealand) started displaying signs of poor health (i.e., shell gapping, slow/sluggish reaction to manipulation, organ discolouration) and expressed specific protein and metabolite biomarkers associated with a thermal stress response (Li et al., 2020), along with other molecular signatures implicated in immune-detection of microbial pathogens (Nguyen & Alfaro, 2020). It is generally thought that interactions between multiple stressors (e.g., temperature and microbial exposure) are responsible for shellfish mortalities during acute ocean warming events (Webb & Duncan, 2019). However, it is not yet established whether increased virulence of pathogens during warmer temperatures are a primary driver for poor health, or whether pathogen loading of opportunistic marine microbes is an opportunistic consequence of an already compromised immune system due to the thermal stress response.

Characterising combined effects of thermal stress and pathogen-based immune stimulation on different biological endpoints may provide insight into how these multiple stressors interact. Mimicking pathogen-associated molecular patterns, endotoxin (lipopolysaccharide) can be used as an exposure agent to elicit the natural innate immune response (Parusel et al., 2017). For example, endotoxins activate cellular and humoral defence mechanisms in mussels, with subsequent impacts on various metabolic processes (Nguyen et al., 2019a). Key physiological responses to immune stimulation and thermal stress can be sought within the fluidic (haemolymph) and cellular (haemocytes) components of the invertebrate circulatory system. Haemolymph and haemocytes are responsible for supplying organs and tissues with essential nutrients and are crucially involved in immunological responses and homeostatic processes (Grandiosa et al., 2016; Grandiosa et al.,

2018). Additionally, the characterisation of haemocyte sub-populations (e.g., hyalinocytes, granulocytes) are an important parameter for cellular immune investigations (Rolton & Ragg, 2020; Muznebin et al., 2022). A number of enzymes associated with the immunological activity are localised in granulocytes (Aladaileh et al., 2007), such as the hydrolytic enzymes acid phosphatase (ACP) and phenoloxidase (PO), as previously reported in mussels (Carballal et al., 1997a; Ray et al., 2020). ACP plays an important role in the degradation of foreign proteins, lipids and carbohydrates in marine organisms (Hu et al., 2015), while PO plays a crucial role in defence mechanisms (Muñoz et al., 2006). To date, the effect of temperature on ACP and PO enzymes in *P. canaliculus* has not been investigated. The identification of biomarkers relevant to thermal stress and immunity is critical to improving health assessment practices on mussel farms.

The current study aimed to investigate the individual and combined effects of acute thermal stress and endotoxin exposure on immunological responses (based on indicators such as immune-related enzymes and metabolite profiles in haemolymph samples) and survival of *P. canaliculus*. Identification of ACP and PO enzyme activities in haemocyte sub-populations of this species are herein reported for the first time, and provide new insights into the relationship between thermal stress and immunostimulatory processes.

6.2 Materials and Methods

6.2.1 Biological samples and experimental setup

Adult mussels ($n = 180$; weight = 36.65 ± 5.43 g; shell length = 81.34 ± 4.06 mm) were obtained from Kaihua Mussel Farms (Whakatiwai, New Zealand: $37^{\circ}02' 51.2''$ S $175^{\circ}18'56.1''$ E) in September 2020 (sea water temperature $\pm 14^{\circ}\text{C}$) and transported immersed to the laboratory (Auckland University of Technology, New Zealand). Animals were cleaned, labelled, and acclimated for 6 days in a re-circulation system (temperature = 15°C ; salinity = 35 ppt; pH = 8.10). Five mussels were randomly placed into each of 36 tanks (2L) [30 tanks + 5 extra tanks], containing filtered and aerated seawater (salinity = 34 ppt; pH = 8.26). Eighteen tanks were maintained at 15°C (ambient temperature) and the remaining eighteen tanks were kept at 26°C (thermal stress temperature) (Fig. 6.1). A water heater was used to reach the desired temperature (26°C) and temperature was checked by using a thermometer. The experimental temperatures were chosen on the basis of the values recorded in the summer 2017-18 during mortality event (April 2018) at a farm in Kaihua. Based on both atmospheric and ocean metrics, the summer 2017/18 heat wave was the most intense on record counts of summer days $\geq 25^{\circ}\text{C}$ were the highest recorded, back to 1973. A total of 60 mussels received an endotoxin injection (100 μL of a 1 mg/mL stock solution dissolved in 0.22 μm -filtered

autoclaved seawater [FSW]; *Salmonella enterica* serotype typhimurium [Sigma-Aldrich L7261-25MG]) (Nguyen et al., 2019a) in the posterior adductor muscle [*Salmonella enterica* was previously isolated from mussel samples during a monitoring programme for the presence of *Salmonella* in shellfish in Galicia, north-west Spain (2012–16) (Lozano-Leon et al., 2019)]. Since, LPS constitutes an integral component of the outer membrane of Gram- negative bacteria and are known to provoke the immune system in both vertebrates and invertebrates, LPS has been compared to other known agents (Gram- negative bacteria) of pathogenicity. Another 60 mussels were injected with 100 μ L of FSW (vehicle control) in the posterior adductor muscle, [the LPS concentrations were determined based on previous publications (Costa et al., 2009; Nguyen et al., 2019a) and our pilot study] and the remaining mussels received no injection (negative control). Injection is a representative method of exposure and this application method follows previous research (Nguyen et al., 2019b). Haemolymph sampling was conducted at three time points (6, 24 and 48h post-injection) from five replicate animals per treatment. Approximately 1.5 mL of haemolymph were withdrawn from the posterior adductor muscle from each individual and divided into subaliquots: 400 μ L were immediately snap-frozen in liquid nitrogen and stored at -80°C for metabolomics analyses, 500 μ L were placed on ice for immediate enzymatic processing, and the remaining haemolymph was used for immediate flow cytometric processing. Mortality checks were conducted from the same 180 mussels (non-injected control, FSW injection and endotoxin injection) after 24, 48, and 120h (mussels were considered dead if their shells were gaping and were non-responsive to being manipulated).

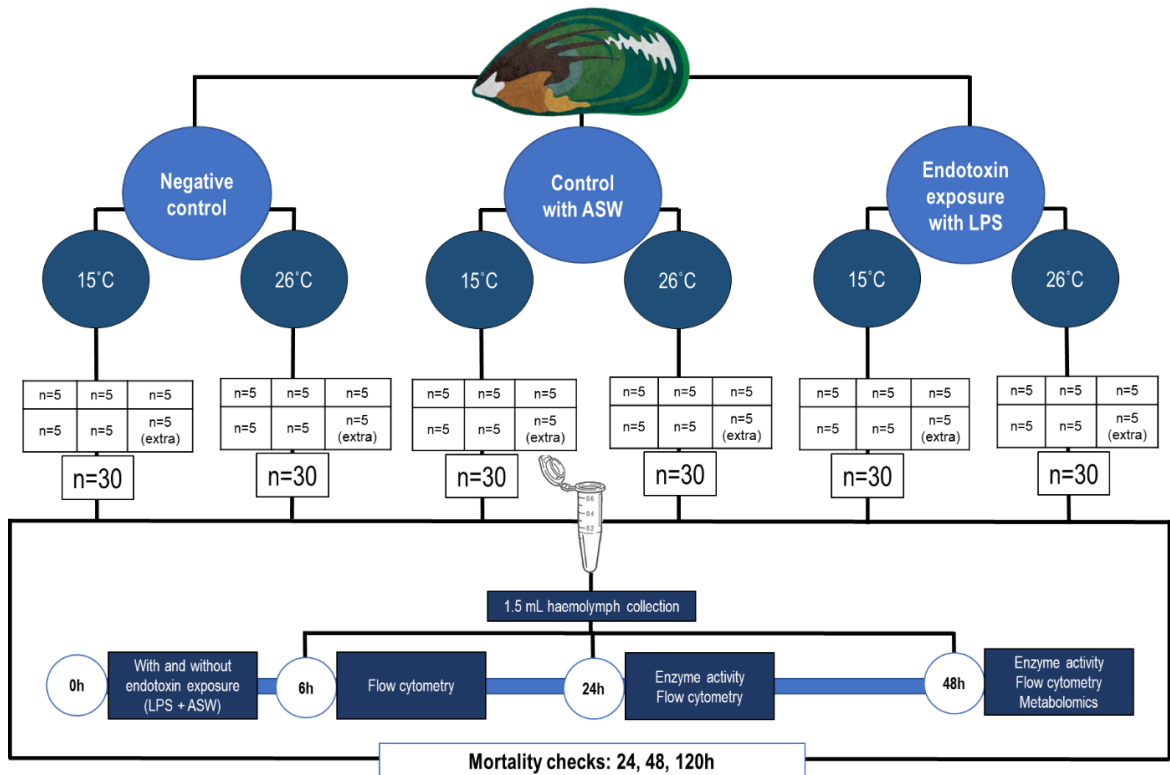


Figure 6.1 Experimental design. Haemolymph was collected after 6h, 24h, and 48h for a combination of flow cytometry, enzyme activity and metabolomic-based analyses. Vehicle controls consisted of 0.22 μ m filtered seawater (FSW) injections.

6.2.2 Enzyme activity

Staining reactions for the presence of acid phosphatase (ACP) and phenoloxidase (PO) enzymes in haemocytes were performed using established protocols (Aladaileh et al., 2007; Wootton & Pipe, 2003). Briefly, haemolymph was diluted 1:1 with cold (4°C) FSW. A total of 50 μ L of this mixture was smeared evenly on glass slides to create a thin monolayer, and then dried for 20 min. Slides were immersed in methanol at room temperature for 1 min and then air-dried. Haemocytes were fixed for 10 minutes in equal volumes of Baker's formol-calcium fixative (10% formalin 100 mL, distilled water 900 mL, calcium chloride 20 g).

Slides were incubated in freshly prepared ACP or PO enzyme-substrate solutions (Dyrynda et al., 1998) with 2% Polypep-P5115 added to each buffer. For the ACP enzyme reaction test, Naphthol-AS-BI-phosphate (20 mg) was dissolved in 1 mL of dimethyl sulfoxide (DMSO) and made up to 50 mL with 0.1 M acetate buffer (pH 4.5) containing 2% sodium chloride. After 2h of incubation, the slides were rinsed in acetate buffer for 2 min at room temperature and then transfer to 0.1 M phosphate-buffered saline (PBS) (pH 7.5) containing 2% NaCl in deionized water, and

followed by air drying for 15 min. For the PO enzyme reaction test, slides were incubated in Coplin jars for 2 h at 30°C with 1 mg mL⁻¹ of L-dopa in 0.1 M PBS (pH 7.4) containing 2% NaCl. Control slides were incubated in buffer alone. After incubation, the slides were rinsed in deionized water. Both control and enzyme (ACP and PO) reacted slides were counterstained for 2 min in methylene blue and rinsed in deionized water and mounted with histomount (DPX) for inspection by light microscopy. The percentages of enzyme reactive haemocytes (Wootton & Pipe, 2003) were enumerated after observing 100 random haemocytes ($\times 100$ magnification).

6.2.3 Flow cytometry

Cell counts, viability, and production of reactive oxygen species (ROS) in haemocytes were recorded via flow cytometry on a Guava[®] Muse[®] Cell Analyzer, using the Muse[®] Cell Count and Viability Kit (MPMCH100102, Abacus DX, New Zealand) and Muse[®] Oxidative Stress Kit (MCH100111) respectively, following the manufacturer's specifications (Delorme et al., 2021). ROS assay quantifies the proportion of ROS-positive haemocytes.

6.2.4 Metabolite profiling

Haemolymph samples were prepared for metabolite profiling as previously described (Nguyen & Alfaro, 2020). Briefly, 300 μ L haemolymph was mixed with 20 μ L internal standard (10 mM L-alanine-2,3,3,3-d₄) and dried with a Speed Vac for 4 hours. Metabolite extractions were performed following two sequential steps of 500 μ L cold methanol: water (ratio 50:50; 80:20). These extractions were added and vortexed for 1 min, followed by cold centrifugation (20,800 g; 5 min; -9°C). The combined extractions were dried overnight and derivatised by methyl chloroformate (MCF) alkylation. Dried samples were re-suspended in 400 μ L of 1 M sodium hydroxide containing 334 μ L of methanol and 68 μ L of pyridine. Whilst vortexing for 30 sec, 40 μ L of MCF reagent was added, followed by another 40 μ L of MCF (vortexed for 30 sec), 400 μ L of chloroform (vortexed for 10 sec), and 800 μ L of a 50 mM sodium bicarbonate solution vortexed for a further 10 sec. Derivatised mixtures were centrifuged (1174 g; 6 min; 6°C) and the upper aqueous layer was discarded. Thirty mg of anhydrous sodium sulphate were added to remove residual water and the chloroform phase containing the MCF derivatives were transferred to vials for GC-MS analyses. Pooled haemolymph samples were similarly prepared to serve as quality control samples (n = 10) (Young et al., 2019).

Metabolite profiling was conducted using a gas chromatograph GC7890B coupled to a quadrupole mass spectrometer MSD5977A (Agilent Technologies, CA, USA), with a quadrupole mass

selective detector (EI) operated at 70 eV according to established protocols and instrument settings (Smart et al., 2010). Samples were extracted, derivatised and analysed in a completely random order, with pooled QC samples being run every three biological samples. Deconvolution of chromatographic data was performed using the Automated Mass Spectral Deconvolution and Identification System (AMDIS v2.66) software. Metabolite identifications and peak integrations (relative quantification) were conducted using Chemstation Software (Agilent Technologies) and customised R xcms-based scripts (Aggio et al., 2011) to interrogate an in-house mass spectral library of MCF derivatised commercial standards. Compound identifications were based on matches to both the MS spectrum of the derivatised metabolite and its respective chromatographic retention time. Data were blank-corrected and aberrant records were removed. The data matrix of peak intensities was pre-processed for QC purposes and to meet the distributional requirements prior to statistical analysis using MetaboAnalyst (Chong et al., 2019). Data were normalised against the internal standard and corrected for analytical drift using pooled QC data and a random forest-based machine learning algorithm (Fan et al., 2019). Missing data were input as half of the minimum value for each variable.

6.2.5 Statistical analyses

Survival data were analysed using non-parametric Kaplan-Meier estimates (XLSTAT® [Addinsoft; NY, USA]). Equality of the survival functions was determined via the log-rank test and pairwise differences were evaluated using the Dunn-Šidák procedure to address multiple hypothesis testing. Enzyme and flow cytometry data were analysed via one-way ANOVA and two-way ANOVA [IBM® SPSS® Statistics Software v.23 (IBM; NY, USA)]. Metabolite data were log-transformed and analysed via two-way ANOVA ($\alpha = 0.05$) using the online server MetaboAnalyst 5.0 (Pang et al., 2021). These analyses incorporated temperature (26°C vs 15°C) and immune stimulation (endotoxin injection vs filtered seawater injection) as a 2×2 factorial design.

6.3 Results

6.3.1 Enzyme activity

Two primary haemocyte types (i.e., granulocytes and hyalinocytes) were observed after methylene blue counterstaining. Granulocytes dominated the cell population (Fig. 6.2A & 6.2E). Positive enzyme reactions for acid phosphatase (ACP) (13%) and phenoloxidase (PO) (15%) were detected only in granulocytes (not in hyalinocytes) (Fig. 6.2B & 6.2F). The mean percentages (\pm SE) of total granulocytes (98%) and hyalinocytes (2%) (Fig. 6.2A & 6.2E), and ACP- and PO-positive granulocytes at 15°C and 26°C after 24h and 48h incubation periods are presented in Table 6.A.1

in the Appendix. No effect of either treatment was detected on haemocyte population profiles or enzyme activities (2-way ANOVA; p -values <0.05 [Appendix Table 6.A.2]). Reaction products of ACP (deposits of white lead phosphate) were localized in the periphery of some specific granules of granulocytes (Fig. 6.2D), whereas PO was stained in the periphery of the granulocytes (Fig. 6.2C).

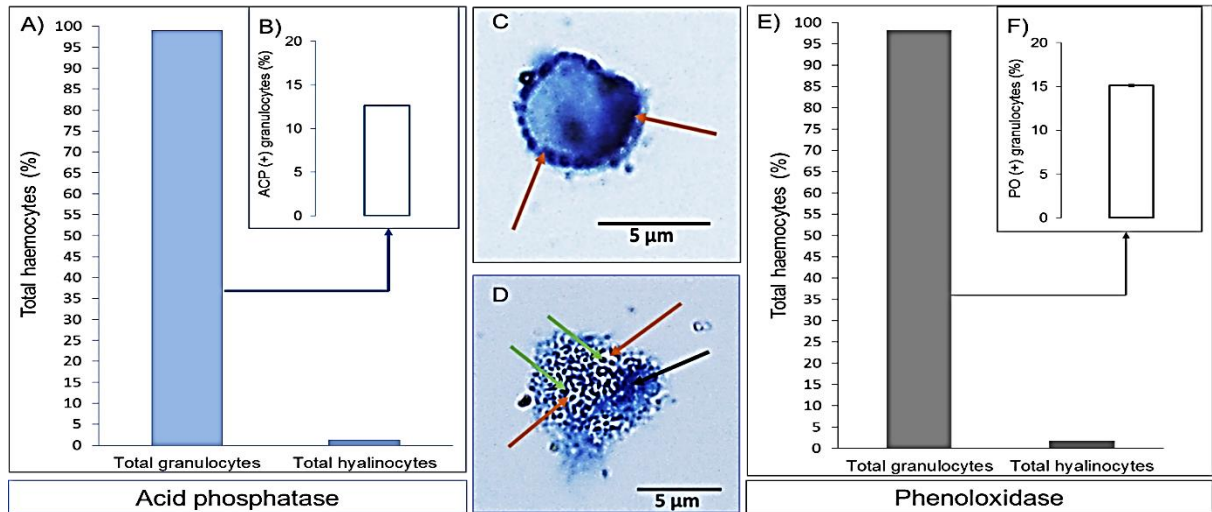


Figure 6.2 Differential haemocyte cell-types and detection of their acid phosphatase (ACP) and phenoloxidase (PO) in *Perna canaliculus*: A) mean percentage (\pm SE) of total granulocytes and hyalinocytes at 15°C and 26°C after 24h and 48h incubation periods which were calculated from the slides incubated in ACP enzyme-substrate solutions, along with B) positively-stained granulocytes for ACP activity (inset bar plot; scale = relative %), C) light micrograph of a granulocyte showing PO enzyme reaction at the peripheral margin (orange arrows), D) light micrograph of a granulocyte showing numerous granules (green arrows) positive for ACP enzyme activity (orange arrows) and nucleus (black arrow), E) mean percentages (\pm SE) of granulocytes and hyalinocytes at 15°C and 26°C after 24h and 48h incubation periods which were calculated from the slides incubated in PO enzyme-substrate solutions, F) along with positively stained granulocytes for PO activity (inset bar plot; scale = relative %).

Differences in the enzyme reactions (ACP and PO) were observed in 24h and 48h incubation periods (Fig. 6.3). Enzyme reactions for incubation periods (24h and 48 h) were significant (One-way ANOVA, P -value <0.05). PO levels were substantially higher after 48h in all treatments (Fig. 6.3). ACP enzyme reactions for treatment groups ($p = 0.981$) and incubation periods ($p = 0.159$) were not significant (One-way ANOVA). PO enzyme reactions for treatment groups ($p = 0.023$) and incubation periods ($p = 0.001$) were significant (One-way ANOVA).

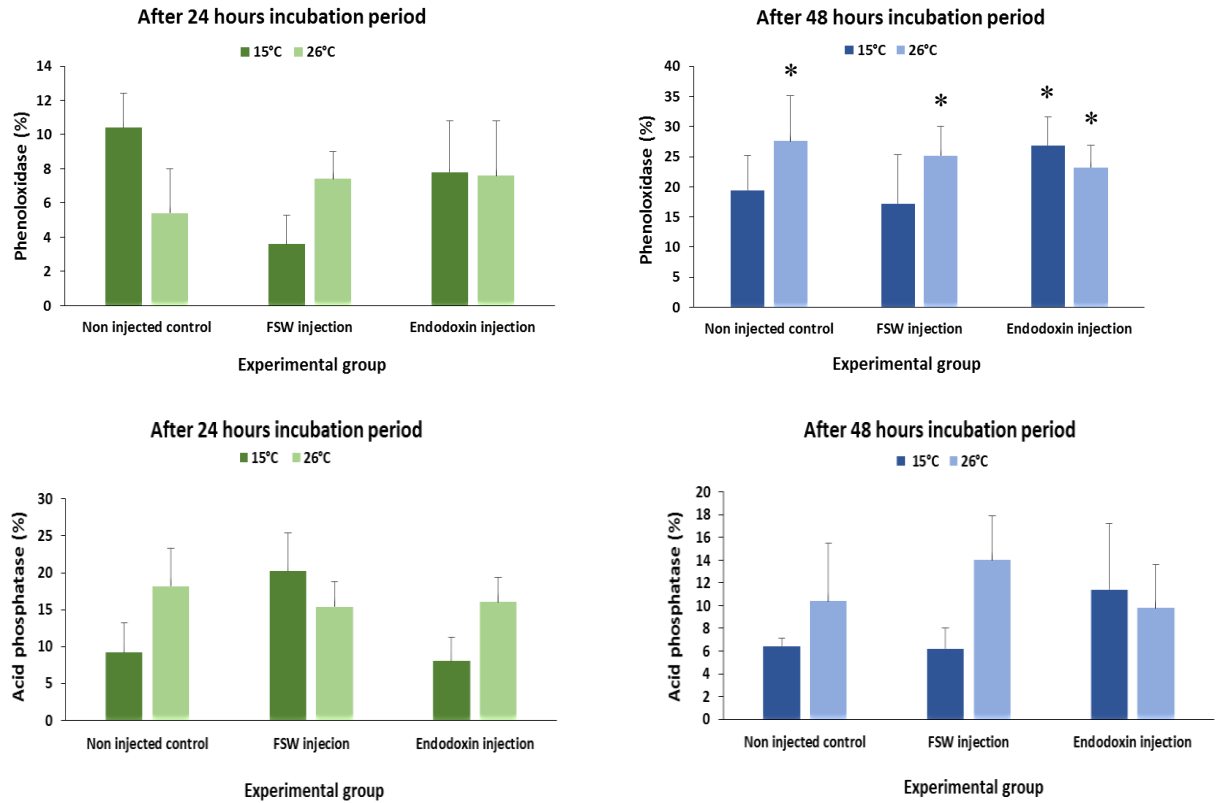


Figure 6.3 Average enzyme activity data (\pm SE) showing mean percentages of acid phosphatase and phenoloxidase, over 2 sampling times (24h and 48h) in all experimental groups (non-injected control, FSW injection and endotoxin injection) housed at 15°C and 26°C.

6.3.2 Flow cytometry

Total haemocyte counts, cell viabilities and relative levels of reactive oxygen species (ROS) of adult mussels showed varying responses over time (6h, 24h and 48h), across temperatures (26°C and 15°C) and endotoxin exposure (Fig. 6.4, Appendix Table 6.A.3). The effect of incubation periods on THC was significant ($p = 0.0448$) and ROS was highly significant ($p = 0.001$) (One-way ANOVA). Highly significant difference in ROS between 6h and 24h incubation period ($p = 0.001$) and 6h and 48h ($p = 0.001$) were recorded but no significant difference between 24h and 48h incubation period ($p = 0.984$) was observed (One-way ANOVA). A substantial elevation in total haemocyte count after 48h exposure to the combined effect of thermal stress and endotoxin was recorded (Fig. 6.4). The values of incubation period ($p = 0.0395$) and temperature ($p = 0.0209$) were associated with significantly different THC (2-way ANOVA; p -values < 0.05). ROS assay provided the quantity and percentage of cells with ROS positive (Fig. 6.4). A significant ($p = 0.038$) but transient reduction in cell viability was detected at 26°C after 24h of incubation (2-way

ANOVA). However, in general, thermal stress and endotoxin exposure did not have major impacts on total haemocyte counts, cell viability, or production of ROS (2-way ANOVA; p -values <0.05).

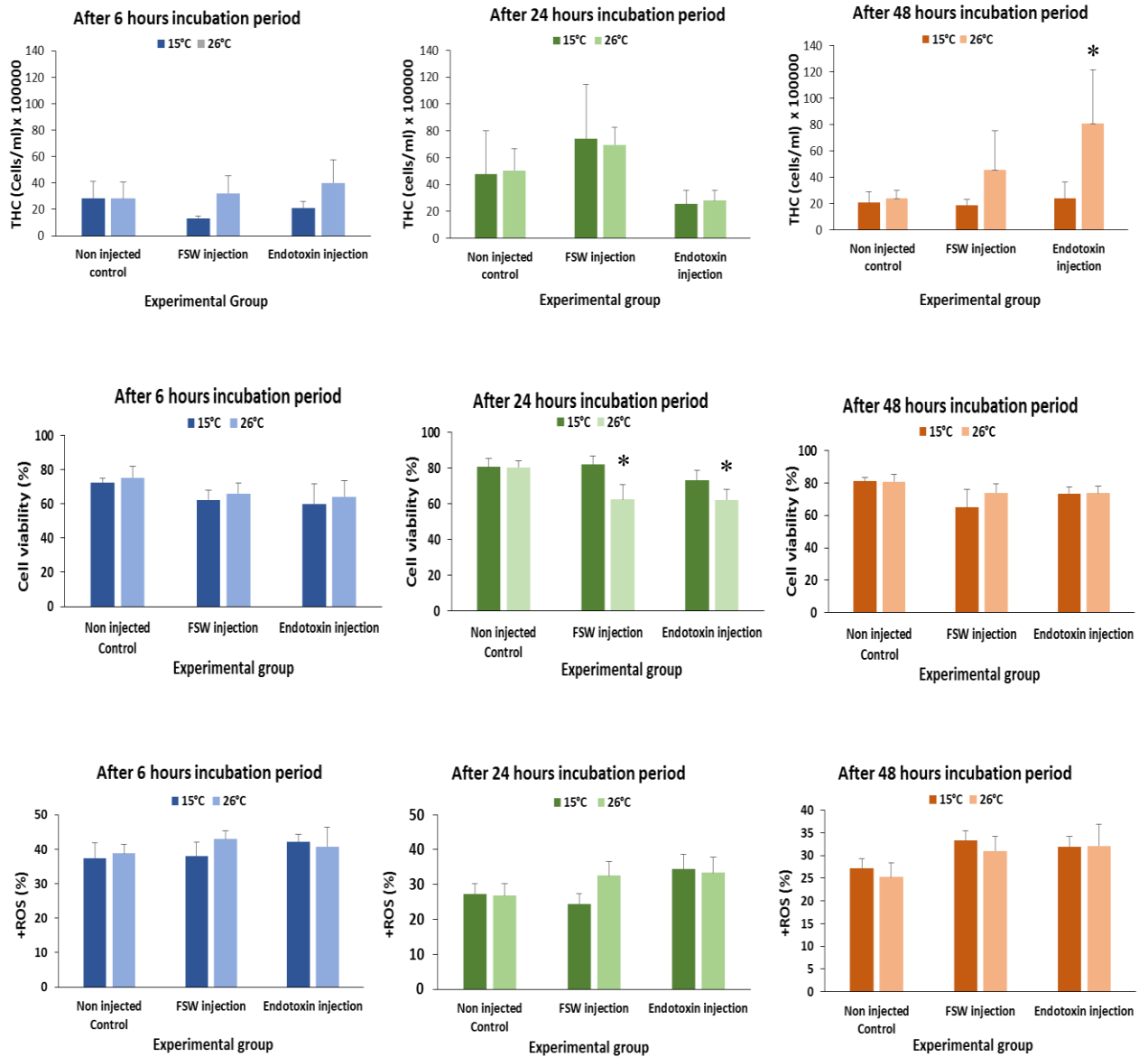


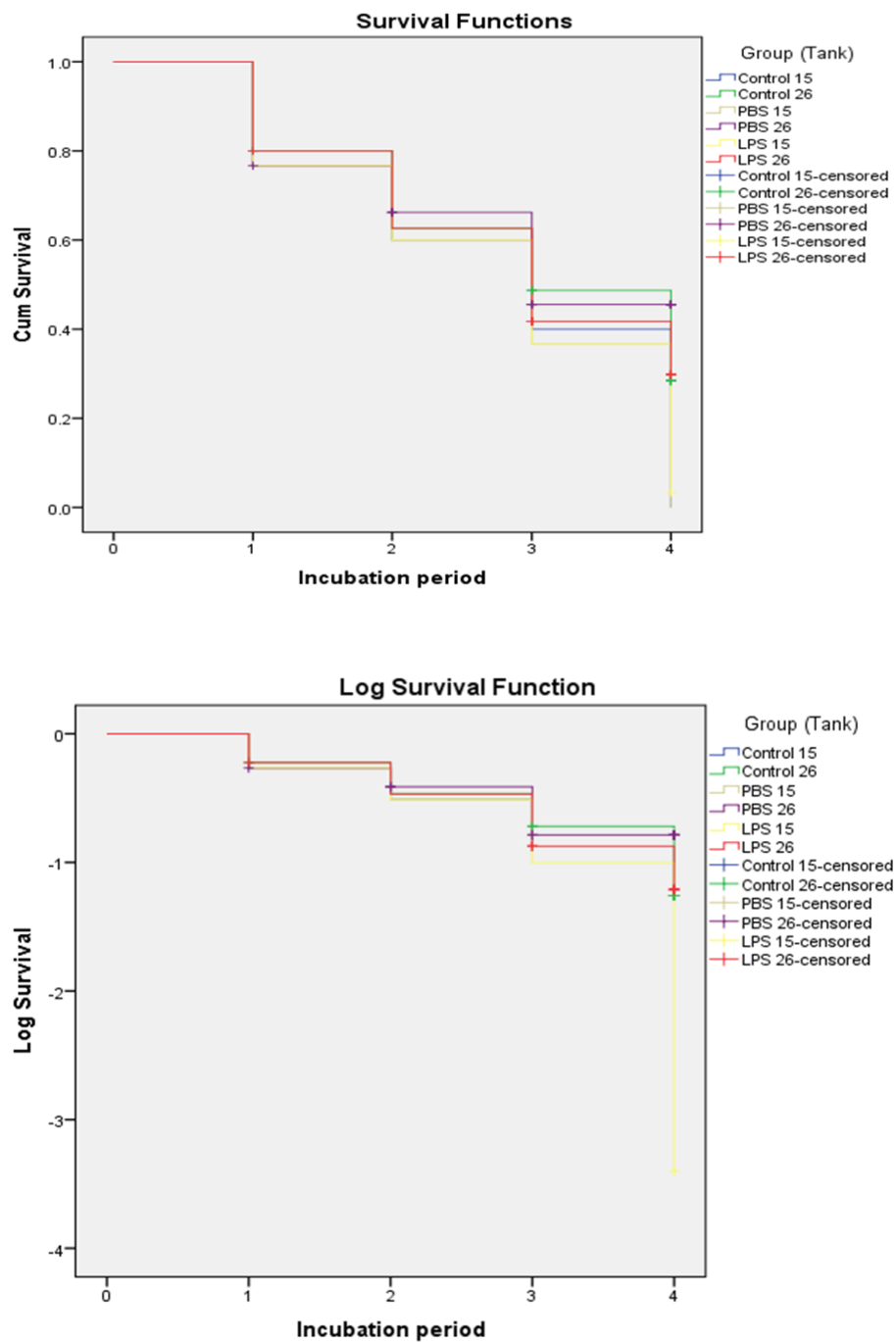
Figure 6.4 Average flow cytometry data (\pm SE) depicting total haemocyte counts, cell viability and reactive oxygen species production over 3 sampling times (6h, 24h and 48h) in all experimental groups (non-injected control, FSW injection and endotoxin injection) housed at 15 and 26°C.

6.3.3 Metabolomics

A main effect of temperature influenced the relative abundances of 42 compounds irrespective of the endotoxin-based immune challenge; of these, 32 metabolites were reliably annotated (Fig. 6.5 & Appendix Table 6.A.4 - 6.A.7). The metabolic response of mussels to thermal stress (26°C vs 15°C) generally comprised a decrease in the free amino acid composition with concomitant increases in free fatty acids in the haemolymph. Immune stimulation via endotoxin exposure induced an increase in the relative abundances of ten compounds compared to non-injected controls (Fig. 6.5). Three metabolites (azelaic acid, phenylalanine and serine) were affected by thermal stress and by endotoxin exposure.

6.3.4 Mortality

Mussel survival was monitored in all treatment groups (non-injected control, FSW injection and endotoxin injection) housed at 15°C and 26°C for an extended duration (after 6, 24, 48, and 120h) to assess major health impacts of thermal stress at 26°C and endotoxin exposure. At the higher temperature, 10-15 individuals per group died, whereas only one mussel perished at 15°C. Kaplan-Meier survival analysis revealed a significant difference among the groups (log-rank test; $p < 0.05$), with pairwise comparisons confirming the main effect of temperature and no effect of endotoxin exposure.



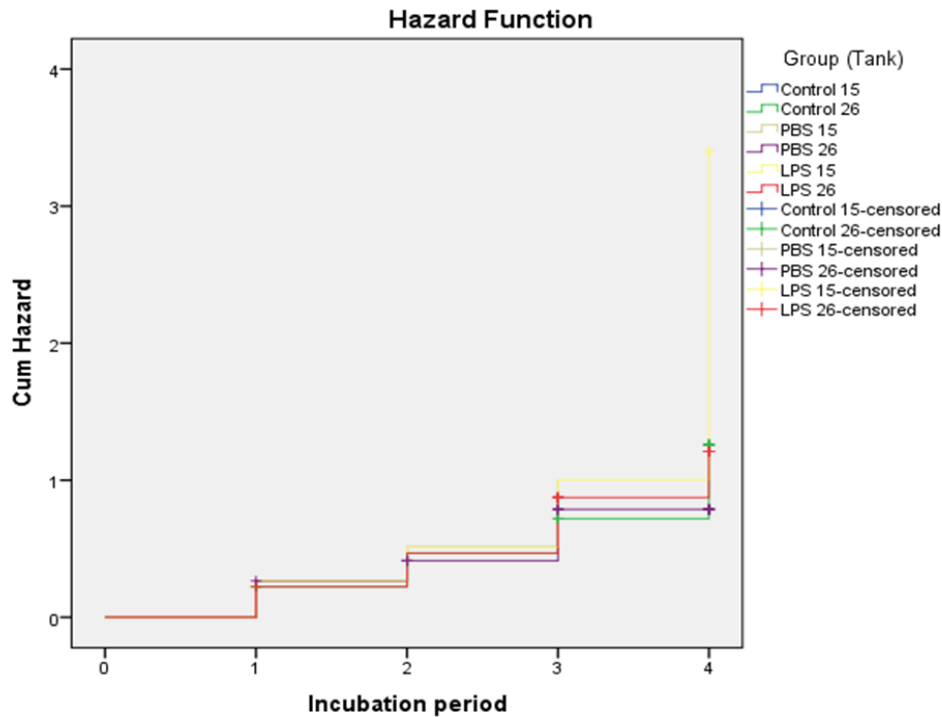


Figure 6.6 Cumulative mussel (*P. canaliculus*) mortality over 120 hours (Incubation period: 0 = 0h, 1 = 6h, 2 = 24h, 3 = 48h, 4 = 120h) in response to a thermal challenge (26°C vs 15°C) and endotoxin exposure.

6.4 Discussion

Circulating haemocytes are important mediators of invertebrate cellular defence mechanisms and are useful for assessing mechanisms underpinning stress responses and poor health. In this study, we conducted a short-term environmentally relevant experiment to investigate the combined effects of thermal stress and immune stimulation via endotoxin exposure on total haemocyte counts and viabilities, haemocyte cell population structure, cell-specific activities of two immune-relevant enzymes, production of haemocyte reactive oxygen species, a comprehensive evaluation of 85 haemolymph metabolites, and mussel survival.

Two primary haemocyte types in *P. canaliculus* were observed, with granulocytes dominating the cell population, representing 98% of the cell population. This proportion falls within the upper range recorded for other bivalve species (44–96%). Allam et al. (2002), noted 92 to 96% granulocytes in the haemolymph of bivalve species (*Ruditapes philippinarum*, *Mercenaria mercenaria* and *Crassostrea virginica*). Muznebin et al. (2022), recorded more than 80% granulocytes and less than 20% hyalinocytes in *P. canaliculus*. Perrigault et al. (2012) recorded a decline in the percentage of granulocytes over time from 48.6% at 2 weeks to 44.3% at 4 months compared to the high salinity treatments. The proportion of circulating hyalinocytes in our study was relatively low compared to a recent flow cytometry-based survey by Rolton et

al. (2020) in the same species. Variations in haemocyte numbers and their population structure can be greatly influenced by season and varying environmental conditions (Carballal et al., 1998; Hégaret & Wikfors, 2005; Parisi et al., 2008; Renwranz et al., 2013). Baseline haemocyte data are currently limited for *P. canaliculus* and there is a need for further characterisations across various spatial and temporal scales. We assessed the occurrence of two immunological marker enzymes (acid phosphatase [ACP] and phenoloxidase [PO] for the first time in this species. Positive enzyme reactions for ACP and PO were detected only in granulocytes. These results are similar to those previously reported in closely-related *Perna perna* (Barracco et al., 1999), and other bivalves (Kuchel et al., 2010; Xing et al., 2002). According to Barracco et al. (1999), the presence of acid phosphatase activity in the granulocytes of *P. perna* suggested that some of its granules were linked to a lysosomal system and act as the intracellular degradation of ingested foreign particles. Furthermore, the ACP reaction products were localised specifically within the periphery of some granules in *P. canaliculus* granulocytes, as was similarly reported in the Mediterranean mussel, *Mytilus galloprovincialis* (Cajaraville & Pal, 1995). Temperature and/or endotoxin exposure did not have a major impact on *P. canaliculus* haemocyte ACP and PO activities at the times sampled, nor on the other haemocyte parameters assessed. However, PO levels appear to double between 24h and 48h, suggesting PO activity may be associated with exposure times. PO plays a significant role in initial immune defense of invertebrates (Shu et al., 2009) and alterations in environmental parameters can modify PO activity (Pankhurst & Van Der Kraak, 2000). Elevated or excessive levels of PO are associated with stress and disease, but low levels can be linked with depleted proteins and immunocompromised animals (Albalat et al., 2019; Luna-Acosta et al., 2017; Perazzolo et al., 2002). The effect of heat stress on enzyme activity is highly variable in other molluscan species. For example, in *M. galloprovincialis* and abalone (*Haliotis* spp.) a slight–moderate reduction in ACP and PO activities have been recorded (Hooper et al., 2014), whereas exposure of the mussel *Mytilus coruscus* to higher water temperatures yielded increased ACP activity (Hu et al., 2015). According to Suzuki and Mori (1990), ACP enzyme is involved in various metabolic processes. Thus, adverse environmental conditions (e.g. high temperature), stress or pathogens can elevate enzyme levels which may change metabolic profiles of mussels. The temperature and/or exposure times we tested were probably not of sufficient magnitude or duration to induce significant changes in enzyme activity. In summary, our cellular-based assessments revealed that acute spikes in sea surface temperatures over a couple of days are likely to have a limited effect on these particular features of immunity in mussels. Further research may focus attention on longer-term impacts of ocean warming (weeks-to-months) which may take place during the summer months, and on other immunological biomarkers.

In contrast to the haemocyte findings, an effect of acute thermal stress and endotoxin exposure was detected at a metabolic level. Increased metabolism as a response to higher temperatures is a common response in mussels, as previously recorded in *P. canaliculus* (Delorme et al., 2021; Dunphy et al., 2015), and confirmed again in this study. Accumulation of metabolites within the tricarboxylic acid (TCA) cycle supports the elevated energy demands and higher metabolic rates experienced due to thermal stress (Dunphy et al., 2018). Increases in aspartic and glutamic acids support replenishing functions towards the TCA cycle (Venter et al., 2019), suggesting increased TCA cycling. To further sustain metabolic function during temperature stress in mussels, amino acids (e.g., glycine, serine and β -alanine) can be channelled to pyruvate, while also enabling the synthesis of adenosine triphosphate (ATP) directly from the phosphorylation of adenosine diphosphate (Delorme et al., 2021; Jiang et al., 2020). A shift towards anaerobic metabolism has been documented in mussels due to various stressors (Nguyen & Alfaro, 2020), and is often associated with increases in lactic acid concentrations, regulation of nicotinamide adenine dinucleotide (NAD⁺), and production of ATP (Venter et al., 2018) as recorded due to thermal stress in the current study. Additionally, during anaerobiosis, catabolism of fatty acids via beta-oxidation directly produces ATP and generates acetyl coenzyme A for usage in the TCA cycle (Delorme et al., 2021).

Added metabolic consequences in response to temperature stress in *P. canaliculus* include decreased branched-chain amino acids (BCAAs) (e.g., isoleucine, valine, leucine) and urea cycle intermediates (e.g., ornithine). Generally, when stressors are experienced BCAAs are used as carbon skeletons in gluconeogenesis to regulate protein turnover and support energy production (Cappello et al., 2017). The decreased urea cycle metabolites are indicative of protein catabolism, where the oxidation of amino acids for energy expenditure is typically achieved via deamination and resulting in ammonia as a product. Furthermore, the urea cycle metabolites assist with the nitrogen/ammonia balance which has clearly been perturbed in our study due to temperature stress (Jiang et al., 2020; Venter et al., 2019). Considering increases in various free amino acid levels measured herein, we hypothesise that proteins are being catabolised during increased energy demands under thermal stress in *P. canaliculus*, as previously reported in clams (Jiang et al., 2020). However, measuring ammonia-nitrogen excretion rates in future studies will be beneficial to reflect the actual rate of protein turnover. The effect of temperature on glutathione metabolism is also highlighted in the current investigation, where abundances of various metabolites (i.e., glutathione, glycine, and glutamic acid) within the glutathione pathway were increased during thermal stress. Glutathione is an important antioxidant molecule with the ability to scavenge reactive oxygen species (ROS), as previously reported in *P. canaliculus* (Delorme et al., 2021; Nguyen et al., 2018b). The release of ROS by haemocytes is considered to be a tightly regulated procedure under normal

physiological conditions, but as soon as the balance between ROS production and antioxidant defences is disturbed (e.g., due to stressors) oxidative damage can be experienced (Sheehan & McDonagh, 2008). Interestingly, apparent ROS production in haemocytes was not altered by either of the treatments applied, which was an unexpected finding. It is possible that the generation of ROS was being enhanced within cells, but their levels were being simultaneously controlled by the antioxidant system (e.g., through glutathione pathway elements). A targeted analysis of ROS and relevant regulatory metabolites and enzymes will need to be conducted within the cellular and cell-free components of the circulatory biofluid to better understand this system in mussels.

Regarding the endotoxin injected group, exposures to the bacterial pathogen mimic caused increases of 4-hydroxyphenylacetic acid, citramalic acid, cysteine, dodecanoic acid (C12), glutaric acid, glyoxylic acid, lactic acid, and octanoic acid (C8) in mussel haemolymph. Increased abundances of metabolites attributed to protein and lipid degradation during immune responses have previously been reported following *Salmonella*-derived endotoxin exposure in *P. canaliculus* (Nguyen et al., 2019a). In support of these findings, fatty acids (increased C8 and C12 in the current study) are known to play important roles in inflammation and immune responses (Geng et al., 2020), 4-hydroxyphenylacetic acid has an ability to reduce excessive release of proinflammatory cytokines which protects against inflammation and disease (Young et al., 2017), cysteine is a prominent component of antimicrobial peptides as seen in *Mytilus* spp. (Bouallegui, 2019), and glutaric acid is produced by the glyoxylate cycle of bacteria (Van Nguyen et al., 2019). The metabolomics results from our study are also in accordance with transcriptomic-level functioning in *M. galloprovincialis* where LPS activates phagocytosis, pathogen recognition, homeostasis, and cell survival processes (Moreira et al., 2020).

Azelaic acid (affected by both endotoxin exposure and thermal stress) is a C9 dicarboxylic acid and typical oxidation product of unsaturated lipid residues. This metabolite has been previously reported as an energy reserve metabolite for the production of acetyl CoA in clams (Jiang et al., 2020), and has been detected at elevated levels in marine aerosols with high bacterial loading (Shibl et al., 2020) and in mussel larvae during mass mortality events (Young et al., unpublished). The source and function of this metabolite in *P. canaliculus* is currently unknown.

A significant difference in survival among the treatment groups was detected after the extended 5-day exposure duration, which confirmed a main and severe impact of thermal stress on gross physiology. These data also reveal that thermal stress, combined with the specific endotoxin treatment, used herein did not lead to a synergistic effect on mortality, which was contrary to our initial expectations. The interactions between water temperatures, host immunity, and the

loading and virulence of opportunistic pathogens still require detailed focus. Endotoxins derived from other bacterial strains and/or use of live pathogens would be appropriate treatments for future multi-stressor experiments in this regard.

6.5 Conclusions

This study provides a snapshot of the individual and combined effects of acute thermal stress and endotoxin exposure on immunological responses and survival of *P. canaliculus*. Neither thermal stress (26°C vs 15°C) nor endotoxin exposure had major impacts on total and differential haemocyte counts, haemocyte viability, or production of reactive oxygen species. The occurrence of two immunological marker enzymes (acid phosphatase [ACP] and phenoloxidase [PO]) were assessed for the first time in this species. Positive enzyme reactions for ACP and PO were detected only in granulocytes (not in hyalinocytes), although their relative expressions also were not affected by the treatments. Conversely, at the higher water temperature, free fatty acid constituents increased in mussel haemolymph and free amino acids decreased which supports higher energy demand and metabolic rate as a result of thermal stress. In addition, branched-chain amino turnover, the urea cycle and the glutathione pathway were affected by the elevated temperature. Survival data confirmed a severe physiological impact of the high temperature treatment through incidences of mortality. However, thermal stress combined with endotoxin exposure did not lead to a synergistic effect on mortality. This study contributes to a better understanding of the mussel immune defence system during acute increases in water temperature, and provides new insights into the relationship between thermal stress and immunostimulatory responses to evaluate host-pathogen interactions.

Chapter 7

General Discussion and Conclusions



Abalone farm, Northland, New Zealand

7.1 General discussion

Marine aquaculture is a rapidly developing industry, but it is threatened by the general emergence and propagation of diseases that can adversely affect production (Rodgers et al., 2015; Stentiford, 2017). These pathogen outbreaks pose a potential risk, especially in summer when the temperature is at its highest. Similarly, mortality rates of New Zealand Greenshell™ mussels (*Perna canaliculus*) of both wild and farm populations have become a common phenomenon with increasing frequency and magnitude in recent years. While their effects on shellfish appear to be related to thermal stress and pathogen loads, there is a lack of information regarding the specific mechanisms of impact, susceptibility and resilience. Thus, a better understanding is needed of the health status and capacity of shellfish to survive and overcome these events. Key to this understanding is the investigation of host-pathogen-environment interactions during mortality events and transmission pathways of infections. This information is crucial to developing improved disease management strategies for aquaculture species and early warning systems. To this end, this thesis was designed to provide information on parasite and pathogen infections of New Zealand aquaculture species, to draw inferences about specific infection patterns relating to disease development and transmission mechanisms, better understand host immune defence systems and evaluate host-pathogen interactions. Utilizing immunological strategies (histopathology, *in situ* hybridization & PCR) in Chapters 2, 3, and 4, detailed identifications of major pathogens and parasites were performed for New Zealand black-footed abalone (*Haliotis iris*), flat oysters (*Ostrea chilensis*) and New Zealand Greenshell™ mussels (*P. canaliculus*). Characterization of haemocytes and phagocytic activity of *P. canaliculus* were examined in Chapter 5 using smear tests and phagocytosis analyses. In Chapter 6, recognition of the marker enzymes and investigation of the individual and combined effect of acute thermal stress and endotoxin exposure on immunological responses and survival of *P. canaliculus* were carried out via enzyme staining reactions, flow cytometry and metabolomic profiling to better understand the immune defence system in mussels.

Notably, histological techniques employed in epidemiological studies are very useful and imperative in the diagnosis of disease agents or pathological lesions (Diggles et al., 2003; Diggles & Hine, 2002). Therefore, these histological techniques were applied throughout the thesis (Chapter 2, 3 & 4) for the detection of potential parasites and pathogens including *Perkinsus olseni*, *Bonamia* spp., apicomplexan X (APX), intracellular microcolonies of bacteria (IMCs) from significant New Zealand aquaculture species and to study the immunological tissue responses and abnormal tissue structures due to pathogens and parasites infections. This thesis encompasses both quantitative and semi-quantitative approaches which were utilized to study pathogens, parasites and tissue conditions of three commercially important shellfish. Following pathogen counting, quantitative scores were used for calculating the prevalence of

parasites (Chapter 2, 3 & 4). In Chapters 2, 3 and 4, the abundance of *B. ostreae*, *P. olsenii* and APX was evaluated semi-quantitatively using grading scales. In addition, inflammatory tissue responses (haemocytosis and ceroid material), gill structure and digestive tubule structure were assessed by semi-quantitative scales (Chapter 2, 3 & 4).

Immunological tissue responses (haemocytosis and ceroid material) were observed in *P. olsenii* associated tissues of abalone (Chapter 2) and both APX and *P. olsenii* associated tissues of mussels (Chapter 4). A significant association (Chi-square test) between *P. olsenii* and swollen gills with ceroid material and haemocytosis was noted (Chapter 2). *P. olsenii* trophozoites were detected in the haemocytosis of mussel tissues and a significant association (Chi-square test) was recorded between *P. olsenii* infection and haemocytosis and brown material accumulation in this study (Chapter 4). Haemocytosis was also often observed in *B. ostreae* infected oyster tissues (Chapter 3). According to Diggles and Oliver (2005), haemocytic inflammatory lesions are noticed due to pathological conditions in abalone, which suggests that haemocytosis may be an immunological response to local and systemic effects of parasites. Bower et al. (2005) observed bacterial clusters surrounded by an accumulation of massive haemocytes in the tissues of oysters which act as a flag to help to locate the pathogens. Therefore, parasites associated with haemocytosis in this study (Chapter 2, 3 & 4) indicates that immunological tissue responses might help to detect parasites in the tissues of abalone, oysters and mussels.

Gill pathology (e.g., without ciliated lateral cilia, destroyed epithelium of gill filament, atrophied/separated ciliary discs in the abfrontal zone of gill filament and very few haemocytes in the gill blood space) and the pathology of digestive tubules (e.g., small or no lumen and large lumen with a thin epithelial wall) were noted from the histological sections of *P. canaliculus* (Chapter 4). A significant association (Chi-square test) between digestive tubule structure and *Perkinsus* infection was recorded. Since the infestation of the *Perkinsus* parasites in digestive tubules may cause digestive tubule atrophy and detrimental effects during food digestion (Lee et al., 2001), likely, the digestive tubule structural abnormalities observed in this study (Chapter 4) may have resulted from pathogen/parasite (*P. olsenii*) infections that lead to disruptions in digestive tubule functions, such as food digestion and nutrition absorption.

The abundance of *B. ostreae* microcells in different tissues of oysters, including gills, mantle, the connective tissue around digestive tubules, and haemocytes surrounding the gut of histological sections were estimated semi-quantitatively by a grading scheme (modified from Hine, 1991a) that included the relative abundance of *B. ostreae* in various tissues and the average number of *B. ostreae* microcells per infected haemocyte per tissue (Chapter 3). The purpose of the whole oyster grading of the modified scale is to measure the overall *B. ostreae* infection, whilst the individual tissue gradings help to clarify the progression of the disease.

This modified grading will assist in assessing the haemocyte presence in a variety of sites within oysters which will indicate *B. ostreae* infections in those sites. In this study (Chapter 3), oysters presented systemic *Bonamia* infection with tissue damages or lesions. In this investigation, *B. ostreae* microcells were detected inside haemocytes and in blood spaces of gills and mantle sinuses of oysters. Diapedesis was noticed in tissues (gut epithelia, gills and mantle) where haemocytes contained *B. ostreae* microcells and suggested a route of disease transmission. In this thesis (Chapter 3), *B. ostreae* infection was detected mostly in live unhealthy oysters rather than the moribund/dead oysters indicating that moribund oysters may have shed their microcells or been ill due to other factors.

A significant discovery of this thesis work was the confirmation of the presence of *P. olsenii* in *H. iris* (Chapter 2). This is the first time that the *in situ* hybridization (ISH) identification of *P. olsenii* has been carried out in New Zealand black-footed abalone, *H. iris* (Chapter 2). ISH is a useful species-specific assay to confirm *P. olsenii* detected in the tissues of *H. iris* by histology. Although OIE notifiable parasite *P. olsenii* has been reported in New Zealand black-footed abalone (*H. iris*), scallops (*Pecten novaezelandiae*) and New Zealand Greenshell™ mussels (*P. canaliculus*) and identified by histopathology and Ray's fluid thioglycollate medium (RFTM) assays (OIE, 2017), there is a lack of information regarding the use of the species-specific ISH assays for detection and confirmation of this potential parasite. Furthermore, the digoxigenin-labelled probes (species-specific ISH assay) and protocol for the confirmation of *P. olsenii* that were developed for *H. iris* in this study (Chapter 2) were also used for demonstrating hybridization to *P. olsenii* cells in the tissue sections of another aquaculture species *P. canaliculus* (Chapter 4).

Undoubtedly, DNA-based PCR assays have improved speed, sensitivity, and specificity in detecting *Bonamia* parasites (Diggles et al., 2003; Flannery et al., 2014). In Chapter 3 of this thesis, *B. ostreae* and *B. exitiosa* were detected by histology and polymerase chain reaction (PCR) from *O. chilensis*, which were collected in the Marlborough Sounds aquaculture area, New Zealand, in 2017, two years after the first detection of *B. ostreae* there, to examine the effects of the new pathogen on the local host. In the present study (Chapter 3), the overall prevalence of *Bonamia* spp. (*B. ostreae* and *B. exitiosa*) in flat oysters detected by PCR was higher than the total prevalence of *Bonamia* spp. observed via histology, highlighting the importance of PCR as an accurate detection tool, especially for detecting light *Bonamia* spp. infections (Flannery et al., 2014).

Potential parasites *P. olsenii* and APX cause serious infections in New Zealand endemic Greenshell™ mussels (*P. canaliculus*) (OIE, 2017; Suong, 2018). Mortality associated with *P. olsenii* infection is severe at times when environmental conditions (e.g., high temperatures,

increased salinity, host density) promote reproduction, activity, and transmission of the parasite (Park & Choi, 2001; Soudant et al., 2013; Villalba et al., 2004). In addition, APX zoites often cause severe disease in oysters during the peak spawning season (summer/fall) (Hine, 2002a). For this research work, a separate chapter (Chapter 4) focused on the observation of these potential parasites (*P. olseni*, APX) and their seasonal fluctuations. This is the first report on seasonal variations of *P. olseni* and APX in *P. canaliculus*. The seasons (summer, winter, spring and autumn) are significantly related (Pearson's Chi-square test) to the presence of *P. olseni* and APX in mussels. Further research may focus attention to find out the link between *P. olseni* and APX infection and seasonal variations of the mussels.

Abalone are susceptible to pathogens and parasites but there are few published studies that focus on their characterization and health effect (Diggle & Oliver, 2005). To fill the knowledge gap, a sampling snapshot of healthy- and unhealthy-looking abalone (samples were selected randomly) was conducted at Moana Blue Abalone Ltd. (Chapter 2). This farm was experienced by diseases which have been mentioned anecdotally. In this thesis (Chapter 2), *P. olseni* was only detected in abalone deemed unhealthy (presence of pustules and nodules) by gross appearance, with a significant association (Chi-square test) between abalone health status and the presence or absence of *P. olseni*. A significant association (Chi-square test) was also found between the abalone gross appearance (healthy and unhealthy) and the presence or absence of unidentified disintegrated ciliates, which were also present around the visible ulcers/pustules that were attributed to *P. olseni* infection. These findings suggest that there is a close relationship between the health status of abalone and the presence or absence of parasites which may assist with identifying and characterising abalone health risks.

The most important mechanism for the elimination of pathogens by aquaculture species is phagocytosis, which is the engulfment of foreign elements (e.g., bacteria, algae, cellular debris, protozoan parasites) by haemocytes. Characterisation of haemocyte sub-populations (e.g., hyalinocytes, granulocytes) is an important parameter for cellular immune investigations (Rolton & Ragg, 2020). Differential haemocyte counts (DHC) were performed on haemolymph smears stained with Giemsa, and *in vitro* phagocytosis activity assays were applied to measure phagocytosis in Chapter 5 of this thesis. A new optimised classification scheme for *P. canaliculus* haemocytes was developed which is an improvement from the previous classifications of Chandurvelan et al. (2013) and is more representative for haemocyte characterization. In this new classification, the eight types of haemocytes were described in detail and all the types were taken into account as part of differential cell count assessment. Therefore, the new scheme is more complete and more accurately describes the distribution and types of haemocytes. Phagocytosis is a temperature-dependent process in bivalve molluscs (Oliver & Fisher, 1999), which can influence haemocyte activity and important immune

functions (Chen et al., 2007; Hegaret et al., 2003; Perrigault et al., 2011; Yu et al., 2009). In the present study (Chapter 5), the phagocytic performance was successfully observed, indicating that granulocytes only exhibited phagocytosis and the phagocytic activity changed with season and temperature (one-way ANOVAs followed by Tukey's post-hoc test). Thus, these findings indicate that the granulocytes might be phagocytic cells and may play distinct roles in the defence system to engulf microorganisms and foreign particles to protect the body and further experiments could be devised to explore this. Subsequently, the results (Chapter 5) confirm that haemocytes are associated with phagocytic activity and play a unique role in the mussel immune system which serves as a reference for future research on the influence of seasonal variations on haemocyte activity and phagocytosis.

In this thesis (Chapter 6), multidisciplinary methods including enzyme staining reactions, flow cytometry, and metabolomic profiling were used to test mussel (*P. canaliculus*) responses. To investigate these responses, adult mussels were exposed to different temperatures (26°C [thermal stress] vs 15°C [ambient]) and a bacterial-derived endotoxin injection (with vs without) to mimic a pathogen infection. Several enzymes associated with the immunological activity are restricted in granulocytes (Aladaileh et al., 2007), for example, the marker enzymes acid phosphatase (ACP) and phenoloxidase (PO), as previously reported in mussels (Carballal et al., 1997a; Ray et al., 2020). ACP plays an important role in the degradation of foreign proteins, lipids and carbohydrates in marine organisms and involves in various metabolic processes (Hu et al., 2015; Suzuki and Mori, 1990), while PO plays a crucial role in defence mechanisms (Muñoz et al., 2006). In this study (Chapter 6), the occurrence and localization of the marker enzymes ACP and PO were confirmed by cytochemical techniques (staining reactions). Positive enzyme reactions for ACP and PO were detected only in granulocytes and the ACP reaction products were localised specifically within the periphery of some granules in *P. canaliculus* granulocytes. This thesis (Chapter 6) reports for the first time the identification of ACP and PO enzyme activities in haemocyte subpopulations of *P. canaliculus* and provides new insights into the relationship between thermal stress and immunostimulatory processes. In this thesis (Chapter 6), although, temperature and/or endotoxin exposure did not have a major impact on *P. canaliculus* haemocyte ACP and PO activities, differences in the enzyme reactions (ACP and PO) were observed in 24h and 48h incubation periods and PO levels appear to double after 48h, suggesting phenoloxidase activity may be associated with exposure times.

Flow cytometry (FCM) is a powerful and routine tool used in immunological studies of the molluscan haemocytes (Nguyen & Alfaro, 2019). In this thesis (Chapter 6), cell counts (total and differential haemocyte), viability and production of reactive oxygen species (ROS) in haemocytes of *P. canaliculus* were recorded via flow cytometry. Adult mussels showed varying responses over time (6h, 24h and 48h), across temperatures (26°C and 15°C) and endotoxin

exposure (with vs without). A substantial elevation in total haemocyte count (THC) after 48h exposure to combined effect of thermal stress and endotoxin was noted. The levels of incubation period and temperature were associated with significant different THC (2-way ANOVA). However, none of the treatments impacted haemocyte viability or production of ROS (2-way ANOVA). An interesting haemocyte proliferation was apparent in different treatments at different incubation period which might be due to rapid haemocyte division or hypermetabolism of haemocyte from tissue to haemocyte. Further research may help to find out the exact reason behind the haemocyte proliferation in over time, across temperatures and endotoxin exposure.

Endotoxins activate cellular and humoral defence mechanisms in mussels, with subsequent impacts on different metabolic cycles (Nguyen et al., 2019). In this study (Chapter 6), the metabolite profile exposed the effects of heat stress and endotoxin exposure at the metabolic level, suggesting physiological changes in energy expenditure and distribution. At higher water temperatures, free fatty acid and amino acid constituents increased and decreased, respectively, supporting a higher energy requirement and a higher metabolic rate due to heat stress. Also, branched-chain amino acids, the urea cycle, and the glutathione pathway were influenced by the higher temperature. In addition, survival data affirmed a severe physiological effect of the high-temperature treatment through the occurrence of mortality but the combination of heat stress and endotoxin exposure did not produce a synergistic effect on mortality (Chapter 6). Therefore, this thesis (Chapter 6) introduces new findings in regards to the immunological responses of farmed mussels to thermal stress and pathogen challenge, indicating that heat stress and endotoxin exposure can cause specific changes in the metabolic and physiological parameters in haemocytes.

7.2 Limitations and future perspectives

Despite the fact that this thesis offers some significant and first-time findings related to aquaculture health, there are still some shortcomings and limitations. In Chapter 2, the investigation was restricted because of the calculation of the mean intensity of *P. olseni* parasites. Mean intensity was calculated quantitatively as the total number of parasites of a particular species in each individual or specified organ or thin section of the entire animal divided by the number of hosts/samples infected with that parasite. In this study, the mean intensity of *P. olseni* is only an index of intensity, because it does not count all the *P. olseni* parasites, only those of the histological section, and it is indicative and comparative, not an absolute value. In this thesis (Chapter 2), focal haemocytosis was observed as huge quantities of haemocytes encompassed *P. olseni* parasites and sometimes also in foci without *Perkinsus*

cells. Moreover, histological lesions were often evident with no noticeable parasites. Therefore, in Chapter 2 of this thesis, histology helped to visually recognise the immunological tissue responses (ceroid material and haemocytosis) but did not provide a conclusive indication of the underlying causes for these conditions, which requires further investigation to detect the early warning signs of health issues in abalone.

To describe the presence of parasites including *P. olseni* and associated pathology as well as to identify and characterise health risks, a targeted sampling event was conducted of healthy- and unhealthy-looking abalone (86 samples) at one land-based farm (Chapter 2). Therefore, it is not appropriate to apply the findings to the species as whole. For future investigation, the study can be designed with larger sample sizes and variations in sampling locations to collect more information about the distribution of the potential parasites. In this study, only a few *H. iris* samples were infected by *P. olseni*. The lower prevalence of *P. olseni* may be related to the fact that sampling was conducted in the austral winter season. Although the sampled abalone are representative of farmed abalone in general, it is necessary to collect data from other seasons especially summer when shellfishes are more susceptible to pathogenic and parasitic infections. Therefore, it is important to monitor *P. olseni* infection continuously throughout all seasons to better understand the susceptibility of *H. iris* to the parasites and this approach will help for monitoring of diseases in molluscs must go hand in hand this way.

Infection with *B. ostreae* was detected for the first time in New Zealand flat oysters (*O. chilensis*) in January 2015 in the Marlborough region (Lane et al., 2016). In this study, flat oysters were collected from the same region two years after the first detection of *B. ostreae* in 2015. It is likely that the animals sampled were therefore more resistant to *Bonamia* and these samples may not be representative of *O. chilensis* as a species. After collecting from farms samples were held for 2-8 days on ice in polystyrene bins in a humid environment for between 2 and 8 days before dissection. Therefore, the samples may not represent the original condition of the oyster and this likely effects the quality and survival of the oysters for a prolonged and variable holding period on ice. Active surveillance in different regions of New Zealand should be conducted for the purposes of early detection of spread of *B. ostreae*, depopulation of all flat oyster farms within areas where *B. ostreae* had been detected and movement controls to manage risk movements of *B. ostreae*.

In this work (Chapter 2 & 4), a species-specific *in situ* hybridization (ISH) assay was used to confirm the histological detection of *P. olseni* in *H. iris* and *P. canaliculus* tissues. ISH can likewise be utilized for future investigations on the pathogenesis of *P. olseni* and can be joined with immunohistochemistry to distinguish the *P. olseni* protein and mRNA of interest. Subsequently, comparative genomics could be utilized for deciding the change in virulence

mechanisms between strains of the same pathogen, it would be exceptionally intriguing to play out some genetic analysis of *P. olseni* for future examinations. Moreover, future PCR and genetic sequencing of the *P. olseni* genome will permit a superior comprehension of the genetic variability of *P. olseni* in the diverse host species. Furthermore, a useful effort would be to sequence the entire genome of *P. olseni* to permit specialists with deeper insights, for example recognizing the sorts of proteins created by *P. olseni*, the connection between *P. olseni* phenotype and host disease, distinguishing the impact of gene changes and possibly help speed up the identification of potential drugs to treat infected hosts.

Very few apicomplexan X (APX) was observed in the connective tissue around digestive tubules and gonads of flat oysters in histological analysis, but a comparatively higher number of APX was found to be PCR positive (Chapter 3). Since histology and PCR analysis were not conducted in this study from the same tissue layer of the samples, APX was not diagnosed by histology when it was in the samples and positive by PCR data. According to Suong et al. (2018), APX zoites are difficult to detect by light microscopy in low-intensity infections and a PCR method is available for the detection of the organism similar to apicomplexan X (APX) coccidia.

In this study (Chapter 3), a coinfection of *B. ostreae* with APX was observed in oysters and an association was found between *B. ostreae* and APX infections (PCR results). Given the relationship of *Bonamia* spp. in the development of APX disease and severity in flat oysters are unclear in this research. Therefore, a more detailed analysis of the existing literature and further experiments are needed to understand how APX interacts with bonamiosis, as this allows for a deeper understanding of its biology and epidemiology, as well as providing a possible way to combat disease more effectively can be decisive. In addition, more work is needed to determine the genetic affinities of this 'APX' and its interactions with oysters and *Bonamia* spp. Further research on the biology of APX should be done to manage a possible outbreak in any of these aquaculture species in New Zealand.

Perkinsus olseni is a key parasite for both abalone and mussels which has a unique life cycle consisting of trophozoite, hypnospore and zoospore (Auzoux-Bordenave et al., 1995; Perkins, 1996; Choi et al., 2005). *Perkinsus* trophozoite occurs in host tissues as a single cell (=tomont) of multi-nucleated form. Once the trophozoites are placed in an anaerobic condition such as in fluid thioglycollate medium (FTM), trophozoites enlarged (keeping the spherical shape) and developed a thick wall, thus becoming a new stage, hypnospore. When the hypnospores are placed in aerated seawater, they undergo zoosporulation (Choi & Park, 2010). The trophozoite (vegetative multiplication stage) is occurring in the tissues of the live host and can be detected by histology. However, hypnospores (growth stage) and zoospore (infectious stage) are also

found in host tissues but remain undetected by histology. Therefore, FTM technique along with histology should be utilized in future study for better understand the life cycle of *P. olseni* in *H. iris* and *P. canaliculus*.

Characterization of mussel (*P. canaliculus*) haemocytes and their phagocytic activity, presented in this study (Chapter 5) is an interesting source of haemocytes classification in mussels. Haemocytes were classified into 8 categories based on cell size, morphology, the nuclear/cytoplasmic (N/C) ratio of the cells, staining affinities of their cytoplasm and cytoplasmic granules by using Giemsa staining. However, in some samples, the hyalinocytes were poorly stained in this experiment (Chapter 5). It may be due to the possibility that the reagents were not exchanged with new reagents at regular intervals. The haemocytes appear rather swollen due to phosphate-buffered saline (PBS) used for differential haemocyte count (Chapter 5) being rather dilute (137 mM NaCl compared to typical seawater or haemolymph plasma 470-500 mM). Therefore it is possible the haemocytes are experiencing osmotic swelling and this may affect both their appearance and physiological performance. The influence from external factors, such as the temperature, pH of the antiaggregants, length of storage (Vargas-Albores & Ochoa, 1992), osmolarity (Hinzmann et al., 2013) and components of the antiaggregant may affect the haemocyte measurement results. Further studies on the mussel haemocytes should consider the external factors that impact the haemocyte profiles.

At the time of sampling (Chapter 6), temperature and/or endotoxin exposure had no significant effect on the ACP and PO activities of *P. canaliculus* haemocytes. However, in Mediterranean mussel (*M. galloprovincialis*) and abalone (*Haliotis* spp.), a slight–moderate decrease in ACP and PO activities have been recorded (Hooper et al., 2014), whereas exposure of the mussel *Mytilus coruscus* to higher water temperatures yielded greater ACP activity (Hu et al., 2015). The temperature and/or exposure times applied in this experiment (Chapter 6) were probably not of adequate magnitude or duration to induce significant changes in enzyme activity. Since the sampling method might influence haemocyte estimations, the haemolymph withdrawal should follow a precise protocol. Furthermore, sampling should make negligible injury to experimental animals, while continued testing of haemolymph from a mussel ought to be carefully evaluated as it can influence parameters such as haemocyte density, protein concentration, and enzyme activities (Ford & Paillard, 2007). It is important to note that future investigations should consider any variations in cell preparation, as well as possible improvements in the specificity and sensitivity of these parameters.

The cellular-based assessments of this thesis work (Chapter 6) revealed that the dramatic rise in sea surface temperatures over a couple of days may have a limited impact on these particular features of immunity in mussels. Further research may focus attention on longer-term effects

of ocean warming (weeks-months) that may occur during the summer months, and on other immunological biomarkers. There was no significant difference in the percentage of hyalinocytes and basophilic granulocytes among mussel samples but there were significant differences among eosinophilic granulocytes-basophilic granulocytes and eosinophilic granulocytes-hyalinocytes (Tukey's tests for pair-wise comparisons for equality) (Chapter 5). Since variations in haemocyte numbers and their population structure can be incredibly affected via season and changing environmental conditions (Carballal et al., 1998; Hégaret & Wikfors, 2005; Parisi et al., 2008; Renwranz et al., 2013), there is a requirement for further characterisations of haemocyte for *P. canaliculus* across various spatial and temporal scales. Since granulocytes are sticky and strongly attached to the smear slides but hyalinocytes are not sticky, in this study (Chapter 5), many hyalinocytes cell types were lost during preparing the Giemsa-stained smear slides. Zhang et al. (2005) reported that small hyalinocytes easily lost from Giemsa-stained smear slides. Therefore, in future, flow cytometry (FCM) analysis can be used to count and differentiate haemocytes without loss of hyalinocytes.

Very high proportion of the cells appear to be undergoing respiratory burst, regardless of treatments (temperatures and endotoxin exposure) (Chapter 6). This could be an artefact of the ROS assay (Muse® Oxidative Stress Kit). Under normal physiological conditions, the release of ROS by haemocytes is considered as a firmly controlled system, but as soon as the balance between ROS production and antioxidant defences is disturbed (because of stressors) oxidative damage can be experienced (Sheehan & McDonagh, 2008). Interestingly, apparent ROS production in haemocytes was not modified by either of the treatments (acute thermal stress and endotoxin exposure) applied, which was an unexpected finding in Chapter 6 of this thesis. Therefore, a targeted analysis of ROS and relevant regulatory metabolites and enzymes will need to be performed within the cellular and cell-free components of the circulating haemocytes to better understand this system in mussels.

7.3 Conclusions

Overall, this thesis provides a detailed histopathological assessment on New Zealand black-footed abalone (*H. iris*), flat oysters (*O. chilensis*) and New Zealand Greenshell™ mussels (*P. canaliculus*) for understanding their general health condition, disease progression, transmission mechanism and host-pathogen interactions. The histological protocol established in this research is now being used in the health assessment of abalone and geoducks in various projects by the Aquaculture Biotechnology Research Group, Auckland University of Technology. This study contributes to a better understanding of the mussels' immune defence system during the rapid increase in water temperature and provides new insights into the relationship between

thermal stress and immune stimulation to assess host-pathogen interactions. The findings of this thesis provide information on host-pathogen interactions, a better understanding of the immune function, the relationship between thermal stress and immunostimulatory responses, and the overall health condition of shellfish for disease mitigation of these important aquaculture species. It is envisaged that the information of this thesis may assist with disease management strategies for the wild and farmed shellfish aquaculture industries.

Chapter 8

References

8. References

- Aagesen, A. M., & Häse, C. C. (2014). Seasonal effects of heat shock on bacterial populations, including artificial *Vibrio parahaemolyticus* exposure, in the Pacific oyster, *Crassostrea gigas*. *Food Microbiology*, 38, 93–103. <https://doi.org/10.1016/j.fm.2013.08.008>
- Aggio, R., Villas-Bôas, S. G., & Ruggiero, K. (2011). Metab: an R package for high-throughput analysis of metabolomics data generated by GC-MS. *Bioinformatics*, 27, 2316–2318. <https://doi.org/10.1093/bioinformatics/btr379>
- Akşit, D., & Mutaf, B. F. (2014). The gill morphology of the date mussel *Lithophaga lithophaga* (Bivalvia: Mytilidae). *Turkish Journal of Zoology*, 38(1), 61–67.
- Aladaileh, S., Nair, S. V., Birch, D., & Raftos, D. A. (2007). Sydney rock oyster (*Saccostrea glomerata*) hemocytes: morphology and function. *Journal of invertebrate pathology*, 96, 48–63. <https://doi.org/10.1016/j.jip.2007.02.011>
- Albalat, A., Johnson, L., Coates, C. J., Dykes, G. C., Hitte, F., Morro, B., Dick, J. R., Todd, K., & Neil, D. M. (2019). The effect of temperature on the physiological condition and immune-capacity of European lobsters (*Homarus gammarus*) during long-term starvation. *Frontiers in Marine Science*, 6, 281. <https://doi.org/10.3389/fmars.2019.00281>
- Allam, B., Paillard, C., & Auffret, M. (2000). Alterations in hemolymph and extrapallial fluid parameters in the Manila clam, *Ruditapes philippinarum*, challenged with the pathogen *Vibrio tapetis*. *Journal of invertebrate pathology*, 76(1), 63–69.
- Allam, B., Ashton-Alcox, K. A., & Ford, S. E. (2002). Flow cytometric comparison of haemocytes from three species of bivalve molluscs. *Fish Shellfish Immunology*, 13, 141–158. <https://doi.org/10.1006/fsim.2001.0389>
- Allam, B., & Raftos, D. (2015). Immune responses to infectious diseases in bivalves. *Journal of Invertebrate Pathology*, 131, 121–136. <http://dx.doi.org/10.1016/j.jip.2015.05.005>
- Alfaro, A. C., & Young, T. (2018). Showcasing metabolomic applications in aquaculture: a review. *Reviews in Aquaculture*, 10, 135–152. <http://doi.org/10.1111/raq.12152>
- Alfaro, A. C., Nguyen, T. V., & Merien, F. (2018). The complex interactions of Ostreid herpesvirus 1, *Vibrio* bacteria, environment and host factors in mass mortality outbreaks of *Crassostrea gigas*. *Reviews in Aquaculture*, 1–21. <https://doi.org/10.1111/raq.12284>
- Alfaro, A. C., & Young, T. (2016). Showcasing metabolomic applications in aquaculture: a review. *Reviews in Aquaculture*, 1–18. <http://doi.org/10.1111/raq.12152>
- Alvarez, M. R., Friedl, F. E., Johnson, J. S., & Hinsch, G. W. (1989). Factors affecting in vitro phagocytosis by oyster hemocytes. *Journal of Invertebrate Pathology*, 54(2), 233–241. [https://doi.org/10.1016/0022-2011\(89\)90033-5](https://doi.org/10.1016/0022-2011(89)90033-5)
- Anderson, T. J., McCault, T. F., Boulo, V., Robledo, J. A. F., & Lester, R. J. G. (1994). Light and electron immune histochemical assays on paramyxean parasites. *Aquatic Living Resources*, 7, 47–52. <https://doi.org/10.1051/alr:1994006>
- Apeti, D. A., Kim, Y., Lauenstein, G., Tull, J., & Warner, R. (2014). Occurrence of Parasites and Diseases in Oysters and Mussels of the U.S. Coastal Waters. National Status and Trends, the Mussel Watch monitoring program. NOAA Technical Memorandum NOSS/NCCOS 182. Silver Spring, MD, p51

Aquaculture New Zealand (2016). Retrieved from <http://www.aquaculture.org.nz/wp-content/uploads/2012/05/NZ-Aquaculture-Facts-2012.pdf>

Araya, M. T., Siah, A., Mateo, D. R., Markham, F., McKenna, P., Johnson, G. R., & Berthe, F. C. (2009). Morphological and molecular effects of *Vibrio splendidus* on hemocytes of softshell clams, *Mya arenaria*. *Journal of Shellfish Research*, 28(4), 751-758. <https://doi.org/10.2983/035.028.0403>

Aranguren, R., & Figueras, A. (2016). Moving from histopathology to molecular tools in the diagnosis of molluscs diseases of concern under EU legislation. *Frontiers in Physiology*, 7, 1-10. <https://doi.org/10.3389/fphys.2016.00538>

Arzul, I., Langlade, A., Chollet, B., Robert, M., Ferrand, S., Omnes, E., ... & Garcia, C. (2011). Can the protozoan parasite *Bonamia ostreae* infect larvae of flat oysters *Ostrea edulis*? *Veterinary parasitology*, 179(1-3), 69-76. <https://doi.org/10.1016/j.vetpar.2011.01.060>

Arzul, I., & Carnegie, R. B. (2015). New perspective on the haplosporidian parasites of molluscs. *Journal of invertebrate pathology*, 131, 32-42. <https://doi.org/10.1016/j.jip.2015.07.014>

Assefa, A., & Abunna, F. (2018). Maintenance of fish health in aquaculture: review of epidemiological approaches for prevention and control of infectious disease of fish. *Veterinary medicine international*, 2018.

Auzoux-Bordenave, S., Vigario, A. M., Ruano, F., Domart-Coulon, I., & Doumenc, D. (1996). In vitro sporulation of the clam pathogen *Perkinsus atlanticus* (Apicomplexa, Perkinsea) under various environmental conditions. *Oceanographic Literature Review*, 9(43), 926.

Azevedo, C., Corra, L., & Cachola, R. (1990). Fine structure of zoosporulation in *Perkinsus atlanticus* (Apicomplexa: Perkinsea). *Parasitology*, 100, 351-358. <https://doi.org/10.1017/S0031182000078616>

Bachere, E., Rosa, R. D., Schmitt, P., Poirier, A. C., Merou, N., Charriere, G. M., & Destoumieux-Garzon, D. (2015). The new insights into the oyster antimicrobial defense: Cellular, molecular and genetic view. *Fish & Shellfish Immunology*, 46(1), 50-64. <http://dx.doi.org/10.1016/j.fsi.2015.02.040>

Bachère, E., Gueguen, Y., Gonzalez, M., de Lorgeril, J., Garnier, J., & Romestand, B. (2004). Insights into the antimicrobial defense of marine invertebrates: the penaeid shrimps and the oyster *Crassostrea gigas*. *Immunological Reviews*, 198, 149-168. <https://doi.org/10.1111/j.0105-2896.2004.00115.x>

Bachère, E., Hervio, D., & Mialhe, E. (1991). Luminol-dependent chemiluminescence by hemocytes of two marine bivalves, *Ostrea edulis* and *Crassostrea gigas*. *Diseases of Aquatic Organisms*, 11, 173-180.

Bachère, E., Chagot, D., & Grizel, H. (1988). Separation of *Crassostrea gigas* hemocytes by density gradient centrifugation and counter flow centrifugal elutriation. *Developmental and Comparative Immunology*, 14, 261-268. [https://doi.org/10.1016/0145-305X\(88\)90071-7](https://doi.org/10.1016/0145-305X(88)90071-7)

Baldwin, J., Wells, R., Low, M., & Ryder, J. (1992). Tauropine and D-Lactate as Metabolic Stress Indicators during Transport and Storage of Live Pāua, (New Zealand Abalone) (*Haliotis iris*). *Journal of Food Science*, 57, 280-282. <https://doi.org/10.1111/j.1365-2621.1992.tb05476.x>

- Balouet, G., Poder, M., & Cahour, A. (1983). Haemocytic parasitosis: morphology and pathology of lesions in the French flat oyster, *Ostrea edulis* L. *Aquaculture*, 34(1-2), 1-14. [https://doi.org/10.1016/0044-8486\(83\)90287-9](https://doi.org/10.1016/0044-8486(83)90287-9)
- Barracco, M. A., Medeiros, I. D., & Moreira, F. M. (1999). Some haemato-immunological parameters in the mussel *Perna perna*. *Fish & Shellfish Immunology*, 9(5), 387-404. <https://doi.org/10.1006/fsim.1998.0196>
- Bayne, C. J., Moore, M. N., Carefoot, T. H., & Thompson, R. J. (1979). Hemolymph functions in *Mytilus californianus*: The cytochemistry of hemocytes and their responses to foreign implants and hemolymph factors in phagocytosis. *Journal of Invertebrate Pathology*, 34, 1-20. [https://doi.org/10.1016/0022-2011\(79\)90048-X](https://doi.org/10.1016/0022-2011(79)90048-X)
- Beaumont, A. R., Turner, G., Wood, A. R., & Skibinski, D.O.F. (2004). Hybridisations between *Mytilus edulis* and *Mytilus galloprovincialis* and performance of pure species and hybrid veliger larvae at different temperatures. *Journal of Experimental Marine Biology and Ecology*, 302(2), 177-188. <https://doi.org/10.1016/j.jembe.2003.10.009>
- Beckmann, N., Morse, M. P., & Moore, C. M. (1992). Comparative study of phagocytosis in normal and diseased hemocytes of the bivalve mollusc *Mya arenaria*. *Journal of Invertebrate Pathology*, 59, 124-132. [https://doi.org/10.1016/0022-2011\(92\)90022-V](https://doi.org/10.1016/0022-2011(92)90022-V)
- Berthe, F. (2004). Report about mollusc diseases. *Mediterranean aquaculture diagnostic laboratories*, 49, 33-48. <https://archimer.ifremer.fr/doc/00000/3300/>
- Berthe, F. C. J., & Hine, P. M. (2003). *Bonamia exitiosa* Hine et al., 2001 is proposed instead of *B. exitiosus* as the valid name of *Bonamia* sp infecting flat oysters *Ostrea chilensis* in New Zealand. *Diseases of Aquatic Organisms*, 57(1-2), 181-181.
- Berthelin, C., Kellner, K., & Mathieu, M. (2000). Storage metabolism in the Pacific oyster (*Crassostrea gigas*) in relation to summer mortalities and reproductive cycle (West Coast of France). *Comparative Biochemistry and Physiology Part B: Biochemistry and Molecular Biology*, 125 (3), 359-369. [https://doi.org/10.1016/S0305-0491\(99\)00187-X](https://doi.org/10.1016/S0305-0491(99)00187-X)
- Bettencourt, R., Dando, P., Collins, P., Costa, V., Allam, B., & Santos, R. S. (2009). Innate immunity in the deep sea hydrothermal vent mussel *Bathymodiolus azoricus*. *Comparative Biochemistry and Physiology Part A: Molecular & Integrative Physiology*, 152(2), 278-289. <https://doi.org/10.1016/j.cbpa.2008.10.022>
- Bingham, P., Brangenberg, N., Williams, R., & Andel, M.V. (2013). Investigation into the first diagnosis of ostreid herpes virus type 1 in Pacific oysters. *Surveillance*, 40(2), 20-24.
- Blackbourn, J., Bower, S. M., & Meyer, G. M. (1998). *Perkinsus qugwadi* sp. nov. (incertae sedis), a pathogenic protozoan parasite of Japanese scallops, *Patinopecten yessoensis*, cultured in British Columbia, Canada. *Canadian Journal of Zoology*, 76, 942-953. <https://doi.org/10.1139/z98-015>
- Bower, S. M. (2010). Synopsis of Infectious Diseases and Parasites of Commercially Exploited Shellfish: *Perkinsus olseni* of Abalone. [https://doi.org/10.1016/0959-8030\(94\)90028-0](https://doi.org/10.1016/0959-8030(94)90028-0)
- Bower, S. M. (2006a). Synopsis of Infectious Diseases and Parasites of Commercially Exploited Shellfish: Fungal Diseases of Abalone. <http://www.dfo-mpo.gc.ca/science/aaah-saa/diseases-maladies/fungusab-eng.html>

- Bower, S. M. (2006b). Synopsis of Infectious Diseases and Parasites of Commercially Exploited Shellfish: Shell-boring Polychaetes of Abalone. http://www-sci.pac.dfo.mpo.gc.ca/shelldis/pages/sbpab_e.htm
- Bower, S. M., Goh, B., Meyer, G. R., Carnegie, R. B., & Gee, A. (2005). Epizootiology and detection of nocardiosis in oysters. *Diseases in Asian Aquaculture V. Diseases in Asian Aquaculture V, Fish Health Section. Asian Fisheries Society, Manila*, 249-262.
- Bower, S. M., McGladdery, S. E., & Price, I. M. (1994). Synopsis of Infectious Diseases and Parasites of commercially exploited shellfish. *Annual Review of Fish Diseases*, 4, 1-199. [https://doi.org/10.1016/0959-8030\(94\)90028-0](https://doi.org/10.1016/0959-8030(94)90028-0)
- Bowmer, C. T., van der Meer, M., & Scholten, M. C. T. (1991). A histopathological analysis of wild and transplanted *Dreissena polymorpha* from the Dutch sector of the River Maas. *Comparative Biochemistry and Physiology, C*, 100, 225-229. [https://doi.org/10.1016/0742-8413\(91\)90158-P](https://doi.org/10.1016/0742-8413(91)90158-P)
- Bouallegui, Y. (2019). Immunity in mussels: An overview of molecular components and mechanisms with a focus on the functional defenses. *Fish & shellfish immunology*, 89, 158-169. <https://doi.org/10.1016/j.fsi.2019.03.057>
- Brauko, K. M., Cabral, A., Costa, N. V., Hayden, J., Dias, C. E., Leite, E. S., ... & Horta, P. A. (2020). Marine heatwaves, sewage and eutrophication combine to trigger deoxygenation and biodiversity loss: A SW Atlantic case study. *Frontiers in Marine Science*, 7, 590258.
- Brehelin, M., Bonami, J. R., Cousserans, F., & Vivares, C. P. (1982). Existence de formes plasmodiales vraies chez *Bonamia ostreae* parasite de l'huitre *Ostrea edulis*. *Comptes rendus des seances de l'Academie des sciences. Serie III: Sciences de la vie. Paris*. 295, 45-48.
- Bruno, D. W., Nowak, B., & Elliott, D. G. (2006). Guide to the identification of fish protozoan and metazoan parasites in stained tissue sections. *Diseases of aquatic organisms*, 70(1-2), 1-36.
- Bucke, D. (1988). Pathology of Bonamiasis. *Parasitology Today*, 4(6), 174-176. [https://doi.org/10.1016/0169-4758\(88\)90154-8](https://doi.org/10.1016/0169-4758(88)90154-8)
- Burge, C. A., Mark Eakin, C., Friedman, C. S., Froelich, B., Hershberger, P. K., Hofmann, E. E., ... & Harvell, C. D. (2014). Climate change influences on marine infectious diseases: implications for management and society. *Annual review of marine science*, 6, 249-277.
- Burreson, E. M. (2000). Disease diagnosis by PCR: foolproof or foolhardy? *Journal of Shellfish Research*, 19(1), 642.
- Bush, A. O., Lafferty, K. D., Lotz, J. M., & Shostak, A. W. (1997). Parasitology meets ecology on its own terms: Margolis et al. revisited. *The Journal of parasitology*, 575-583. <https://doi.org/10.7939/R3J38KV04>
- Cajaraville, M. P., & Pal, S. G. (1995). Morphofunctional study of the haemocytes of the bivalve mollusc *Mytilus galloprovincialis* with emphasis on the endolysosomal compartment. *Cell structure and function*, 20, 355-367.
- Cappello, T., Maisano, M., Mauceri, A., & Fasulo, S. (2017). 1H NMR-based metabolomics investigation on the effects of petrochemical contamination in posterior adductor muscles of caged mussel *Mytilus galloprovincialis*. *Ecotoxicology and environmental safety*, 142, 417-422. <https://doi.org/10.1016/j.ecoenv.2017.04.040>

- Carballal, M. A. J., Villalba, A., & López, C. (1998). Seasonal variation and effects of age, food availability, size, gonadal development, and parasitism on the hemogram of *Mytilus galloprovincialis*. *Journal of invertebrate pathology*, *72*, 304-312. <https://doi.org/10.1006/jipa.1998.4779>
- Carella, F., Feist, S. W., Bignell, J. P., & De Vico, G. (2015a). Comparative pathology in bivalves: Aetiological agents and disease processes. *Journal of invertebrate pathology*, *131*, 107-120. <http://dx.doi.org/10.1016/j.jip.2015.07.012>
- Carella, F., Sardo, A., Mangoni, O., Di Cioccio, D., Urciuolo, G., De Vico, G., & Zingone, A. (2015b). Quantitative histopathology of the Mediterranean mussel (*Mytilus galloprovincialis* L.) exposed to the harmful dinoflagellate *Ostreopsis cf. ovata*. *Journal of invertebrate pathology*, *127*, 130-140. <https://doi.org/10.1016/j.jip.2015.03.001>
- Casas, S. M. L. (2002). Estudio de la perkinsosis en la almeja fina, *Tapes decussatus* (Linnaeus, 1758), de Galicia. Universidad de Santiago de Compostela, PhD Thesis, pp. 272.
- Castinel, A., Webb, S. C., Jones, J. B., Peeler, E. J., & Forrest, B. M. (2019). Disease threats to farmed green-lipped mussels *Perna canaliculus* in New Zealand: review of challenges in risk assessment and pathway analysis. *Aquaculture Environment Interactions*, *11*, 291-304. <https://doi.org/10.3354/aei00314>.
- Canesi, L., Gavioli, M., & Pruzzo, C., Gallo, G. (2002). Bacteria hemocyte interactions and phagocytosis in marine bivalves. *Microscopy Research and Technique*, *57*, 469-476. <https://doi.org/10.1002/jemt.10100>
- Cano, I., Ryder, D., Webb, S. C., Jones, B. J., Brosnahan, C. L., Carrasco, N., ... & Feist, S. W. (2020). Cosmopolitan Distribution of Endozoicomonas-Like Organisms and Other Intracellular Microcolonies of Bacteria Causing Infection in Marine Mollusks. *Frontiers in microbiology*, *11*, 2778. <https://www.frontiersin.org/articles/10.3389/fmicb.2020.577481/full>
- Cajaraville, M. P., Olabarrieta, I., & Marigomez, I. (1996). In vitro activities in mussel hemocytes as biomarkers of environmental quality: a case study in the Abra Estuary (Biscay Bay). *Ecotoxicology and Environmental Safety*, *35*(3), 253-260. <https://doi.org/10.1006/eesa.1996.0108>
- Carballal, M. J., López, C., Azevedo, C., & Villalba, A. (1997a). Enzymes involved in defense functions of hemocytes of mussel *Mytilus galloprovincialis*. *Journal of invertebrate pathology*, *70*(2), 96-105. <https://doi.org/10.1006/jipa.1997.4670>
- Carballal, M. J., Lopez, M. C., Azevedo, C., & Villalba, A. (1997b). Hemolymph cell types of the mussel *Mytilus galloprovincialis*. *Diseases of aquatic organisms*, *29*(2), 127-135.
- Carballal, M. J., López, C., Azevedo, C., & Villalba, A. (1997c). In vitro study of phagocytic ability of *Mytilus galloprovincialis* Lmk. haemocytes. *Fish & Shellfish Immunology*, *7*(6), 403-416. <https://doi.org/10.1006/fsim.1997.0094>
- Carnegie, R. B., Arzul, I., & Bushek, D. (2016). Managing marine mollusc diseases in the context of regional and international commerce: policy issues and emerging concerns. *Philosophical Transactions of the Royal Society B: Biological Sciences*, *371*(1689), 20150215.
- Carnegie, R. B., Bureson, E. M., Hine, P. M., Stokes, N. A., Audemard, C., Bishop, M. J., & Peterson, C. H. (2006). *Bonamia perspora* n. sp. (Haplosporidia), a parasite of the oyster *Ostreola equestris*, is the first *Bonamia* species known to produce spores. *Journal of Eukaryotic Microbiology*, *53*, 232-245. <https://doi.org/10.1111/j.1550-7408.2006.00100.x>

- Carnegie, R. B., Barber, B. J., & Distel, D. L. (2003). Detection of the oyster parasite *Bonamia ostreae* by fluorescent *in situ* hybridization. *Diseases of aquatic organisms*, 55(3), 247-252.
- Castinel, A., Webb, S. C., Jones, J. B., Peeler, E. J., & Forrest, B. M. (2019). Disease threats to farmed green-lipped mussels *Perna canaliculus* in New Zealand: review of challenges in risk assessment and pathway analysis. *Aquaculture Environment Interactions*, 11, 291–304. <https://doi.org/10.3354/aei00314>
- Castinel, A., Forrest, B., & Hopkins, G. (2014). Review of diseases of potential concern for New Zealand shellfish aqua culture: perspectives for risk management. Cawthron Rep No. 2297.
- Castinel, A., Forrest, B., & Hopkins, G. (2013). Review of disease risks for New Zealand shellfish aquaculture: perspectives for management. Prepared for Ministry for Business, Innovation and Employment. Cawthron Report No. 2297. 31 pp.
- Cáceres-Martínez, J., & Vásquez-Yeomans, R. (1997). Presence and Histopathological Effects of the Copepod *Pseudomyicola spinosus*, *Mytilus galloprovincialis* and *Mytilus californianus*. *Journal of invertebrate pathology*, 70(2), 150-155. <https://doi.org/10.1006/jipa.1997.4679>
- Casas, S. M., Reece, K. S., Li, Y., Moss, J. A., Villalba, A., & La Peyre, J. F. (2008). Continuous culture of *Perkinsus mediterraneus*, a parasite of the European flat oyster *Ostrea edulis*, and characterization of its morphology, propagation, and extracellular proteins *in vitro*. *Journal of Eukaryotic Microbiology*, 55, 34–43. <https://doi.org/10.1111/j.1550-7408.2008.00301.x>
- Chandurvelan, R., Marsden, I. D., Gaw, S., & Glover, C. N. (2013). Waterborne cadmium impacts immunocytotoxic and cytogenotoxic endpoints in green-lipped mussel, *Perna canaliculus*. *Aquatic toxicology*, 142, 283-293. <http://dx.doi.org/10.1016/j.aquatox.2013.09.002>
- Chakraborty, S., Ray, M., & Ray, S. (2009). Evaluation of phagocytic activity and nitric oxide generation by molluscan haemocytes as biomarkers of inorganic arsenic exposure. *Biomarkers*, 14(8), 539-546. <https://doi.org/10.3109/13547500903240473>
- Chang, S. J., Tseng, S. M., & Chou, H. Y. (2005). Morphological characterization via light and electron microscopy of the hemocytes of two cultured bivalves: a comparison study between the hard clam (*Meretrix lusoria*) and Pacific oyster (*Crassostrea gigas*). *Zoological studies*, 44(1), 144-153.
- Chen, M., Yang, H., Delaporte, M., & Zhao, S. (2007). Immune condition of *Chlamys farreri* in response to acute temperature challenge. *Aquaculture*, 271(1-4), 479-487. <https://doi.org/10.1016/j.aquaculture.2007.04.051>
- Cheyney, D., MacDonald, B., & Elston, R. (1998). Summer Mortality of Pacific Oysters, *Crassostrea gigas* (Thunberg): Initial Findings on Multiple Environmental Stressors in Puget Sound, Washington.
- Chu, F. L. C., & La Peyre, J. F. (1993). Development of disease caused by the parasite, *Perkinsus marinus* and defense-related hemolymph factors in 3 populations of Oysters from the Chesapeake Bay, USA. *Journal of Shellfish Research*, 12(1), 21.
- Chu, F. L. E. (1996). Laboratory investigations of susceptibility, infectivity and transmission of *Perkinsus marinus* in oysters. *Journal of Shellfish Research*, 15(1), 57-66.

- Cheng, T. C. (1981). Bivalves, in: N.A. Ratcliffe & A.F. Rowly (Eds.), *Invertebrate blood cells*, Academic Press, London, United Kingdom, pp. 233-300.
- Cheng, T. C., & Foley, D. A. (1975). Hemolymph cells of the bivalve mollusc *Mercenaria mercenaria*: an electron microscopical study. *Journal of Invertebrate Pathology*, 26, 341-351. [https://doi.org/10.1016/0022-2011\(75\)90232-3](https://doi.org/10.1016/0022-2011(75)90232-3)
- Cheyney, D., MacDonald, B., & Elston, R. (1998). Summer Mortality of Pacific Oysters, *Crassostrea gigas* (Thunberg): Initial Findings on Multiple Environmental Stressors in Puget Sound, Washington.
- Choi, K. S., & Park, K. I. (1997). Report on the occurrence of *Perkinsus* sp. in the Manila clams, *Ruditapes philippinarum* in Korea. *Journal of Aquaculture*, 10, 227-237.
- Choi, K. S., & Park, K.I. (2010). Review on the protozoan parasite *Perkinsus olseni* (Lester and Davis, 1981) infection in Asian waters Coast. *Environ Ecos Issues East China Sea*, 269-281.
- Choi, K. S., Park, K. L., Lee, K. W., & Matsuoka, K. (2002). Infection intensity, prevalence and histopathology of *Perkinsus* sp. in the Manila clam, *Ruditapes philippinarum*, in Isahaya Bay, Japan. *Journal of Shellfish Research*, 21, 119-125.
- Choi, K. S., Park, K. I., Cho, M. J., & Soudant, P. (2005). Diagnosis, pathology, and taxonomy of *Perkinsus* sp. isolated from the Manila clam *Ruditapes philippinarum* in Korea. *Journal of aquaculture*, 18(3), 207-214.
- Chiswell, S. M., & Sutton, P. J. (2020). Relationships between long-term ocean warming, marine heat waves and primary production in the New Zealand region. *New Zealand Journal of Marine and Freshwater Research*, 54, 614-635. <https://doi.org/10.1080/00288330.2020.1713181>
- Chong, J., Wishart, D. S., & Xia, J. (2019). Using MetaboAnalyst 4.0 for comprehensive and integrative metabolomics data analysis. *Current protocols in bioinformatics*, 68, e86. <https://doi.org/10.1002/cpbi.86>
- Cigarría, J., & Elston, R. (1997). Independent introduction of *Bonamia ostreae*, a parasite of *Ostrea edulis*, to Spain. *Diseases of Aquatic Organisms*, 29, 157-158.
- Cima, F., Matozzo, V., Marin, M. G., & Ballarin, L. (2000). Haemocytes of the clam *Tapes philippinarum* (Adams & Reeve, 1850): morpho functional characterisation. *Fish & Shellfish Immunology*, 10, 677-693. <https://doi.org/10.1006/fsim.2000.0282>
- Ciocan, C., & Sunila, I. (2005). Disseminated neoplasia in blue mussels, *Mytilus galloprovincialis*, from the Black Sea, Romania. *Marine Pollution Bulletin*, 50 (11), 1335-1339. <https://doi.org/10.1016/j.marpolbul.2005.04.042>
- Cochennec-Laureau, N., Auffret, M., Renault, T., & Langlade, A. (2003). Changes in circulating and tissue-infiltrating hemocyte parameters of European flat oysters, *Ostrea edulis*, naturally infected with *Bonamia ostreae*. *Journal of invertebrate pathology*, 83(1), 23-30. [https://doi.org/10.1016/S0022-2011\(03\)00015-6](https://doi.org/10.1016/S0022-2011(03)00015-6)
- Cochennec, N., LeRoux, F., Berthe, F., & Gerard, A. (2000). Detection of *Bonamia ostreae* based on small subunit ribosomal probe. *Journal of Invertebrate Pathology*, 76, 26-32. <https://doi.org/10.1006/jipa.2000.4939>

- Coles, J., & Pipe, R. (1994). Phenoloxidase activity in the haemolymph and haemocytes of the marine mussel *Mytilus edulis*. *Fish & Shellfish Immunology*, 4, 337-352. <https://doi.org/10.1006/fsim.1994.1030>
- Comps, M. (1983). Recherches histologiques et cytologiques sur les infections intracellulaires des mollusques bivalves marins. PhD Thesis, Université des Sciences et Techniques du Languedoc, Montpellier.
- Cone, J. B. (2001). Inflammation. *American Journal of Surgery*, 182, 558-562. [https://doi.org/10.1016/S0002-9610\(01\)00822-4](https://doi.org/10.1016/S0002-9610(01)00822-4)
- Cook, P. A. (2019). Worldwide abalone production statistics. *Journal of Shellfish Research*, 38(2), 401-404. <https://doi.org/10.2983/035.038.0222>
- Cook, P., & Gordon, G. (2010). World abalone supply, markets and pricing. *Journal of Shellfish Research*, 29, 569-571. <https://doi.org/10.2983/035.029.0303>
- Cordier, G. (1986). Flow cytometry for immunology. *Biology of the Cell*, 58, 147-150. <https://doi.org/10.1111/j.1768-322X.1986.tb00499.x>
- Cossarizza, A., Chang, H. D., Radbruch, A., Akdis, M., Andrä, I., Annunziato, F., ... & Oxenius, A. (2017). Guidelines for the use of flow cytometry and cell sorting in immunological studies. *European journal of immunology*, 47(10), 1584-1797.
- Costa, M., Prado-Álvarez, M., Gestal, C., Li, H., Roch, P., Novoa, B., & Figueras, A. (2009). Functional and molecular immune response of Mediterranean mussel (*Mytilus galloprovincialis*) haemocytes against pathogen-associated molecular patterns and bacteria. *Fish & Shellfish Immunology*, 26, 515-523. <https://doi.org/10.1016/j.fsi.2009.02.001>
- Costa, M. M., Prado-Álvarez, M., Gestal, C., Li, H., Roch, P., Novoa, B. & Figueras, A. (2009). Functional and molecular immune response of Mediterranean mussel (*Mytilus galloprovincialis*) haemocytes against pathogen-associated molecular patterns and bacteria. *Fish & shellfish immunology*, 26(3), 515-523.
- Couch, J. A. (1985). Prospective study of infectious and non infectious diseases in oysters and fishes in three Gulf of Mexico estuaries. *Diseases of Aquatic Organisms*, 1, 59-82.
- Cruz-Flores, R., & Cáceres-Martínez, J. (2020). Rickettsiales-like organisms in bivalves and marine gastropods: a review. *Reviews in Aquaculture*, 12(4), 1-17.
- Cranfield, H. J., Dunn, A., Doonan, I. J., & Michael, K. P. (2005). *Bonamia exitiosa* epizootic in *Ostrea chilensis* from Foveaux Strait, southern New Zealand between 1986 and 1992. *ICES Journal of Marine Science*, 62, 3-13. <https://doi.org/10.1016/j.icesjms.2004.06.021>
- Culloty, S. C., & Mulcahy, M. F. (1996). Season-, age-, and sex-related variation in the prevalence of bonamiasis in flat oysters (*Ostrea edulis* L.) on the south coast of Ireland. *Aquaculture*, 144(1-3), 53-63. [https://doi.org/10.1016/S0044-8486\(96\)01290-2](https://doi.org/10.1016/S0044-8486(96)01290-2)
- Culloty, S. C., & Mulcahy, M. F. (2007). *Bonamia ostreae* in the native oyster *Ostrea edulis*. *A Review. Marine Environment and Health Series*, 29, 200.
- da Silva, P. M., Vianna, R. T., Guertler, C., Ferreira, L. P., Santana, L. N., Fernández-Boo, S., & Villalba, A. (2013). First report of the protozoan parasite *Perkinsus marinus* in South America, infecting mangrove oysters *Crassostrea rhizophorae* from the Paraíba River (NE, Brazil). *Journal of invertebrate pathology*, 113(1), 96-103. <https://doi.org/10.1016/j.jip.2013.02.002>

- da Silva, P. M., Comesaña, P., Fuentes, J., & Villalba, A. (2008). Variability of haemocyte and haemolymph parameters in European flat oyster *Ostrea edulis* families obtained from brood stocks of different geographical origins and relation with infection by the protozoan *Bonamia ostreae*. *Fish & Shellfish Immunology*, 24 (5), 551-563. <https://doi.org/10.1016/j.fsi.2007.11.003>
- da Silva, P. M., Fuentes, J., & Villalba, A. (2005). Growth, mortality and disease susceptibility of oyster *Ostrea edulis* families obtained from brood stocks of different geographical origins, through on-growing in the Ria de Arousa (Galicia, NW Spain). *Marine Biology*, 147(4), 965-977. <http://dx.doi.org/10.1007/s00227-005-1627-4>
- da Silva, P. M., & Villalba, A. (2004). Comparison of light microscopic techniques for the diagnosis of the infection of the European flat oyster *Ostrea edulis* by the protozoan *Bonamia ostreae*. *Journal of Invertebrate Pathology*, 85, 97–104. <https://doi.org/10.1016/j.jip.2003.12.010>
- Dang, C., Tan, T., Moffit, D., Deboutteville, J. D., & Barnes, A. C. (2012). Gender differences in hemocyte immune parameters of bivalves: the Sydney rock oyster *Saccostrea glomerata* and the pearl oyster *Pinctada fucata*. *Fish & shellfish immunology*, 33(1), 138-142. <https://doi.org/10.1016/j.fsi.2012.04.007>
- Dang, C., De Montaudouin, X., Caill-Milly, N., & Trumbić, Ž. (2010). Spatio-temporal patterns of perkinsosis in the Manila clam *Ruditapes philippinarum* from Arcachon Bay (SW France). *Diseases of aquatic organisms*, 91(2), 151-159. <https://doi.org/10.3354/dao02243>
- Danovaro, R., Corinaldesi, C., Dell'Anno, A., Fuhrman, J. A., Middelburg, J. J., Noble, R. T., & Suttle, C. A. (2011). Marine viruses and global climate change. *FEMS microbiology reviews*, 35(6), 993-1034.
- Darriba Couñago, S. (2017). Atlas de Histopatología Moluscos bivalvos mariños Histopathological Atlas Marine bivalve molluscs Cancellara do Mar Santiago de Compostela. Edita: Intecmar. Xunta de Galicia (Consellería do Mar). 1.ª edición: Santiago de Compostela, marzo de 2017 162p.
- Desriac, F., Le Chevalier, P., Brillet, B., Leguerinel, I., Thuillier, B., Paillard, C., & Fleury, Y. (2014). Exploring the hologenome concept in marine bivalvia: haemolymph microbiota as a pertinent source of probiotics for aquaculture. *FEMS microbiology letters*, 350(1), 107-116.
- de Oliveira David, J. A., Salaroli, R. B., & Fontanetti, C. S. (2008). Fine structure of *Mytella falcata* (Bivalvia) gill filaments. *Micron*, 39(3), 329-336. <https://doi.org/10.1016/j.micron.2007.06.002>
- Diggles, B. K., Hine, P. M., Handley, S., & Boustead, N. C. (2002a). *A handbook of diseases of importance to aquaculture in New Zealand*. NIWA Science and Technology Series No. 49. 200 p.
- Diggles, B. K., Nichol, J., Hine, P. M., Wakefield, S., Cochennec-Laureau, N., Roberts, R. D., & Friedman, C. S. (2002b). Pathology of cultured paua *Haliotis iris* infected with a novel haplosporidian parasite, with some observations on the course of disease. *Diseases of Aquatic Organisms*, 50(3), 219-231. <https://doi.org/10.3354/dao050219>
- Diggles, B. K., & Oliver, M. (2005). Diseases of cultured paua (*Haliotis iris*) in New Zealand. *Disease in Asian Aquaculture*, V, 275–287.

- Diggles, B. K., Cochenne-Laureau, N., & Hine, P. M. (2003). Comparison of diagnostic techniques for *Bonamia exitiosus* from flat oysters *Ostrea chilensis* in New Zealand. *Aquaculture*, 220, 145–156. [https://doi.org/10.1016/S0044-8486\(02\)00635-X](https://doi.org/10.1016/S0044-8486(02)00635-X)
- Diggles, B. K., & Hine, P. M. (2002). *Bonamia exitiosus* epidemiology in Foveaux Strait oysters. Final research report, OYS1999/01, Ministry of Fisheries. Unpublished report held at National Institute of Water and Atmospheric Research.
- Dinamani, P., Hine, M., & Jones, J. B. (1987). Occurrence and characteristics of the haemocyte parasite *Bonamia ostreae* in the New Zealand dredge oyster *Tiostrea lutaria*. *Diseases of aquatic organisms*, 3, 37-44. <https://doi.org/10.3354/dao003037>
- Dinamani, P. (1986). Potential disease-causing organisms associated with mantle cavity of Pacific oyster *Crassostrea gigas* in northern New Zealand. *Diseases of Aquatic Organisms*, 2, 55–63. <https://doi.org/10.3354/dao002055>
- Dinamani, P. (1971). Occurrence of the Japanese oyster, *Crassostrea gigas* (Thunberg), in Northland, New Zealand. *New Zealand Journal of Marine and Freshwater Research*, 5, 352-35.
- Delorme, N. J., Venter, L., Rolton, A., & Ericson, J. A. (2021). Integrating animal health and stress assessment tools using the green-lipped mussel *Perna canaliculus* as a case study. *Journal of Shellfish Research*, 40(1), 93-112.
- Donaghy, L., Kraffe, E., Le Goïc, N., Lambert, C., Volety, A. K., & Soudant, P. (2012). Reactive oxygen species in unstimulated hemocytes of the Pacific oyster *Crassostrea gigas*: a mitochondrial involvement. *PLoS One*, 7 (10), e46594.
- Doonan, I. J., Cranfield, H. J., & Michael, K. P. (1994). Catastrophic reduction of the oyster, *Tiostrea chilensis* (Bivalvia: Ostreidae), in Foveaux Strait, New Zealand, due to an infestation by the protistan *Bonamia* sp. *New Zealand Journal of Marine and Freshwater Research*, 28, 335–344. <https://doi.org/10.1080/00288330.1994.9516623>
- Dundon, W. G., Arzul, I., Omnes, E., Robert, M., Magnabosco, C., Zambon, M., ... & Arcangeli, G. (2011). Detection of Type 1 Ostreid Herpes variant (OsHV-1 μ var) with no associated mortality in French-origin Pacific cupped oyster *Crassostrea gigas* farmed in Italy. *Aquaculture*, 314(1-4), 49-52. <https://doi.org/10.1016/j.aquaculture.2011.02.005>
- Dungan, C. F., Reece, K. S., Moss, J. A., Hamilton, R. M., & Diggles, B. K. (2007). *Perkinsus olseni* in vitro Isolates from the New Zealand Clam *Austrovenus stutchburyi*. *Journal of Eukaryotic Microbiology*, 54(3), 263-270. <https://doi.org/10.1111/j.1550-7408.2007.00265.x>
- Dungan, C. F., & Reece, K. S. (2006). *In vitro* propagation of two *Perkinsus* spp. parasites from Japanese Manila clams, *Venerupis philippinarum*, and description of *Perkinsus honshuensis* n. sp. *Journal of Eukaryotic Microbiology*, 53, 316-326. <https://doi.org/10.1111/j.1550-7408.2006.00120.x>
- Dunphy, B., Ruggiero, K., Zamora, L., & Ragg, N. (2018). Metabolomic analysis of heat-hardening in adult green-lipped mussel (*Perna canaliculus*): a key role for succinic acid and the GABAergic synapse pathway. *Journal of thermal biology*, 74, 37-46. <https://doi.org/10.1016/j.jtherbio.2018.03.006>
- Dunphy, B. J., Watts, E., & Ragg, N. L. (2015). Identifying thermally-stressed adult green-lipped mussels (*Perna canaliculus* Gmelin, 1791) via metabolomic profiling. *American Malacological Bulletin*, 33(1), 127-135. <https://doi.org/10.4003/006.033.0110>

- Dunphy, B. J., & Wells, R. M. (2001). Endobiont infestation, shell strength and condition index in wild populations of New Zealand abalone, *Haliotis iris*. *Marine and Freshwater Research*, 52(5), 781-786. <https://doi.org/10.1071/MF99189>
- Dunn, A., Cranfield, H. J., Doonan, I. J., & Michael, K. P. (2000). Revised estimates of natural mortality for the Foveaux Strait oyster (*Ostrea chilensis*). *New Zealand Journal of Marine and Freshwater Research*, 34(4), 661-667.
- Dyrynda, E. A., Pipe, R. K., Burt, G. R., & Ratcliffe, N. A. (1998). Modulations in the immune defences of mussels (*Mytilus edulis*) from contaminated sites in the UK. *Aquatic Toxicology*, 42, 169-185. [https://doi.org/10.1016/S0166-445X\(97\)00095-7](https://doi.org/10.1016/S0166-445X(97)00095-7)
- Ellis, R. P., Parry, H., Spicer, J. I., Hutchinson, T. H., Pipe, R. K., & Widdicombe, S. (2011). Immunological function in marine invertebrates: Responses to environmental perturbation. *Fish Shellfish Immunology*, 30 (6), 1209-1222. <https://doi.org/10.1016/j.fsi.2011.03.017>
- Ellis, A. E. (2001). Innate host defense mechanisms of fish against viruses and bacteria. *Dev. Comp. Developmental and Comparative Immunology*, 25, 827-839. [https://doi.org/10.1016/S0145-305X\(01\)00038-6](https://doi.org/10.1016/S0145-305X(01)00038-6)
- Ellis, M. S., Barber, R. D., Hillman, R. E., Kim, Y., & Powell, E. N. (1998). Histopathology analysis. In: Lauenstein, G.G., Cantillo, A.Y. (ed.), Sampling and Analytical Methods of the National Status and Trends Program Mussel Watch Projects: 1993-1996 update. National Oceanic and Atmospheric Administration Technical Memorandum, NOS/ORCA, 130. pp. 198-215.
- Elston, R. A., Dungan, C. F., Meyers, T. R., & Reece, K. S. (2003). *Perkinsus* sp infection risk for manila clams, *Venerupis philippinarum* (A. Adams and Reeve, 1850) on the Pacific coast of North and Central America. *Journal of Shellfish Research*, 22(3), 661.
- Elston, R. A., Moore, J. D., & Brooks, K. (1992). Disseminated neoplasia of bivalve molluscs. *Reviews in Aquatic Science*, 6, 405-466.
- Elston, R. A., Kent, M. L., & Wilkinson, M. T. (1987). Resistance of *Ostrea edulis* to *Bonamia ostreae* infection [Short Communication]. *Aquaculture*, 64(3), 237-242. [https://dx.doi.org/10.1016/0044-8486\(87\)90328-0](https://dx.doi.org/10.1016/0044-8486(87)90328-0)
- Elston, R. A., Farley, C. A., & Kent, M. L. (1986). Occurrence and significance of bonamiasis in European flat oysters *Ostrea edulis* in North America. *Diseases of aquatic organisms*, 2(49-54). <https://doi.org/10.3354/dao003037>
- Elvitigala, D., Premachandra, H., Whang, I., Nam, B., & Lee, J. (2013). Molecular insights of the first gastropod TLR counterpart from disk abalone (*Haliotis discus discus*), revealing its transcriptional modulation under pathogenic stress. *Fish & Shellfish Immunology*, 35, 334-342. <https://doi.org/10.1016/j.fsi.2013.04.031>
- Engelsma, M. Y., Culloty, S. C., Lynch, S. A., Arzul, I., & Carnegie, R. B. (2014). *Bonamia* parasites: a rapidly changing perspective on a genus of important mollusc pathogens. *Diseases of Aquatic Organisms*, 110, 5-23.
- Fan, S., Kind, T., Cajka, T., Hazen, S. L., Tang, W. W., Kaddurah-Daouk, R., Irvin, M. R., Arnett, D. K., Barupal, D. K., & Fiehn, O. (2019). Systematic error removal using random forest for normalizing large-scale untargeted lipidomics data. *Analytical chemistry*, 91, 3590-3596.

- FAO. (2020). The State of World Fisheries and Aquaculture 2020. Sustainability in action. Rome. <https://doi.org/10.4060/ca9229en>
- FAO. (2019). *Global aquaculture production 1950-2014 (online query)* [Online]. FAO. Available: <http://www.fao.org/fishery/statistics/global-aquaculture-production/query/en>
- Farley, C. A., Wolf, P. H., & Elstons, R. A. (1988). A long-term study of 'microcell' disease in oysters with a description of a new genus, *Mikrocytos* (g.n.), and two new species, *Mikrocytos mackini* (sp.n.) and *Mikrocytos roughleyi* (sp.n.). *Fishery Bulletin*, 86(3), 581-593.
- Fisher, W. S., & Tamplin, M. (1988). Environmental influence on activities and foreign-particle binding by hemocytes of American oysters, *Crassostrea virginica*. *Canadian Journal of Fisheries and Aquatic Sciences*, 45(7), 1309-1315. <https://doi.org/10.1139/f88-153>
- Flannery, G., Lynch, S.A., Longshaw, M., Stone, D., Martin, P., Ramilo, A., Villalba, A., & Culloty, S. C. (2014). Interlaboratory variability in screening for *Bonamia ostreae*, a protistan parasite of the European flat oyster *Ostrea edulis*. *Diseases of Aquatic Organisms*, 110, 93-99. <https://doi.org/10.3354/dao02717>
- Fleisher, T. A., & Oliveira, J. B. (2019). 92 - Flow Cytometry. In: Rich, R. R., Fleisher, T. A., Shearer, W. T., Schroeder, H. W., Frew, A. J. & Weyand, C. M. (eds.) *Clinical Immunology (Fifth Edition)*. London: Elsevier. 1239-1251.
- Flye-Sainte-Marie, J., Soudant, P., Lambert, C., Le Goïc, N., Goncalvez, M., Travers, M. A., & Jean, F. (2009). Variability of the hemocyte parameters of *Ruditapes philippinarum* in the field during an annual cycle. *Journal of Experimental Marine Biology and Ecology*, 377(1), 1-11.
- Friedman, C. S., Andree, K. B., Beauchamp, K. A., Moore, J. D., Robbins, T. T., Shields, J. D., & Hedrick, R. P. (2000). '*Candidatus Xenohaliotis californiensis*', a newly described pathogen of abalone, *Haliotis* spp., along the west coast of North America. *International Journal of Systematic and Evolutionary Microbiology*, 50(2), 847-855. <https://doi.org/10.1099/00207713-50-2-847>
- Ford, S. E., & Chintala, M. M. (2006). Northward expansion of a marine parasite: Testing the role of temperature adaptation. *Journal of experimental marine biology and ecology*, 339(2), 226-235. <https://doi.org/10.1016/j.jembe.2006.08.004>
- Ford, S., & Paillard, C. (2007). Repeated sampling of individual bivalve mollusks I: Intraindividual variability and consequences for haemolymph constituents of the Manila clam, *Ruditapes philippinarum*. *Fish & Shellfish Immunology*, 23, 280-291.
- Ford, S. E., & Smolowitz, R. (2007). Infection dynamics of an oyster parasite in its newly expanded range. *Marine Biology*, 151(1), 119-133. <https://doi.org/10.1007/s00227-006-0454-6>
- Friedman, C. S., Thompson, M., Chun, C., Haaker, P. L., & Hedrick, R. P. (1997). Withering syndrome of the black abalone *Haliotis cracherodii*: water temperature, food availability and parasites as possible causes. *Journal of Shellfish Research*, 16, 403-411.
- Fuentes, J., López, J. L., Mosquera, E., Vázquez, J., Villalba, A., Álvarez, G. (2002). Growth, mortality, pathological conditions and protein expression of *Mytilus edulis* and *M. galloprovincialis* crosses cultured in the Ría de Arousa (NW of Spain). *Aquaculture*, 213, 233-251. [https://doi.org/10.1016/S0044-8486\(02\)00046-7](https://doi.org/10.1016/S0044-8486(02)00046-7)

- Gagnaire, B., Gay, M., Huvet, A., Daniel, J. Y., Saulnier, D., & Renault, T. (2007). Combination of a pesticide exposure and a bacterial challenge: in vivo effects on immune response of Pacific oyster, *Crassostrea gigas* (Thunberg). *Aquatic Toxicology*, 84(1), 92–102. <https://doi.org/10.1016/j.aquatox.2007.06.002>
- Gagnaire, B., Frouin, H., Moreau, K., Thomas-Guyon, H., & Renault, T. (2006). Effects of temperature and salinity on haemocyte activities of the Pacific oyster, *Crassostrea gigas* (Thunberg). *Fish Shellfish Immunology*, 20, 536-547. <https://doi.org/10.1016/j.fsi.2005.07.003>
- Gerdol, M., Gomez-Chiarri, M., Castillo, M. G., Figueras, A., Fiorito, G., Moreira, R., ... & Vasta, G. R. (2018). Immunity in molluscs: recognition and effector mechanisms, with a focus on bivalvia. In: Cooper, E. (ed.) *Advances in Comparative Immunology*. Springer, pp. 225-341. https://doi.org/10.1007/978-3-319-76768-0_11
- Geng, C., Guo, Y., Wang, C., Cui, C., Han, W., Liao, D., & Jiang, P. (2020). Comprehensive evaluation of lipopolysaccharide-induced changes in rats based on metabolomics. *Journal of inflammation research*, 13, 477.
- Genin, A., Levy, L., Sharon, G., Raitsos, D. E., & Diamant, A. (2020). Rapid onsets of warming events trigger mass mortality of coral reef fish. *Proceedings of the National Academy of Sciences*, 117, 25378-25385. <https://doi.org/10.1073/pnas.2009748117>
- Giamberini, L., Auffret, M., & Pihan, J. C. (1996). Haemocytes of the freshwater mussel, *Dreissena polymorpha pallas*: Cytology, cytochemistry and x-ray microanalysis. *Journal of Molluscan Studies*, 62, 367–379. <https://doi.org/10.1093/mollus/62.3.367>
- Goggin, C. L., & Lester, R. J. G. (1995). *Perkinsus*, a protistan parasite of abalone in Australia: a review. *Marine and Freshwater Research*, 46, 639-646. <https://doi.org/10.1071/MF9950639>
- Goggin, C. L., & Lester, R. J. G. (1995). *Perkinsus*, a protistan parasite of abalone in Australia: a review. *Marine and Freshwater Research*, 46(3), 639-646. <https://doi.org/10.1071/MF9950639>
- Gosling, E. (2015). *Marine bivalve molluscs*. John Wiley & Sons.
- Grandiosa, R., Bouwman, M. L., Young, T., Mérien, F., & Alfaro, A. C. (2018). Effect of antiaggregants on the in vitro viability, cell count and stability of abalone (*Haliotis iris*) haemocytes. *Fish & shellfish immunology*, 78, 131-139. <https://doi.org/10.1016/j.fsi.2018.04.038>
- Grandiosa, R., Mérien, F., Pillay, K., & Alfaro, A. C. (2016). Innovative application of classic and newer techniques for the characterization of haemocytes in the New Zealand black-footed abalone (*Haliotis iris*). *Fish Shellfish Immunology*, 48, 175-184. <https://doi.org/10.1016/j.fsi.2015.11.039>
- Grandiosa, R., Mérien, F., Pillay, K., & Alfaro, A. C. (2015). Innovative Application of Classic and Newer Techniques for the Characterization of Haemocytes in the New Zealand black-footed abalone (*Haliotis iris*). *Fish & Shellfish Immunology*, 48, 175-184. <https://doi.org/10.1016/j.fsi.2015.11.039>
- Gregory, M. A., George, R. C., & McClurg, T. P. (1996). The architecture and fine structure of gill filaments in the brown mussel, *Perna perna*. *African Zoology*, 31(4), 193-207.

- Grindley, R. M., Keogh, J. A., & Friedman, C. S. (1998). Shell lesions in New Zealand *Haliotis* spp. (Mollusca, Gastropoda). *Journal of Shellfish Research*, 17, 805-811.
- Goedken, M., & De Guise, S. (2004). Flow cytometry as a tool to quantify oyster defence mechanisms. *Fish & shellfish immunology*, 16(4), 539-552.
- Handler J, Bastianello S, Callinan R, Carson J, Creeper J, Deveney M, et al. (2006). Abalone Aquaculture Subprogram: A National Survey of Diseases of Commercially Exploited Abalone Species to Support Trade and Translocation Issues and the Development of Health Surveillance Programs. Tasmanian Aquaculture and Fisheries Institute, pp. 170.
- Handler, J., Bastianello, S., Callinan, R., Carson, J., Creeper, J., Deveney, M., ... & Stephens, F. (2002). Abalone aquaculture subprogram: A national survey of diseases of commercially exploited abalone species to support trade and translocation issues and the development of health surveillance programs. *FRDC project Report*, 201.
- Handley, S. J. (1995). Spionid polychaetes in Pacific oysters, *Crassostrea gigas* (Thunberg) from Admiralty Bay, Marlborough Sounds, New Zealand. *New Zealand Journal of Marine and Freshwater Research*, 29, 305-309. <https://doi.org/10.1080/00288330.1995.9516665>
- Handley, S. J., & Bergquist, P. R. (1997). Spionid polychaete infestations of intertidal Pacific oysters *Crassostrea gigas* (Thunberg), Mahurangi Harbour, northern New Zealand. *Aquaculture*, 153, 191-205. [https://doi.org/10.1016/S0044-8486\(97\)00032-X](https://doi.org/10.1016/S0044-8486(97)00032-X)
- Hauton, C., Hawkins, L., & Hutchinson, S. (2000). The effects of salinity on the interaction between a pathogen (*Listonella anguillarum*) and components of a host (*Ostrea edulis*) immune system. *Comparative Biochemistry and Physiology, Part B: Biochemistry and Molecular Biology*, 127, 203-212. [https://doi.org/10.1016/S0305-0491\(00\)00251-0](https://doi.org/10.1016/S0305-0491(00)00251-0)
- Hégaret, H., & Wikfors, G. H. (2005). Time-dependent changes in hemocytes of eastern oysters, *Crassostrea virginica*, and northern bay scallops, *Argopecten irradians irradians*, exposed to a cultured strain of *Prorocentrum minimum*. *Harmful Algae*, 4, 187-199. <https://doi.org/10.1016/j.hal.2003.12.004>
- Hégaret, H., Wikfors, G. H., & Soudant, P. (2003). Flow cytometric analysis of haemocytes from eastern oysters, *Crassostrea virginica*, subjected to a sudden temperature elevation: II. Haemocyte functions: aggregation, viability, phagocytosis, and respiratory burst. *Journal of Experimental Marine Biology and Ecology*, 293 (2), 249-265. [https://doi.org/10.1016/S0022-0981\(03\)00235-1](https://doi.org/10.1016/S0022-0981(03)00235-1)
- Hervio, D., Bower, S. M., & Meyer, G. R. (1996). Detection, isolation, and experimental transmission of *Mikrocytos mackini*, a microcell parasite of Pacific oysters *Crassostrea gigas* (Thunberg). *Journal of Invertebrate Pathology*, 67(1), 72-79. <https://doi.org/10.1006/jipa.1996.0011>
- Hervio, D., Bachere, E., Boulo, V., Cochenec, N., Vuillemin, V., Le Coguc, Y., ... & Mialhe, E. (1995). Establishment of an experimental infection protocol for the flat oyster, *Ostrea edulis*, with the intrahaemocytic protozoan parasite, *Bonamia ostreae*: application in the selection of parasite-resistant oysters. *Aquaculture*, 132(3-4), 183-194. [https://doi.org/10.1016/0044-8486\(94\)00342-L](https://doi.org/10.1016/0044-8486(94)00342-L)
- Hine, P. M., Diggles, B. K., Parsons, M. J. D., & Pringles, A. B. B. (2002). The effects of stressors on the dynamics of *Bonamia exitiosus* Hine, Cochenec-Laureau & Berthe, infections in flat oysters *Ostrea chilensis* (Philippi). *Journal of Fish Diseases*, 25, 545-554. <https://doi.org/10.1046/j.1365-2761.2002.00410.x>

- Hine, P. M. (2002a). Severe apicomplexan infection in the oyster *Ostrea chilensis*: a possible predisposing factor in bonamiosis. *Diseases of Aquatic Organisms*, 51, 49-60. <https://doi.org/10.3354/dao051049>
- Hine, P. M. (2002b). Results of a survey on shellfish health in New Zealand in 2000. *Surveillance* 29(1), 3-7. <http://www.sciquest.org.nz/node/47220>
- Hine, P. M., Cochenec-Laureau, N., & Berthe, A. F. (2001). *Bonamia exitiosus* n. sp. (Haplosporidia) infecting flat oysters *Ostrea chilensis* in New Zealand. *Diseases of Aquatic Organisms*, 47(1), 63-72. <http://dx.doi.org/10.3354/dao047063>
- Hine, P. M. (1999). The inter-relationships of bivalve hemocytes. *Fish Shellfish Immunology*, 9, 367-385. <https://doi.org/10.1006/fsim.1998.0205>
- Hine, P. M. (1997). Health status of commercially important molluscs in New Zealand. *Surveillance*, 24(1), 25-28. <http://www.sciquest.org.nz/node/46985> Accessed 17 September 2020.
- Hine, P. M. (1996). The ecology of *Bonamia* and decline of bivalve molluscs. *New Zealand Journal of Ecology*, 20(1): 109-116. <http://www.jstor.org/stable/24053738>
- Hine, P. M., & Wesney, B. (1994). Interaction of phagocytosed *Bonamia* sp. (Haplosporidia) with haemocytes of oysters *Tiostrea chilensis*. *Diseases of aquatic organisms*, 20, 219-229.
- Hine, P. M., & Jones, J. B. (1994). *Bonamia* and other aquatic parasites of importance to New Zealand. *New Zealand Journal of Zoology*, 21(1), 49-56. <https://doi.org/10.1080/03014223.1994.9517975>
- Hine, P. M., Wesney, B., & Hay, B. E. (1992). Herpes viruses associated with mortalities among hatchery-reared Pacific oysters, *Crassostrea gigas*. *Diseases of Aquatic Organisms*, 25, 143-149.
- Hine, P. M. (1991a). The annual pattern of infection by *Bonamia* sp. in New Zealand flat oysters, *Tiostrea chilensis*. *Aquaculture*, 93(3), 241-251. [https://doi.org/10.1016/0044-8486\(91\)90236-Z](https://doi.org/10.1016/0044-8486(91)90236-Z)
- Hine, P. M. (1991b). Ultrastructural observations on the annual infection pattern of *Bonamia* sp. in flat oysters *Tiostrea chilensis*. *Diseases of aquatic organisms*, 11, 163-171.
- Hinzmann, M. F., Lopes-Lima, M., Gonçalves, J., & Machado, J. (2013). Antiaggregant and toxic properties of different solutions on hemocytes of three freshwater bivalves. *Toxicological & Environmental Chemistry*, 95(5), 790-805.
- Hooker, S., & Creese, R. (1995). Reproduction of Paua, *Haliotis iris* Gmelin 1791 (Mollusca: Gastropoda), in North-Eastern New Zealand. *Marine and Freshwater Research*, 46, 617-622. <https://doi.org/10.1071/MF9950617>
- Hooper, C., Day, R., Slocombe, R., Benkendorff, K., Handlinger, J., & Goulias, J. (2014). Effects of severe heat stress on immune function, biochemistry and histopathology in farmed Australian abalone (hybrid *Haliotis laevigata* × *Haliotis rubra*). *Aquaculture*, 432, 26-37. <https://doi.org/10.1016/j.aquaculture.2014.03.032>
- Hooper, C., Hardy-Smith, P., & Handlinger, J. (2007). Ganglioneuritis causing high mortalities in farmed Australian abalone (*Haliotis laevigata* and *Haliotis rubra*). *Australian Veterinary Journal*, 85(5), 188-193. <https://doi.org/10.1111/j.1751-0813.2007.00155.x>

- Hooper, C., Day, R., Slocombe, R., Handler, J., & Benkendorff, K. (2006). Stress and immune responses in abalone: limitations in current knowledge and investigative methods based on other models. *Fish & Shellfish Immunology*, 22, 363-379. <https://doi.org/10.1016/j.fsi.2006.06.009>
- Howard, D. W. (2004). *Histological techniques for marine bivalve mollusks and crustaceans*. NOAA, National Ocean Service, National Centers for Coastal Ocean Service, Center for Coastal Environmental Health and Biomolecular Research, Cooperative Oxford Laboratory. NOAA Technical Memorandum NOS NCCOS, 5, pp218.
- Howard, D. W., Lewis, E. J., Keller, B. J., & Smith, C. S. (2004). Histological techniques for marine bivalve molluscs and crustaceans. NOAA Technical Memorandum NOS NCCOS, 5, 218.
- Howell, M. J. (1963). Preliminary identification made of trematode parasite infecting Foveaux Strait oysters. *New Zealand commercial fishing*, 1(11), 16-18.
- Hu, M., Li, L., Sui, Y., Li, J., Wang, Y., Lu, W., & Dupont, S. (2015). Effect of pH and temperature on antioxidant responses of the thick shell mussel *Mytilus coruscus*. *Fish & shellfish immunology*, 46, 573-583. <https://doi.org/10.1016/j.fsi.2015.07.025>
- Hwang, J. Y., Park, J. J., Yu, H. J., Hur, Y. B., Arzul, I., Couraleau, Y., & Park, M. A. (2013). Ostreid herpes virus 1 infection in farmed Pacific oyster larvae *Crassostrea gigas* (Thunberg) in Korea. *Journal of Fish Diseases*, 36, 969–972. <https://doi.org/10.1111/jfd.12093>
- Jenkins, C., Hick, P., Gabor, M., Spiers, Z., Fell, S. A., Gu, X., . . . Frances, J. (2013). Identification and characterisation of an ostreid herpes virus-1 microvariant (OsHV-1 microvar) in *Crassostrea gigas* (Pacific oysters) in Australia. *Diseases of Aquatic Organisms*, 105(2), 109-126. <https://doi.org/10.3354/dao02623>
- Jenkins, R. J., & Meredyth-young, J. L. (1979). Occurrence of the pacific oyster, *Crassostrea gigas*, off the South Island of New Zealand. *New Zealand Journal of Marine and Freshwater Research*, 13(1), 173–174. <https://doi.org/10.1080/00288330.1979.9515791>
- Jiang, Y., Jiao, H., Sun, P., Yin, F., & Tang, B. (2020). Metabolic response of *Scapharca subcrenata* to heat stress using GC/MS-based metabolomics. *PeerJ*, 8, e8445. <https://doi.org/10.7717/peerj.8445>
- Jones, J., Scotti, P., Dearing, S., & Wesney, B. (1996). Virus-like particles associated with marine mussel mortalities in New Zealand. *Diseases of Aquatic Organisms*, 25, 143-149. <https://doi.org/10.3354/dao025143>
- Jones, J. B. (1981). A new microsporidium from the oyster *Ostrea lutaria* in New Zealand. *Journal of invertebrate pathology*, 38 (1), 67–70. [https://doi.org/10.1016/0022-2011\(81\)90035-5](https://doi.org/10.1016/0022-2011(81)90035-5)
- Jones, J. B. (1975). Studies on animals closely associated with some New Zealand shellfish. Unpublished PhD thesis, pp192, Victoria University, Wellington New Zealand.
- Karp, R. D., & Coffaro, K. A. (1980). Cellular defense systems of the Echinodermata. In: Manning ED, ed. *Phylogeny of Immunological Memory*. Amsterdam, The Netherlands: Elsevier/North Holland, 257-282.
- Karvonen, A., Rintamäki, P., Jokela, J., & Valtonen, E. T. (2010). Increasing water temperature and disease risks in aquatic systems: climate change increases the risk of some, but not all, diseases. *International journal for parasitology*, 40(13), 1483-1488.

- Kesarcodi-Watson, A., Kaspar, H., Lategan, M. J., & Gibson, L. (2009a). Two pathogens of Greenshell™ mussel larvae, *Perna canaliculus*: *Vibrio splendidus* and a *V. coralliilyticus/neptunius*-like isolate. *Journal of fish diseases*, 32(6), 499-507. <https://doi.org/10.1111/j.1365-2761.2009.01006.x>
- Kesarcodi-Watson, A., Kaspar, H., Lategan, M. J., & Gibson, L. F. (2009b). Challenge of New Zealand Greenshell™ mussel *Perna canaliculus* larvae using two *Vibrio* pathogens: a hatchery study. *Diseases of aquatic organisms*, 86(1), 15-20. <https://doi.org/10.3354/dao02100>
- Kim, Y., & Powell, N. E. (2007). Distribution of parasites and pathologies in sentinel bivalves: NOAA status and trends “Mussel Watch” program. *Journal of Shellfish Research*, 26 (4), 1115–1151. [https://doi.org/10.2983/0730-8000\(2007\)26\[1115:DOPAPI\]2.0.CO;2](https://doi.org/10.2983/0730-8000(2007)26[1115:DOPAPI]2.0.CO;2)
- Kim, Y., Powell, E. N., & Ashton-Alcox, K. A. (2006). Histopathology analysis. In: Kim Y, Ashton-Alcox, KA, Powell EN (Eds.), *Histological Techniques for Marine Bivalve Molluscs: Update*, NOAA Technical Memorandum NOS NCCOS 27 pp19–52.
- Kim, Y., & Powell, E. N. (2004). Surfclam histopathology survey along the Delmarva mortality line. *Journal of Shellfish Research*, 23, 429–441. <http://shellfish.org/pubs/jsrtoc/toc.htm>
- Klassen, A., Faccio, A. T., Canuto, G. A. B., da Cruz, P. L. R., Ribeiro, H. C., Tavares, M. F. M., & Sussulini, A. (2017). Metabolomics: definitions and significance in systems biology. *Metabolomics: From Fundamentals to Clinical Applications*, 3-17. https://doi.org/10.1007/978-3-319-47656-8_1
- Kroeck, M. A., & Montes, J. (2005). Occurrence of the haemocyte parasite *Bonamia* sp. in flat oysters *Ostrea puelchana* farmed in San Antonio Bay (Argentina). *Diseases of Aquatic Organisms*, 63(2-3), 231-235. <https://doi.org/10.3354/dao063231>
- Kuchel, R. P., Raftos, D. A., Birch, D., & Vella, N. (2010). Haemocyte morphology and function in the Akoya pearl oyster, *Pinctada imbricata*. *Journal of invertebrate pathology*, 105, 36-48. <https://doi.org/10.1016/j.jip.2010.04.011>
- Lafont, M., Petton, B., Vergnes, A., Pauletto, M., Segarra, A., Gourbal, B., & Montagnani, C. (2017). Long-lasting antiviral innate immune priming in the Lophotrochozoan Pacific oyster, *Crassostrea gigas*. *Scientific reports*, 7(1), 1-14. <https://doi.org/10.1038/s41598-017-13564-0>
- La Peyre, J. F., Schafhauser, D. Y., Rizkalla, E. H., & Faisal, M. (1995). Production of serine proteases by the oyster pathogen *Perkinsus marinus* (Apicomplexa) in vitro. *Journal of Eukaryotic Microbiology*, 42(5), 544-551. <https://doi.org/10.1111/j.1550-7408.1995.tb05903.x>
- Lachambre, S., Day, R., Boudry, P., Huchette, S., Rio-Cabello, A., Fustec, T., & Roussel, S. (2017). Stress response of farmed European abalone reveals rapid domestication process in absence of intentional selection. *Applied Animal Behaviour Science*, 196, 13-21.
- Lallias, D., Arzul, I., Heurtebise, S., Ferrand, S., Chollet, B., Robert, M., ... & Lapègue, S. (2008). *Bonamia ostreae*-induced mortalities in one-year old European flat oysters *Ostrea edulis*: experimental infection by cohabitation challenge. *Aquatic Living Resources*, 21(4), 423-439. <https://doi.org/10.1051/alr:2008053>
- Lane, H. S. (2018). Studies on *Bonamia* parasites (Haplosporidia) in the New Zealand flat oyster *Ostrea chilensis* (Thesis, Doctor of Philosophy). University of Otago. Retrieved from <http://hdl.handle.net/10523/7967>

- Lane, H. S., Webb, S. C., & Duncan, J. (2016). *Bonamia ostreae* in the New Zealand oyster *Ostrea chilensis*: a new host and geographic record for this haplosporidian parasite. *Diseases of Aquatic Organisms*, 118(1), 55-63. <https://doi.org/10.3354/dao02960>
- Lassalle, G., De Montaudouin, X., Soudant, P., & Paillard, C. (2007). Parasite co-infection of two sympatric bivalves, the Manila clam (*Ruditapes philippinarum*) and the cockle (*Cerastoderma edule*) along a latitudinal gradient. *Aquatic Living Resources*, 20(1), 33-42. <https://doi.org/10.1051/alr:2007013>
- Lau, Y. T., Gambino, L., Santos, B., Espinosa, E. P., & Allam, B. (2018). Transepithelial migration of mucosal hemocytes in *Crassostrea virginica* and potential role in *Perkinsus marinus* pathogenesis. *Journal of invertebrate pathology*, 153, 122-129. <https://doi.org/10.1016/j.jip.2018.03.004>
- Le, D. V., Alfaro, A. C., Ragg, N. L., Hilton, Z., Watts, E., & King, N. (2017). Functional morphology and performance of New Zealand geoduck clam (*Panopea zelandica*) larvae reared in a flow-through system. *Aquaculture*, 468, 32-44. <https://doi.org/10.1016/j.aquaculture.2016.09.047>
- Lee, M. K., Cho, B. Y., Lee, S. J., Kang, J. Y., Do Jeong, H., Huh, S. H., & Huh, M. D. (2001). Histopathological lesions of Manila clam, *Tapes philippinarum*, from Hadong and Namhae coastal areas of Korea. *Aquaculture*, 201(3-4), 199-209. [https://doi.org/10.1016/S0044-8486\(01\)00648-2](https://doi.org/10.1016/S0044-8486(01)00648-2)
- Le Gall, G., Bachère, E., & Mialhe, E. (1991). Chemiluminescence analysis of the activity of *Pecten maximus* hemocytes stimulated with zymosan and host-specific Rickettsiales-like organisms. *Diseases of aquatic organisms*, 11, 181-186.
- Lester, R. J. G., & Davis, G. H. G. (1981). A new *Perkinsus* species (Apicomplexa, Perkinsea) from the abalone *Haliotis ruber*. *Journal of Invertebrate Pathology*, 37(2), 181-187. [https://doi.org/10.1016/0022-2011\(81\)90073-2](https://doi.org/10.1016/0022-2011(81)90073-2)
- Li, S., Alfaro, A. C., Nguyen, T. V., Young, T., & Lulijwa, R. (2020). An integrated omics approach to investigate summer mortality of New Zealand Greenshell™ mussels. *Metabolomics*, 16 (9), 100. <https://doi.org/10.1007/s11306-020-01722-x>
- Lester, R. J. G., & Hayward, C. J. (2005). Control of *Perkinsus* disease in abalone. Fisheries Research and Development Corporation Project 2000/151 Final Report. University of Queensland, Brisbane, pp.50.
- Lester, R. J. G., Kleeman, S. N., Barker, S. C., & McCallum, H. I. (2001). Epidemiology of *Perkinsus olseni*, pathogen of abalone. (Abstract). Book of Abstracts, European Association of Fish Pathologists, Tenth International Conference "Diseases of Fish and Shellfish. Trinity College Dublin, Ireland, 9-14 September 2001, pp.O-006.
- Li, X., Li, J., Wang, Y., Fu, L., Fu, Y., Li, B., & Jiao, B. (2011). Aquaculture Industry in China: Current State, Challenges, and Outlook. *Reviews in Fisheries Science*, 19(3), 187–200. <https://doi.org/10.1080/10641262.2011.573597>
- Lin, T., Zhang, D., Lai, Q., Sun M., Quan, W., & Zhou, K. (2014). A modified method to detect the phagocytic ability of eosinophilic and basophilic haemocytes in the oyster *Crassostrea plicatula*. *Fish & Shellfish Immunology*, 40, 337-343. <https://doi.org/10.1016/j.fsi.2014.07.016>
- Liggins, G. W., & Upston, J. (2010). Investigating and managing the *Perkinsus*-related mortality of blacklip abalone in NSW, 184 pp. New South Wales: Industry & Investment

NSW. Final report to the Fisheries Research and Development Corporation, Project No. 2004/084.

Longshaw, M., Feist, S. W., Matthews, R. A., & Figueras, A. (2001). Ultrastructural characterization of *Marteilia* species (Paramyxea) from *Ostrea edulis*, *Mytilusedulis* and *Mytilus galloprovincialis* in Europe. *Diseases of Aquatic Organisms*, 44, 137–142. <http://dx.doi.org/10.3354/dao044137>

López, C., Carballal, M. J., Azevedo, C., & Villalba, A. (1997a). Morphological characterization of the hemocytes of the clam, *Ruditapes decussatus* (Mollusca: Bivalvia). *Journal of Invertebrate Pathology*, 69(1), 51-57. <https://doi.org/10.1006/jipa.1996.4639>

Lopez, C., Carballal, M. J., Azevedo, C., & Villalba, A. (1997b). Enzyme characterisation of the circulating haemocytes of the carpet shell clam, *Ruditapes decussatus* (Mollusca: Bivalvia). *Fish & Shellfish Immunology*, 7(8), 595-608. <https://doi.org/10.1006/fsim.1997.0112>

Lozano-Leon, A., Garcia-Omil, C., Dalama, J., Rodriguez-Souto, R., Martinez-Urtaza, J., & Gonzalez-Escalona, N. (2019). Detection of colistin resistance mcr-1 gene in *Salmonella enterica* serovar Rissen isolated from mussels, Spain, 2012 to 2016. *Eurosurveillance*, 24(16), 1900200.

Lupo, C., Bougeard, S., Le Bihan, V., Blin, J. L., Allain, G., Azéma, P., Benoit, F., Béchemin, C., Bernard, I., & Blachier, P. (2021). Mortality of marine mussels *Mytilus edulis* and *M. galloprovincialis*: Systematic literature review of risk factors and recommendations for future research. *Reviews in Aquaculture*, 13, 504-536. <https://doi.org/10.1111/raq.12484>

Luna-Acosta, A., Breitwieser, M., Renault, T., & Thomas-Guyon, H. (2017). Recent findings on phenoloxidases in bivalves. *Marine Pollution Bulletin*, 122, 5–16.

Luna, L. G. (ed). (1968). Manual of histologic staining methods of the Armed Forces Institute of Pathology, 3rd edn, McGraw-Hill, New York, pp. 38–39.

Mackenzie, C. L., Lynch, S. A., Culloty, S. C., & Malham, S. K. (2014). Future oceanic warming and acidification alter immune response and disease status in a commercial shellfish species, *Mytilus edulis* L. *PLoS One*, 9(6), e99712. <https://doi.org/10.1371/journal.pone.0099712>

Mackin, J. G. (1951). Histopathology of infection of *Crassostrea virginica* (Gmelin) by *Dermocystidium marinum* Mackin, Owen, and Collier. *Bulletin of Marine Science*, 1(1), 72-87.

Mackin, J. G., Owen, H. M., & Collier, A. (1950). Preliminary note on the occurrence of a new protistan parasite, *Dermocystidium marinum* n. sp. in *Crassostrea virginica* (Gmelin). *Science*, 111, 328-329. <https://doi.org/10.1126/science.111.2883.328>

Maedel, L. B., & Doig K. (2012). Examination of the peripheral blood film and correlation with the complete blood count. In: Rodak BF, Fritsma GA, Keohane EM, editors. Hematology clinical principles and applications. 4th ed. China: Elsevier Saunders; pp.197-199.

Malham, S. K., Cotter, E., O'Keeffe, S., Lynch, S., Culloty, S. C., King, J. W., ... & Beaumont, A. R. (2009). Summer mortality of the Pacific oyster, *Crassostrea gigas*, in the Irish Sea: the influence of temperature and nutrients on health and survival. *Aquaculture*, 287(1-2), 128-138. <https://doi.org/10.1016/j.aquaculture.2008.10.006>

Malham, S., Lacoste, A., Gelebart, F., Cueff, A., & Poulet, S. (2003). Evidence for a direct link between stress and immunity in the mollusc *Haliotis tuberculata*. *Journal of*

Experimental Zoology Part A: Comparative Experimental Biology, 295(A), 136–144.
<https://doi.org/10.1002/jez.a.10222>

Malek, J. C., & Byers, J. E. (2018). Responses of an oyster host (*Crassostrea virginica*) and its protozoan parasite (*Perkinsus marinus*) to increasing air temperature. *PeerJ*, 6, e5046.
<https://doi.org/10.7717/peerj.5046>

Martello, L., & Tjeerdema, R. (2001). Combined effects of pentachlorophenol and salinity stress on chemiluminescence activity in two species of abalone. *Aquatic Toxicology*, 51, 351–62. [https://doi.org/10.1016/S0166-445X\(00\)00110-7](https://doi.org/10.1016/S0166-445X(00)00110-7)

Mateo, D. R., Siah, A., Araya, M. T., Berthe, F. C. J., Johnson, G. R., & Greenwood, S. J. (2009). Differential in vivo response of soft-shell clam hemocytes against two strains of *Vibrio splendidus*: Changes in cell structure, numbers and adherence. *Journal of Invertebrate Pathology*, 102, 50-56. <https://doi.org/10.1016/j.jip.2009.06.008>

Matozzo, V., & Bailo, L. (2015). A first insight into haemocytes of the smooth Venus clam *Callista chione*. *Fish & Shellfish Immunology*, 42, 494-502.
<https://doi.org/10.1016/j.fsi.2014.11.034>

Matozzo, V., Chinellato, A., Munari, M., Finos, L., Bressan, M., & Marin, M. G. (2012). First Evidence of Immunomodulation in Bivalves under Seawater Acidification and Increased Temperature. *Plos One*, 7 (3), e33820. <https://doi.org/10.1371/journal.pone.0033820>

Matozzo, V., & Marin, M. G. (2011). Bivalve immune responses and climate changes: is there a relationship? *Invertebrate survival journal*, 8(1), 70-77.

Matozzo, V., & Marin, M. G. (2010). First evidence of gender-related differences in immune parameters of the clam *Ruditapes philippinarum* (Mollusca, Bivalvia). *Marine biology*, 157(6), 1181-1189.

Matozzo, V., Rova, G., & Marin, M. G. (2007). Haemocytes of the cockle *Cerastoderma glaucum*: morphological characterisation and involvement in immune responses. *Fish & shellfish immunology*, 23(4), 732-746. <https://doi.org/10.1016/j.fsi.2007.01.020>

Maynard, J., Van Hooijdonk, R., Harvell, C. D., Eakin, C. M., Liu, G., Willis, B. L., ... & Shields, J. D. (2016). Improving marine disease surveillance through sea temperature monitoring, outlooks and projections. *Philosophical Transactions of the Royal Society B: Biological Sciences*, 371(1689), 20150208.

McGladdery, S. E., Drinnan, R. E., & Stephenson, M. F. (1993). A manual of parasites, pests and diseases of Canadian Atlantic bivalves. Canadian Technical Reports on Fisheries and Aquatic Science No. 1931, pp.121.

McCormick-Ray, M. G., & Howard, T. (1991). Morphology and mobility of oyster hemocytes: evidence for seasonal variations. *Journal of Invertebrate pathology*, 58(2), 219-230. [https://doi.org/10.1016/0022-2011\(91\)90066-](https://doi.org/10.1016/0022-2011(91)90066-)

McLaughlin, S. M., Tall, B. D., Shaheen, A., Elsayed, E. E., & Faisal, M. (2000). Zoosporulation of a new *Perkinsus* species isolated from the gills of a soft-shell clam *Mya arenaria*. *Parasite*, 7, 115-122. <https://doi.org/10.1051/parasite/2000072115>

Michael, K. P., Forman, J., Hulston, D., & Sutherland, J. (2016). A survey of the Foveaux Strait oyster (*Ostrea chilensis*) population (OYU 5) in commercial fishery areas and the status of *Bonamia* (*Bonamia exitiosa*) in February 2016. Report, Ministry of Fisheries.

Millar, R. H. (1963). Oysters killed by Trematode Parasites. *Nature*, 197, 616.
<https://doi.org/10.1038/197616b0>

- Ministry for Primary Industries (2020). <https://www.mpi.govt.nz/dmsdocument/15895-The-Governments-Aquaculture-Strategy-to-2025>
- Mitta, G., Vandenbulcke, F., & Roch, P. (2000). Original involvement of antimicrobial peptides in mussel innate immunity. *Federation of European Biochemical Societies Letters*, 486, 185–190. [https://doi.org/10.1016/S0014-5793\(00\)02192-X](https://doi.org/10.1016/S0014-5793(00)02192-X)
- Mohandas, A., Cheng, T. C., & Cheng, L. B. (1985). Mechanism of lysosomal release from *Mercenaria mercenaria* granulocytes: a scanning electron microscope study. *Journal of invertebrate pathology*, 46, 189–197. [https://doi.org/10.1016/0022-2011\(85\)90148-X](https://doi.org/10.1016/0022-2011(85)90148-X)
- Monari, M., Matozzo, V., Foschi, J., Cattani, O., Serrazanetti, G. P., & Marin, M. G. (2007). Effects of high temperatures on functional responses of haemocytes in the clam *Chamelea gallina*. *Fish & shellfish immunology*, 22(1-2), 98-114. <https://doi.org/10.1016/j.fsi.2006.03.016>
- Montes, J., Anadon, R., & Azevedo, C. (1994). A possible life cycle for *Bonamia ostreae* on the basis of electron microscopy studies. *Journal of Invertebrate Pathology*, 63(1), 1-6. <https://doi.org/10.1006/jipa.1994.1001>
- Mortensen, S., & Glette, J. (1996). Phagocytic activity of scallop (*Pecten maximus*) haemocytes maintained in vitro. *Fish & Shellfish Immunology*, 6(2), 111-121. <https://doi.org/10.1006/fsim.1996.0012>
- Moss, J. A., Xiao, J., Dungan, C. F., & Reece, K. S. (2008). Description of *Perkinsus beihaiensis* n. sp., a new *Perkinsus* sp. parasite in oysters of Southern China. *Journal of Eukaryotic Microbiology*, 55, 117–130. <https://doi.org/10.1111/j.1550-7408.2008.00314.x>
- Moss, J. A., Burrenson, E. M., & Reece, K. S. (2006). Advanced *Perkinsus marinus* infections in *Crassostrea ariakensis* maintained under laboratory conditions. *Journal of Shellfish Research*, 25, 65–72. [https://doi.org/10.2983/0730-8000\(2006\)25\[65:APMIIC\]2.0.CO;2](https://doi.org/10.2983/0730-8000(2006)25[65:APMIIC]2.0.CO;2)
- Moreira, R., Romero, A., Rey-Campos, M., Pereiro, P., Rosani, U., Novoa, B., & Figueras, A. (2020). Stimulation of *Mytilus galloprovincialis* hemocytes with different immune challenges induces differential transcriptomic, miRNomic, and functional responses. *Frontiers in immunology*, 11, 3318. <https://doi.org/10.3389/fimmu.2020.606102>
- Morton, B. (1970). The tidal rhythm and rhythm of feeding and digestion in *Cardium edule*. *Journal of the Marine Biological Association of the United Kingdom*, 50(2), 499-512.
- Moore, J. D., Robbins, T. T., & Friedman, C. S. (2000). Withering syndrome in farmed red abalone *Haliotis rufescens*: thermal induction and association with a gastrointestinal Rickettsiales-like prokaryote. *Journal of Aquatic Animal Health*, 12(1), 26-34. [https://doi.org/10.1577/1548-8667\(2000\)012<0026:WSIFRA>2.0.CO;2](https://doi.org/10.1577/1548-8667(2000)012<0026:WSIFRA>2.0.CO;2)
- Moss, J. A., Burrenson, E. M., & Reece, K. S. (2006). Advanced *Perkinsus marinus* infections in *Crassostrea ariakensis* maintained under laboratory conditions. *Journal of Shellfish Research*, 25, 65–72. [https://doi.org/10.2983/0730-8000\(2006\)25\[65:APMIIC\]2.0.CO;2](https://doi.org/10.2983/0730-8000(2006)25[65:APMIIC]2.0.CO;2)
- Moss, J. A., Xiao, J., Dungan, C. F., & Reece, K. S. (2008). Description of *Perkinsus beihaiensis* n. sp., a new *Perkinsus* sp. parasite in oysters of southern China. *Journal of Eukaryotic Microbiology*, 55, 117–130. <https://doi.org/10.1111/j.1550-7408.2008.00314.x>
- Mourton, C., Boulo, V., Chagot, D., Hervio, D., Bachere, E., Mialhe, E., & Grizel, H. (1992). Interactions between *Bonamia ostreae* (Protozoa: Ascetospora) and hemocytes of *Ostrea edulis* and *Crassostrea gigas* (Mollusca: Bivalvia): in vitro system establishment. *Journal of Invertebrate Pathology*, 59(3), 235-240. [https://doi.org/10.1016/0022-2011\(92\)90127-P](https://doi.org/10.1016/0022-2011(92)90127-P)

- Mouton, A., & Gummow, B. (2011). The occurrence of gut associated parasites in the South African abalone, *Haliotis midae*, in Western Cape aquaculture facilities. *Aquaculture*, 313(1-4), 1-6. <https://doi.org/10.1016/j.aquaculture.2011.01.003>
- Mouritsen, K. N., & Jensen, K. T. (1997). Parasite transmission between soft-bottom invertebrates: temperature mediated infection rates and mortality in *Corophium volutator*. *Marine Ecology Progress Series*, 151, 123-134. <https://doi.org/10.3354/meps151123>
- Munari, M., Matozzo, V., & Marin, M. G. (2011). Combined effects of temperature and salinity on functional responses of haemocytes and survival in air of the clam *Ruditapes philippinarum*. *Fish Shellfish Immunology*, 30, 1024–1030. <https://doi.org/10.1016/j.fsi.2011.01.025>
- Munford, J. G., DaRos, L., & Strada, R. (1981). A study on the mass mortality of mussels in the *Laguna Veneta*. *Journal of the World Mariculture Society*, 12(2), 186-199. <http://dx.doi.org/10.1111/j.1749-7345.1981.tb00294.x>
- Muñoz, P., Meseguer, J., & Esteban, M. Á. (2006). Phenoloxidase activity in three commercial bivalve species. Changes due to natural infestation with *Perkinsus atlanticus*. *Fish & shellfish immunology*, 20, 12-19. <https://doi.org/10.1016/j.fsi.2005.02.002>
- Muznebin, F., Alfaro, A. C., Webb, S. C., & Merien, F. (2022). Characterization of mussel (*Perna canaliculus*) haemocytes and their phagocytic activity across seasons. *Aquaculture Research*. <https://doi.org/10.1111/are.15926>
- Muznebin, F., Alfaro, A. C., & Webb, S. C. (2021). Occurrence of *Perkinsus olseni* and other parasites in New Zealand black-footed abalone (*Haliotis iris*). *New Zealand Journal of Marine and Freshwater Research*, 1-21. <https://doi.org/10.1080/00288330.2021.1984950>
- Nakatsugawa, T., Nagai, T., Hiya, K., Nishizawa, T., & Muroga, K. (1999). A virus isolated from juvenile Japanese black abalone *Nordotis discus discus* affected with amyotrophia. *Diseases of Aquatic Organisms*, 36, 159-161. <https://doi.org/10.3354/dao036159>
- Nakayama, K., Nomoto, A. M., Nishijima, M., & Maruyama, T. (1997). Morphological and Functional Characterization of Hemocytes in the Giant Clam *Tridacna crocea*. *Journal of Invertebrate Pathology*, 69(2), 105-111. <https://doi.org/10.1006/jipa.1996.4626>
- Navas, J. I. (2008). Principales patologías de la almeja fina, *Ruditapes decussatus* (Linnaeus, 1758), del litoral onubense con especial referencia a la parasitosis por *Perkinsus olseni* Lester y Davis, 1981: diagnóstico, transmisión y efectos sobre la almeja PhD. Thesis Dissertation. Universidad de Sevilla.
- Neves, R. A. F., Figueiredo, G. M., Valentin, J. L., da Silva Scardua, P. M., & Hégaret, H. (2015). Immunological and physiological responses of the periwinkle *Littorina littorea* during and after exposure to the toxic dinoflagellate *Alexandrium minutum*. *Aquatic Toxicology*, 160, 96-105. <https://doi.org/10.1016/j.aquatox.2015.01.010>
- Newton, M., & Webb, S. C. (2019). *Summer Mortality of Green-Lipped Mussels 2017-18: A Survey of New Zealand Mussel Farmers* (No. 3258). Cawthron Report. 29 p. plus appendix.
- New Zealand Aquaculture. (2019). <https://www.aquaculture.org.nz/wp-content/uploads/2019/10/New-Zealand-Aquaculture-sector-overview-2019.pdf>
- New Zealand Aquaculture Facts. (2012). Retrieved from <https://www.aquaculture.org.nz/2012/05/29/new-zealand-aquaculture-facts-2012/>

- Nguyen, T. V., & Alfaro, A. C. (2020). Metabolomics investigation of summer mortality in New Zealand Greenshell™ mussels (*Perna canaliculus*). *Fish & Shellfish Immunology*, 106, 783-791. <https://doi.org/10.1016/j.fsi.2020.08.022>.
- Nguyen, T. V., Alfaro, A. C., Merien, F., & Young, T. (2019a). *In vitro* study of apoptosis in mussel (*Perna canaliculus*) haemocytes induced by lipopolysaccharide. *Aquaculture*, 503, 8-15. <https://doi.org/10.1016/j.aquaculture.2018.12.086>
- Nguyen, T. V., Alfaro, A. C., Young, T., & Merien, F. (2019b). Tissue-specific immune responses to *Vibrio* sp. infection in mussels (*Perna canaliculus*): A metabolomics approach. *Aquaculture*, 500, 118-125.
- Nguyen, T. V., & Alfaro, A. C. (2019). Applications of flow cytometry in mollusc immunology: current status and trends. *Fish & Shellfish Immunology*, 94, 239-248.
- Nguyen, T. V., Alfaro, A. C., & Merien, F. (2018a). Omics approaches to investigate host-pathogen interactions in mass mortality outbreaks of *Crassostrea gigas*. *Review in Aquaculture*, 1-17. <https://www.doi.org/10.1111/raq.12294>
- Nguyen, T. V., Alfaro, A. C., Young, T., Ravi, S., & Merien, F. (2018b). Metabolomics study of immune responses of New Zealand greenshell™ mussels (*Perna canaliculus*) infected with pathogenic *Vibrio* sp. *Marine Biotechnology*, 20, 396-409. <https://doi.org/10.1007/s10126-018-9804-x>
- Nguyen, T. V., Alfaro, A. C., Merien, F., Young, T. & Grandiosa, R. (2018c). Metabolic and immunological responses of male and female New Zealand Greenshell™ mussels (*Perna canaliculus*) during *Vibrio* sp. infection. *Journal of Invertebrate Pathology*, 157, 80-89. <https://doi.org/10.1016/j.jip.2018.08.008>
- Nollens, H. H., Keogh, J. A., & Probert, P. K. (2004). Haematological pathology of shell lesions in the New Zealand abalone, *Haliotis iris* (Mollusca: Gastropoda). *Comparative Clinical Pathology*, 12(4), 211-216.
- NZMFA. (2010). New Zealand marine farming association. Online at: <http://www.nzmfa.co.nz>
- Oidtmann, B. C., Thrush, M. A., Denham, K. L., & Peeler, E. J. (2011). International and national biosecurity strategies in aquatic animal health. *Aquaculture*, 320(1-2), 22-33.
- OIE. (2019a). Aquatic Animal Health Code. Chapter 1.3. Diseases listed by the OIE. https://www.oie.int/en/what-we-do/standards/codes-and-manuals/aquatic-code-online-access/?id=169&L=1&htmfile=chapitre_diseases_listed.htm
- OIE. (2019b). Infection with *Perkinsus olseni*. Chapter 2.4.7. Manual of Diagnostic Tests for Aquatic Animals. https://www.oie.int/index.php?id=2439&L=0&htmfile=chapitre_perkinsus_olseni.htm
- OIE. (2018a). Aquatic Animal Health Code, Chapter 1.4. Aquatic Animal Health Surveillance Article 1.4.8. https://www.oie.int/index.php?id=171&L=0&htmfile=chapitre_aqua_ani_surveillance.htm Accessed 20 February 2019.
- OIE. (2018b). Aquatic Animal Health Code Chapter 1.5 Criteria for listing species as susceptible to infection with a specific pathogen. <https://www.oie.int/standard-setting/aquatic-code/>

- OIE. (2017). Quarterly aquatic animal disease report (Asia and Pacific Region) October – December 2017. <https://rr-asia.oie.int/wp-content/uploads/2019/09/qaad-2017-4q.pdf>
- OIE. (2016). Manual of Diagnostic Tests for Aquatic Animals. Aquatic Manual 7th Edition, 2016, pp.589. <https://www.oie.int/standard-setting/aquatic-manual/>
- OIE. (2014). Chapter 5.1. General obligations related to certification. In: Aquatic Animal Health Code. Accessed 7 September 2016. <https://www.oie.int/doc/ged/D13873.PDF>
- OIE. (2012). Infection with *Bonamia ostreae*. Manual of Diagnostic Tests for Aquatic Animals. Chapter 2.4.3.
- OIE. (2000). Diagnostic Manual for Aquatic Diseases, 3rd edition 2000, pp. 237.
- Oliver, L. M., & Fisher, W. S. (1999). Appraisal of perspective bivalve immune markers. *Biomarkers*, 4, 510-530. <https://doi.org/10.1080/135475099230679>
- Ottaviani, E. (2006). Molluscan immune recognition. *Invertebrate Survival Journal*, 3(1), 50-63.
- Pampanin, D. M., Marin, M. G., & Ballarin, L. (2002). Morphological and cytoenzymatic characterization of haemocytes of the venus clam *Chamelea gallina*. *Diseases of aquatic organisms*, 49(3), 227-234.
- Pankhurst, N. W., & Van Der Kraak, G. (2000). Evidence that acute stress inhibits ovarian steroidogenesis in rainbow trout *in vivo*, through the action of cortisol. *General and comparative endocrinology*, 117(2), 225-237.
- Pang, Z., Chong, J., Zhou, G., De Lima Morais, D. A., Chang, L., Barrette, M., Gauthier, C., Jacques, P.-É., Li, S., & Xia, J. (2021). MetaboAnalyst 5.0: narrowing the gap between raw spectra and functional insights. *Nucleic acids research*, 49 (W1), 388–396. <https://doi.org/10.1093/nar/gkab382>
- Parisi, M.-G., Li, H., Jouvét, L. B., Dyrinda, E. A., Parrinello, N., Cammarata, M., & Roch, P. (2008). Differential involvement of mussel hemocyte sub-populations in the clearance of bacteria. *Fish & shellfish immunology*, 25, 834-840. <https://doi.org/10.1016/j.fsi.2008.09.005>
- Parusel, R., Steimle, A., Lange, A., Schäfer, A., Maerz, J. K., Bender, A., & Frick, J.-S. (2017). An important question: Which LPS do you use? *Virulence*, 8, 1890-1893. <https://doi.org/10.1080/21505594.2017.1361100>
- Park, K. I., Donaghy, L., Kang, H. S., Hong, H. K., Kim, Y. O., & Choi, K. S. (2012). Assessment of immune parameters of Manila clam *Ruditapes philippinarum* in different physiological conditions using flow cytometry. *Ocean Science Journal*, 47(1), 19-26. <https://doi.org/10.1007/s12601-012-0002-x>
- Park, K. I., Tsutsumi, H., Hong, J. S., & Choi, K. S. (2008). Pathology survey of the short-neck clam *Ruditapes philippinarum* occurring on sandy tidal flats along the coast of Ariake Bay, Kyushu, Japan. *Journal of invertebrate pathology*, 99(2), 212-219. <https://doi.org/10.1016/j.jip.2008.06.004>
- Park, K.I., & Choi, K.S. (2001). Spatial distribution of the protozoan parasite, *Perkinsus* sp., found in the Manila clams, *Ruditapes philippinarum* in Korea. *Aquaculture*, 203, 9-22. [https://doi.org/10.1016/S0044-8486\(01\)00619-6](https://doi.org/10.1016/S0044-8486(01)00619-6)

- Park, K. I., Choi, K. S., & Choi, J. W. (1999). Epizootiology of *Perkinsus* sp. found in the Manila clam, *Ruditapes philippinarum* in Komsoe Bay, Korea. *Korean Journal of Fisheries and Aquatic Sciences*, 32(3), 303-309.
- Peeler, E. J., Reese, R. A., Cheslett, D. L., Geoghegan, F., Power, A., & Thrush, M. A. (2012). Investigation of mortality in Pacific oysters associated with Ostreid herpes virus-1 μ Var in the Republic of Ireland in 2009. *Preventive Veterinary Medicine*, 105, 136–143. <http://dx.doi.org/10.1016/j.prevetmed.2012.02.001>.
- Perkins, F. O. (1996). The structure of *Perkinsus marinus* (Mackin, Owen and Collier, 1950) Levine, 1978 with comments on taxonomy and phylogeny of *Perkinsus* spp. *Journal of Shellfish Research*, 15(1), 67.
- Perrigault, M., Dahl, S. F., Espinosa, E. P., & Allam, B. (2012). Effects of salinity on hard clam (*Mercenaria mercenaria*) defense parameters and QPX disease dynamics. *Journal of Invertebrate Pathology*, 110 (1), 73-82. <https://doi.org/10.1016/j.jip.2012.02.004>
- Perrigault, M., Dahl, S. F., Espinosa, E. P., Gambino, L., & Allam, B. (2011). Effects of temperature on hard clam (*Mercenaria mercenaria*) immunity and QPX (Quahog Parasite Unknown) disease development: II. Defense parameters. *Journal of invertebrate pathology*, 106(2), 322-332. <https://doi.org/10.1016/j.jip.2010.11.004>
- Perazzolo, L. M., Gargioni, R., Ogliari, P., & Barracco, M. A. (2002). Evaluation of some hemato-immunological parameters in the shrimp *Farfantepenaeus paulensis* submitted to environmental and physiological stress. *Aquaculture*, 214, 19–33.
- Pichot, Y., Comps, M., Tige, G., Grizel, H., & Rabouin, M. A. (1979). Recherches sur *Bonamia ostreae* gen. n., sp. n., parasite nouveau de l'huître plate *Ostrea edulis* L. *Revue des Travaux de l'Institut des Pêches Maritimes*, 43(1), 131-140.
- Pipe, R. K., Farley, S. R., & Coles, J. A. (1997). The separation and characterisation of haemocytes from the mussel *Mytilus edulis*. *Cell and Tissue Research*, 289, 537-545. <https://doi.org/10.1007/s004410050899>
- Poder, M., Cahour, A., & Balouet, G. (1983). Etudes histologiques et ultrastructurales des lésions de parasitose hemocytaire chez *Ostrea edulis*. *Comptes Rendus Mathématiques des l'Académie des Sciences*, 107(2), 175-186.
- Portela, J., Duval, D., Rognon, A., Galinier, R., Boissier, J., Coustau, C., Mitta, G., Théron, A., & Gourbal, B. (2013). Evidence for Specific Genotype-Dependent Immune Priming in the Lophotrochozoan *Biomphalaria glabrata* Snail. *Journal of Innate Immunity*, 5, 261-276. <https://doi.org/10.1159/000345909>
- Poulin, R. (2006). Global warming and temperature-mediated increases in cercarial emergence in trematode parasites. *Parasitology*, 132(1), 143-151.
- Prado-Álvarez, M., Romero, A., Balseiro, P., Dios, S., Novoa, B., & Figueras, A. (2012). Morphological characterization and functional immune response of the carpet shell clam (*Ruditapes decussatus*) haemocytes after bacterial stimulation. *Fish & Shellfish Immunology*, 32, 69-78. <https://doi.org/10.1016/j.fsi.2011.10.019>
- Prado, S., Dubert, J., da Costa, F., Martínez-Patiño, D., & Barja J. L. (2014). Vibrios in hatchery cultures of the razor clam, *Solen marginatus* (Pulteney). *Journal of Fish Diseases*, 37, 209–217. <https://doi.org/10.1111/jfd.12098>

- Pretto, T., Zambon, M., Civettini, M., Caburlotto, G., Boffo, L., Rossetti, E., & Arcangeli, G. (2014). Massive mortality in Manila clams (*Ruditapes philippinarum*) farmed in the Lagoon of Venice, caused by *Perkinsus olseni*. *Bulletin- European Association of Fish Pathologists*, 34(2), 43-53.
- Pruzzo, C., Gallo, G., & Canesi, L. (2005). Persistence of vibrios in marine bivalves: the role of interactions with hemolymph components. *Environmental microbiology*, 7, 761–772. <https://doi.org/10.1111/j.1462-2920.2005.00792.x>
- Quick, J. A., & Mackin, J. G. (1971). Oyster parasitism by *Labyrinthomyxa marina* in Florida. Fl. Dept. Nat. Resour. Marine Research Laboratory Professional Paper Series, 13, 1-55.
- Rahman, M. A., Henderson, S., Miller-Ezzy, P., Li, X. X., & Qin, J. G. (2019). Immune response to temperature stress in three bivalve species: Pacific oyster *Crassostrea gigas*, Mediterranean mussel *Mytilus galloprovincialis* and mud cockle *Katylusia rhytiphora*. *Fish & shellfish immunology*, 86, 868-874. <https://doi.org/10.1016/j.fsi.2018.12.017>
- Rajalakshmi, S., & Mohandas, A. (2005). Copper-induced changes in tissue enzyme activity in a freshwater mussel. *Ecotoxicology and Environmental Safety*, 62, 140–143. <https://doi.org/10.1016/j.ecoenv.2005.01.003>
- Ramilo, A., Navas, J. I., Villalba, A., & Abollo, E. (2013). Species-specific diagnostic assays for *Bonamia ostreae* and *B. exitiosa* in European flat oyster *Ostrea edulis*: conventional, real-time and multiplex PCR. *Diseases of aquatic organisms*, 104(2), 149-161.
- Ramilo, A., Carrasco, N., Reece, K. S., Valencia, J. M., Grau, A., Aceituno, P., ... & Villalba, A. (2015). Update of information on perkinsosis in NW Mediterranean coast: Identification of *Perkinsus* spp. (Protista) in new locations and hosts. *Journal of invertebrate pathology*, 125, 37-41. <https://doi.org/10.1016/j.jip.2014.12.008>
- Rasband, W. S. Image J, U. S. National Institutes of Health, Bethesda, Maryland, USA.
- Ray, A., Gautam, A., Das, S., Pal, K., Das, S., Karmakar, P., Ray, M., & Ray, S. (2020). Effects of copper oxide nanoparticle on gill filtration rate, respiration rate, hemocyte associated immune parameters and oxidative status of an Indian freshwater mussel. *Comparative Biochemistry and Physiology Part C: Toxicology & Pharmacology*, 237, 108855. <https://doi.org/10.1016/j.cbpc.2020.108855>
- Ray, S. M. (1954). *Biological studies of Dermocystidium marinum, a fungus parasite of oysters*. Rice University (Doctoral dissertation).
- Reece, K. S., & Stokes, N. A. (2003). Molecular analysis of a haplosporidian parasite from cultured New Zealand abalone *Haliotis iris*. *Diseases of Aquatic Organisms*, 63, 61-66. <https://doi.org/10.3354/dao053061>
- Renault, T., & Novoa, B. (2004). Viruses infecting bivalve molluscs. *Aquatic Living Resources*, 17, 397–409. <https://doi.org/10.1051/alr:2004049>
- Renwrandt, L., Siegmund, E., & Woldmann, M. (2013). Variations in hemocyte counts in the mussel, *Mytilus edulis*: Similar reaction patterns occur in disappearance and return of molluscan hemocytes and vertebrate leukocytes. *Comparative Biochemistry and Physiology Part A: Molecular & Integrative Physiology*, 164, 629-637. <https://doi.org/10.1016/j.cbpa.2013.01.021>
- Robledo, D., Ronza, P., Harrison, P. W., Losada, A. P., Bermúdez, R., Pardo, B. G., María José Redondo, M. J., Sitjà-Bobadilla, A., Quiroga, M. I., & Martínez, P. (2014). RNA-seq

- analysis reveals significant transcriptome changes in turbot (*Scophthalmus maximus*) suffering severe enteromyxosis. *BMC Genomics*, *15*, 1149-1166.
<https://doi.org/10.1186/1471-2164-15-1149>
- Robledo, J. A. F., Santarém, M. M., & Figueras, A. (1994). Parasite loads of rafted blue mussels (*Mytilus galloprovincialis*) in Spain with special reference to the copepod, *Mytilicola intestinalis*. *Aquaculture*, *127*, 287–302. [https://doi.org/10.1016/0044-8486\(94\)90232-1](https://doi.org/10.1016/0044-8486(94)90232-1)
- Rodgers, C. J., Carnegie, R. B., Chávez-Sánchez, M. C., Martínez-Chávez, C. C., Nozal, M. F., & Hine, P. M. (2015). Legislative and regulatory aspects of molluscan health management. *Journal of invertebrate pathology*, *131*, 242-255.
<https://doi.org/10.1016/j.jip.2015.06.008>
- Rolton, A., & Ragg, N. L. (2020). Green-lipped mussel (*Perna canaliculus*) hemocytes: A flow cytometric study of sampling effects, sub-populations and immune-related functions. *Fish & shellfish immunology*, *103*, 181-189. <https://doi.org/10.1016/j.fsi.2020.05.019>
- Rolton, A., Webb, S. C., & Lopez San Martin, M. (2019). Digestive epithelial virosis (DEV) in bivalves: a review. Cawthron Report No. 3249, pp. 25.
- Roque, A., Carrasco, N., Andree, K. B., Lacuesta, B., Elandaloussi, L., Gairin, I., Rodgers, C. J., & Furones, M. D. (2012). First report of OsHV-1 microvar in Pacific oyster (*Crassostrea gigas*) cultured in Spain. *Aquaculture*, *324–325*, 303-306.
<http://dx.doi.org/10.1016/j.aquaculture.2011.10.018>
- Rowley, A., & Powell, A. (2007). Invertebrate immune systems—specific, quasi-specific, or nonspecific? *The Journal of Immunology*, *179*, 7209-7214.
<https://doi.org/10.4049/jimmunol.179.11.7209>
- Russell-Pinto, F., Reimão, R., & de Sousa, M. (1994). Haemocytes in *Cerastoderma edule* (Mollusca, Bivalvia): distinct cell types engage in different responses to sheep erythrocytes. *Fish & Shellfish Immunology*, *4*(5), 383-397. <https://doi.org/10.1006/fsim.1994.1033>
- Ryder, J., Wells, R., & Baldwin, J. (1994). Tauropine and D-lactate as indicators of recovery of live Pāua (New Zealand abalone) (*Haliotis iris*) from handling stress, and post- mortem quality. *Food Australia*, *46*, 523-526.
- Sagrìstà, E., Durfort, M., & Azevedo, C. (1995). *Perkinsus* sp. (Phylum Apicomplexa) in Mediterranean clam *Ruditapes semidecussatus*: ultrastructural observations of the cellular response of the host. *Aquaculture*, *132*, 153-160. [https://doi.org/10.1016/0044-8486\(94\)00391-Z](https://doi.org/10.1016/0044-8486(94)00391-Z)
- Sahaphong, S., Linthong, V., Wanichanon, C., Riengrojpitak, S., Kangwanrangsan, N., Viyanant, V., Upatham, E. S., Pumthong, T., Chansue, N., & Sobhon, P. (2001). Morpho functional study of the haemocytes of *Haliotis asinina*. *Journal of Shellfish Research*, *20*, 711-716.
- Salinger, M. J., Renwick, J., Behrens, E., Mullan, A. B., Diamond, H. J., Sirguey, P., Smith, R. O., Trought, M. C., Cullen, N. J., & Fitzharris, B. B. (2019). The unprecedented coupled ocean-atmosphere summer heatwave in the New Zealand region 2017/18: drivers, mechanisms and impacts. *Environmental Research Letters*, *14*, 044023.
- Sánchez-Martínez, J. G., Aguirre-Guzmán, G., & Mejía-Ruíz, H. (2007). White spot syndrome virus in cultured shrimp: A review. *Aquaculture Research*, *38* (13), 1339-1354.
<https://doi.org/10.1111/j.1365-2109.2007.01827.x>

- Schmitt, P., Duperthuy, M., Montagnani, C., Bachère, E., & Destoumieux-Garzón, D. (2012). “Immune responses in the Pacific oyster *Crassostrea gigas* an overview with focus on summer mortalities,” in *Oysters Physiology, Ecological Distribution and Mortality*, ed. J. Qin (New York: Nova Science Publishers, Inc.).
- Segarra, A., Pepin, J. F., Arzul, I., Morga, B., Faury, N., & Renault, T. (2010). Detection and description of a particular Ostreid herpes virus 1 genotype associated with massive mortality outbreaks of Pacific oysters, *Crassostrea gigas*, in France in 2008. *Virus Research*, 153, 92–99. <http://dx.doi.org/10.1016/j.virusres.2010.07.011>
- Seafood New Zealand (2016). New Zealand Seafood Exports, Report 7, Seafood exports by product type Calendar year to December 2016 (final). <https://www.seafood.org.nz/publications/export-information/2016>
- Stentiford, G. D., Neil, D. M., Peeler, E. J., Shields, J. D., Small, H. J., Flegel, T. W., ... & Lightner, D. V. (2012). Disease will limit future food supply from the global crustacean fishery and aquaculture sectors. *Journal of invertebrate pathology*, 110(2), 141-157.
- Sheehan, D., & Mcdonagh, B. (2008). Oxidative stress and bivalves: a proteomic approach. *Invertebrate Survival Journal*, 5, 110-123.
- Shibl, A. A., Isaac, A., Ochsenkühn, M. A., Cárdenas, A., Fei, C., Behringer, G., Arnoux, M., Drou, N., Santos, M. P., Gunsalus, K. C., & Woolstra, C. R. (2020). Diatom modulation of microbial consortia through use of two unique secondary metabolites. *bioRxiv*, 117(44), 27445–27455. <https://doi.org/10.1101/2020.06.11.144840>
- Shu, W., Wang, S. H., Wang, Y. L., & Zhang, Z. P. (2009). Phenoloxidase in mollusca and crustacean. *Chinese Journal of Zoology*, 44 (5), 137-146.
- Smart, K. F., Aggio, R. B., Van Houtte, J. R., & Villas-Bôas, S. G. (2010). Analytical platform for metabolome analysis of microbial cells using methyl chloroformate derivatization followed by gas chromatography–mass spectrometry. *Nature protocols*, 5, 1709-1729. <https://doi.org/10.1038/nprot.2010.108>
- Smith, P. J., & Conroy, A. M. (1992). Loss of genetic variation in hatchery produced abalone, *Haliotis iris*. *New Zealand Journal of Marine and Freshwater Research*, 26, 81-85. <https://doi.org/10.1080/00288330.1992.9516503>
- Smolowitz, R., & Shumway, S. E. (1997). Possible cytotoxic effects of the dinoflagellate, *Gyrodinium aureolum*, on juvenile bivalve molluscs. *Aquaculture International*, 5(4), 291-300. <https://doi.org/10.1023/A:1018355905598>
- Soudant, P., Chu, F. L. E., & Volety, A. (2013). Host–parasite interactions: Marine bivalve molluscs and protozoan parasites, Perkinsus species. *Journal of invertebrate pathology*, 114(2), 196-216. <https://doi.org/10.1016/j.jip.2013.06.001>
- Song, L., Wang, L., Qiu, L., & Zhang, H. (2010). Bivalve Immunity. In: Söderhäll, K. (ed.) *Invertebrate Immunity*. Boston, MA: Springer. 44-65.
- Soares-da-Silva, I. M., Ribeiro, J., Valongo, C., Pinto, R., Vilanova, M., Bleher, R., & Machado, J. (2002). Cytometric, morphologic and enzymatic Characterisation of haemocytes in *Anodonta cygnea*. *Comparative Biochemistry and Physiology - Part A: Molecular & Integrative Physiology Special Issues*, 132, 541–553. [https://doi.org/10.1016/S1095-6433\(02\)00039-9](https://doi.org/10.1016/S1095-6433(02)00039-9)

- Sparks, A. K. (1972). Invertebrate pathology, non communicable diseases. London, UK: Academic Press.
- Stillman, J. H. (2019). Heat waves, the new normal: summer time temperature extremes will impact animals, ecosystems, and human communities. *Physiology*, *34*, 86-100. <https://doi.org/10.1152/physiol.00040.2018>
- Stentiford, G. D., Sritunyaluksana, K., Flegel, T. W., Williams, B. A., Withyachumnarnkul, B., Itsathitphaisarn, O., & Bass, D. (2017). New paradigms to help solve the global aquaculture disease crisis. *PLoS pathogens*, *13*(2), e1006160. <https://doi.org/10.1371/journal.ppat.1006160>
- Stokes, N. A., & Burreson, E. M. (1995). A sensitive and specific DNA probe for the oyster pathogen *Haplosporidium nelsoni*. *Journal of Eukaryotic Microbiology*, *42*(4), 350-357.
- Sunila, I., & Lindström, R. (1985). The structure of the interfilamentar junction of the mussel (*Mytilus edulis* L.) gill and its uncoupling by copper and cadmium exposures. *Comparative Biochemistry and Physiology Part C: Comparative Pharmacology*, *81*(2), 267-272.
- Suong, N. T., Banks, J. C., Fidler, A., Jeffs, A., Wakeman, K. C., & Webb, S. (2019). PCR and histology identify new bivalve hosts of Apicomplexan-X (APX), a common parasite of the New Zealand flat oyster *Ostrea chilensis*. *Diseases of Aquatic Organisms*, *132* (3), 181–189. <https://doi.org/10.3354/dao03318>
- Suong, N. T. (2018). Molecular detection of the apicomplexan parasite ‘X’ (APX) in bivalves in New Zealand. PhD thesis.
- Suong, N. T., Banks, J. C., Webb, S. C., Jeffs, A., Wakeman, K. C., & Fidler, A. (2018). PCR test to specifically detect the apicomplexan ‘X’ (APX) parasite found in flat oysters *Ostrea chilensis* in New Zealand. *Diseases of aquatic organisms*, *129*(3), 199-205. <https://doi.org/10.3354/dao03244>
- Soudant, P., Paillard, C., Choquet, G., Lambert, C., Reid, H. I., Marhic, A., ... & Birkbeck, T. H. (2004). Impact of season and rearing site on the physiological and immunological parameters of the Manila clam *Venerupis* (= *Tapes*, = *Ruditapes*) philippinarum. *Aquaculture*, *229*(1-4), 401-418.
- Suzuki, T., & Mori, K. (1990). Hemolymph lectin of the pearl oyster, *Pinctada fucata martensii*: a possible non-self recognition system. *Developmental & Comparative Immunology*, *14*(2), 161-173.
- Svärdh, L. (1999). Bacteria, granulocytomas, and trematode metacercariae in the digestive gland of *Mytilus edulis*: seasonal and inter population variation. *Journal of Invertebrate Pathology*, *74*, 275–280. <https://doi.org/10.1006/jipa.1999.4880>
- Symonds, J. E., Clarke, S. M., King, N., Walker, S. P., Blanchard, B., Sutherland, D., Roberts, R., Preece, M. A., Tate, M., & Buxton, P. (2019). Developing successful breeding programs for New Zealand aquaculture: a perspective on progress and future genomic opportunities. *Frontiers in genetics*, *10*, 27. <https://doi.org/10.3389/fgene.2019.00027>
- Tame, A., Yoshida, T., Ohishi, K., & Maruyama, T. (2015). Phagocytic activities of hemocytes from the deep-sea symbiotic mussels *Bathymodiolus japonicus*, *B. platifrons*, and *B. septemdiarum*. *Fish Shellfish Immunology*, *45*, 146-156.

- Tiscar, P., & Mosca, F. (2004). Defense mechanisms in farmed marine molluscs. *Veterinary Research Communications*, 28, 57-62.
- Travers, M. A., Miller, K. B., Roque, A., & Friedman, C. S. (2015). Bacterial diseases in marine bivalves. *Journal of invertebrate pathology*, 131, 11-31. <https://archimer.ifremer.fr/doc/00274/38532/37049.pdf>
- Travers, M., Le Goïc, N., Huchette, S., Koken, M., & Paillard, C. (2008). Summer immune depression associated with increased susceptibility of the European abalone, *Haliotis tuberculata* to *Vibrio harveyi* infection. *Fish & Shellfish Immunology*, 25, 800-808. <https://doi.org/10.1016/j.fsi.2008.08.003>
- Tripp, M. R. (1992). Phagocytosis by hemocytes of the hard clam, *Mercenaria mercenaria*. *Journal of invertebrate pathology*, 59(3), 222-227. [https://doi.org/10.1016/0022-2011\(92\)90125-N](https://doi.org/10.1016/0022-2011(92)90125-N)
- Uddin, M. J., Yang, H. S., Choi, K. S., Kim, H. J., Hong, J. S., & Cho, M. (2010). Seasonal changes in *Perkinsus olseni* infection and gametogenesis in Manila clam, *Ruditapes philippinarum*, from Seonjaedo Island in Incheon, off the west coast of Korea. *Journal of the World Aquaculture Society*, 41, 93-101. <https://doi.org/10.1111/j.1749-7345.2009.00337.x>
- Usheva, L. N., Vaschenko, M. A., & Durkina, V. B. (2006). Histopathology of the digestive gland of the bivalve mollusk *Crenomytilus grayanus* (Dunker, 1853) from southwestern Peter the Great Bay, Sea of Japan. *Russian Journal of Marine Biology*, 32(3), 166-172. <https://doi.org/10.1134/S1063074006030047>
- Vaillant, G. E. (2001). Defense Mechanisms. In: Smelser, N. J. & Baltes, P. B. (eds.) International Encyclopedia of the Social & Behavioral Sciences. Oxford: Pergamon. 3355-3359.
- Vakalia, S., & Benkendorff, K. (2005). Antimicrobial activity in the haemolymph of *Haliotis laevigata* and the effects of a dietary immunostimulant, A. Fleming (Ed). The 12th Annual Abalone Aquaculture Workshop, Abalone Aquaculture Subprogram, Fisheries Research and Development Corporation, Canberra, Australia, Mc Larren Vale, South of Australia.
- Vargas-Albores, F., & Ochoa, J. (1992). Variation of pH, osmolality, sodium and potassium concentrations in the haemolymph of sub-adult blue shrimp (Ps) according to size. *Comparative Biochemistry and Physiology Part A: Physiology*, 102, 1-5.
- Van Nguyen, T., Alfaro, A. C., Young, T., Green, S., Zarate, E., & Merien, F. (2019). Itaconic acid inhibits growth of a pathogenic marine *Vibrio* strain: A metabolomics approach. *Scientific reports*, 9(1), 1-9. <https://doi.org/10.1038/s41598-019-42315-6>
- Venter, L., Mienie, L. J., Vosloo, A., Loots, D. T., Jansen Van Rensburg, P., & Lindeque, J. Z. (2019). Effect of proline-enriched abalone feed on selected metabolite levels of slow-growing adult *Haliotis midae*. *Aquaculture Research*, 50, 1057-1067. <https://doi.org/10.1111/are.13978>
- Venter, L., Loots, D. T., Vosloo, A., Jansen Van Rensburg, P., & Lindeque, J. Z. (2018). Abalone growth and associated aspects: now from a metabolic perspective. *Reviews in Aquaculture*, 10, 451-473. <https://doi.org/10.1111/raq.12181>
- Viergutz, C., Linn, C., & Weitere, M. (2012). Intra-and interannual variability surpasses direct temperature effects on the clearance rates of the invasive clam *Corbicula fluminea*. *Marine Biology*, 159(11), 2379-2387. <https://doi.org/10.1007/s00227-012-1902-0>

- Villalba, A., Gestal, C., Casas, S. M., & Figueras, A. (2011). Perkinsosis en moluscos. *Figueras A, Novoa B. Enfermedades de moluscos bivalvos de interés en acuicultura. Madrid: Fundación Observatorio Español de Acuicultura*, Madrid, pp. 181-242.
- Villalba, A., Casas, S. M., López, C., & Carballal, M. J. (2005). Study of perkinsosis in the carpet shell clam *Tapes decussatus* in Galicia (NW Spain). II. Temporal pattern of disease dynamics and association with clam mortality. *Diseases of aquatic organisms*, 65(3), 257-267. <https://doi.org/10.3354/dao065257>
- Villalba, A., Reece, K. S., Ordás, M. C., Casas, S. M., & Figueras, A. (2004). Perkinsosis in molluscs: a review. *Aquatic living resources*, 17(4), 411-432. <https://doi.org/10.1051/alr:2004050>
- Villalba, A., Mourelle, S. G., Carballal, M. J., & Lopez, C. (1997). Symbionts and diseases of farmed mussels *Mytilus galloprovincialis* throughout the culture process in the Rias of Galicia (NW Spain). *Diseases of Aquatic Organisms*, 31, 127-139. <https://doi.org/10.3354/dao031127>
- Wang, Y., Hu, M., Chiang, M. W. L., Shin, P. K. S., & Cheung, S. G. (2012). Characterization of subpopulations and immune-related parameters of hemocytes in the green-lipped mussel *Perna viridis*. *Fish & shellfish immunology*, 32(3), 381-390. <https://doi.org/10.1016/j.fsi.2011.08.024>
- Webb, S. C., & Duncan, J. (2019). New Zealand shellfish health monitoring 2007 to 2017: insights and projections. Prepared for the Ministry of Business, Innovation and Employment (MBIE). Cawthron Report No. 2568, pp. 67, plus appendices.
- Webb, S. C. (2013). Assessment of pathology threats to the New Zealand Shellfish industry. Prepared for Ministry of Science and Innovation, Programme CAWX0802. Cawthron Report No. 1334, pp. 69, plus appendices.
- Webb, S. C. (2012). Studies on ostreid herpes virus-1: a causal agent implicated in summer mortality in the oyster *Crassostrea gigas* by PCR of archival histological specimens. Cawthron Report, 2093, 5.
- Webb, S. C. (2008). Pathogens and parasites of the mussels *Mytilus galloprovincialis* and *Perna canaliculus*: Assessment of threats face by New Zealand aquaculture. Cawthron Report No.1334, pp. 28.
- Webb, S. C., Fidler, A., & Renault, T. (2007). Primers for PCR-based detection of ostreid herpes virus-1 (OsHV-1): application in a survey of New Zealand molluscs. *Aquaculture*, 272, 126-139. <https://doi.org/10.1016/j.aquaculture.2007.07.224>
- Webb, S. C. (1999). Aspects of stress with particular reference to mytilid mussels and their parasites. Unpublished PhD Thesis, University of Cape Town, pp. 472.
- Weddeburn, J., Mcfadzen, I., Sanger, R., Beesley, A., Heath, C., Hornsby, M., & Lowe, D. (2000). The field application of cellular and physiological biomarkers, in the mussel *Mytilus edulis*, in conjunction with early life stage bioassays and adult histopathology. *Marine Pollution Bulletin*, 40, 257-267. [https://doi.org/10.1016/S0025-326X\(99\)00214-3](https://doi.org/10.1016/S0025-326X(99)00214-3)
- Wendling, C. C., Batista, F. M., & Wegner, K. M. (2014). Persistence, seasonal dynamics and pathogenic potential of *Vibrio* communities from Pacific oyster hemolymph. *PLoS One*, 9(4), e94256.

- Wilson-Ormond, E. A., Ellis, M. S., Powell, E. N., Kim, Y., & Li, S. I. (2000). Effects of Gas-Producing Platforms on Continental Shelf Megafauna in the Northwest Gulf of Mexico: Reproductive Status and Health. *International Review of Hydrobiology: A Journal Covering all Aspects of Limnology and Marine Biology*, 85(2-3), 293-323. [https://doi.org/10.1002/\(SICI\)1522-2632\(200004\)85:2/3<293::AID-IROH293>3.0.CO;2-U](https://doi.org/10.1002/(SICI)1522-2632(200004)85:2/3<293::AID-IROH293>3.0.CO;2-U)
- Winstead, J. T. (1998). A histological study of digestive tubules in intertidal and subtidal oysters, *Crassostrea virginica*, collected at high and low tides. *Journal of Shellfish Research*, 17(1), 275-280.
- Winstead, J. T. (1995). Digestive tubule atrophy in eastern oysters, *Crassostrea virginica* (Gmelin, 1791), exposed to salinity and starvation stress. *Journal of Shellfish Research*, 14(1), 105-112.
- Wood, E. M., & Yasutake, W. T. (1956). Ceroid in fish. *The American journal of pathology*, 32(3), 591-603.
- Wootton, E. C., & Pipe, R. K. (2003). Structural and functional characterization of the blood cells of the bivalve mollusc, *Scrobicularia plana*. *Fish Shellfish Immunology*, 15, 249-262. [https://doi.org/10.1016/S1050-4648\(02\)00164-X](https://doi.org/10.1016/S1050-4648(02)00164-X)
- Wootton, E. C., Dyrinda, E. A., & Ratcliffe, N. A. (2003). Bivalve immunity: comparisons between the marine mussel (*Mytilus edulis*), the edible cockle (*Cerastoderma edule*) and the razor-shell (*Ensis siliqua*). *Fish & Shellfish Immunology*, 15(3), 195-210. [https://doi.org/10.1016/S1050-4648\(02\)00161-4](https://doi.org/10.1016/S1050-4648(02)00161-4)
- Xing, J., Zhan, W. B., & Zhou, L. (2002). Endoenzymes associated with haemocyte types in the scallop (*Chlamys farreri*). *Fish & Shellfish Immunology*, 13, 271-278. <https://doi.org/10.1006/fsim.2001.0402>
- Xue, Q. G., Renault, T., & Chilmonczyk, S. (2001). Flow cytometric assessment of haemocyte sub-populations in the European flat oyster, *Ostrea edulis*, haemolymph. *Fish & Shellfish Immunology*, 11(7), 557-567. <https://doi.org/10.1006/fsim.2001.0335>
- Yang, H. S., Park, K. I., Donaghy, L., Adhya, M., & Choi, K. S. (2012). Temporal variation of *Perkinsus olseni* infection intensity in the Manila clam *Ruditapes philippinarum* in Gomso Bay, off the west coast of Korea. *Journal of shellfish Research*, 31(3), 685-690. <https://doi.org/10.2983/035.031.0312>
- Young, T., Walker, S. P., Alfaro, A. C., Fletcher, L. M., Murray, J. S., Lulijwa, R., & Symonds, J. (2019). Impact of acute handling stress, anaesthesia, and euthanasia on fish plasma biochemistry: implications for veterinary screening and metabolomic sampling. *Fish physiology and biochemistry*, 45, 1485-1494. <https://doi.org/10.1007/s10695-019-00669-8>
- Young, T., Kesarcodi-Watson, A., Alfaro, A. C., Merien, F., Nguyen, T. V., Mae, H., Le, D. V., & Villas-Bôas, S. (2017). Differential expression of novel metabolic and immunological biomarkers in oysters challenged with a virulent strain of OsHV-1. *Developmental & Comparative Immunology*, 73, 229-245. <https://doi.org/10.1016/j.dci.2017.03.025>
- Young, T., Alfaro, A. C., & Villas-Bôas, S. G. (2016). Metabolic profiling of mussel larvae: effect of handling and culture conditions. *Aquaculture International*, 24, 843-856.
- Yu, J. H., Song, J. H., Choi, M. C., & Park, S. W. (2009). Effects of water temperature change on immune function in surf clams, *Macra veneriformis* (Bivalvia: Mactridae). *Journal of invertebrate pathology*, 102(1), 30-35. <https://doi.org/10.1016/j.jip.2009.06.002>

- Zannella, C., Mosca, F., Mariani, F., Franci, G., Folliero, V., Galdiero, M., Tiscar, P. G., & Galdiero, M. (2017). Microbial diseases of bivalve mollusks: infections, immunology and antimicrobial defense. *Marine Drugs*, 15, 182. <https://doi.org/10.3390/md15060182>
- Zaroogian, G., & Yevich, P. (1993). Cytology and biochemistry of brown cells in *Crassostrea virginica* collected at clean and contaminated stations. *Environmental Pollution*, 79(2), 191-197. [https://doi.org/10.1016/0269-7491\(93\)90069-Z](https://doi.org/10.1016/0269-7491(93)90069-Z)
- Zhang, W., Wu, X., & Wang, M. (2006). Morphological, structural, and functional characterization of the haemocytes of the scallop, *Argopecten irradians*. *Aquaculture*, 251(1), 19-32. <https://doi.org/10.1016/j.aquaculture.2005.05.020>
- Zhang, W., Wu, X., Sun, J., & Li, D. (2005). Morphological and functional characterization of the hemocytes of the scallop, *Chlamys farreri*. *Journal of Shellfish Research*, 24(4), 931-936.
- Zhengli, S., & Handler, J. (2004). Abalone viral mortality–disease card. *Developed to support the NACA/FAO/OIE regional quarterly aquatic disease (QAAD) reporting system in the Asia-Pacific*. NACA, Bangkok.
- Zhou, L., Yang, A., Liu, Z., Wu, B., Sun, X., Lv, Z., Tian, J.-T. & Du, M. (2017). Changes in hemolymph characteristics of ark shell *Scapharaca broughtonii* dealt with *Vibrio anguillarum* challenge in vivo and various of anticoagulants in vitro. *Fish & Shellfish Immunology*, 61, 9-15.
- <https://www.aquaculture.org.nz/>
- <https://www.paua.org.nz/>
- <https://www.niwa.co.nz>

Chapter 9

Appendixes

9.1 Appendixes (Chapter 1)

Table 2.A.1 Statistical analysis: Chi-square test for the association between *P. olsenii* and other pathogens and parasites.

Pathogens and parasites		<i>Perkinsus olsenii</i>		Chi-square test for association (P-value)
		No	Yes	
Intracellular microcolonies of bacteria (IMCs)	Absent	76	2	0.042
	Present	6	2	
<i>Scyphidia</i> -like ciliates	Absent	37	2	1.000
	Present	45	2	
<i>Sphenophrya</i> -like ciliates	Absent	38	2	1.000
	Present	44	2	
Unidentified disintegrated Ciliates	Absent	61	3	1.000
	Present	21	1	

Table 2.A.2 Statistical analysis: Chi-square test for the association between *P. olsenii* and gills pathology.

Pathological condition of gills		<i>Perkinsus olsenii</i>		Chi-square test for association (P-value)
		No	Yes	
Swollen gills with ceroid material and haemocytosis (grade 4)	Absent	77	2	0.032
	Present	5	2	
Disrupted gills with ceroid material and ciliate parasites and without haemocytosis (grade 3)	Absent	78	3	0.217
	Present	4	1	
Gills with ceroid material and ciliate parasites (grade 2)	Absent	47	2	1.000
	Present	35	2	
Normal gills without ceroids and parasites (grade 1)	Absent	43	4	0.123
	Present	39	0	

Table 2.A.3 Statistical analysis: Chi-square test for the association between *P. olsenii* and gross appearance of abalone.

Gross appearance		<i>Perkinsus olseni</i>		Chi-square test for association (<i>P</i> -value)
		No	Yes	
Healthy or Unhealthy	Healthy	59	0	0.008
	Unhealthy	23	4	

Table 2.A.4 Statistical analysis: Chi-square test for the association between *P. olseni* and unhealthy gross appearance of abalone.

Unhealthy gross appearance		<i>Perkinsus olseni</i>		Chi-square test for association (<i>P</i> -value)
		No	Yes	
Pustules	Absent	82	1	0.024
	Present	0	1	
Nodules	Absent	82	1	0.001
	Present	0	3	
Others	Absent	59	3	0.383
	Present	23	0	

Table 2.A.5 Statistical analysis: Chi-square test for the association between unidentified disintegrated ciliates and gross appearance of abalone.

Gross appearance		Unidentified disintegrated ciliates		Chi-square test for association (<i>P</i> -value)
		No	Yes	
Healthy or Unhealthy	Healthy	48	11	0.036
	Unhealthy	16	11	

9.2 Appendixes (Chapter 6)

Table 6.A.1 Mean percentage±SE of PO positive granulocytes, ACP positive granulocytes, total granulocytes and total hyalinocytes were calculated from the slides incubated in ACP and PO enzyme-substrate solutions at 15°C and 26°C temperature after 24 hours and 48 hours incubation period from non-injected control, FSW injected and endotoxin injected mussels. [Total sample number (n) = 60 and 100 cell counts from each sample].

Phenoloxidase (mean percentage±SE)		
Time	24h incubation	48h incubation

Groups		PO+ granulocytes	Total granulocytes in PO-reaction slides	Total hyalinocytes in PO-reaction slides	PO + granulocytes	Total granulocytes in PO-reaction slides	Total hyalinocytes in PO-reaction slides
15°C	Non-injected control	10.4±2.0	99±1.8	3.8±1.8	19.4±5.8	99.4±0.4	0.6±0.4
	FSW injection	3.6±1.7	96.4±1.7	3.6±1.7	17.2±8.1	98.2±1.6	1.8±1.6
	Endotoxin injection	7.8±3.0	96.8±1.8	3.2±1.8	26.8±4.8	99.8±0.2	0.2±0.2
26°C	Non-injected control	5.4±2.6	99±0.5	1±0.5	27.6±7.5	99±0.6	1±0.6
	FSW injection	7.4±1.6	98.8±0.4	1.2±0.4	25.2±4.8	99.6±0.4	0.4±0.4
	Endotoxin injection	7.6±3.2	97±1.3	3±1.3	23.2±3.7	98.4±1.0	1.6±1.0
Acid phosphatase (mean percentage±SE)							
Time		24h incubation			48h incubation		
Groups		ACP + granulocytes	Total granulocytes in ACP-reaction slides	Total hyalinocytes in ACP-reaction slides	ACP + granulocytes	Total granulocytes in ACP-reaction slides	Total hyalinocytes in ACP-reaction slides
15°C	Non-injected control	9.2±4	89±0.6	1.8±0.6	6.4±0.8	98.6±0.6	1.4±0.6
	FSW injection	20.2±5.2	99.2±0.4	0.8±0.4	6.2±1.8	99.2±0.8	0.8±0.8
	Endotoxin injection	8±3.2	98.2±1.4	1.6±1.4	11.4±5.8	99.2±0.6	0.8±0.6
26°C	Non-injected control	18.2±5.1	99±0.6	2±0.6	10.4±5.1	99.8±0.2	0.2±0.2
	FSW injection	15.4±3.4	97.8±1.7	2.2±1.7	14±3.9	99±0.6	1±0.6
	Endotoxin injection	16±3.4	99±0.6	1±0.6	9.8±3.8	98.8±1.0	1.2±1.0

Table 6.A.2 2-Way ANOVA summary table for Enzyme reactions.

	Response	Factors	df	Sum Square	Mean Square	F-value	P-value
	24h	Total Hyalinocytes (%) in PO-reaction slides	Tank groups (non-injected control, FSW injection and endotoxin injection)	2	3.27	1.633	0.174
Temperature (15 & 26)			1	24.30	24.300	2.585	0.121
Interaction: Tank groups × Temperature			2	9.80	4.900	0.521	0.600
Total Granulocytes (%) in PO-reaction slides		Tank groups (non-injected control, FSW injection and endotoxin injection)	2	3.27	1.633	0.174	0.842
		Temperature (15 & 26)	1	24.30	24.300	2.585	0.121
		Interaction: Tank groups × Temperature	2	9.80	4.900	0.521	0.600
PO enzyme positive granulocytes (%)		Tank groups (non-injected control, FSW injection and endotoxin injection)	2	35.5	17.73	0.595	0.559
		Temperature (15 & 26)	1	1.6	1.63	0.055	0.817

		Interaction: Tank groups × Temperature	2	97.1	48.53	1.630	0.217
	Total Hyalinocytes (%) in ACP-reaction slides	Tank groups (non-injected control, FSW injection and endotoxin injection)	2	0.07	0.033	0.007	0.993
		Temperature (15 & 26)	1	0.03	0.033	0.007	0.935
		Interaction: Tank groups × Temperature	2	8.07	4.033	0.826	0.450
	Total Granulocytes (%) in ACP-reaction slides	Tank groups (non-injected control, FSW injection and endotoxin injection)	2	4.27	2.133	0.859	0.436
		Temperature (15 & 26)	1	3.33	3.333	1.342	0.258
		Interaction: Tank groups × Temperature	2	0.27	0.133	0.054	0.948
	ACP enzyme positive granulocytes (%)	Tank groups (non-injected control, FSW injection and endotoxin injection)	2	4.27	2.133	0.471	0.630
		Temperature (15 & 26)	1	3.33	3.333	0.362	0.553
		Interaction: Tank groups × Temperature	2	0.27	0.133	1.262	0.948
48h	Total Hyalinocytes (%) in PO-reaction slides	Tank groups (non-injected control, FSW injection and endotoxin injection)	2	0.47	0.233	0.067	0.301
		Temperature (15 & 26)	1	0.13	0.133	0.038	0.846
		Interaction: Tank groups × Temperature	2	10.07	5.033	1.452	0.254
	Total Granulocytes (%) in PO-reaction slides	Tank groups (non-injected control, FSW injection and endotoxin injection)	2	0.47	0.233	0.067	0.935
		Temperature (15 & 26)	1	0.13	0.133	0.038	0.846
		Interaction: Tank groups × Temperature	2	10.07	5.033	1.452	0.254
	PO enzyme positive granulocytes (%)	Tank groups (non-injected control, FSW injection and endotoxin injection)	2	73	36.63	0.204	0.817
		Temperature (15 & 26)	1	132	132.30	0.737	0.399
		Interaction: Tank groups × Temperature	2	228	114.10	0.636	0.538
	Total Hyalinocytes (%) in ACP-reaction slides	Tank groups (non-injected control, FSW injection and endotoxin injection)	2	0.2	0.100	0.046	0.955
		Temperature (15 & 26)	1	0.3	0.300	0.137	0.714
		Interaction: Tank groups × Temperature	2	3.8	1.900	0.870	0.432
	Total Granulocytes (%) in ACP-reaction slides	Tank groups (non-injected control, FSW injection and endotoxin injection)	2	0.27	0.1333	0.060	0.942
		Temperature (15 & 26)	1	0.53	0.5333	0.241	0.628
		Interaction: Tank groups × Temperature	2	3.47	1.7333	0.782	0.469
	ACP enzyme positive granulocytes (%)	Tank groups (non-injected control, FSW injection and endotoxin injection)	2	26.6	13.30	0.172	0.843
		Temperature (15 & 26)	1	86.7	86.70	1.118	0.301

		Interaction: Tank groups × Temperature	2	111.8	55.90	0.721	0.497
--	--	--	---	-------	-------	-------	-------

Table 6.A.3 2Way ANOVA summary table for Flow cytometry

	Response	Factors	df	Sum Square	Mean Square	F-value	p-value
6h	THC (cells/ ml)	Tank groups (non-injected control, FSW injection and endotoxin injection)	2	3.228e+12	1.614e+12	0.226	0.799
		Temperature (15 & 26)	1	1.188e+13	1.188e+13	1.665	0.209
		Interaction: Tank groups × Temperature	2	6.304e+12	3.152e+12	0.442	0.648
	Viability (%)	Tank groups (non-injected control, FSW injection and endotoxin injection)	2	803	401.3	1.378	0.271
		Temperature (15 & 26)	1	98	98.1	0.337	0.567
		Interaction: Tank groups × Temperature	2	3	1.3	0.004	0.996
	ROS (%)	Tank groups (non-injected control, FSW injection and endotoxin injection)	2	60.8	30.39	0.422	0.661
		Temperature (15 & 26)	1	19.4	19.44	0.270	0.608
		Interaction: Tank groups × Temperature	2	49.6	24.80	0.344	0.712
24h	THC (cells/ ml)	Tank groups (non-injected control, FSW injection and endotoxin injection)	2	1.013e+14	5.064e+13	1.842	0.180
		Temperature (15 & 26)	1	3.893e+09	3.893e+09	0.000	0.991
		Interaction: Tank groups × Temperature	2	8.023e+11	4.011e+11	0.015	0.986
	Viability (%)	Tank groups (non-injected control, FSW injection and endotoxin injection)	2	848	424.1	2.636	0.0923
		Temperature (15 & 26)	1	776	775.6	4.820	0.0380 *

48h		Interaction: Tank groups × Temperature	2	473	236.3	1.468	0.2502
	ROS (%)	Tank groups (non-injected control, FSW injection and endotoxin injection)	2	257.0	128.52	1.833	0.182
		Temperature (15 & 26)	1	35.6	35.62	0.508	0.483
		Interaction: Tank groups × Temperature	2	131.3	65.66	0.937	0.406
	THC (cells/ ml)	Tank groups (non-injected control, FSW injection and endotoxin injection)	2	4.682e+13	2.341e+13	0.977	0.391
		Temperature (15 & 26)	1	6.198e+13	6.198e+13	2.586	0.121
		Interaction: Tank groups × Temperature	2	3.611e+13	1.805e+13	0.753	0.482
	Viability (%)	Tank groups (non-injected control, FSW injection and endotoxin injection)	2	677	338.4	1.863	0.177
		Temperature (15 & 26)	1	66	65.9	0.363	0.553
		Interaction: Tank groups × Temperature	2	134	67.2	0.370	0.695
	ROS (%)	Tank groups (non-injected control, FSW injection and endotoxin injection)	2	234.6	117.29	2.494	0.104
		Temperature (15 & 26)	1	13.2	13.20	0.281	0.601
Interaction: Tank groups × Temperature		2	9.2	4.59	0.098	0.907	

Table 6.A.4 Metabolites significantly affected ($p < 0.05$) in green-lipped mussels due to the effect of temperature, immune stimulation or the interaction of both.

Metabolites	Temperature ($p < 0.05$)	Immune Stimulation ($p < 0.05$)	Interaction ($p < 0.05$)
2-Aminoadipic acid	1.04E-03	1.29E-01	2.60E-01
2-Ketoglutaramate	3.46E-03	9.13E-01	8.68E-01
4-Hydroxyphenylacetic acid	3.59E-01	3.58E-03	8.51E-01
Aspartic acid	2.25E-02	9.05E-02	5.23E-01
Azelaic acid	4.14E-01	1.54E-01	1.07E-02
beta-Alanine	9.99E-03	9.02E-01	6.48E-01

Cabamic acid	2.33E-02	8.98E-02	3.91E-01
Citramalic acid	8.13E-01	3.95E-02	2.57E-01
Creatinine	6.20E-07	2.13E-01	1.02E-01
Cysteine	5.40E-01	6.96E-03	6.74E-01
Docosahexaenoic acid (DHA)	3.82E-02	6.31E-01	6.90E-01
Dodecanoic acid (C12)	9.76E-01	4.17E-03	9.53E-01
Eicosapentaenoic acid (EPA)	2.10E-02	6.45E-01	6.29E-01
Fumaric acid	2.62E-03	6.74E-01	7.31E-01
gamma-Linolenic acid (C18:3)	4.90E-02	9.00E-01	4.44E-01
Glutamic acid	1.89E-02	4.14E-01	2.69E-01
Glutaric acid	1.24E-03	1.83E-02	5.68E-02
Glutathione	3.28E-03	6.62E-02	3.11E-01
Glycine	4.61E-02	3.98E-01	5.97E-01
Glyoxylic acid	4.27E-01	4.28E-02	6.13E-01
Histidine	1.04E-03	7.24E-01	7.85E-01
Isoleucine	5.96E-07	5.06E-01	9.20E-02
Itaconic acid	4.66E-02	5.18E-01	5.00E-01
Lactic acid	2.27E-02	3.80E-02	1.36E-01
Leucine	2.45E-07	5.28E-01	1.21E-01
Lysine	4.31E-03	8.26E-01	6.83E-01
Malic acid	4.31E-03	8.88E-01	7.08E-01
Margaric acid (C17)	2.13E-02	4.56E-01	9.83E-01
Methionine	2.97E-05	9.48E-01	4.42E-01
Octanoic acid (C8)	2.08E-01	6.17E-03	1.02E-01
Ornithine	2.39E-05	9.30E-01	6.14E-02
Pentadecanoic acid (C15)	3.04E-02	4.51E-01	9.67E-01
Phenylalanine	2.50E-05	7.08E-01	3.83E-02
Proline	1.92E-05	2.83E-01	2.26E-01
Serine	3.81E-04	8.04E-01	3.18E-02
trans-Vaccenic acid	2.89E-02	7.60E-01	8.48E-01
Tryptophan	2.08E-02	6.80E-01	1.17E-01
Tyrosine	5.49E-03	6.62E-01	1.77E-01
Valine	3.68E-06	4.90E-01	7.01E-02
Unknown 1	8.51E-03	6.22E-01	6.27E-02
Unknown 2	4.77E-04	4.23E-01	4.62E-01
Unknown 3	1.06E-04	8.21E-01	9.72E-02
Unknown 4	3.30E-06	4.35E-01	1.51E-01
Unknown 5	2.62E-03	6.74E-01	7.31E-01
Unknown 6	4.27E-01	1.73E-02	4.44E-01
Unknown 7	5.55E-03	7.21E-01	8.92E-01
Unknown 8	7.44E-03	4.81E-01	1.96E-01
Unknown 9	2.97E-05	9.65E-01	8.42E-01
Unknown 10	1.11E-03	9.99E-01	7.29E-01
Unknown 11	1.13E-01	2.63E-02	8.11E-02
Unknown 12	4.86E-02	9.63E-01	9.11E-01

Table 6.A.5 Average metabolite abundance of metabolites found in green-lipped mussels significantly affected by temperature.

Metabolites	[Ave metabolite] 17°C group	[Ave metabolite] 26°C group	Response of 26°C group
2-Amino adipic acid	0.03	0.05	↑
Aspartic acid	9.72	12.37	↑
beta-Alanine	0.03	0.04	↑
Cabamic	0.14	0.32	↑
Creatinine	0.21	0.07	↓

DHA	0.25	0.44	↑
2-ketoglutaramate	0.03	0.01	↓
EPA	0.16	0.33	↑
Fumaric acid	0.01	0.03	↑
C18:3	0.04	0.07	↑
Glutamic acid	1.01	1.38	↑
Glutaric acid	0.00	0.00	↑
Glutathione	0.16	0.23	↑
Glycine	31.52	38.62	↑
Histidine	0.24	0.09	↓
Isoleucine	1.55	0.43	↓
Itaconic acid	0.00	0.00	↑
Lactic acid	0.08	0.12	↑
Leucine	3.06	0.78	↓
Lysine	2.83	1.37	↓
Malic acid	0.03	0.10	↑
C17	0.09	0.15	↑
Methionine	0.30	0.11	↓
Ornithine	0.48	0.15	↓
C15	0.07	0.12	↑
Phenylalanine	0.68	0.29	↓
Proline	5.59	3.13	↓
Serine	1.65	1.05	↓
trans-Vaccenic acid	0.08	0.15	↑
Tryptophan	0.19	0.11	↓
Tyrosine	1.27	0.67	↓
Valine	4.14	1.50	↓

Table 6.A.6 Average metabolite abundance of metabolites found in green-lipped mussels significantly affected by immune stimulation.

Metabolites	[Ave metabolite] Endotoxin group	[Ave metabolite] FSW group	Endotoxin reaction
4-Hydroxyphenylacetic acid	0.05	0.02	↑
Citramalic acid	2.32	1.50	↑
Cysteine	0.09	0.05	↑
C12	0.04	0.02	↑
Glutaric acid	0.00	0.00	↑
Glyoxylic acid	0.06	0.03	↑
Lactic acid	0.12	0.08	↑
C8	0.02	0.01	↑

Table 6.A.7 Average metabolite abundance of metabolites found in green-lipped mussels significantly affected by the interaction of temperature and immune stimulation.

Temperature	17°C	17°C	25°C	25°C
Immune stimulation	FSW	Endotoxin	FSW	Endotoxin
Azelaic acid	0.004	0.008	0.006	0.005
Phenylalanine	0.571	0.785	0.333	0.254
Serine	1.466	1.829	1.172	0.929